GEOLOGICAL SURVEY
of
WESTERN AUSTRALIA

ANNUAL REPORT 1974

GEOLOGICAL SURVEY OF WESTERN AUSTRALIA

ANNUAL REPORT

FOR THE YEAR

1974

EXTRACT FROM THE REPORT OF THE DEPARTMENT OF MINES

Minister: The Hon. A. Mensaros, M.L.A.

Under Secretary: B. M. Rogers

Director, Geological Survey: J. H. Lord

By Authority: WILLIAM C. BROWN, Government Printer

1975

46009/4/75

DIVISION IV

Annual Report of the Geological Survey Branch of the Mines Department for the Year 1974

CONTENTS

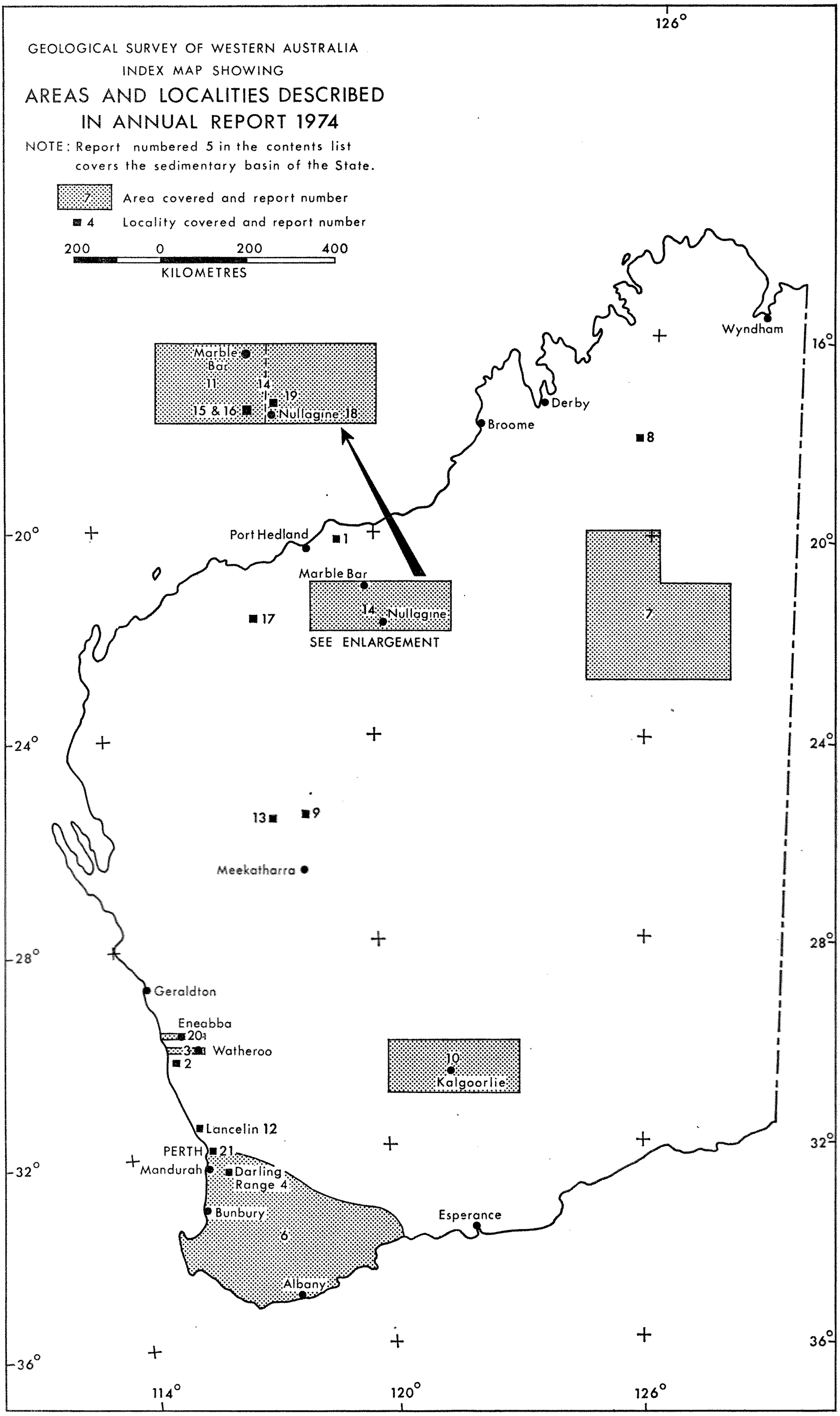

Figure 1. Index map showing areas and localities described in Annual Report for 1974.

LIST OF FIGURES

DIVISION IV

•

Annual Report of the Geological Survey Branch of the Mines Department for the Year 1974

•

Under Secretary for Mines:

My report on the activities on the Geological Survey of Western Australia during 1974, together with some of the reports on investigations made for departmental purposes, are submitted for the information of the Honourable Minister for Mines.

INTRODUCTION

The reduction trend in exploration which was evident in 1973, continued in 1974 mainly due to the unfavourable Commonwealth Government policy towards overseas explorers, which in turn has adversely affected the smaller-Australian companies.

During the year 47 new temporary reserves for mineral exploration were granted, as compared with 182 in 1973.

Iron ore exploration has been continued by interested companies on a similar scale to 1973. Most work was done in extending the knowledge of known occurrences. While producing companies were able to extend existing sales contracts, no new major contracts were written. Goldsworthy Mining Limited announced that by about 1978 it would commence mining a production rate of 10 million tonnes per year from its "Mining Area C" deposits. These ore bodies have reserves of 750 million tonnes of high grade ore with a low phorphorus content. The small Koolanooka mine, which was the first to export iron ore in March 1966, closed, having exhausted its ore body and fulfilled the contract of 5.1 million tonnes.

Bauxite exploration is at a standstill. The feasibility study for Alwest to establish an alumina plant at Worsley near Collie was completed favourably, but agreement could not be reached with the Commonwealth Government on several aspects, particularly that of the environment.

The great interest in uranium exploration decreased during 1974, probably due to the lack of further potentially economic finds since Yeelirrie, and also to the uncertainty of permission being granted to develop any discoveries. The search this year has concentrated on the Murchison, Gascoyne, Ashburton and Kimberley areas.

Exploration for nickel continues, but on a reduced scale. The results of exploration by Australian Selection near Agnew has proved an ore body containing about 40 million tonnes, averaging 2 per cent nickel. Good drilling results are still being reported from Forrestania. No new finds have been reported to the Department of Mines. The Carr Boyd rocks mine commenced production, while mines at Widgiemooltha and Redross are being developed.

Gold prospecting continues to be active due to the increased price. The Paterson Range gold find has reported reserves of 3.8 million tonnes, averaging 8.78 gm (0.31 oz) per tonne and the development of a mine is planned. Preparations are being made to reopen the Blue Spec mine near Nullagine for the production of gold and antimony.

The main mineral sands activity has been the development of earlier discoveries, particularly at Eneabba where Jennings Mining Ltd. (reserves 9.5 million tonnes) has commenced production, Allied Minerals (reserves 9.0 million tonnes) should commence production in 1975, and Western Titanium (reserves 9.8 million tonnes) plan to commence production late in 1976. The Geological Survey has studied the mineral sands deposits of the State and estimates the resources as 72.9 million tonnes, of which 20 million tonnes are uneconomic at present.

General exploration for other metallic and nonmetallic minerals continued on a reduced scale. Mining and export of talc commenced at Mount Seabrook. Full scale plant for the production of diatomite is being established near Dongara, while there is a proposal to ship a large parcel of magnesite from near Ravensthorpe. Exploration and drilling have outlined a prospective copper-zinc deposit near Golden Grove 93 km northwest of Paynes Find. Additional work is being done to determine its economic importance.

The amount of oil exploration work done, both onshore and offshore, showed a continued decline. Only 16 test wells were completed in 1974, a decrease of 20 per cent as compared with 1973. Total footage for all wells drilled was 51 487 m, a decrease of 19 per cent. There was a decrease of 69 per cent in land seismic work and 21 per cent decrease in marine seismic work, as compared with 1973.

This decrease in exploration for oil and gas at the time of an energy crisis throughout the world must have a serious adverse effect on Australia's future ability to attain any self-sufficiency in this form of energy.

The present situation of about 70 per cent self-sufficiency, has been achieved only by continuous exploration over many years and we cannot afford to allow this decrease in the exploration rate to continue.

The only significant results during the year were from the West Tryal Rocks No. 2, 75 km northwest of Barrow Island, where a gas flow of 255 000 to 314 000 cubic metres per day was reported and from Lambert No. 1 where some oil showings occurred.

The upsurge in prospecting for coal, which developed in 1973, tapered off towards the end of 1974 without any significant economic discoveries being made.

Two lecture evenings followed by field excursions were conducted. One was at Marble Bar where the lectures were given in conjunction with a three day excursion on the Marble Bar and Nullagine 1 : 250 000 geological sheets. The other was in Perth where the lecture evening was held at the University, followed by a two day excursion on the Precambrian of the Perth 1 : 250 000 sheet. About 73 and 58 persons respectively attended the field excursions.

STAFF

Continued difficulties were experienced in filling vacancies which required experience or training in sedimentary geology or hydrogeology. It is hoped that all such positions will be filled early in 1975.

Two geologists were engaged to specialise in environmental geology while two additional staff were appointed to the Sedimentary (Oil) Division to assist in particular with the handling of technical information being received from companies.

Difficulty is being experienced in retaining geological and technical assistants. Staff recruited for such positions soon loose interest in routine work and resign.

PROFESSIONAL

Appointments

Name	Position	Effective Date
Elias, M., B.Sc. (Hons.)	Geologist, Level 1	7/1/74
Briese, E., B.Sc. (Hons.)	Geologist, Level 1	7/6/74
Drake, J. R. B.Sc. (Hons.)	Geologist, Level 1	14/6/74
Davy, R., Ph.D.	Geochemist, Level 4	17/6/74
Biggs, E. R., B.Sc. (Hons.)	Geologist, Level 2	1/7/74
Archer, R. H., B.Sc. (Hons.)	Geologist, Level 1	26/8/74
Megallaa, M. N., B.Sc.	Geophysisict, Level 3	1/10/74
Hocking, R. M., B.Sc. (Hons.)	Geologist, Level 1	11/12/74

Temporary Relief

Drake, J. R. B.Sc. (Hons.)	Geologist, Level 1	14/1/74
Novak, V., B.Sc.	Geologist, Level 1	30/1/74
Hirschberg, K. J. B., Ph.D.	Geologist, Level 1	15/5/74

Promotions

Davidson, W. A.	Geologist, Level 2	15/11/74

Resignations

Janse, R.	Geologist, Level 1	8/2/74
Novak, V.	Geologist (temp.) Level 1	22/2/74
Barnes, R. J.	Geologist, Level 1	24/4/74
Forth, J. R.	Geologist, Level 2	26/9/74
Boegli, J. -C.	Geologist, Level 1	29/11/74

Transfer Out

Cope, R. N.	Geologist, Level 4	27/5/74

CLERICAL AND GENERAL

Appointments

Name	Position	Effective Date
Muldownie, C.	Technical Assistant	17/1/74
Rankin, P.	Geological Assistant	21/1/74
Bazely, M. J.	Typist	4/2/74
Williams, S. J., B.Sc. (Hons.)	Geological Assistant	6/2/74
Douglas, S. K.	Geophysical Assistant	5/2/74
Berkmann, S.	Typist	15/3/74
Pearman, M.	Messenger	22/3/74
Ridley, J.	Typist	1/4/74
Green, M.	Technical Assistant	16/4/74
Lutter, M. D.	Technical Assistant	30/4/74
Hargrave, D. J.	Typist	30/4/74
Yule, J. G. C.	Geophyisical Assistant	27/5/74
O'Brien, B.	Geological Assistant	4/6/74
Dowling, N.	Technical Assistant	7/5/74
Wakeham, J. I.	Library Assistant	1/7/74
Baints, R.	Technical Assistant	8/7/74
Ritchie, L.	Geological Assistant	29/7/74
Bontemps, T. H.	Geological Assistant	29/8/74
Thomas, H.	Geological Assistant	26/8/74
Butherway, P.	Geohpysical Assistant	10/10/74
Hammill, N. C.	Clerical Assistant	23/9/74
Slater, R. M.	Geophysical Assistant	9/12/74

Resignations

Formato, E.	Geophysical Assistant	11/1/74
Darby, N. D.	Geological Assistant	15/2/74
Nutt, M. D.	Typist	8/3/74
Muldownie, C. E.	Technical Assistant	22/3/74
Butherway, P.	Geophysical Assistant	22/3/74
Grenfell, R. A.	Messenger	22/3/74
Marrell, G.	Technical Assistant	29/3/74
Berkmann, S.	Typist	1/4/74
Douglas, S. R.	Geophysical Assistant	26/4/74
Bazely, M. J.	Typist	2/5/74
Pearson, J.	Library Assistant	23/4/74
O'Brien, B.	Geological Assistant	8/7/74
Beere, M.	Clerical Assistant	20/9/74
Yule, J. G. C.	Geophysical Assistant	5/9/74
Ritchie, L.	Geological Assistant	22/11/74

Transfers Out

Mouritzen, C.	Geological Assistant	31/5/74
Lyons, W. A.	Senior Clerk	17/6/74

Transfers In

McNamara, T.	Senior Clerk	17/6/74

OPERATIONS

HYDROGEOLOGY AND ENGINEERING GEOLOGY DIVISION

E. P. O'Driscoll (Chief Hydrogeologist), T. T. Bestow, R. P. Mather (Supervising Geologists), K. Berliat, A. D. Allen (Senior Geologists), C. C. Sanders, G. W. A. Marcos, W. A. Davidson, A. S. Harley, R. E. J. Leech, J. C. Barnett, D. P. Commander, J. M. Campbell, G. Klenowski and E. H. Briese.

Hydrogeology

Further progress was made with the programme of exploratory drilling for water in the Perth Basin sediments. Two of the deepest bores ever to be drilled for ground water investigation were drilled at Picton Junction and Yoganup to depths of 1 200 and 1 120 metres respectively. The latter, known as Quindalup No. 6, intersected sediments containing water of domestic quality to a depth of nearly 1 000 metres, confirming the existence of a very large water resource.

The deep drilling west of Winchester along the Eneabba cross-section was completed. This established that large reserves of potable water exist down to at least 750 metres at and east of Eneabba. Drilling has commenced on a new cross-section between Moora and Grey.

The long term investigation of the shallow aquifers in and near the Perth Metropolitan area has made considerable progress. A further seventeen sites have been drilled as part of the Joondalup programme and the Metropolitan Water Board has continued exploration in the vicinity of Lake Thompson, 21 bores being drilled to depths of up to 64 metres. Further shallow production bores have been drilled at Wanneroo, and deep bores at Mirrabooka and at Wanneroo Reservoir. One deep stratigraphic bore has been drilled at Whitfords. Close liaison continues to be maintained with the Metropolitan Water Board in all aspects of groundwater exploration and development.

The investigation into the water resources of the western part of the Canning Basin has continued. A further nine boreholes were drilled and an extensive seismic programme has been completed. At Millstream nine exploratory bores were drilled east of the area investigated in 1968, these being part of a project to better define the limits of the important calcrete groundwater storage. Further drilling has also been carried out along the De Grey River where seismic work has indicated the presence of a deep buried channel.

Several inter-departmental committees have been set up to study the effects of the bauxite mining and Manjimup woodchip industries on the various aspects of hydrology in the region of the Darling Range. This Branch has actively participated so far as the availability of staff would allow.

Twenty boreholes were drilled in a wide area at Del Park, and it is expected that subsequent monitoring will delineate the groundwater response to mining and dieback *(Phytopthora cinnamomi)* in the adjoining forest.

Advice continues to be provided in connexion with work done by groundwater consultants for mining and other companies. However, activity remains at a low level. Landholders throughout the State continue to seek advice regarding the development of groundwater supplies and although there has been an increase in enquiries at the office, there has been a reduction in the number of on-site inspections.

Engineering Geology

A number of proposed dam sites were investigated for the Department of Public Works, including:

(a) Dogger Gorge and Gregory Gorge—geological mapping and drilling to compare the sites.

(b) Moochalabra Creek dam—additional geological mapping and drilling for the proposed raising of the wall.

(c) Harvey dam site—report completed and issued.

(d) Burekup dam site—detailed study with drilling—report issued.

(e) Bullinnarwa Pool dam site—report prepared.

(f) Robe River dam site—a reconnaissance and report on a proposed site.

The following investigations were made for the Metropolitan Water Board:

(a) South Dandalup dam—geological information updated during construction of this dam.

(b) Wungong, South Canning and North Dandalup dam sites—detailed study including mapping, drilling and seismic work continuing.

(c) Minor work has been done on the Wungong tunnel site and the Beenyup waste water plant outfall tunnel.

SEDIMENTARY (OIL) DIVISION

P. E. Playford (Supervising Geologist), G. H. Low, W. J. E. van de Graaff (Senior Geologists), M. N. Megallaa (Geophysicist), R. W. A. Crowe, R. M. Hocking.

Information received from petroleum companies was evaluated and collated, and methods for accession, storage, retrieval, and distribution of data were further developed. The flow of information from companies greatly increased during the year, largely due to the requirement for submission of comprehensive data packages when permits or parts of permits are relinquished. These data are microfilmed and are made available to the public in this form when required.

The Division continued to deal with numerous enquiries from companies and other Government departments on exploration for petroleum and coal in the State.

The Geological Survey's contribution to the Officer Basin project (which is being carried out in conjunction with the Bureau of Mineral Resources) was completed in draft form. Preliminary editions of 1 : 250 000 geological maps of the basin are being issued progressively and a bulletin on the geology of the basin is to be produced.

The Noonkanbah 1 : 250 000 Sheet in the Canning Basin was mapped (jointly with the Bureau of Mineral Resources). Preliminary compilation of data for the basin study of the Carnarvon Basin was commenced during 1974 and mapping will begin in 1975.

REGIONAL GEOLOGY DIVISION

R. D. Gee (Supervising Geologist), I. R. Williams (Senior Geologist), P. C. Muhling, J. A. Bunting, A. T. Brakel, R. J. Chin, M. Elias and S. Williams.

The programme of regional mapping of the Precambrian area of the State for publication on a scale of 1 : 250 000 continued. Progress is shown in Figure 2.

Field mapping on the Nullagine, Sir Samuel and Collier Sheets, plus the Precambrian portions of Mt. Bannerman, Patterson Range and Yarrie, was completed. The latter two sheets were mapped in conjunction with the Mineral Resources Division. Mapping continued on the Southern Cross Sheet and commenced on Robinson Range Sheet.

Work continued on the bulletin on the area covered by the Kalgoorlie and Esperance 1:1 000 000 Sheets.

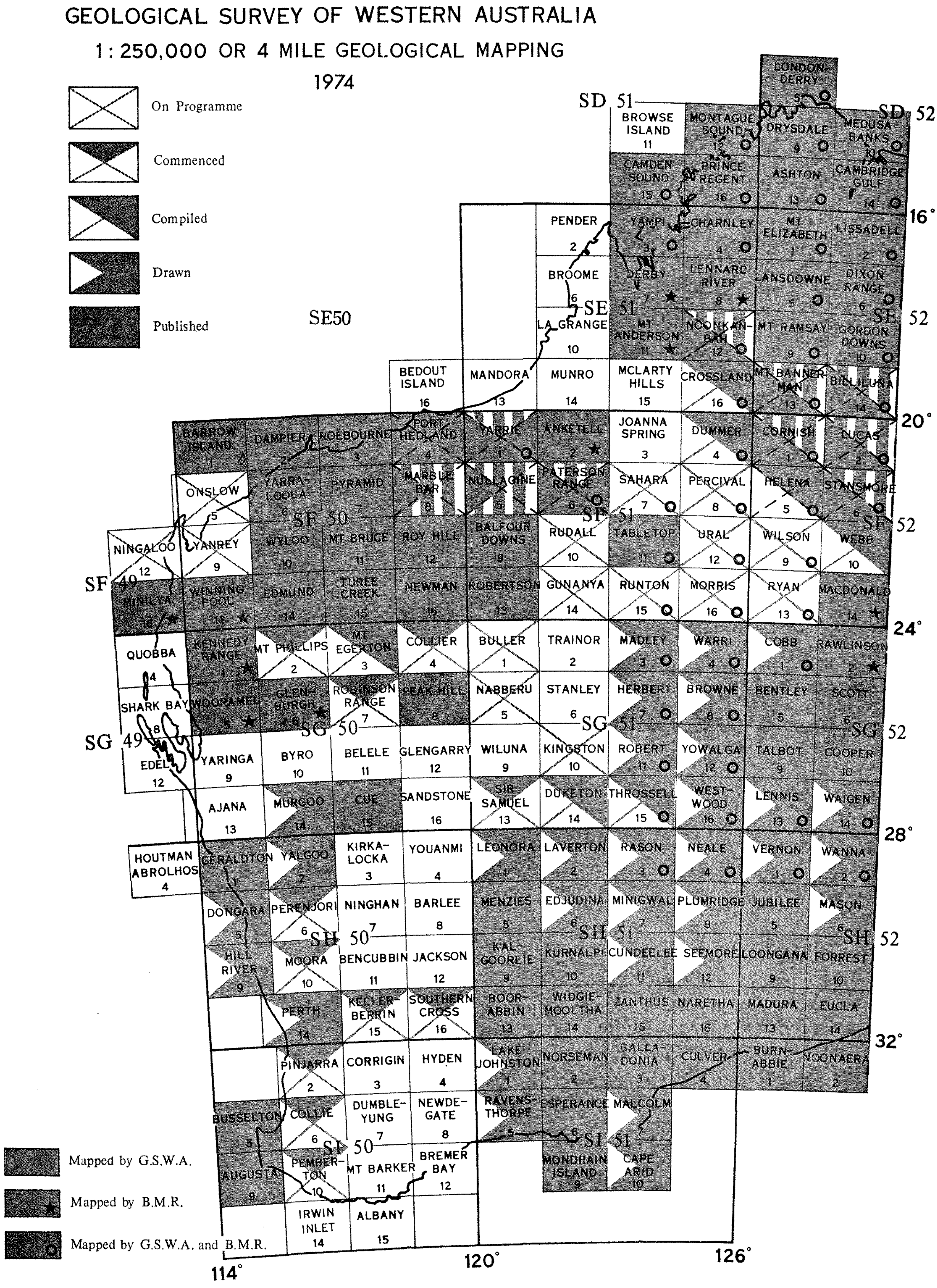
GEOLOGICAL SURVEY OF WESTERN AUSTRALIA
1: 250,000 OR 4 MILE GEOLOGICAL MAPPING
1974
On Programme
Commenced
Compiled
Drawn
Published
Mapped by G.S.W.A.
Mapped by B.M.R.
Mapped by G.S.W.A. and B.M.R.
Broken lines or shading indicates remapping
SD 51
SD 52
SE50
SE 51
SE 52
SF 49
SF 50
SF 51
SF 52
SG 49
SG 50
SG 51
SG 52
SH 50
SH 51
SH 52
SI 50
SI 51
16°
20°
24°
28°
32°
114°
120°
126°
LONDONDERRY
BROWSE ISLAND
MONTAGUE SOUND
DRYSDALE
MEDUSA BANKS
CAMDEN SOUND
PRINCE REGENT
ASHTON
CAMBRIDGE GULF
PENDER
YAMPI
CHARNLEY
MT ELIZABETH
LISSADELL
BROOME
DERBY
LENNARD RIVER
LANSDOWNE
DIXON RANGE
LA GRANGE
MT ANDERSON
NOONKANBAH
MT RAMSAY
GORDON DOWNS
BEDOUT ISLAND
MANDORA
MUNRO
MCLARTY HILLS
CROSSLAND
MT BANNERMAN
BILLILUNA
BARROW ISLAND
DAMPIER
ROEBOURNE
PORT HEDLAND
YARRIE
ANKETELL
JOANNA SPRING
DUMMER
CORNISH
LUCAS
ONSLOW
YARRALOOLA
PYRAMID
MARBLE BAR
NULLAGINE
PATERSON RANGE
SAHARA
PERCIVAL
HELENA
STANSMORE
NINGALOO
YANREY
WYLOO
MT BRUCE
ROY HILL
BALFOUR DOWNS
RUDALL
TABLETOP
URAL
WILSON
WEBB
MINILYA
WINNING POOL
EDMUND
TUREE CREEK
NEWMAN
ROBERTSON
GUNANYA
RUNTON
MORRIS
RYAN
MACDONALD
QUOBBA
KENNEDY RANGE
MT PHILLIPS
MT EGERTON
COLLIER
BULLER
TRAINOR
MADLEY
WARRI
COBB
RAWLINSON
SHARK BAY
WOORAMEL
GLENBURGH
ROBINSON RANGE
PEAK HILL
NABBERU
STANLEY
HERBERT
BROWNE
BENTLEY
SCOTT
EDEL
YARINGA
BYRO
BELELE
GLENGARRY
WILUNA
KINGSTON
ROBERT
YOWALGA
TALBOT
COOPER
AJANA
MURGOO
CUE
SANDSTONE
SIR SAMUEL
DUKETON
THROSSELL
WESTWOOD
LENNIS
WAIGEN
HOUTMAN ABROLHOS
GERALDTON
YALGOO
KIRKALOCKA
YOUANMI
LEONORA
LAVERTON
RASON
NEALE
VERNON
WANNA
DONGARA
PERENJORI
NINGHAN
BARLEE
MENZIES
EDJUDINA
MINIGWAL
PLUMRIDGE
JUBILEE
MASON
HILL RIVER
MOORA
BENCUBBIN
JACKSON
KALGOORLIE
KURNALPI
CUNDEELEE
SEEMORE
LOONGANA
FORREST
PERTH
KELLERBERRIN
SOUTHERN CROSS
BOORABBIN
WIDGIEMOOLTHA
ZANTHUS
NARETHA
MADURA
EUCLA
PINJARRA
CORRIGIN
HYDEN
LAKE JOHNSTON
NORSEMAN
BALLADONIA
CULVER
BURNABBIE
NOONAERA
BUSSELTON
COLLIE
DUMBLEYUNG
NEWDEGATE
RAVENSTHORPE
ESPERANCE
MALCOLM
AUGUSTA
PEMBERTON
MT BARKER
BREMER BAY
MONDRAIN ISLAND
CAPE ARID
IRWIN INLET
ALBANY

Figure 2.

MINERAL RESOURCES DIVISION

J. G. Blockley (Supervising Geologist), J. D. Carter, A. A. Gibson (Senior Geologists), J. L. Baxter, A. H. Hickman, S. L. Lipple, S. A. Wilde, W. B. Hill (Geologists) and K. J. B. Hirschberg (Geologist, temporarily attached).

The manuscript was completed for a bulletin on the State's mineral sands. Compilation and writing of bulletins on copper, tin, vanadium, tungsten, molybdenum and chromium continued.

Mapping continued on the Darling Range bauxite province. This included, the completion of the Precambrian portions of the Perth Sheet, most of the Pinjarra Sheet and some of the Moora Sheet.

In conjunction with the Regional Geology Division the Nullagine Sheet was completed and compiled, and the Precambrian parts of the Paterson Range and Yarrie Sheets mapped.

Miscellaneous investigations include inspections of talc, kaolin and copper-zinc deposits, an examination of the proposed site for the new Kalgoorlie airport and a survey of the limestone resources of the Perth Metropolitan area.

The evaluation section dealt with 137 requests for information on former mining tenements, and added a further 1 188 accessions to the Survey's collection of confidential mineral exploration data. Particular attention was given to reports dealing with uranium exploration.

COMMON SERVICES DIVISION

Petrology (W. G. Libby, J. D. Lewis, J. R. Drake)

Demand for petrological services continued to increase through 1974. One hundred and thirty seven Petrological Reports were written on 2 263 samples. Most of these samples were thin sections, but at least 46 were polished mineral mounts, hand specimens or grain mounts for heavy mineral analysis. The increase in work over the last four years has necessitated the streamlining of the form of the Petrological Report. Retrieval of the increasing mass of petrological data has been facilitated by the introduction of a computerised data system early in the year. Records of more than 6 000 samples have been processed.

In addition to service petrology, studies were made on the Nullagine meteorite, the Black Range Dolerite, the Cooglegong Granite, and metramorphosed anorthositic gabbros. The programme on the petrology of the Eastern Goldfields is nearing completion.

The co-operative geochronological programme with the Western Australian Institute of Technology continues to grow. Twelve geochronology projects are active and the results of two additional projects have been published during 1974. Two further projects have been deferred.

The laboratory prepared 1 855 thin sections of which 1 464 were petrological, 32 rock or mineral mounts and 225 rock slabs were polished, 39 mineral separations were performed, 222 rocks were prepared for chemical analysis and 292 discs were made for X-ray fluorimetry. One hundred and thirty three granite slabs were stained for modal analysis.

The Government Chemical Laboratories continued to provide valuable chemical analyses and mineral determinations.

Palaeontology (A. E. Cockbain, J. Backhouse, K. Grey)

One hundred file reports and one record were written during the year. The accompanying table shows that, as in previous years, the main demand for palaeontological work came from the Hydrogeology and Engineering Geology Division. Some reports covered more than one field of palaeontology and hence the number of reports shown in the table is greater than 100.

Report requested by	Field of palaeontology		
	Palynology	Micro-palaenotology	Macro-palaeontology
Hydrology and Engineering Geology Division	77	2	....
Sedimentary Division	1	....	1
Regional Mapping and Mineral Resources Divisions	2	4	5
Other Survey requests	1	....	4
Other organisations	4	2	3

Studies of the Mesozoic palynology of the Perth Basin have resulted in a biostratigraphic zonation which is applicable to the Watheroo and Eneabba Lines of boreholes and further work will be done to extend this zonation to other areas in the Perth Basin. Work continued on the Devonian fauna and microflora of the Lennard Shelf and a study of the stromatoporoids from this region was started.

Geophysics (D. L. Rowston, I. R. Nowak)

Geophysical activities were again dominated by investigations for the Hydrogeology and Engineering Geology Division. Groundwater studies included completion of the West Canning Basin seismic refraction survey, experimental work at Cooya Pooya and a minor involvement in paired catchment projects associated with the woodchip industry near Manjimup. Dam sites at Burekup, South Canning and at Dogger Gorge on the Fortescue River were also investigated.

Geophysical bore logging continued at the high level experienced over the past few years. During 1974, 133 bores were logged (138 in 1973) yielding, for all runs, logs equivalent to 32 000 m (27 000 m) of hole. The usual laboratory services were provided for the repair and calibration of equipment and field salinities determined for 830 water samples.

Geochemistry (R. Davy).

Analysis of samples submitted during the previous year in connexion with the regional rock geochemistry survey of the Leonora, Laverton and Rason 1 : 250 000 Sheets has proceeded at the Government Chemical Laboratories. This analytical programme is expected to be complete by mid 1975.

A study of geochemical changes at the transition from the Marra Mamba Iron Formation to the Wittenoom Dolomite in the Millstream No. 9 diamond drillhole has been completed.

An investigation of the trace element content and behaviour of *in situ* laterite and bauxite profiles in the Darling Range area (Perth and Pinjarra 1 : 250 000 Sheets) has commenced.

Environmental Geology (E. R. Biggs, R. H. Archer)

A study was initiated into the usage and availability of clays (for bricks, tiles and pipes) close to the Perth Metropolitan area. Examination of geological and company data was completed and preliminary field work commenced.

Nearly 200 applications for mineral tenements were processed to detemine if any conditions should be imposed to protect the environment.

Where applicable, exploration or exploitation conditions were recommended to the Principal Registrar, following field visits where necessary.

A system of recording geological data exposed in temporary excavations in the Metropolitan area is currently under trial with the objective of improving geological knowledge of the urban area.

A substantial proportion of the section's activities provided information for and liaison with other Departments and the public on topics such as the geology of possible waste disposal sites (acid effluent, arsenical waste), soil erosion, stream and dam salinity, mining in dunes or beaches and dredging in estuaries. Various committee meetings were attended on these and similar topics.

Technical Information (K. H. Green, M. M. Harley, M. E. Wenham, S. M. Fawcett)

This section's function of distributing geological information to the general public and internally was well patronised during the year. Twenty seven Records were edited and issued, and seven Explanatory Notes published. Three information pamphlets are currently in press, and a pamphlet detailing the Museum's rock and mineral collection was issued.

Requisitions raised on the Surveys and Mapping Branch for drafting services and photography for the Survey totalled 1 087. Photocopying for the public of out-of-date publications numbered 800 requisitions; many of these contained several items.

During the year 1 861 members of the public visited the library for research purposes. Book loans to the staff totalled 4 254, and loans to other libraries 264.

An automatic Reader-Printer (Kodak Model MPG-TL) has been installed as a further development of our microfilm library. All company reports and plans are being photographed on 35 mm film and placed in cassettes. When completed, this will form a valuable reference for information as the reports are released to the public.

ACTIVITIES OF THE COMMONWEALTH BUREAU OF MINERAL RESOURCES.

Geological and geophysical projects carried out by the Bureau of Mineral Resources in Western Australia included the following:

(i) Compilation of bulletins on the Kimberley Division as a joint project with the Survey, whose portion has been completed for some years.

(ii) Preparation of a bulletin and completion of compilation of geological mapping on the Officer Basin as a joint project with the Survey.

(iii) Continuation of mapping in the Canning Basin as a joint project with the Survey.

The aeromagnetic survey of the Officer Basin was not commenced as programmed, and was once again deferred for a year.

PROGRAMME FOR 1975

HYDROGEOLOGY AND ENGINEERING DIVISION

A. Hydrogeology

1. Continuation of the hydrogeological survey of the Perth Basin, including deep drilling.
2. Hydrogeological investigations and/or exploratory drilling for groundwater in the following areas:
   (a) Millstream, Weelamurra Creek, George River and Lower Harding River.
   (b) West Canning Basin.
   (c) Murchison and East Murchison—regional assessments.
3. Town water supply investigations for the following: Albany, Port Hedland, Esperance, Geraldton.
4. Hydrogeological investigations for Metropolitan Water Supply Board:
   (a) Regional studies.
   (b) Deep drilling at Wanneroo and Whitfords.
   (c) Shallow drilling at Salvado, Wanneroo, Gwelup, Yanchep, Joondalup and Lake Thompson.
5. Kimberley Division—hydrogeological assistance to pastoralists as required.
6. Continuation of bore census of selected areas.
7. Inter-departmental studies concerning groundwater salinity problems in the Darling Range area.
8. Miscellaneous investigations and inspections as requested by Government Departments and the public.

B. Engineering

1. Pilbara area—further investigations at the following dam sites: Dogger Gorge, Gregory Gorge, Kangan Pool, Robe River—complete reports on Bullinarwa Pool dam site.
2. Darling Range area—continuation of field work or completion of reports and plans at the following dam sites: Wungong, South Canning, North Dandalup, South Dandalup, completion of report on Wungong tunnel.
3. Beenyup outfall tunnel (Mullaloo).
4. Miscellaneous investigations as requested by Government departments.

SEDIMENTARY (OIL) DIVISION

1. Maintain an active interest in the progress and assessment of oil exploration in Western Australia.
2. Completion of the bulletin on the Perth Basin.
3. Mapping the following map sheets of the Canning Basin in conjunction with the Bureau of Mineral Resources: Tabletop, Ural, Wilson, Runton, Morris, Ryan, Rudall, Percival and Sahara.
4. Commence surface and sub-surface study of the Carnarvon Basin, including Onslow, Yanrey, and Ningaloo 1 : 250 000 Sheets.

REGIONAL GEOLOGIAL DIVISION

1. Continuation of mapping of the Bangemall Basin and adjacent areas including the Robinson Range, Buller, Nabberu, Rudall, Runton and Tabletop 1 : 250 000 Sheets.

2. Continuation of mapping on the Southern Cross 1 : 250 000 Sheet.

3. Mapping of the pre-Bangemall rocks of the Kingston 1 : 250 000 Sheet.

4. Completion of the re-assessment of the regional geology of the Eastern Goldfields.

MINERAL RESOURCES DIVISION

1. Maintain records and assess mineral exploration in Western Australia.

2. Completion of mineral resources bulletins on tin, copper, vanadium, chromium, tungsten, and molybdenum deposits of Western Australia.

3. Remapping of the Port Hedland 1 : 250 000 Sheet and commence re-assessment of the regional and economic geology of the Pilbara Block.

4. Continuation of regional mapping of the Darling Range on the Pinjarra, Collie and Moora 1 : 250 000 Sheets and study of the bauxite occurrences.

5. Mapping of the Precambrian of the Yanrey 1 : 250 000 Sheet and examination of copper occurrences in the Ashburton area.

The various specialist groups in the Common Services Division will provide support wherever required.

PUBLICATIONS AND RECORDS

Issued during 1974

Annual Report, 1973.

Bulletin 123: The geology of the Blackstone Region, Western Australia.

Geological map 1 : 2 500 000 Western Australia.

Geological map of Balladonia 1 : 250 000 Sheet (SI/51-3 International Grid) with explanatory notes.

Geological map of Bentley 1 : 250 000 Sheet (SG/52-5 International Grid) with explanatory notes.

Geological map of Cue 1 : 250 000 Sheet (SG/50-15 International Grid) with explanatory notes.

Geological map of Esperance-Mondrain Island 1 : 250 000 Sheet (SH/51-6 and 10 International Grid) with explanatory notes.

Geological map of Norseman 1 : 250 000 Sheet (SI/51-2 International Grid) with explanatory notes.

Geological map of Yampi 1 : 250 000 Sheet (SE/51-3 International Grid) with explanatory notes.

Geological map of Zanthus 1 : 250 000 Sheet (SH/51-15 International Grid) with explanatory notes.

In Press

Memoir No. 2: The geology of Western Australia.

Information Pamphlets; 2nd Edition: Tin, Copper. Precious and Semiprecious stones.

Geological map of Edjudina 1 : 250 000 Sheet (SH/51-6 International Grid) with explanatory notes.

Geological may of Dongara-Hill River 1 : 250 000 Sheet (SH/50-5 and 9 International Grid) with explanatory notes.

Geological map of Herbert 1 : 250 000 Sheet (SG/51-7 International Grid) with explanatory notes.

Geological map of Lake Johnston 1 : 250 000 Sheet (SI/51-1 International Grid) with explanatory notes.

Geological map of Mason 1 : 250 00 Sheet (SH/52-6 International Grid) with explanatory notes.

Geological map of Murgoo 1 : 250 000 Sheet (SH/50-14 International Grid) with explanatory notes.

Geological map of Plumridge 1 : 250 000 Sheet (SH/51-8 International Grid) with explanatory notes.

Geological map of Ravensthorpe 1 : 250 000 Sheet (SI/51-5 International Grid) with explanatory notes.

Geological map of Seemore 1 : 250 000 Sheet (SH/51-12 International Grid) with explanatory notes.

Geological map of Yalgoo 1 : 250 000 Sheet (SH/50-2 International Grid) with explanatory notes.

Reprints

Geological map of Mount Bruce 1 : 250 000 Sheet (SF/50-11 International Grid).

Geological map of Yarraloola 1 : 250 000 Sheet (SF/50-6 International Grid).

In Preparation

Bulletin 124: The geology of the Perth Basin.

Bulletin 125: The geology of the Eastern Goldfields.

Mineral Resources Bulletins: Tin, Heavy mineral sands, Copper.

Geological maps 1 : 250 000 with explanatory notes, the field work having been completed: Billiluna, Browne, Cobb, Cundeelee, Duketon, Laverton, Lennis, Leonora, Lucas, Madley, Marble Bar, Minigwal, Mount Bannerman, Mount Egerton, Neale, Nullagine, Paterson Range, Perth, Rason, Robert, Sir Samuel, Stansmore, Throssell, Vernon, Waigen, Wanna, Warri, Westwood, Yarrie, Yowalga.

Geological map 1 : 1 000 000 Kalgoorlie.

Geological map 1 : 1 000 000 Esperance.

Records Produced

1972/25 vol. 2. The geology of the proposed North Pole dam site, Shaw River, by J. M. Campbell (restricted).

1974/1 Dolerite geochemical study, Northampton district, W.A., by A. A. Gibson.

1974/2 Wells drilled for petroleum exploration in W.A. to the end of 1973, by G. H. Low.

1974/3 Lower Wungong proposed dam site—rock quarry site 2 km upstream (Site No. 2), by G. Marcos (restricted).

1974/4 Explanatory notes on the Cobb 1 : 250 000 geological sheet, W.A., by W. J. E. van de Graaff.

1974/5 Explanatory notes on the Vernon 1 : 250 000 geological sheet, W.A., by W. J. E. van de Graaff.

1974/6 West Canning Basin hydrology: investigation geophysics, 1973 progress report, by D. L. Rowston (restricted).

1074/7 Burekup proposed dam site—seismic refraction survey, by I. R. Nowak (restricted).

1974/8 Explanatory notes on the Leonora 1 : 250 000 geological sheet, by R. Thom and R. G. Barnes.

1974/9 Explanatory notes on the Neale 1 : 250 000 geological sheet, W.A., by W. J. E. van de Graff and J. A. Bunting.

1974/10 Robe River dam site "D"—geological reconnaissance, by R. P. Mather (restricted).

1974/11 Explanatory notes on the Plumridge 1 : 250 000 geological sheet, W.A., by W. J. E. van de Graaff and J. A. Bunting.

1974/12 Explanatory notes on the Cundeelee 1 : 250 000 geological sheet, W.A., by J. A. Bunting and W. J. E. van de Graaff.

1974/13 Lower Wungong proposed dam site, rock quarry site No. 1 (6 km upstream): geological investigation, by G. Marcos (restricted).

1974/14 Lower Wungong proposed dam site: construction area geological conditions, by G. Marcos (restricted).

1974/15 Explanatory notes on the Archaean rocks of the Perth 1 : 250 000 geological sheet, W.A., by S. A. Wilde.

1974/16 Devonian brachiopods from the reef complexes of the Canning Basin, by K. Grey.

1974/17 Explanatory notes on the Minigwal 1 : 250 000 geological sheet, W.A., by J. A. Bunting and J.-C. Boegli.

1974/18 West Canning Basin groundwater investigations: progress report, March, 1974, by R. E. J. Leech (restricted).

1974/19 Kangan Pool dam site, Sherlock River: seismic refraction survey, by D. L. Rowston (restricted).

1974/20 Explanatory notes on the Marble Bar 1 : 250 000 geological sheet, W.A., by A. H. Hickman and S. L. Lipple.

1974/21 Burekup proposed dam site, Collie River: geological investigation progress report, by G. Klenowski (restricted).

1974/22 Dogger Gorge proposed dam site: seismic refraction survey, by I. R. Nowak (restricted).

1974/23 The hydrogeology of the Watheroo-Jurien Bay line, Perth Basin, by A. S. Harley.

1974/24 Lime resources between Lancelin and Mandurah, W.A., by J. L. Baxter and J. P. Rexilius.

1974/25 Heavy mineral reserves in Western Australia, March, 1973, by J. L. Baxter (confidential).

Reports in other publications

Trendall, A. F., 1974, Time, Life and Iron: West Australia Institute of Technology, Gazette v. 7, no. 2, p. 10-13.

1st February, 1975.

J. H. LORD,
Director.

HYDROGEOLOGY OF THE DE GREY RIVER AREA

by W. A. Davidson

ABSTRACT

The De Grey River groundwater investigation comprised part of the search for supplies for Port Hedland. It included a bore census, exploratory drilling, geophysics, and test-pumping of alluvial sediments along the De Grey, Strelley and Shaw Rivers. Test-pumping showed that 2 000 m^3/day should be obtainable.

The volume of groundwater in storage was estimated to be 82 x 10^6 m^3. As much as 40 per cent of this quantity has a salinity of 1 000-2 000 ppm TDS and the remainder, which falls in the potable range (300-1 000 ppm TDS), includes the annual recharge over 170 km^2. These estimates are based on an assumed storage co-efficient of 0.1.

Without drawing on storage and neglecting the effects of increased river recharge and reduced transpiration losses, 7 600 m^3/day of potable water should be obtainable from the aquifer. Under prolonged pumping this estimate could be conservative.

INTRODUCTION.

The rapidly increasing demand for water, as a result of population growth and industrial development in Port Hedland, has made it necessary to find additional reserves of groundwater.

To identify areas having groundwater possibilities a pastoral property bore and well census was made during 1969. As a result the De Grey River system and its associated alluvium was chosen for a more intensive investigation between 1969 and 1972.

The aim was to find a groundwater source capable of producing more that 30 000 m^3 per day of groundwater with a salinity of less than 1 000 ppm of Total Dissolved Solids (TDS). These minimal requirements were set by the Public Works Department.

The De Grey River system is at the northern edge of the Pilbara Block, and the area investigated is approximately 100 km east of Port Hedland (Fig. 3, inset).

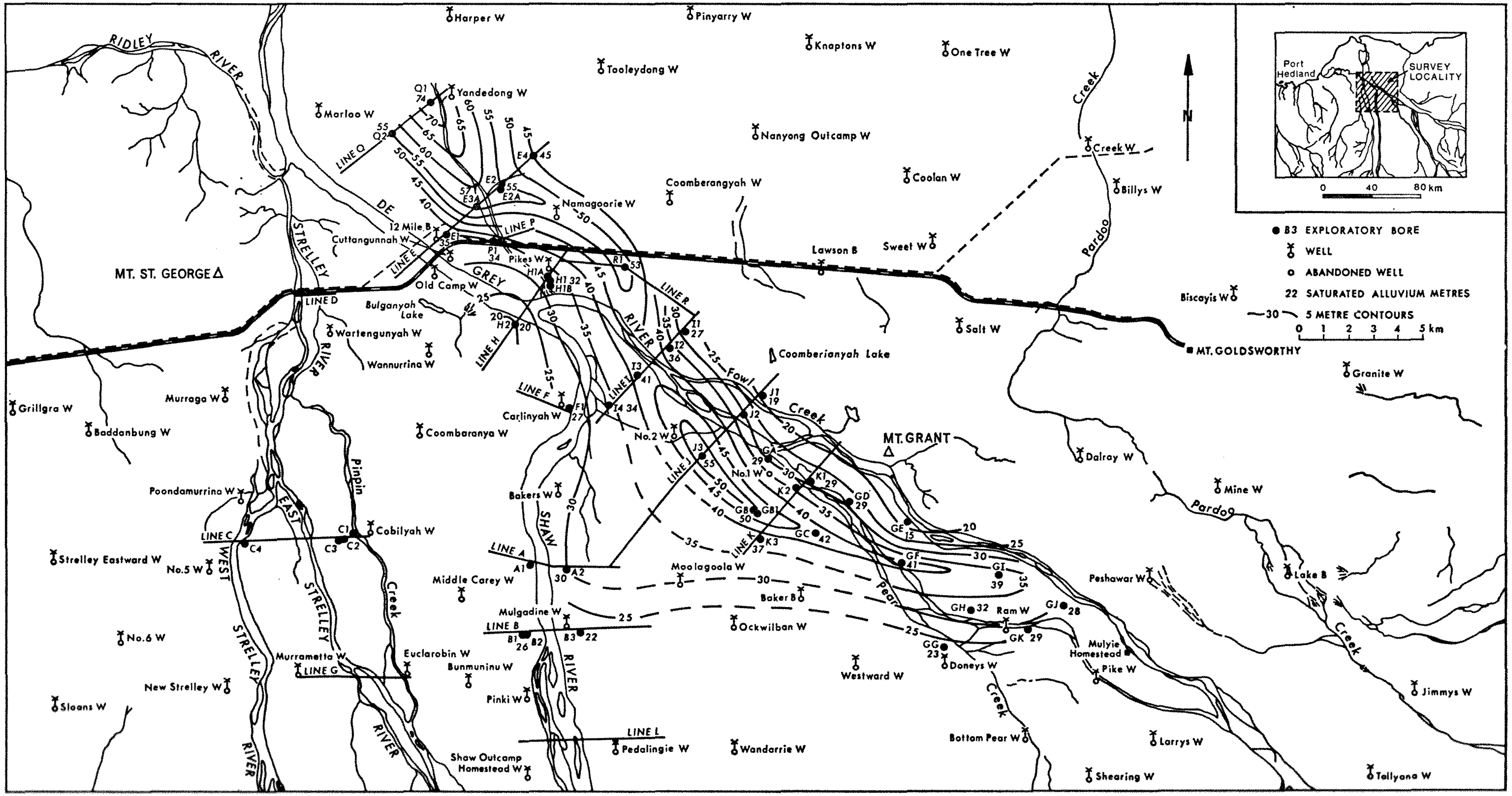

14150

Figure 3. De Grey River groundwater—isopachs of saturated alluvium in metres for 23/8/72.

Investigations.

Forty nine bores were drilled through the alluvium to weathered and sometimes fresh bedrock. Depths ranged between 18 m and 119 m and the aggregate depth was 2 972 m. Details of the boreholes are given in Table 1.

The bores were sited by geophysical methods (seismic refraction and resistivity profiling) in an attempt to delineate ancient buried river channels.

The seismic lines, boreheads, wells and river pools were accurately levelled and related to standard mean sea level datum.

TABLE 1. BOREHOLE DETAILS OF THE DE GREY RIVER AREA

Bore	Commenced	Completed	Reduced levels		Total depth m	Casing		Screens		Developed by surging (hours)	Drilling method
			Casing m	NS m		Length m	Diam. OD mm	Interval m	Diam. OD mm		
A1	24/8/69	2/9/69	34·49	33·83	48·8	28·7	76	4·6–28·7	76	....	Cable tool
A2	7/11/70	20/11/70	36·99	36·39	42·7	27·4	203	27·4–42·1	178	36	Cable tool
B1	2/10/69	6/10/69	38·92	38·15	47·2	47·2	76	3·1–47·2	76	....	Cable tool
B2	7/10/69	28/10/69	38·85	38·24	52·4	44·9	152	open hole		....	Cable tool
B3	28/10/69	8/11/69	39·08	38·28	37·5	35·1	76	35·1–37·5	76	....	Cable tool
C1	4/9/69	29/9/69	30·45	29·92	23·5	23·5	76	3·1–23·5	76	....	Cable tool
C2	7/9/69	10/9/69	31·78	31·08	23·8	23·8	76	3·7–23·8	76	....	Cable tool
C3	10/9/69	10/12/69	31·30	30·89	55·5	38·2	152	open hole		....	Cable tool
C4	30/9/69	1/10/69	33·91	33·11	18·3	18·3	76	4·6–18·3	76	....	Cable tool
E1	11/11/69	4/12/69	23·25	22·34	118·9	39·6	76	4·6–39·6	76	....	Cable tool
E2	24/4/70	24/5/70	24·21	23·34	112·8	61·0	76	15·2–61·0	76	....	Cable tool
E2A	22/10/70	29/11/70	23·73	23·29	54·6	17·8	203	17·8–54·4	178	84	Cable tool
E3	22/6/71	10/8/71	23·80	23·80	59·4	24·7	305	24·7–59·1	152	70	Cable tool and Rotary
E3A	5/7/71	29/7/71	24·04	23·81	91·4	24·4	76	24·4–59·7	76	Air lifted	Cable tool
E3B	11/8/71	19/8/71	23·87	23·35	59·4	59·4	101	8·2–59·4	101	Air lifted	Rotary
E4	20/8/71	13/9/71	21·56	20·93	105·4	21·3	76	21·3–51·8	76	Air lifted	Rotary
E4A	4/10/71	13/10/71	20·99	20·88	51·8	24·1	305	24·1–51·8	152	40	Rotary
E4B	14/9/71	1/10/71	21·66	20·90	51·8	21·3	76	21·3–51·8	76	Air lifted	Rotary
F1	27/10/70	5/11/70	31·05	30·58	44·2	11·0	203	11·0–29·3	178	48	Cable tool
H1	27/5/70	4/6/70	27·55	26·93	93·0	93·0	76	11·6–93·0	76	....	Cable tool
H1A	30/9/70	23/11/70	27·33	26·77	51·8	7·8	203	7·8–21·6	178	48	Cable tool
H1B	7/10/70	....	27·35	26·88	79·3	58·6	203	58·6–80·0	178	24	Cable tool
H2	8/7/70	16/7/70	27·40	26·44	48·2	48·2	76	12·2–48·2	76	....	Cable tool
I1	5/6/70	10/6/70	28·65	27·66	53·0	53·0	76	18·3–30·5	76	....	Cable tool
I2	11/6/70	21/6/70	29·96	28·98	77·4	77·4	76	15·2–42·7	76	....	Cable tool
I3	10/7/70	18/7/70	31·01	29·72	82·3	79·3	76	9·1–79·3	76	....	Cable tool
I4	14/10/70	24/11/70	29·09	28·17	70·1	17·9	203	17·9–40·5	178	24	Cable tool
J1	22/6/70	29/6/70	33·56	32·39	42·7	42·2	76	12·2–27·4	76	....	Cable tool
J2	30/6/70	7/7/70	33·55	32·03	58·8	51·8	76	21·3–33·5	76	....	Cable tool
J3	24/8/71	13/9/71	31·74	31·45	78·3	25·6	319	25·6–63·1	152	16	Cable tool
K1	31/7/70	4/8/70	34·04	33·14	36·0	35·1	76	9·1–35·1	76	....	Cable tool
K2	23/7/70	30/7/70	33·08	32·16	40·2	40·2	114	9·1–40·2	114	....	Cable tool
K3	2/8/71	21/8/71	36·30	36·07	103·0	25·3	273	25·3–95·4	Casing 152	20	Cable tool
P1	5/11/70	15/11/70	24·55	24·01	45·7	17·8	203	17·8–36·7	178	48	Cable tool
Q1	14/10/71	3/11/71	20·56	20·41	108·8	22·3	305	22·3–54·3	152	35	Rotary
Q2	3/11/71	25/11/71	18·30	18·41	100·9	22·9	305	22·9–95·4	152	70	Rotary
R1	16/9/71	14/10/71	25·84	25·39	94·5	28·7	319	28·7–62·5	152	14	Cable tool
GA	19/6/70	22/8/70	32·51	32·14	36·3	16·1	203	16·1–35·4	178	60	Cable tool
GB	18/7/70	7/8/70	35·51	35·14	106·7	59·5	203	59·5–105·2	178	72	Cable tool
GB1	8/8/70	17/8/70	35·51	35·29	47·2	22·7	203	22·7–46·2	178	60	Cable tool
GC	22/8/70	8/9/70	35·44	35·04	70·1	17·4	203	17·4–45·1	178	48	Cable tool
GD	6/8/70	15/8/70	35·31	34·80	36·0	12·0	203	12·0–36·1	178	48	Cable tool
GE	18/8/70	27/8/70	38·22	37·60	31·7	12·1	203	12·1–30·5	178	24	Cable tool
GF	28/8/70	7/9/70	37·62	37·37	50·3	22·3	203	22·3–41·8	178	36	Cable tool
GG	8/9/70	17/10/70	40·05	39·71	45·1	23·2	203	23·2–43·9	178	36	Cable tool
GH	19/9/70	4/11/70	40·66	40·28	40·5	16·1	203	16·1–39·6	178	36	Cable tool
GI	9/9/70	....	39·34	38·97	56·4	18·2	203	18·2–48·2	178	48	Cable tool
GJ	23/9/70	29/9/70	41·84	41·20	43·9	17·9	203	17·9–41·6	178	24	Cable tool
GK	21/9/70	....	42·44	42·04	44·5	11·9	203	11·9–43·0	178	60	Cable tool

TABLE 2. STRATIGRAPHIC UNITS OF THE PORT HEDLAND 1 : 250 000 GEOLOGICAL SHEET

Age	Map Symbol	Name of Unit	Lithology	Occurrence	Topography	Economic Geology
Quaternary	Qr	....	Alluvial clay, silt, sand, gravel and conglomerate	In some areas adjacent to major drainages the alluvium is up to 82 m thick	Valley floors, flats and river systems	Water
Tertiary	Tk	....	Pisolitic ironstone and kankar	Areas along Strelley River	Limited exposures on edge of some drainage channels. Isolated, small, flat-topped hills	Water—some station wells
	To	Oakover Formation	Siltstone, limestone and chalcedony	Areas along Strelley River		
	M	Anketell Sandstone	Sandstone, shale and claystone	Bore E1 proved a thickness greater than 76 m	Hill capping, small mesas and buttes	Water—some station wells
Jurassic-Triassic	M	Callawa Formation	Current-bedded, coarse sandstone and conglomerates	Possibly intersected in bores E2, E3A, E4, H1, H2, I1, I2, I3, I4, P1, Q1, Q2, and R1	Hill capping, small mesas and buttes	Water—some station wells
			ANGULAR UNCONFORMITY			
Archaean	q	....	Quartz reefs and blows	Many of the bores	Ridges or elongated hills	Water
	d	....	Quartz dolerite dykes	H2 and possibly I2, I4 and GB		Road metal
	Agr	....	Granite, granite gneiss	Many bores	Scattered outcrops and low level sand-covered plains	Ballast for railways
	Agn	....	Partly granitized Archaean			Water
			STRONG FOLDING AND GRANITE INTRUSION			
	Ai	Gorge Creek Formation	Argillite, quartz and conglomerate with iron-bearing formations and volcanics	Many of the bores	Dissected ranges and hills	Iron ore and manganese
	Aw	Warrawoona 'series'	Basic volcanic pillow lavas, serpentines, coarse-grained basic intrusives, conglomerate sandstone, shale, jaspilite and associated schistose rocks		Dissected ranges and hills	Iron ore

GEOLOGY

The lowermost sediments of the De Grey valley are Coongan and Shaw alluvium, overlain by Oakover and Nullagine River sediments deposited after river capture. The uppermost sediments consist of recent alluvium from all four rivers. This sequence of sediments rests on a basement floor consisting of granite, volcanics and indurated sediments of the Gorge Creek Formation, all of Archaean age.

The regional geology is shown on the Port Hedland 1 : 250 000 Geological Sheet and described by Low (1965). Table 2 illustrates the stratigraphic units.

HYROGEOLOGY

The six different aquifers that have been recognized are considered in order of increasing storage potential.

Granite. Many of the bores terminated in weathered to fresh granite, which yielded small supplies. For example bore grant B was pumped at 1 156 m^3/day for 48 hours with a drawdown of 10 m.

Drilling samples from bore A1 show exfoliation of the granite basement. Immediately below the exfoliation plates there is a build up of water-bearing clean quartz sand. This weathering profile is thought not to be very extensive and can be regarded only as a source of windmill-water for stock.

There are two types of weathered granitic material, one is a series of exfoliated plates, and the other is probably colluvial in origin. The colluvial granitic material seems to be the better aquifer because useful thicknesses can be expected (e.g. K3, 45-94.5 m).

Volcanics and Gorge Creek Formation. Several bores ended in volcanic rocks, and two were tested by pumping; e.g. H1A was pumped at 785 m^3/day for 7½ hours with about 7 m of drawdown.

Although the rocks do not have a large potential, Goldsworthy Mining Ltd. reported pumping "large volumes" of water from their open cut, presumably from joints and fractures in the cherts of the iron formation.

Mesozoic sediments. Fourteen of the exploratory bores penetrated sediments of possible Mesozoic age; most of the samples were very rich in clay and silt. Borehole E1, which terminated in a grey shale, possibly belonging to the Anketell Sandstone, had a very low yield. Others could be better, such as R1, which ended in quartz sand (possibly Callawa Formation), but was not tested.

In borehole cuttings weathered Mesozoic sandy siltstone is similar to the sandy siltstone of the Archaean Gorge Creek Formation. Gamma-ray logging has shown that the sediments at 35.5 m depth in borehole I1 have the same radiation pattern as the sediments in I2 at 45 m and I3 at 50 m. Bores I1, I2 and I3 may have terminated in either Mesozoic or Archaean sediments.

Kankar. Their are two sets of geological conditions under which the kankar has developed.

The water table kankar is the more important, and is usually the source of stock and domestic water supplies. Essentially it is a calcareous, weakly cemented alluvium about 1 m-thick and therefore not a large individual producer of water.

The kankar which develops at the top of the granite weathering profile can be quite thick, e.g. 45-62 m in bore K3. It appears to be *in situ* and is probably a product of a chemically weathered basement.

Alluvium. The aquifers in the river alluvium range in thickness from a few metres to about 75 metres, and may be roughly grouped into an upper and lower unit. This division is fairly arbitrary along the De Grey River, where there is often a hydraulic connection between the two.

The upper sand or water table aquifers usually have coarse-grained sand and gravel at the water table and sometimes a thin kankar horizon. The water in these sands may be fully confined, as in bore B2, but this is not commonly so.

The lower sands vary in thickness and permeability and are sometimes separated from the upper sands by silty clay. They occur as thin beds and lenses, so that through 75 m several sandy beds may be intersected. Occasionally a thick gravel bed is present.

The lower sand aquifers associated with the De Grey River are more extensive and also less clayey than those of the Shaw and Strelley Rivers.

Alluvial Trough

The present course of the De Grey River no longer coincides with the axis of the alluvial filled trough (Fig. 3). In its downstream part the river has migrated several kilometres southwestward, although farther up-stream it has moved to the northeast. The positions roughly coincide between cross-section lines H and I.

HYDROCHEMISTRY

There is a wide range of salinities, the better quality water generally occurring close to the present river course.

Throughout the area the salinity of the groundwater is suitable for stock consumption, and beneath nearly half of the area it is suitable for domestic use.

The isohaline map (Fig. 4) shows the regional groundwater salinity pattern and reflects the presence of the buried river channel downstream from near bore H1. Drilling has shown that the aquifer in this area has a comparatively high permeability.

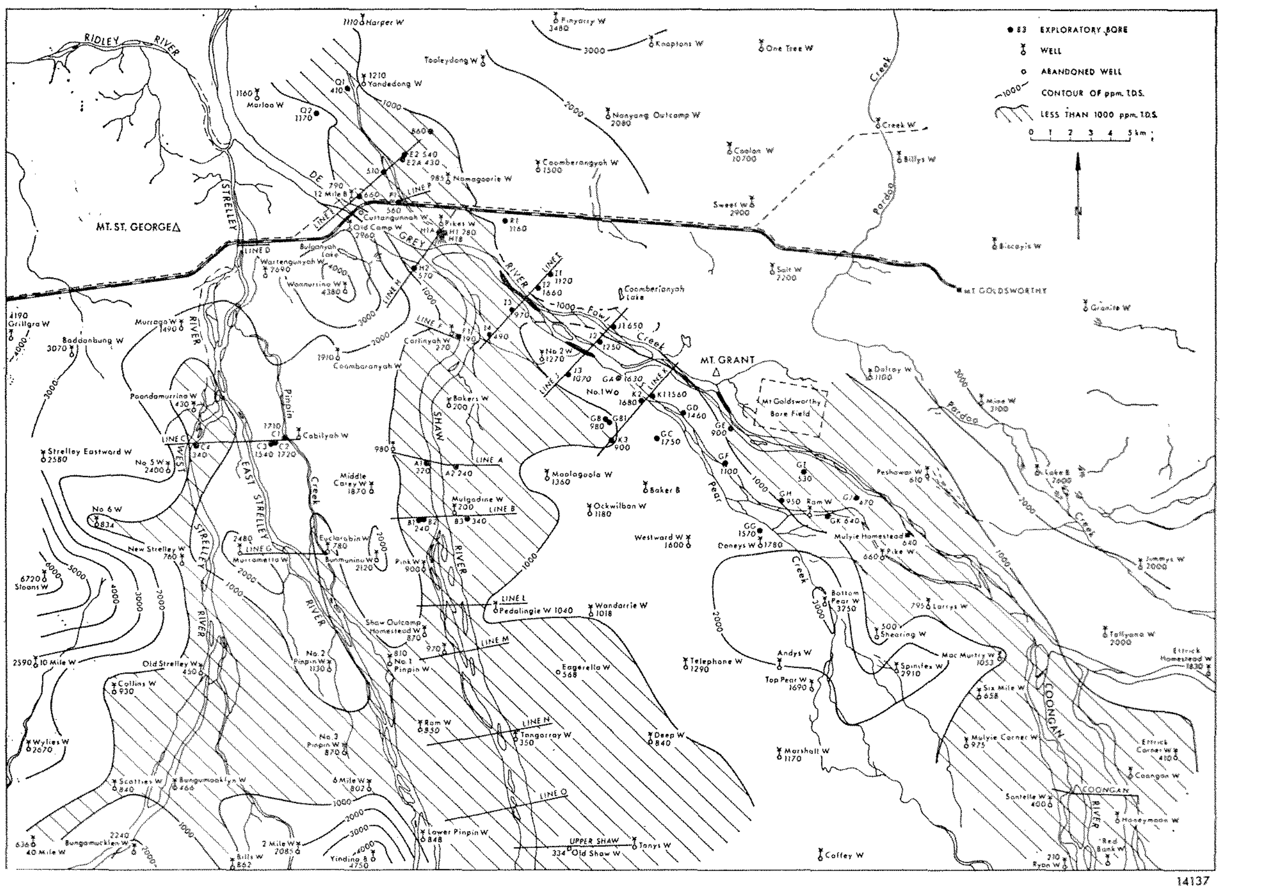

Figure 4. De Grey River groundwater—hydrochemistry and isohalines in ppm TDS.

PUMPING TESTS

Twenty-seven bores were tested for periods of up to 48 hours.

Because of the heterogeneous nature of the aquifer, and because both confined and unconfined conditions could occur at each site, leaky artesian, delayed yield, water table and boundary conditions were likely to be experienced in any one test. Most of the bores were pumped without observation bores and many were only partially penetrating.

Time-drawdown curves plotted from pumping-test data proved very difficult to analyse. A summary of results is shown in Table 3.

GROUNDWATER MOVEMENT

The direction of groundwater movement, along flow lines, is perpendicular to the poteniometric contours indicated on the flow net diagram (Fig. 5). The flow channels are defined by flow lines passing through points of origin distributed along the 18 metre poteniometric contour at equal intervals.

TABLE 3. DE GREY RIVER PROJECT PUMPING-TEST DATA

Bore	Screened Interval m	Pumping-Test			Transmissivity		Hydraulic Conductivity	
		Duration Hours	Rate m^3/d	Total Drawdown m	T $m^3/d/m$	Method	Saturated Alluvium m	K $m^3/d/m^2$
A2	27·4-42·1	1·5	200	13·41	15	Specific capacity	29·8	0·5
B3	28·0-35·1	8	349	10·13	30	Specific capacity	21·8	1·4
C3	Open Hole	0·9	273	20·91	Bore pumped on the fork			
E2A	17·8-54·4	48	2 400	2·13	1 400	Specific capacity	54·7 E2	25·6
E3	24·7-59·1	48	3 100	6·17	940	Part penetration	57·3 E3A	16·4
E4A	24·1-51·8	48	3 060	8·85	1 940	Theis curve	44·7 E4	43·4
F1	11·0-29·3	1	160		Bore pumped on the fork			
H1A	7·8-21·6	7·7	786	6·86	50·70	Delay	32·3 H1	2·2
H1B	58·6-80·0	Pumped Test Failed						
I4	17·9-40·5	48	1 266	4·72	220	Specific capacity	33·6	6·6
J3	25·6-63·1	48	4 580	8·53	500	Specific capacity	55·0	9·1
K3	25·3-95·4	48	2 620	7·77	200	Delay	36·7	5·4
Q1	22·3-54·3	48	3 900	8·38	510	Specific capacity	73·8	6·9
Q2	22·9-95·4	48	4 580	5·48	600	Specific capacity	54·9	10·9
R1	28·7-62·5	48	4 866	6·40	1 440	Const. D.D.	52·8	27·3
GA	16·1-35·4	48	1 593	4·12	370	Specific capacity	29·2	12·7
GB	59·5-105·2	48	1 156	9·91	58	Delayed yield	50·1	1·2
GB1	22·7-46·2	48	3 338	15·85	220	Theis curve	50·1 GB	4·4
GC	17·4-45·1	48	2 837	4·57	300	Delayed yeild	41·8	7·2
GD	12·0-36·1	48	1 440	2·29	300	Delayed yeild	28·8	10·4
GE	12·1-30·5	48	1 309	7·92	inadequate test		15·2	....
GF	22·3-41·8	48	1 527	2·44	280	Delayed yield	41·1	6·8
GG	23·2-43·9	0·7	854	20·12	50	Specific capacity	23·0	2·2
GH	16·1-39·6	48	2 837	6·10	200	Delayed yield	?32·4	6·2
GI	18·2-48·2	48	1 746	2·74	270	Delayed yield	38·5	7·0
GJ	17·9-41·6	40	1 811	18·29	60	Delayed yield	28·4	2·1
GK	11·9-43·0	48	2 837	2 ·90	Inadequate, not conclusive test		29·4	....

(2)—46009

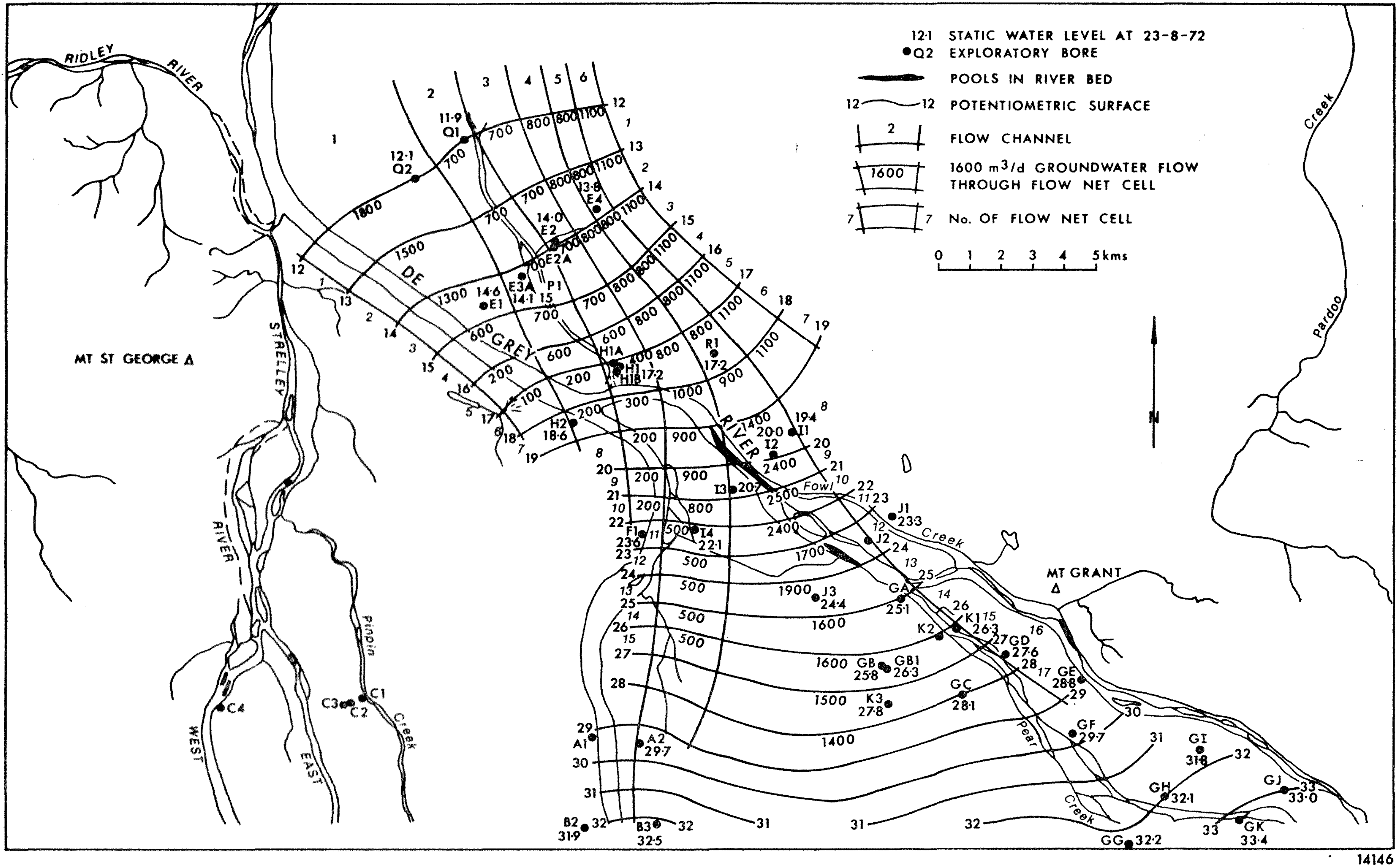

Figure 5. De Grey River groundwater—flow net for 23/8/72 potentiometric surface.

To evaluate the volume of water passing through individual cross-sectional areas defined by the flow net, the transmissivities, gradients and cross-section lengths, have to be determined. This volume can then be calculated by using the simple expression $Q = Til$.

Where Q = volume passing through section, m^3/d.

T = transmissivity, $m^3/d/m$.

i = gradient, dimensionless.

l = cross-section length, m.

The hydraulic gradient and cross section lengths may be directly measured from the flow net but the transmissivity for each section has to be estimated from the distribution of values derived by test pumping. This estimate, together with the derived flow volumes, is only roughly correct because of the variability of these values.

The flow net has six flow channels. In channel 1 there is a large net groundwater gain from the De Grey River. Along channel 2 there is a large net gain from the De Grey-Shaw River junction, with no gain or loss throughout the rest of the flow channel. Along channel 3 there is a large net gain from the De Grey River near the Shaw River junction; the remainder of the flow channel showing no gains or losses. Channel 4 shows a small net gain from the Shaw and De Grey Rivers and also some net loss which is possibly a transpiration loss. Above the granitic basement between the De Grey and the Shaw Rivers, channel 5 shows a steady increase in groundwater volumes from both rainfall and De Grey River flow. The net loss where permanent pools occur in the De Grey River, on lines J and I, is due to evaporation and transpiration. The remainder of the flow channel shows no gains or losses. Channel 6 is probably in a state of balance, though this might not be so if the channel were extended along the De Grey past Mount Grant, where evaporation and transpiration losses would be large.

The quantity of groundwater moving through the area can be calcluated by adding the contributions made by each flow channel. For example at the northern end of the flow net system a total of 5 900 m^3 per day is moving through the section indicated by the 12 m potentiometric line (i.e. about 1.3 x 10^6 imperial gallons per day).

Recharge Systems

The recharge-discharge regime is shown diagrammatically on Figure 6, the relative importance of each element being shown by the numbers on the arrows.

Recharge comes from river flow and from direct rainfall percolation.

River flow recharge is the most important source of intake to the alluvium, even though the rivers flow only for short periods. Typically the De Grey may flow twice in one year and not at all in the next, which means that there are long periods during which discharge from the aquifers takes place.

Most of the rain falling directly on the riverbed sands soaks in, whereas a high percentage of the rainfall on the interfluvial areas is lost by evaporation. In areas not affected by river recharge, if all the chloride ion in the groundwater comes from directly percolating rainfall, then the chloride concentration in the groundwater is a measure of the proportion of rainwater which becomes recharged after evapotranspiration losses.

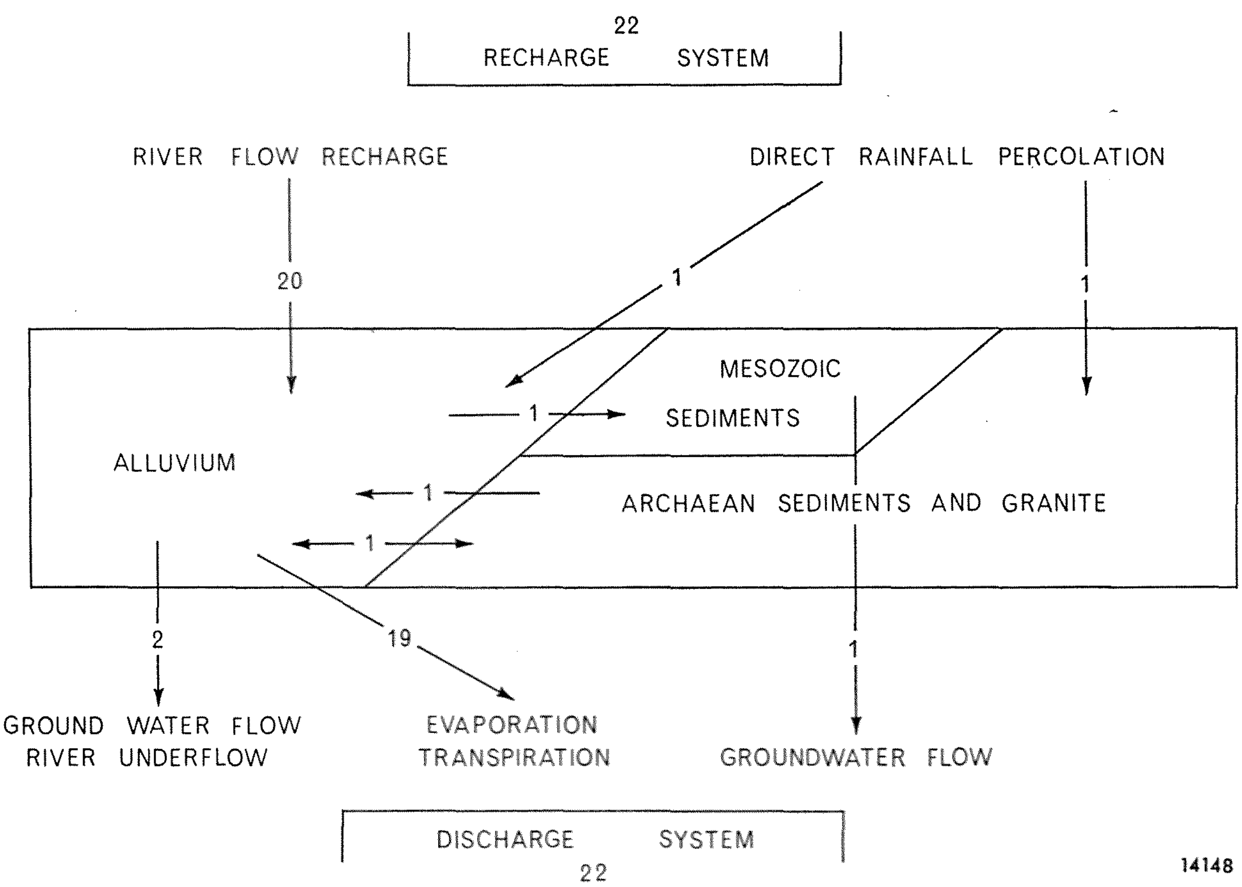

Figure 6. De Grey River groundwater—recharge-discharge regime.

There is about 8 ppm chloride in rainwater in this district, and it can be assumed that all the chloride in the groundwater in the areas listed in Table 4 comes from rainfall. It follows that about 3 per cent of the rainfall reaches the water table in an average rainfall year.

TABLE 4. RAINFALL RECHARGE BASED ON CHLORIDE CONCENTRATION.

Well bore	ppm chloride ground-water	ppm chloride rainfall	Distance from coast km	per cent rain recharged	per cent rain evapor-ated
J3	270	8	40	$\frac{8}{270}$ x 100 = 3	97
GB1	324	8	40	$\frac{8}{324}$ x 100 = 2	98
K3	225	8	40	$\frac{8}{225}$ x 100 = 4	96
Moolagoola	309	8	40	$\frac{8}{309}$ x 100 = 3	97
Ockwilban	210	8	40	$\frac{8}{210}$ x 100 = 4	96

The figure of 3 per cent can probably be applied to the whole area to derive the total volume of recharge from rainfall.

The area of interest, as shown by the flow net, is about 170 km² and the average annual rainfall is 275 mm.

$$\therefore \text{volume of infiltration} = 170 \text{ x } 1000^2 \text{ x } \frac{275}{1000} \text{ x } \frac{3}{100}$$

$$= 1\,400\,000 \text{ m}^3/\text{year.}$$

The average rise in water table, during recharging periods, is about 1 m per year. By assuming an average storage coefficient of 0.1 for the upper unconfined part of the aquifer, the total annual recharge to 170 km² of alluvium can be calculated.

$$\text{Total recharge} = 170 \text{ x } 1000^2 \text{ x } 1 \text{ x } 0.1$$

$$= 17\,000\,000 \text{ m}^3 \text{ per year}$$

If 1.4 x 10^6 m³ per year results from direct rainfall the remaining 15.6 x 10^6 m³ per year appears to come from river recharge. This means that only 8 per cent of the annual recharge of the groundwater in the alluvial flats is the result of direct downward infiltration of rain falling on the surface, the remaining 92 per cent being leakage from river flows.

Discharge Systems

The discharge components consist of transpiration, evaporation, groundwater flow and river underflow leaving the system.

From aerial photographs it has been estimated that approximately 11 x 10^6 m² of vegetation along river banks is contributing to transpiration. According to the Forestry Department a transpiration rate of 50 per cent pan evaporation could be applicable, and may even be conservative. If this premise is accepted, the amount of discharge through transpiration can be calculated as follows:

Annual pan evaporation = 2.5 m

Transpiration = 50 per cent evaporation
= 1.25 m

Area of vegetation = 11 000 000 m²

∴total volume water transpired per year

= 1.25 x 11 000 000

= 13 750 000 m³ per year

The amount of evaporation from surface water, such as pools in the De Grey River, has been calculated as follows:

Estimate of pool surface area = 250 000 m²

Surface evaporation per year (Bureau of Meteorology) = 2.5 m

∴volume evaporated = 250 000 x 2.5 per year

= 625 000 m³ per year

Groundwater and river underflow leaving the system was calculated by flow net analysis to be 5 900 m³ per day or approximately 2.2 x 10^6 m³ per year.

Groundwater Balance

Input m³/year		Losses m³/year	
Recharge from river	15 600 000	Transpiration	13 750 000
Rainfall	1 400 000	Pool evaporation	650 000
		Groundwater outflow	2 200 000
Total	17 000 000		16 575 000
		i.e. approx.	17 000 000

Groundwater Resources

When a relatively shallow aquifer is pumped for a long period of time the water levels fall, full drainage conditions are achieved, and the areas over which confined conditions occur are progressively eliminated. In this circumstance a specific yield of 0.1 or more is thought reasonable for use in calculating abstractable storage from a material that is predominantly sandy.

An isopach map (Fig. 3) was drawn of the saturated alluvium for 23/8/72 when the water table was very low. The amount of groundwater within the area shown by Figure 7 is the volume in storage, at a particular moment, and excludes the annual recharge from rain or river flow.

The area has been divided into three sub-regions, two containing groundwater of less than 1 000 ppm TDS, and the third exceeding 1 000 ppm TDS. Volumes were calculated using an assumed storage coefficient of 0.1. The volume of good quality water was found to be 37.9 x 10^6 m³, and of poor quality water 27.1 x 10^6 m³. Mixing the two gives 65 x 10^6 m³ of water in storage at minimum water table level. After average annual recharge the total water in storage would be 65 x 10^6 m³ + 17 x 10^6 m³ or 82 x 10^6 m³ of which about 17 x 10^6 m³ will be lost to transpiration, evaporation and groundwater outflow per year.

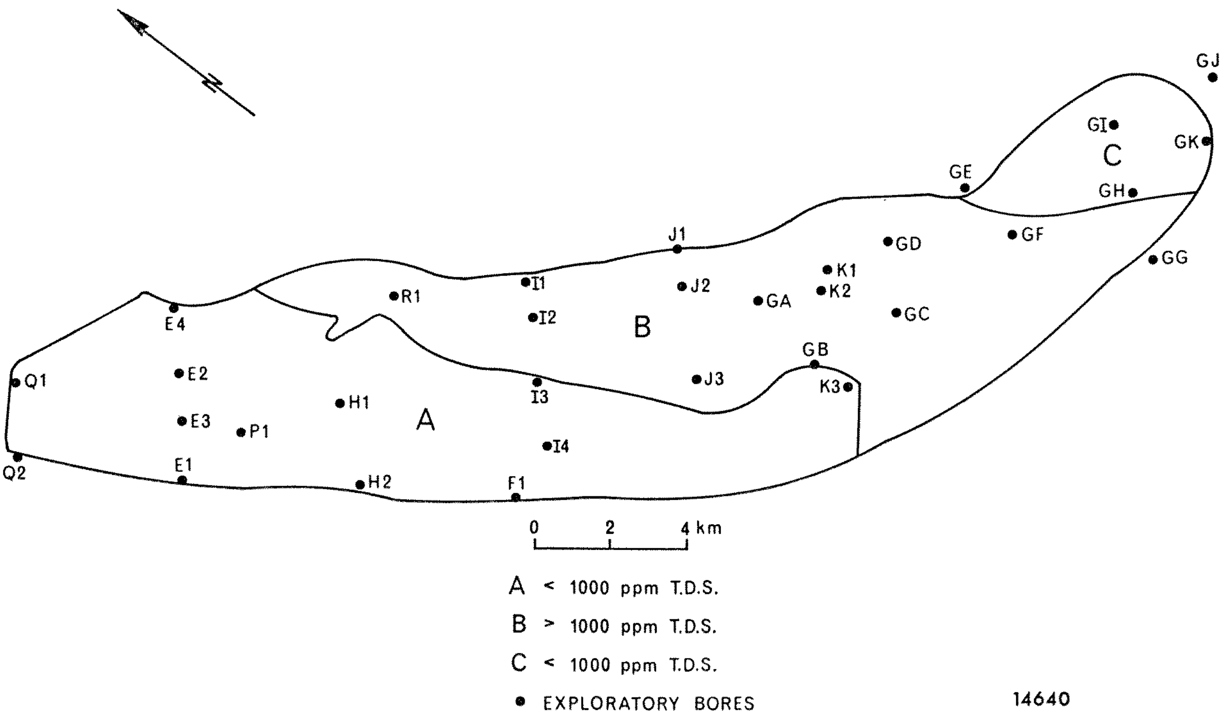

Figure 7. De Grey groundwater—salinity sub-regions.

Groundwater available for pumping

In summary, the volume of available groundwater is expressed by:

$$\begin{aligned} Q &= GF + IR + RT + E \\ &= 5\,900 \text{ m}^3 + IR + RT + 1\,700 \text{ m}^3 \\ &= 7\,600 \text{ m}^3 + RT \end{aligned}$$

Where Q = volume of groundwater available for pumping in m^3 per day.

GF = groundwater outflow in m^3 per day.

IR = portion of groundwater which is held in storage and which will be gained by induced additional recharge.

RT = the amount by which transpiratory loss is reduced by lowering the water table. This could be substantial.

E = the saving in evaporative loss when the water table is sufficiently lowered by pumping.

At present the safe yield of the aquifer is 7 600 m^3 per day, exclusive of any gain due to reduced transpiratory losses, and assuming that no additional recharge due to lowering of the water table takes place. It is not known what effect these other factors will have on the value of a new safe yield which might be arrived at after prolonged pumping, and a changed water balance. The effect could be assessed only by pumping at a rate in excess of 7 600 m^3/day and by monitoring the water levels and salinities.

REFERENCES

Davidson, W. A., 1973, De Grey Groundwater Investigation: West. Australia Geol. Survey Rec. 1973/27 (unpublished).

Low, G., 1965, Port Hedland, W.A.: West. Australia Geol. Survey 1:250 000 Geol. Series Explan. Notes.

EARTH TIDE INFLUENCE ON GROUND WATER LEVELS, HILL RIVER AREA, PERTH BASIN

by A. S. Harley

ABSTRACT

Hydrographs from two unconnected bores to the east of Jurien Bay, in the Perth Basin, show water level fluctuations in confined aquifers. The generally larger more random fluctuations can be attributed to atmospheric pressure changes. The smaller, periodic, semi-diurnal fluctuations correspond closely to fluctuations of lunar-solar origin in the earth's gravity field. The ocean tides have no discernable effect on the water levels. Only the water level in bore Watheroo Line 11 shows any obvious response to rainfall. Similar fluctuations due to earth tides are noted in other bores in Western Australia.

INTRODUCTION

Bores on the Watheroo Line, W.L. 11 and W.L. 12A, are on the western end of a line of deep bores drilled by the Geological Survey along the 30° 19′ S latitude between Watheroo and Jurien Bay. Bore W.L. 11 penetrated interbedded sandstones and mudstones of the Cockleshell Gully Formation, and bore W.L. 12A intersected the Lesueur Sandstone. Regionally the geology is complicated by a series of faults (Fig. 8).

Both bores are screened in confined aquifers but, as the bores were exploratory, the extent of the aquifers and the intake areas are unknown. When formation testing was completed, water level recorders were set up on the two bores.

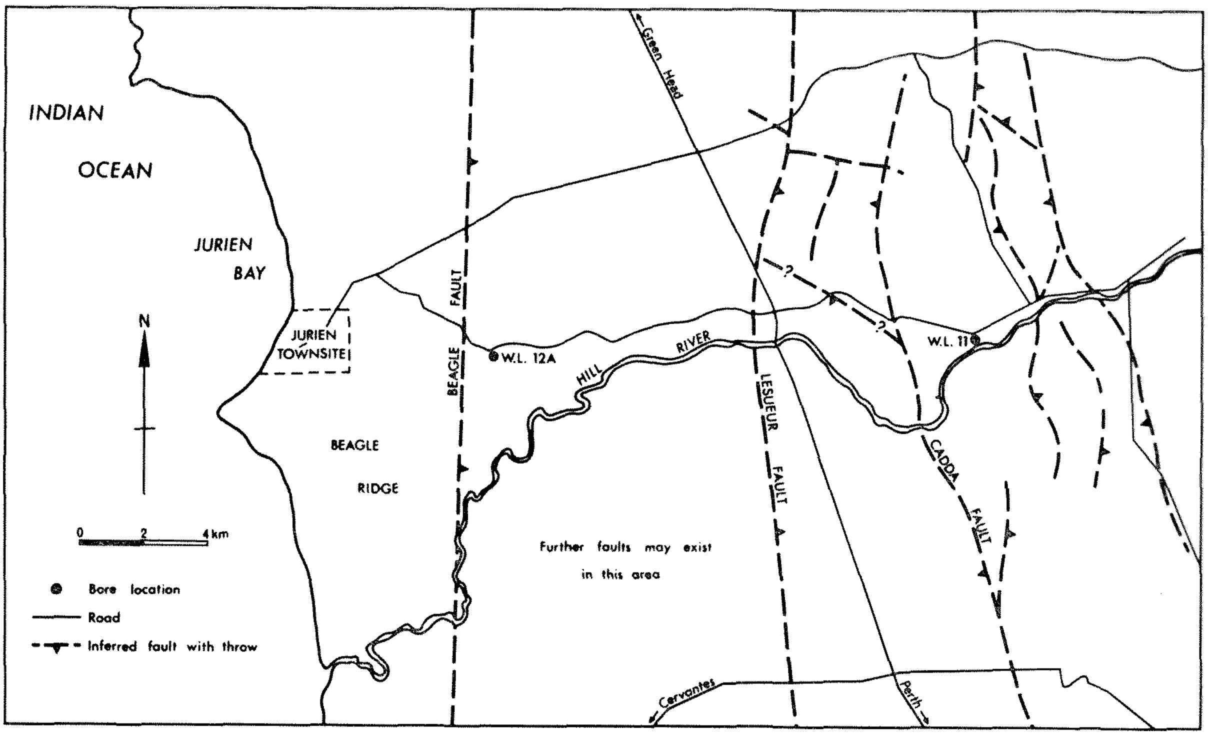

Figure 8. Hill River area—borehole locations and inferred faults.

HYDROGRAPHIC FLUCTUATIONS

Fluctuations in the water levels of both bores were analyzed with respect to atmospheric pressure, rainfall, ocean and earth tides. The periodic, semi-diurnal fluctuations were of special interest.

It was not possible to run the hydrographic and barographic recorders simultaneously, but it was possible to compare for a short time the W.L. 11 hydrographs with barographs at W.L. 12, and later compare both the W.L. 11 and W.L. 12A hydrographic records with barographs from near Eneabba, 53 km to the northeast. The hydrographs showed an inverse relationship with the barographs (Fig. 9), and the relatively large fluctuations were more frequent in the variable winter climate. The water levels are therefore affected by atmospheric pressure variations.

Small semi-diurnal barometric fluctuations were observed approximately at the same time each day, and had a constant amplitude, whereas the hydrographic semi-diurnal fluctuations varied in amplitude and had a semi-diurnal time lag of approximately 23 minutes. This indicates that the two types of semi-diurnal fluctuations have different origins.

Rainfall over the summer months was very low and intermittent, and so can be ruled out as the cause of the semi-diurnal fluctuations. However the W.L. 11 hydrographs do show a response to heavy or continuous rain.

Ocean and earth tides are generally semi-diurnal and are caused by fluctuations in the earth's gravity field due to the varying attraction of the moon, and to a lesser extent, the sun. However the ocean tides are modified by physiographic factors, thus on the west coast the tides are predominantly diurnal with a small range (Hodgkin and Di Lollo, 1958). Ocean tides can cause fluctuations in adjacent confined aquifers, but although the Watheroo hydrographs show the same spatial variation in amplitude intensities, the fluctuations are semi-diurnal and not diurnal (Fig. 10).

Assuming that the earth tide dilations are in phase with the gravity fluctuations, the inverted computed gravity corrections (Goguel, 1972), plotted at 3-hour intervals, compare favourably with the hydrographic semi-diurnal fluctuations. In particular the alternating large and small troughs, due to the upper and lower lunar culminations, correspond well.

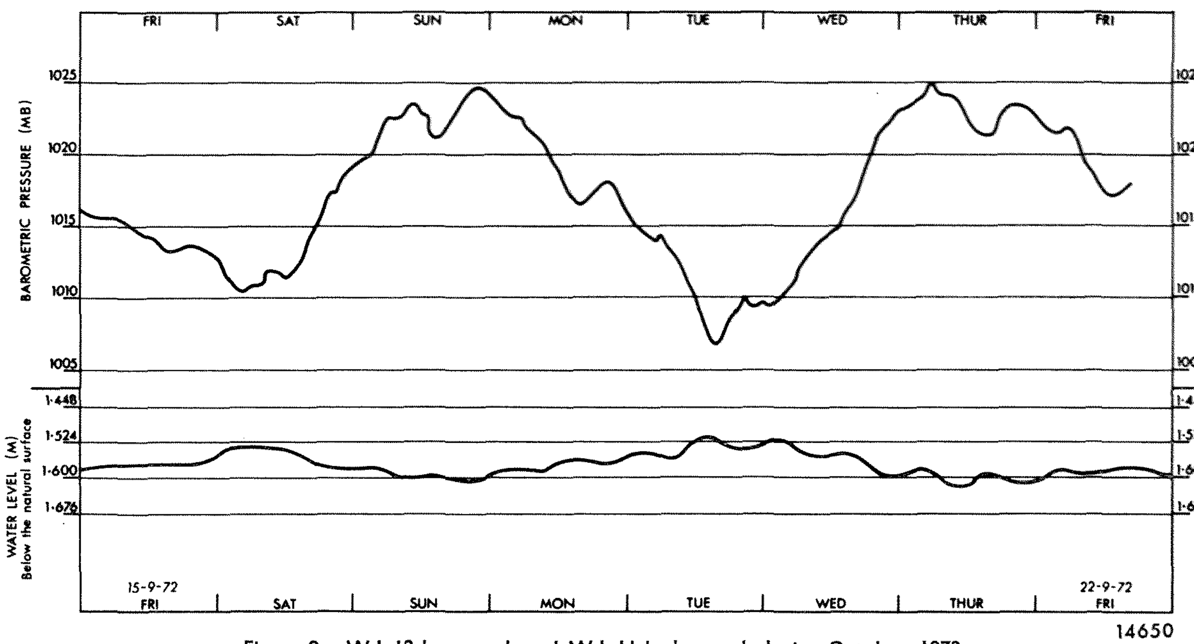

Figure 9. W.L.12 barograph and W.L.11 hydrograph during October, 1972.

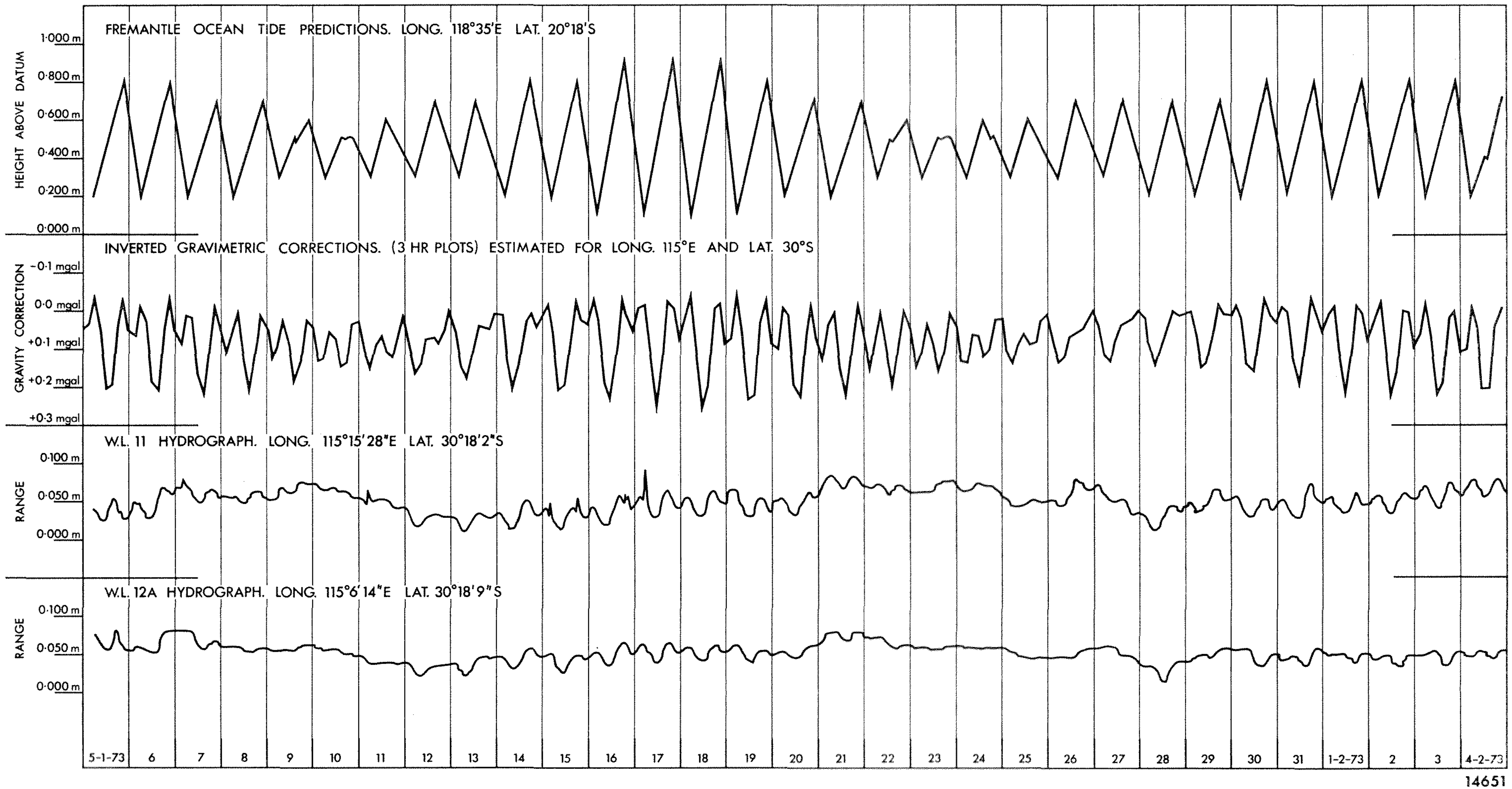

Figure 10. Hydrographs, gravimetric correction and ocean tidal predictions.

ADDITIONAL SEMI-DIURNAL RECORDINGS

Similar semi-diurnal fluctuations, attributed to earth tides, have been observed in Early Jurassic sediments near Pinjarra in the Perth Basin, and reported from a Tertiary calcreted drainage near Agnew in the Eastern Goldfields (Geotechnics, 1972), and in Recent alluvium just southwest of Mount Goldsworthy in the Pilbara (Davidson, 1973).

The maximum range of the semi-diurnal fluctuations lies between 10 mm and 40 mm, although the bore near Mount Goldsworthy is an exception with a maximum of 210 mm.

CONCLUSIONS

Critical examination of the data has reasonably established that although water level fluctuations in the Watheroo bores are affected by changes in the atmospheric pressure, and to a lesser extent rainfall, the periodic semi-diurnal fluctuations can be attributed to earth tides. Ocean tides appear to have no effect.

ACKNOWLEDGEMENTS

Sincere thanks are expressed to the Commonwealth Bureau of Meterology and the West Australian Astronomical Observatory for the help and information that their officers have given.

REFERENCES

Davidson, A., 1973, The De Grey River groundwater investigation: West. Australia Geol. Survey Rec. 1973/27 (unpublished).

Australian National Tide Tables 1973: Aust. Gov. Pub. Service, Canberra.

Geotechnics (Aust.) Pty. Ltd., 1972, The water resources of the Agnew area, Western Australia: Geotechnics (Aust.) Pty. Ltd. (Confidential).

Goguel, J., 1972, Tidal Gravity corrections for 1973: Geophysical prospecting Jour., v. 20, Supp. No. 1.

Hodgkin, E. P., and Di Lollo, V., 1958, The Tides of South-Western Australia: Royal Soc. West. Australia Jour., v. 41, p. 42-54.

THE GEOHYDROLOGY OF THE WATHEROO-JURIEN BAY DRILLHOLE LINE, PERTH BASIN

by A. S. Harley

ABSTRACT

The line completed a further section of the continuing deep-drilling project investigating the pressure waters of the Perth Basin. Twelve sites were drilled to a maximum depth of 762 m on a line extending across the Perth Basin from near Watheroo in the east, to Jurien Bay on the coast. Additional information has been used from 8 State Government and private bores on, or adjacent to, the line.

Predominantly continental sediments of Early Triassic to Recent age were intersected across the graben-faulted Dandaragan Trough between the Precambrian shield and the Beagle Ridge. Movements occurred at the end of the Jurassic, in the Neocomian, and in either the Late Cretaceous or Tertiary or both.

Aquifers containing potable water, and with good permeabilities, are recognized in the Coastal Limestone, the Warnbro Group, the Yarragadee Unit I, and the Lesueur Sandstone. The Yarragadee Unit III mudstones are an important confining unit separating the Agaton groundwater system from that at Badgingarra.

INTRODUCTION

The Watheroo-Jurien Bay Line is part of a long-term drilling investigation of the hydrogeology of the Perth Basin. The line of bores was drilled along an east-west section on the 30° 19′ S parallel, about 185 km north of Perth, and extends 86 km from the salt lakes, 7.6 km southwest of Watheroo, westward to the coast at Jurien Bay. Figure 11A shows the positions of the bore sites.

Drilling on Watheroo Line (W.L.) bore 1 started in May, 1967, but after W.L.4 the Mines Department was asked to investigate the area to the north and south of the bores then drilled, to determine whether a potable groundwater supply could be found to supplement the Northern Comprehensive Water Supply Scheme. By September, 1969, a further 22 sites were drilled for the Agaton Project (Balleau and Passmore, 1973), which covered an area of about 500 km^2 within latitudes 30° 11′ S and 30° 32′ S, and longitudes 115° 39′ E and 115° 55′ E. The Watheroo-Jurien Bay project recommenced in February, 1971, and was completed with W.L.12 in October, 1972.

The bores were drilled to a maximum depth of 762 m at an average spacing of 7 km. Agaton bores (A) 7, 18, 19, 24 and W.L.9 were additional bores to further clarify the hydrogeology. Bores W.L.11 and 12 had a spacing of 14.4 km because information from the oil well, Cadda 1, was available (Elie and others, 1965). The Jurien Bay (J.B.) 1 bore, on the western end of the line, was drilled in 1962. On sites W.L.2, 5, 6, 7, 8, 10, 11, and 12, one or more observation bores were drilled to test shallower aquifers. Information from the Magnetic Observatory bore, drilled in 1936, and from J.B.11 bore has also been used.

Suitable bores were capped and left for long-term water level observation, others being either abandoned or converted for use by the landowner.

DRILLING AND TESTING PROCEDURES

Four bores were drilled by percussion cable tool rig, the others by rotary methods. Sludge samples from the deepest bore on each site were logged every 3m, and conventional cores from the earlier rotary-drilled bores were taken at approximately 60 m intervals. From W.L.7 onwards sidewall cores were recovered on the completion of drilling, together with one or more conventional cores from the adjacent observation bores. The sidewall coring supplied the most useful samples for palynological examination, although the conventional cores gave a better idea of the rock type.

Gamma-ray and electric logs were run on each deep bore with additional logs on W.L.7, and W.L.12B. Step-out bores W.L.7A, W.L.11A, and W.L. 12B were also geophysically logged. Only gamma-ray logs could be taken in percussion bores A.7 and A.18 because of the casing. No geophysical logs were run in J.B.1, J.B.11, or the Magnetic Observatory bore, all drilled some years ago.

Drill-stem tests using both Johnson and Halliburton test-strings were made in open-hole conditions in bores W.L.1, W.L.2, W.L.3, W.L.5, W.L.6, and W.L.9. However, only two water samples, those recovered in W.L.1, appeared to be uncontaminated with drilling mud, and only one other sample, from the upper interval in W.L.6, approached the expected formation water salinity. Although pressure heads could be calculated using the Halliburton tester, the pressure records were not good enough to determine aquifer characteristics.

All the bores, except W.L.9, were cased and water samples collected from selected screened or slotted intervals either by bailing, pumping or air lifting.

Bore data are summarized in Table 5. All potentiometric levels are related to the State mean sea level datum.

TABLE 5. CHEMICAL ANALYSES OF WATER SAMPLES FROM WATHEROO-JURIEN BAY LINE

Bore	Screened interval (metres b.n.s.)	Formation	Appearance	TDS Evap.	TDS Cond.	pH	Ca ppm	Ca epm	Mg ppm	Mg epm	Na ppm	Na epm	K ppm	K epm	Fe ppm	HCO₃ ppm	HCO₃ epm	CO₃ ppm	SO₄ ppm	SO₄ epm	Cl ppm	Cl epm	NO₃ ppm	SiO₂ ppm	Remarks	No. Points on Fig. 11B
W.L.1	208·5–217·6	Leederville	Clear	8 610	9 160	6·1	110	5·49	249	20·48	2 630	114·35	76	1·94	0·1	55	0·90	0	575	11·97	4 580	129·16	1	11	....	....
W.L.1	506·0–515·1	Yarragadee Unit V	Clear	14 300	13 600	6·1	230	11·48	450	37·0	4 210	183·05	118	3·02	0·1	18	0·30	0	877	18·26	7 660	216·01	<1	11	....	....
A.18	206·4–213·7	Leederville	Clear with sl. brown deposit	650	710	5·3	7	0·35	19	1·56	186	8·09	10	0·26	1·4	12	0·20	0	42	0·87	325	9·17	<1	31	....	....
A.18	260·9–272·8	Leederville	Very sl. cloudy	750	830	5·3	3	0·15	21	1·73	207	9·00	23	0·59	5·6	6	0·10	0	42	0·87	370	10·43	2	49	Total Fe content	....
W.L.2	224·3–229·8	Leederville	Very pale yellow with black deposit	620	700	8·9	13	0·65	10	0·82	193	8·39	32	0·82	<0·1	278	4·56	15	2	0·04	194	5·47	7	<1	Probably cement contamination	....
W.L.2	342·9–349·0	Yarragadee Unit VI	Clear with brown deposit	800	950	6·7	16	0·80	24	1·97	247	10·74	15	0·38	3·1	137	2·25	0	39	0·81	381	10·74	6	12	....	....
W.L.2A	143·3–164·6	Leederville	Clear with sl. brown deposit	640	710	7·5	12	0·60	10	0·82	200	8·70	8	0·20	0·7	61	1·00	0	31	0·65	307	8·66	<1	35	....	....
A.24	91·0–146·7	Leederville	Clear with sl. brown deposit	350	370	5·3	2	0·10	11	0·90	92	4·00	9	0·23	5·0	6	0·10	0	38	0·79	154	4·34	<1	26	....	....
A.7	203·0–212·1	Yarragadee Unit VI	Clear	570	640	5·6	4	0·20	24	1·97	133	5·78	15	0·38	0·3	18	0·30	0	13	0·27	276	7·78	<1	32	....	....
W.L.3	151·5–160·0	Yarragadee Unit V	Clear with sl. brown deposit	560	610	6·5	12	0·60	20	1·64	145	6·30	15	0·38	0·1	49	0·80	0	21	0·44	273	7·70	1	31	....	....
W.L.4	130·2–177·1	Yarragadee Unit VI	Clear with grey deposit	480	660	6·8	15	0·75	11	0·90	141	6·13	2	0·05	<0·1	55	0·90	0	18	0·37	232	6·54	<1	14	....	....
W.L.5	391·5–398·0	Yarragadee Unit II	Clear with sl. brown deposit	1 630	1 850	7·6	60	2·99	25	2·06	509	22·13	17	0·43	0·14	195	3·20	0	106	2·21	787	22·19	1	23	....	....
W.L.5	740·3–746·9	Yarragadee Unit II	Clear with sl. brown deposit	1 570	1 780	7·9	58	2·89	27	2·22	476	20·70	16	0·41	0·05	177	2·90	0	66	1·37	778	21·94	<1	21	....	....
W.L.5A	255·4–258·6	Yarragadee Unit III	Clear with sl. brown deposit	1 480	1 730	7·9	13	0·65	24	1·97	511	22·22	14	0·36	0·06	183	3·00	0	94	1·96	718	20·25	<1	41	....	....
W.L.6	392·6–399·0	Yarragadee Unit II	Sl. cloudy with sl. brown deposit	1 410	1 550	6·9	14	0·70	35	2·88	388	16·87	29	0·74	5·0	7	1·15	0	82	1·71	649	18·30	1	52	....	....
W.L.6	392·6–399·0	Yarragadee Unit II	Sl. cloudy with sl. brown deposit	1 260	1 390	7·2	19	0·95	28	2·30	346	15·04	27	0·69	5·0	110	1·80	0	74	1·54	554	15·62	2	54	Probably downhole contamination	....
W.L.6	672·1–678·2	Yarragadee Unit II	Clear with heavy brown deposit	1 400	1 600	8·5	60	2·99	22	1·81	419	18·22	33	0·84	<0·05	156	2·56	12	158	3·29	623	17·57	4	4	Probably cement contamination	....
W.L.6A	177·4–183·5	Yarragadee Unit II	Clear with heavy deposit	1 220	1 390	6·9	8	0·40	41	3·37	348	15·13	18	0·46	<0·05	92	1·51	0	46	0·96	601	16·95	<1	6	....	....
W.L.7	714·6–724·2	Yarragadee Unit I	Clear with sl. brown deposit	430	500	7·6	10	0·49	12	0·99	124	5·39	12	0·31	0·25	128	2·10	0	18	0·37	167	4·71	<1	22	....	14
W.L.7A	521·9–528·2	Yarragadee Unit II	V. pale yellow with sl. deposit	900	1 030	7·0	7	0·35	19	1·56	274	11·91	12	0·31	0·6	82	1·34	0	46	0·96	420	11·84	0	47	....	....
W.L.7B	178·9–181·3	Yarragadee Unit II	Clear	740	850	7·3	19	0·95	15	1·23	203	8·83	19	0·49	<0·05	67	1·10	0	12	0·25	359	10·12	1	48	....	....
W.L.8	586·8–596·5	Yarragadee Unit I	Clear with brown deposit	560	640	5·5	10	0·50	29	2·38	116	5·04	17	0·43	1·2	3	0·05	0	13	0·27	284	8·01	<1	44	....	16
W.L.8A	170·7–174·3	Yarragadee Unit II	V. pale yellow with sl. brown deposit	720	760	6·6	9	0·45	15	1·23	188	8·17	16	0·41	2·8	34	0·56	0	55	1·15	298	8·40	<1	83	....	....
W.L.10	381·1–387·5	Yarragadee Unit I	V. sl. cloudy with deposit	300	320	7·7	32	1·60	3	0·25	55	2·39	12	0·31	0·05	134	2·20	0	16	0·33	71	2·00	<1	27	....	18
W.L.10A	224·5–230·8	Yarragadee Unit II	Cloudy	340	360	6·6	9	0·45	7	0·58	81	3·52	11	0·28	0·05	46	0·75	0	18	0·37	130	3·67	2	19	....	....
W.L.11	207·0–213·4	Cockleshell Gully	Clear with black deposit	4 340	4 480	7·5	172	8·59	90	7·40	1 200	52·18	24	0·61	0·15	183	3·00	0	252	5·25	2 150	60·63	<1	16	....	....
W.L.11	207·0–213·4	Formation Cattamara	Clear with sl. brown deposit	2 770	3 140	8·0	86	4·29	29	2·39	870	37·83	17	0·44	<0·05	192	3·15	0	138	2·87	1 380	38·92	<1	18	Downhole contamination	....
W.L.11A	692·8–699·2	Coal Measures	Clear with brown deposit	4 920	5 550	7·9	136	6·79	67	5·51	1 610	70·00	31	0·79	<0·05	177	2·90	0	290	6·04	2 630	74·17	<1	18	....	....
W.L.11B	14·0– 20·1	Member.	Cloudy with deposit	710	750	7·6	5	0·25	12	0·99	213	9·26	4	0·10	<0·05	58	0·95	0	65	1·35	266	7·50	50	67	....	....
Midland No. 7	36·6– 42·7	Coastal Limestone	Clear	460	540	7·0	48	2·40	16	1·32	95	4·13	4	0·10	<0·05	164	2·69	0	18	0·37	173	4·48	1	17	....	26
W.L.12	712·4–718·6	Woodada	Clear with sl. brown deposit	570	680	8·0	13	0·65	19	1·56	160	6·94	30	0·77	<0·05	152	2·51	0	42	0·87	232	6·54	<1	15	....	24
W.L.12A	135·2–141·5	Lesueur	Clear with sl. brown deposit	340	410	7·1	8	0·40	9	0·74	99	4·30	7	0·18	0·15	95	1·56	0	15	0·31	133	3·75	<1	16	....	22
W.L.12B	572·2–578·5	Lesueur	Clear with sl. brown deposit	400	470	7·4	24	1·20	15	1·23	83	3·61	20	0·51	<0·05	98	1·61	0	15	0·31	164	4·62	<1	18	....	23
J.B.11	23·7– 26·8	Coastal Limestone	Clear	620	690	7·4	88	4·39	16	1·32	113	4·91	4	0·10	<0·1	268	4·39	0	19	0·40	209	5·89	2	13	....	27
J.B.1	153·9–181·4	Woodada	....	49 300	....	6·7	1 280	63·88	1 210	99·51	15 400	669·59	570	14·58	....	64	1·05	0	3 160	65·79	27 700	781·14	2	....	....	25

Analyses : Government Chemical Laboratories.

CLIMATE

The climate is typically mediterranean, characterized by cool, wet, winters and warm, dry, summers. The annual average rainfall is 452 mm at Jurien Bay, 564 mm at the Badgingarra Research Station, and 428 mm at Watheroo.

GEOLOGY

Figure 12A shows the geological cross section. The geology has been described in detail in an earlier report (Harley, 1974).

In summary, the bores intersected predominantly continental sediments of Early Triassic to Recent age across the deep, graben-faulted, Dandaragan Trough between the Precambrian shield and the structural "high" of the Beagle Ridge. Marine transgressions occurred in the Early Triassic, Middle Jurassic, and the Late Cretaceous. Faulting and gentle folding occurred at the end of the Jurassic during the Neocomian when there was a period of non-deposition, and during Tertiary time.

Continuous erosion has taken place since the Cretaceous, but lateritization during the Pleistocene or Tertiary or both has formed a residual surface resistant to erosion. The coastal plain has developed as a result of marine erosion with subsequent modification and the deposition of several Pleistocene to Recent dune systems.

Since the writing of of the Agaton report by Balleau and Passmore (1972) there have been revisions of the Cretaceous stratigraphical nomenclature and further drilling of the Yarragadee Formation. Consequently the Molecap Greensand (Coolyena Group), Dandaragan Sandstone (Warnbro Group), and the non-marine Leederville Formation (Warnbro Group) have been recognized, and the subdivision of the Yarragadee has been altered.

GEOHYDROLOGY

Aquifers exist in all the formations from Quaternary to Triassic in age, and are described according to their geological form, rather than by groundwater systems. The Agaton bore field in the east has been comprehensively described and evaluated by Balleau and Passmore. Figure 12B is a cross section showing the potentiometric levels and groundwater salinities in the individual bores. Detailed results are given in Tables 5 and 6.

QUATERNARY

Agaton Area

Thin, localized, perched aquifers are found in the Quaternary sands overlying the less permeable late Cretaceous marine formations, the salinities ranging from 100 ppm to 1 800 ppm, the higher salinities resulting from evaporation and transpiration. Recharge is by infiltration of rainfall and groundwater movement down dip above the underlying impermeable beds. As yet there appears to be no problem with high nitrate values caused by the leaching of artificial fertilizers.

TABLE 6. SUMMARY OF BORE DATA

Bore	Total depth (m)	*R or †P	Natural surface elevation m.s.l. (m)	Potentiometric level elevation m.s.l. (m)	Observation interval: Depth (m) b.n.s.	Observation interval: Screen or slots	Test pumping rate m³/day	Air-lift flow rate m³/day	Formation tester	Recovered salinity (by conductivity) ppm	Status abd: abandoned obs: observation
W L.1	551·7	R	234·1	209·8	208·5–217·6	....	....	....	Johnson	9 160	abd
W'L.1	....	....	....	211·3	506·0–515·1	....	....	....	Johnson	13 600	....
Magnetic Observatory	106·7	P	238·7	232·5	15·2– 21·3	slots	....	....	....	11 400	abd
A.19	588·3	R	237·4	210·9	216·4–225·6					....	....
A.19	....	....	....	....	276·8–289.0	slots	....	....	....	820	obs
A.19	....	....	....	....	314·2–320·3					....	....
A.18	282·9	P	255·5	....	206·4–213·7	screen	218	....	....	710	cased off
A.18	....	....	....	211·1	260·9–272·8	screen	163	....	....	830	obs
W.L.2	637·0	R	261·2	210·3	224·3–229·8	casing gap	....	....	....	(contaminated 700)	obs (blocked)
W.L.2	....	....	....	162·9	342·9–349·0	slots	....	....	....	950	cemented off
W.L.2A	164·6	P	261·0	211·1	143·3–164·6	?	....	....	....	710	obs (blocked)
A.24	371·2	R	262·1	211·0	91·0–102·9						
A.24	....	....	....	....	112·2–127·7	slots	....	....	....	370	....
A.24	....	....	....	....	134·2–146·7						
A.7	304·8	P	256·6	211·1	Below 125·0	open hole	....	....	....	....	obs (blocked)
A.7	....	....	....	211·9	203·0–212.1	screen	1 253	....	....	640	casing withdrawn
W.L.3	603·5	R	314·2	217·4	151·5–160·0	screen	....	....	....	610	in use by farmer
W.L.9	319·4	R	323·95	(resistivity log 220·4)	Not tested	....	....	....	....	....	abd
W.L.4	573·9	R	334·9	221·3	130·2–141·4	slots	....	....	....	660	obs (blocked)
					167·9–177·1						
W.L.5	765·3	R	286·2	101·2	391·5–398·0	slots	....	10	....	1 850	obs
W.L.5	....	....	....	102·4	489·0–502·9	....	....	....	Halliburton	....	....
W.L.5	....	....	....	100·1	593·1–616·6	....	....	....	Halliburton	....	....
W.L.5	....	....	....	101·1	740·3–746·9	slots	....	13	....	1 780	cemented off
W.L.5A	258·6	R	286·5	192·6	255·4–258·6	screen	....	15	....	1 730	obs
W.L.6	762·3	R	216·9	101·0	392·6–399·0	slots	....	55	....	1 550	obs
W.L.6	....	....	....	99·1	465·4–485·5	....	....	....	Halliburton	(1 850)	....
W.L.6	....	....	....	98·0	672·1–678·2	slots	....	....	....	(contaminated 1 600)	cemented off
W.L.6A	183·8	R	216·8	100·9	177·4–183·5	screen	....	....	....	1 390	abd
W.L.7	757·7	R	186·5	105·7	714·6–724·2	screen	....	143	....	500	obs
W.L.7A	547·1	R	186·9	105·1	521·9–528·2	screen	....	143	....	1 030	obs
W.L.7B	198·1	R	187·0	104·9	178·9–181·3	screen	....	93	....	850	obs
W.L.8	755·0	R	148·6	120·7	586·8–596·5	screen	....	196	....	640	obs
W.L.8A	202·7	R	147·1	118·9	170·7–174·3	screen	....	196	....	760	obs
W.L.10	764·7	R	141·0	116·8	381·1–387·5	screen	....	44	....	320	obs
W.L.10A	304·0	R	141·2	117·3	224·5–230·8	screen	....	11	....	360	obs
W.L.11	762·0	R	78·6	77·2	207·0–213·4	screen	....	196	....	4 480	obs
W.L.11 (annulus)	....	....	....	76·8	Below 97·5	....	....	....	....	....	obs
W.L.11A	746·6	R	78·3	65·0	692·8–699·2	screen	....	225	....	5 550	obs
W.L.11A (annulus)	....	....	....	73·0	Below 59·4	....	....	....	....	....	obs
W.L.11B	26·8	R	77·7	69·4	14·0– 20·1	screen	....	58	....	750	obs
Midland No. 7	42·7	P	50·8	15·8	36·6– 42·7	slotted	....	....	....	540	Farmer's bore
W.L.12	762·3	R	49·7	25·8	712·4–718·6	screen	....	185	....	680	obs
W.L.12 (annulus)	....	....	....	18·6	Below 41·6	....	....	....	....	....	obs
W.L.12A	155·4	R	48·8	18·4	135·2–141·5	screen	....	157	....	410	obs
W.L.12B	583·7	R	48·7	19·6	572·2–578·5	screen	....	202	....	470	obs
W.L.12B (annulus)	....	....	....	18·6	Below 48·8	....	....	....	....	....	obs
J.B.11	45·7	P	19·5	0·2	23·7 –26·8	screen	1 177	....	....	690	obs
J.B.1.	191·4	P	3·6	0	6·1					4 710	abd
				0	26·5	open hole	....	....	....	2 760	
				1·8	153·9–181·4					49 300	

*R: Rotary drilled

†P: Percussion drilled

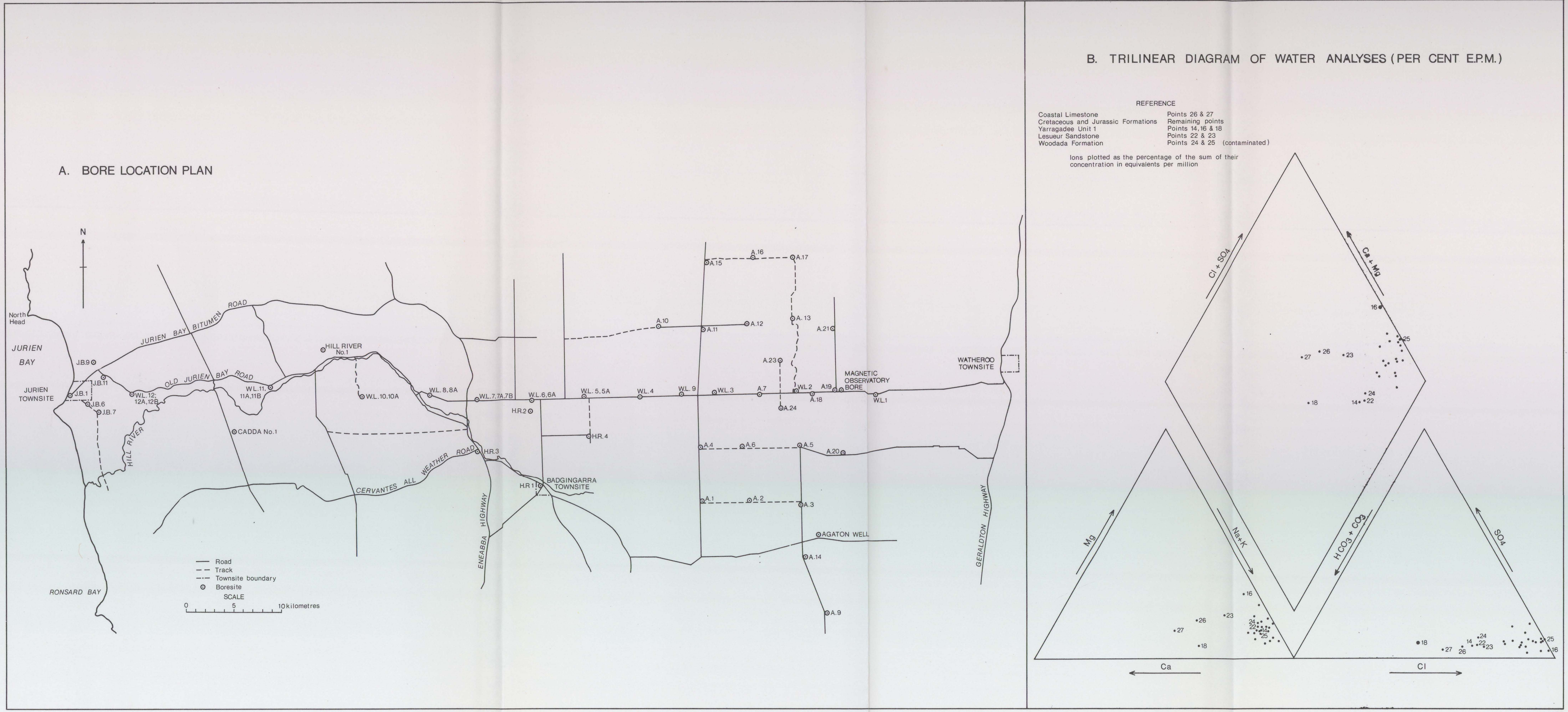

Fig. 11. Watheroo—Jurien Bay drillhole line.

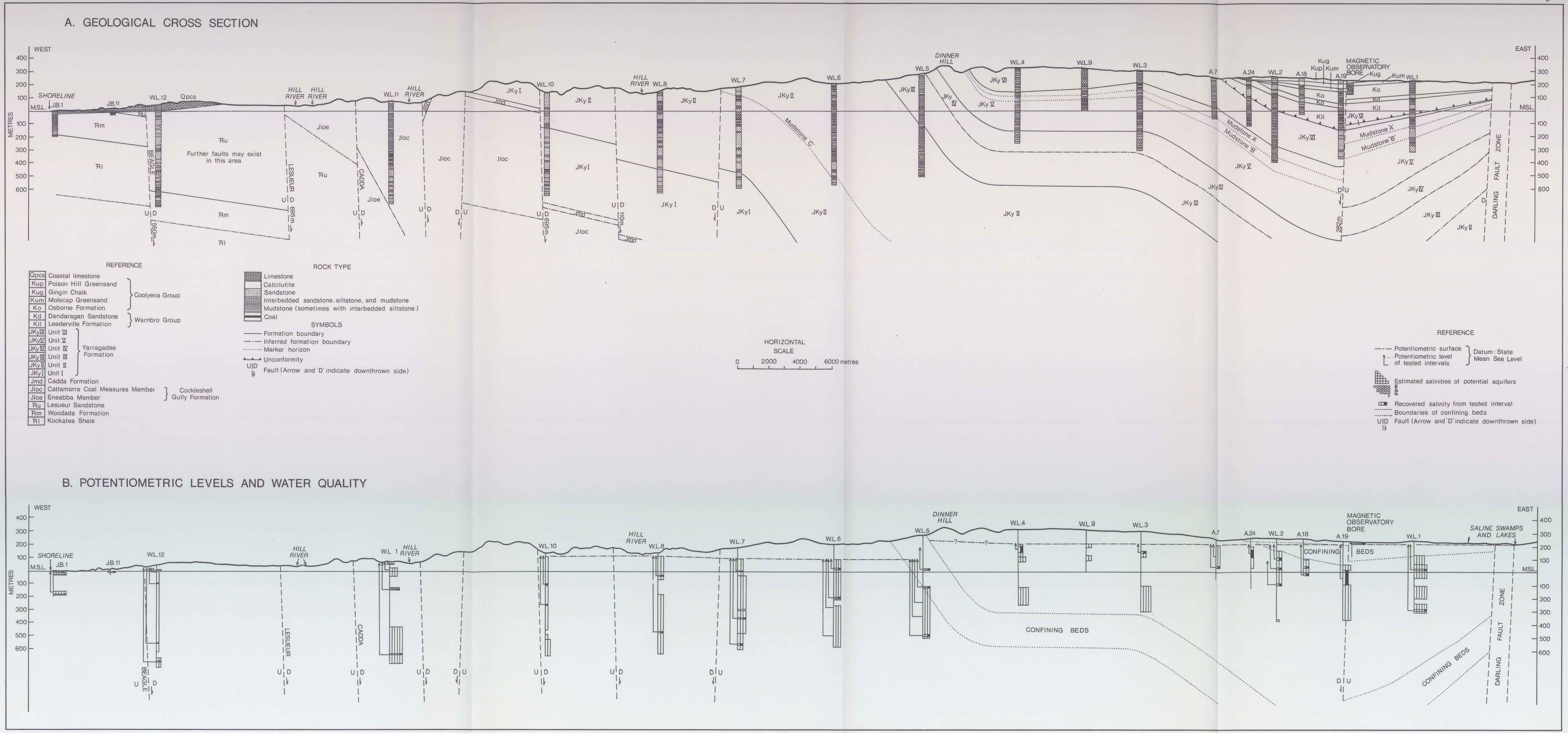

Fig. 12. Watheroo—Jurien Bay drillhole line.

Dandaragan Scarp

Thin, localized, perched aquifers occur along the Dandaragan Scarp (Low, 1972) in the vicinity of Dinner Hill. The line of shallow soaks and wells tapping Quaternary sands is parallel to the apparent strike of the underlying impermeable Yarragadee Unit III mudstone.

Salinities vary from less than 100 ppm to more than 2 000 ppm but most are less than 500 ppm. Nitrate contents range from 1 ppm to 33 ppm, indicating pollution from artificial fertilizers. The higher salinities result from evaporation and transpiration. Recharge is from rainfall.

Coastal Limestone

The Coastal Limestone is a sandy calcarenite which extends westward to the coast from about 10 km inland, and crops out offshore. It varies in thickness from about 40 m, near W.L. 12, to 17 m at the coast near J.B. 1. East of the Beagle Ridge the aquifer is probably partially confined by the underlying laterite, and on the Beagle Ridge is underlain by relatively impermeable, argillaceous sediments of the Woodada Formation. Where exposed, the top part of the Coastal Limestone is lithified, but at depth the sediments are poorly consolidated and very permeable.

In J.B. 11 a pumping rate of 49 m^3/hour produced a drawdown of 0.71 m and similar results were reported from several other bores. Salinities increased from about 600 ppm, 4 km east of Jurien Bay, to 1 400 ppm near the townsite. In J.B. 1 the salinity increased with depth from 4 700 ppm, near the water table, to 27 600 ppm at the base of the aquifer (Berliat and Morgan, 1962) because of salt water intrusion.

The potentiometric levels in most of the bores are very close to mean sea level. Higher levels recorded in bores J.B. 1 and 10 were associated with deeper confined aquifers, while the level of + 15.8 m in the bore near W.L. 12 is probably due to the proximity to an intake, and recharge from the underlying Lesueur Sandstone aquifer. The salinity contours indicate that groundwater movement is from the northeast (Milbourne, 1966). Recharge is by infiltrating rainfall moving from the northeast through solution tubes and cavities in the limestone, and pressure water may also move upward from the underlying Lesueur Sandstone.

COOLYENA GROUP

Except for the Poison Hill Greensand the Coolyena Group beds are clayey and relatively impermeable, and act as a hydraulic barrier between the Poison Hill Greensand and the Warnbro Group, although the Molecap Greensand and the Osborne Formation become more sandy to the westward. Perched waters occur on the more sandy beds, but are normally of a fairly high salinity, exceeding 1 000 ppm in the Gingin Chalk in A. 18 and 5 000 ppm in the Observatory bore. The high salinities reflect low permeability of the aquifers, and evapotranspiration losses. Perched waters could perhaps be found in the sandy sediments of the Poison Hill Greensand but there is no evidence for this.

Recharge is direct from rainfall. Because some of the perched aquifers are above the potentiometric surface of the underlying pressure waters, there is a potential for downward leakage. Balleau and Passmore (1972) have demonstrated this from examination of the Ca + Mg/Na + K ratios in recovered water samples.

WANBRO GROUP

Dandaragan Sandstone

The Dandaragan Sandstone is a fine to coarse-grained marine sandstone, about 40 m thick in the Watheroo section. It is confined at the top and bottom by clayey beds, but crops out on the western edge of the marine basin. Although this Sandstone was not tested in the Watheroo bores, results from the Agaton bore field suggest that the permeability may be relatively high. Hydraulic conductivities between 26 and 27 $m^3/d/m^2$ have been reported.

Salinities calculated from the resistivity logs indicate values less than 1 000 ppm on the western side of the marine basin, but the salinity increases eastward. The high salinity in W.L. 1 is probably caused by leakage from the saline drainage along the Darling Fault zone, but the fault west of the Magnetic Observatory bore prevents contamination of the aquifer by westerly movement of the saline water. This also applies to the water in the Leederville and the Yarragadee aquifers.

Results from the Agaton bore field show that the potentiometric levels in the Dandaragan Sandstone are very similar to those in the underlying Leederville and Yarragadee aquifers, and therefore the groundwater flow is in a south-easterly direction. Recharge is from rainfall, where the formation crops out along the margin of the marine basin, by horizontal flow from the Leederville Formation, and by leakage from the overlying sediments of the Coolyena Group.

Leederville Formation

This is an interbedded sandstone, siltstone, and mudstone with generally fairly thin and sometimes discontinuous aquifers confined by the more impermeable beds, except where the formation crops out along the western margin of the marine basin. The hydraulic conductivity is less than that in the overlying Dandaragan Sandstone.

Water samples were recovered from several bores, the salinity being less than 500 ppm in A.24, but gradually increasing eastward. In W.L. 1 the salinity exceeded 5 000 ppm, due to local intake from the saline drainage along the Darling Fault zone. Some of the samples had several parts per million iron content.

Potentiometric levels were fairly constant from east to west and may decrease slightly with depth. The level in W.L. 1 was recorded in a drill-stem test and was not reliable. Balleau and Passmore (1972) show the groundwater flow to be in a southeasterly direction. Recharge is from rain falling where the formation crops out along the western and northern margins of the marine basin, upward movement from the underlying Yarragadee Formation, and downward leakage from the overlying Dandaragan Sandstone.

YARRAGADEE FORMATION

Units IV, V and VI

These units are a series of interbedded sandstone, siltstone, and mudstone beds, and their several aquifers are confined except on the western edge of the basin. The permeability is similar to that in the Leederville Formation, an average hydraulic conductivity of 4.7 $m^3/d/m^2$ having been calculated for the two formations (Balleau and Passmore, 1972).

Salinities in the western section of the basin are less than 1 000 ppm but increase both to the eastward and with depth. The high salinity in W.L. 1 is probably due to local intake.

The potentiometric levels are very similar between bores W.L. 1 and A. 7 but show a rise westward of A. 7. However the level in W.L. 1 was recorded in a drill-stem test and is not reliable.

The relatively steep decline between W.L. 3 and A. 7 is probably due to the influence of the small anticline near W.L. 3. The easterly gradient indicates an apparent direction of groundwater flow, but when the Agaton bore field is considered, the overall movement is southeasterly. Potentiometric levels may decrease slightly with depth. The unusually low water level in W.L. 2 is thought to be unrepresentative of the aquifer and caused by silting up of the slotted interval. Recharge is from rainfall in the west, leakage from overlying aquifers, and direct downward infiltration through the unsaturated zone.

On the Watheroo-Jurien Bay Line the Agaton groundwater system is confined by the underlying Yarragadee Unit III mudstone and the Darling Fault. There is groundwater flow into the area from the north, and a discharge to the south.

Unit III

This thick mudstone is considered to be an important confining unit separating the Agaton and the Badgingarra groundwater systems (Fig. 12B). From the W.L. 5 geophysical logs the interval between 291 m and 340 m appears to be particularly impermeable. Two thin interbedded sandstones were tested in bores W.L. 5A and Hill River (potentiometric level 186.2 m and salinity 2 190 ppm), the results suggesting that these thin aquifers are independent of either the Agaton or the Badgingarra groundwater systems.

Units I and II

These units are essentially sandstone with minor mudstone beds. The aquifers are confined at depth but are unconfined where they crop out to the westward. Because of the fines and poor sorting in the upper sediments of Unit II their permeability is low, but the sandstone towards the base of Unit II and in Unit I are coarser grained and have less intergranular clay, so their permeability is relatively greater.

The groundwater salinity around W.L. 10 is less than 500 ppm, but it gradually increases to the eastward and also increases with depth. The markedly higher resistivity values on the electric logs of the top section of Unit I indicate a decrease in salinity. Several of the tested horizons had an iron content high enough to necessitate treatment.

The potentiometric surface rises slightly from W.L. 10 to W.L. 8, and then falls gradually to the eastward. The rise to the W.L. 8 level is slightly unusual because the salinity increases uniformly to the eastward from W.L. 10. However, local factors may be involved such as discharge near W.L. 10 to Hill River, or recharge near W.L. 8 from Hill River. Except in W.L. 10 the potentiometric level decreases slightly with depth. It is suggested that the flow of groundwater is in a southeasterly direction, but this cannot be confirmed with the present information. Recharge is from rainfall to the basically unconfined aquifer system, and there is possibly some seasonal recharge from the Hill River in the vicinity of W.L. 8.

The Badgingarra groundwater system is bounded to the west by the faulted blocks of older sediments.

CADDA FORMATION

This was not intersected and little is known of its hydrogeological characteristics.

COCKLESHELL GULLY FORMATION

Cattamarra Coal Measures Member

The member is an interbedded sandstone and mudstone. Bore W.L. 11 intersected several discrete aquifers separated by thick mudstones.

Except in the top aquifer, the groundwater salinity in W.L. 11 is more than 1 000 ppm, and increases with depth to more than 5 000 ppm. The top aquifer is thin, unconfined, probably not continuous because of surface erosion, and the water has a high nitrate content which may result from contamination from artificial fertilizers. Aquifers in the Cattamarra Coal Measures Member rarely have salinities of less than 1 000 ppm.

The different aquifers show marked variations between their potentiometric levels (Table 6). W.L. 11 was drilled in a narrow fault block and it is not known whether the faults are boundaries to the groundwater flow. The topography indicates that the groundwater flow is probably southward to the Hill River. Recharge is from infiltration where the aquifers crop out, and by leakage through the confining beds.

Eneabba Member

This was not intersected by the Watheroo bores but other evidence indicates that it is an interbedded sandstone and mudstone. Cadda 1 water bore gave a salinity of 1 100 ppm, and aquifer characteristics in the Eneabba Member probably resemble those in the overlying Cattmarra Coal Measures Member.

LESUEUR SANDSTONE

This is a thick, permeable sandstone with infrequent thin mudstone beds becoming more numerous near the base of the formation. It appears to be confined under a thin "laterite" around W.L. 12, but to the east is probably unconfined.

In the section drilled the groundwater salinity was less than 500 ppm, but there was a noticeable iron content. The potentiometric levels appear to increase with depth, and as these levels are higher than that in the overlying Coastal Limestone there may be upward movement. Recharge into the Lesueur aquifers is probably from rainfall farther east beyond the Coastal Limestone.

It is not known whether the Lesueur and Beagle Faults are hydraulic boundaries, but the general direction of groundwater flow is probably southward towards the Hill River.

WOODADA FORMATION

This is an interbedded sandstone and mudstone and tests in W.L. 12 and J.B. 1 indicate that the aquifers are confined by the more argillaceous beds.

The recovered salinity in W.L. 12 was about 700 ppm, whereas the reported salinity in J.B. 1 was 49 300 ppm due to salt water contamintation. Although the yield by air-lifting was relatively good in W.L. 12, the resistivity logs from W.L. 12 suggest a relatively low permeability.

The potentiometric level in W.L. 12 is higher than those from the Lesueur Sandstone in the same bore, indicating potential for leakage into the overlying aquifer in which the water is hydrochemically very similar. The source of recharge is unknown.

KOCKATEA SHALE

This is a thick silty mudstone unit and from present evidence has little groundwater potential.

HYDROCHEMISTRY

Water analyses are listed in Table 5 and plotted on a trilinear diagram (Fig. 11B).

The measured pH values generally range between 6.5 and 8.0, but the true pH could be very different because of aeration of the water samples.

Iron is only present in sufficient quantities to be a problem in the Leederville Formation and Yarragadee Unit II waters, but most water samples contained some precipitated iron. Nitrate is the only other significant ion, and was found in noticeable amounts in the perched aquifers along the Dandaragan Scarp and on top of the Cockleshell Gully Formation. However where there is rainwater intake to a shallow aquifer through an artificially fertilized soil, the nitrate content should be monitored.

Waters from the Jurassic and Cretaceous aquifers are essentially sodium chloride-rich (Fig. 11B). The more calcium bicarbonate-rich waters are those from the sandstones of Yarragadee Unit I (points 14, 18), the Lesueur Sandstone (22, 23), and surprisingly the Woodada Formation in W.L. 12 (24). Not unexpectedly the water from the Coastal Limestone is also calcium bicarbonate-rich (26, 27). Sample 16 from the Yarragadee Unit I aquifer, in W.L. 8, appears to be magnesium chloride-rich, and is rather unusual. It is thought that the relatively calcium bicarbonate-rich waters in the Lesueur and Woodada Formations in W.L. 12 are the result of recharge through the calcareous dune systems. The origin of the Yarragadee Unit I water is uncertain, but there could be some connection with the calcaresous Cadda Formation.

The high proportion of sodium chloride in the groundwater is due to recharge by rainfall, concentrated to some extent by evapotranspiration near the surface.

CONCLUSIONS

Aquifers were found in all the formations above the Early Triassic Kockatea Shale, with water salinities as high as 50 000 ppm. There are four major aquifer systems with salinities of less than 1 000 ppm.

The Coastal Limestone is an important permeable non-pressure aquifer containing potable water (less than 1 000 ppm) east of Jurien Bay, but the salinity increases towards the coast. Recharge is from the northeast.

The Agaton groundwater system in the east includes the Warnbro Group and upper units of the Yarragadee Formation. It is confined below, and to the west, by the mudstones of Yarragadee Unit III, and to the east by the Darling Fault. Potable water can be obtained from the aquifers west of the synclinal axis. However the best economic prospects are the water-bearing beds of the Warnbro Group, which are largely overlain by the confining beds of the Coolyena Group. The Dandaragan Sandstone has good hydraulic conductivities of the order of 26.5 $m^3/d/m^2$ with estimated salinities less than 1 000 ppm west of the synclinal axis. The Leederville Formation has slightly better quality water but is high in iron. Hydraulic conductivities are lower, an average of 4.7 $m^3/d/m^2$, because of the more argillaceous nature of the sediments. In the Agaton groundwater system the groundwater movement is southeastward across the Watheroo-Jurien Bay Line.

The Badgingarra groundwater system farther west includes the basal two units of the Yarragadee Formation. It is bounded on the west by faulted, older sedimentary blocks and to the east by the mudstones of Unit III. Salinities increase from less than 500 ppm, in W.L. 10, to nearly 2 000 ppm in W.L. 5. The best aquifer is the thick, permeable sandstone in the upper part of Unit I. The groundwater flow has an easterly component and possibly moves southeastward.

The Lesueur Sandstone intersected in W.L. 12 contains thick aquifers with salinities of less than 500 ppm, and apparent good permeabilities. The aquifers are bounded to the westward by the Beagle Fault, and probably to the eastward by the Lesueur Fault. The general groundwater movement is probably southward towards the Hill River, but there may be some discharge into the overlying Coastal Limestone, which has a lower potentiometric level.

REFERENCES

Balleau, W. P., and Passmore, J. R., 1972, Geology and groundwater at the Agaton exploratory bore field: West. Australia Geol. Survey Rec. 1972/11 (unpublished).

Berliat, K., and Morgan, K. H., 1962, Report on exploratory drilling for water at Jurien Bay, W.A.: West. Australia Geol. Survey Rec. 1962/1 (unpublished).

Elie, R., Cooper, R., Tricot, P. L., and Sweeney, P., 1965, Cadda No. 1 Well completion report: French Petroleum Co. (Australia) Pty. Ltd. Petroleum Search Subsidy Act. Rept. 65/4164 (unpublished).

Harley, A. S., 1974, The hydrogeology of the Watheroo-Jurien Bay Line, Perth Basin: West. Australia Geol. Survey Rec. 1974/23 (unpublished).

Low, G. H., 1972, Explanatory notes on the Proterozoic and Phanerozoic rocks of the Moora 1 : 250 000 Geological Sheet, W.A.: West. Australia Geol. Survey Rec. 1972/21 (unpublished).

Milbourne, R., 1967, Exploratory drilling for groundwater at Jurien Bay: West. Australia Geol. Survey Ann. Rept. 1966, p. 18-20.

SHEAR ZONES IN PRECAMBRIAN ROCKS OF THE DARLING RANGE: NATURE, ORIGIN AND ENGINEERING SIGNIFICANCE

by G. Klenowski

ABSTRACT

Two sets of shear zones are common in Precambrian rocks of the Darling Range. One set has a northerly trend and occurs in the margins of metadolerite dykes and the adjacent country rock. Southwards from the Canning Tunnel to the Burekup area the shearing nature changes from predominantly dolerite deformation, associated with hydrothermal activity, to predominantly country rock deformation under increasing metamorphic grade, and movement direction changes from dip-slip to strike-slip. The other set, of more variable trend, becomes more extensive southwards to the Burekup area, and offsets some dykes.

Tectonites derived from deformation of dolerite include hornblende schist, actinolite schist, biotite schist and chloritic schist. Deformation of country rock produced porphyroclastic augen gneiss, augen schist and mica schist. Mylonitic rocks also occur.

Shear zones are important in engineering geology because they form zones of weak rock which, where closely fractured, may act as pathways for water percolation, and lead to localized deep weathering. Such zones occurred in the excavations at the South Dandalup dam site and the Canning Tunnel, and remedial work was necessary.

INTRODUCTION

The western margin of the Yilgarn Block is characterized by numerous shear zones developed in the margins of metadolerite dykes and in the adjacent country rock. These zones have been investigated in the Canning Tunnel, North and South Dandalup and Burekup dam sites (Fig. 13). Both the 5.5 km Canning Tunnel and the deeply incised Collie River Valley near Burekup present excellent rock exposure for structural analysis.

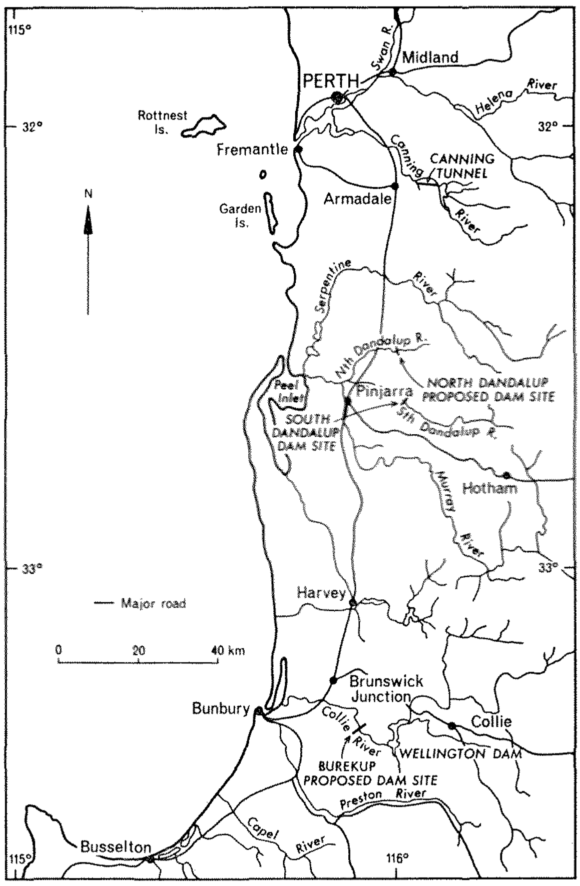

Figure 13. Darling Range area—engineering geology investigation sites.

Shear zones are important in engineering geology because they form zones of weak rock which where closely fractured, may act as pathways for water percolation and lead to localized deep weathering. These require remedial work.

TECTONIC SETTING

The four areas studied are east of the northerly trending Darling Fault, which has displaced the west block 10 000 to 15 000 m downward, and are underlain by Archaean granitic rocks intruded by Upper Proterozoic dolerite (now metadolerite). The granitic complex includes hybrid gneiss, granitic gneiss, augen gneiss, massive granite, pegmatite and aplite. The granitic gneiss of the Yilgarn Block has been dated at 3 000 m.y. and the massive granite at 2 700 m.y. (Compston and Arriens, 1968). The dolerite of the western margin of the Yilgarn Block is considered to be 650 m.y. (Wilson and others, 1958).

The tectonic history in the areas investigated may be divided into pre-dolerite and post-dolerite tectonism. Pre-dolerite tectonism involved the formation of the granitic complex and subsequent deformation which included shearing, faulting and minor folding. Post-dolerite tectonism is recognized by shearing occurring in the margins of metadolerite dykes and in the adjacent country rock, and by faulting which off-sets some dykes. A Rb-Sr age of 560-590 m.y. has been obtained from sheared and metasomatized dyke margins (Compston and Arriens, 1968). This tectonic episode is important because it occurs on a regional scale, and has produced considerable variation of the original rock types. Southwards from the Canning Tunnel to the Burekup area, the shearing nature in the margins of metadolerite dykes and in the adjacent country rock changes from predominantly dolerite deformation, associated with hydrothermal activity, to predominantly country rock deformation under increasing regional metamorphic grade.

STRUCTURAL ANALYSIS

Data for detailed structural analysis were collected from the Canning Tunnel and the North Dandalup and Burekup proposed dam site areas. Modal attitudes of dykes and shear zones were determined using Rose and Pi diagrams (Klenowski, 1973, 1974). The metadolerite dykes generally strike north and dip steeply east or west. Many have well jointed sheared margins, with the shearing showing considerable variation in intensity. No definite controlling pattern of shearing could be identified, but generally the westerly dipping dykes are more intensely sheared on their western margins. In all areas, shear zones vary in width from less than one centimetre to 35 metres. Shearing always increases in intensity towards the contacts between the metadolerite and the country rock.

In the Canning Tunnel the metadolerite dykes generally trend NNW. The metadolerite is always more intensely sheared than the country rock (Fig. 14). The direction of movement was dip-slip, west blocks down, determined by S-shaped drag structures in the metadolerite, dragging of adjacent gneissic foliation (Fig. 16A), displacement of pegmatite veins on either side of metadolerite dykes, and the development of slickensides. A secondary strike-slip component was also identified from slickensides.

At North Dandalup the metadolerite dykes generally trend NNW. Although exposure is poor, the metadolerite appears to be less extensively sheared, and the country rock more extensively sheared than in the Canning Tunnel. Shear zones up to one metre wide, and varying in trend from NW to NE, are also common in the country rock. General movement directions could not be established because of insufficient evidence.

Around the Burekup dam site the metadolerite dykes generally trend NE. Movement directions in shear zones were determined by the alignment of microcline porphyroclasts, offsetting of metadolerite dykes, shear-step structures developed in quartz

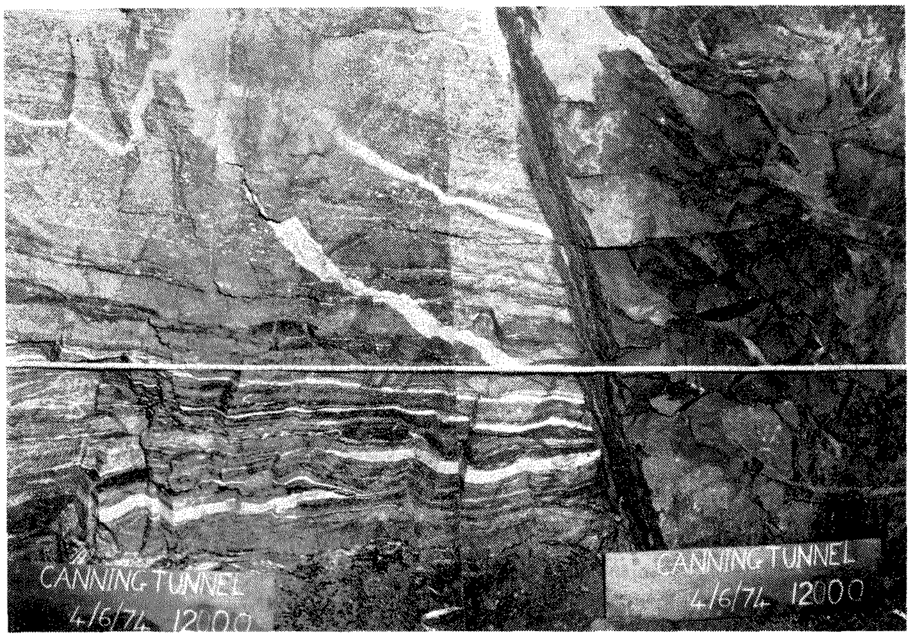

3682·45 m

3684·91 m

Figure 14. Canning Tunnel—sheared, westerly dipping margin of metadolerite dyke. Country rock is hybrid gneiss.

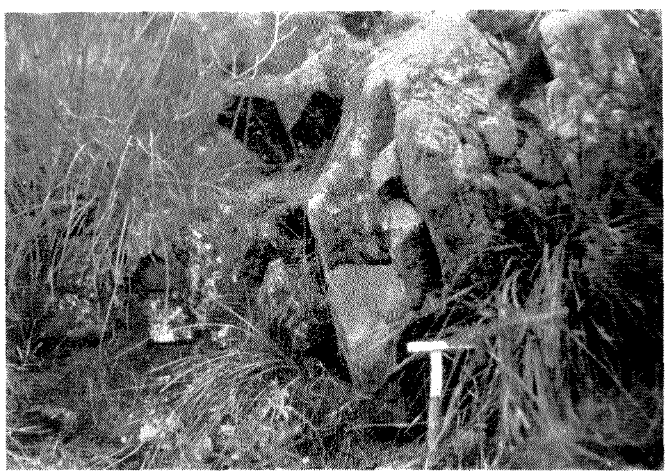

A

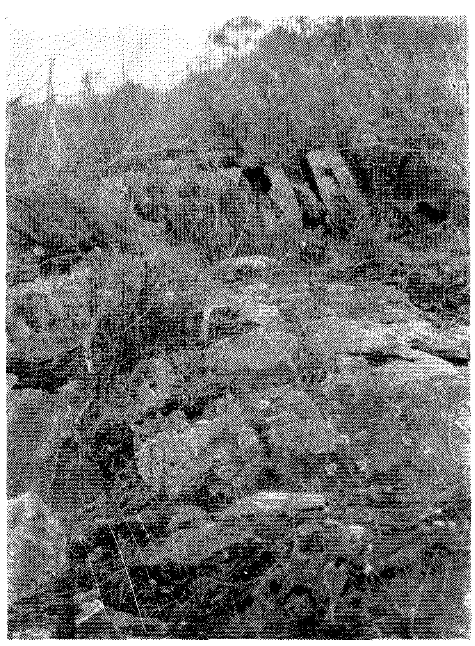

B

Figure 15. Burekup proposed dam site.

A. Right bank—shear zone in margin of metadolerite dyke and adjacent country rock.

B. Left bank—shear zone in country rock adjacent to metadolerite dyke.

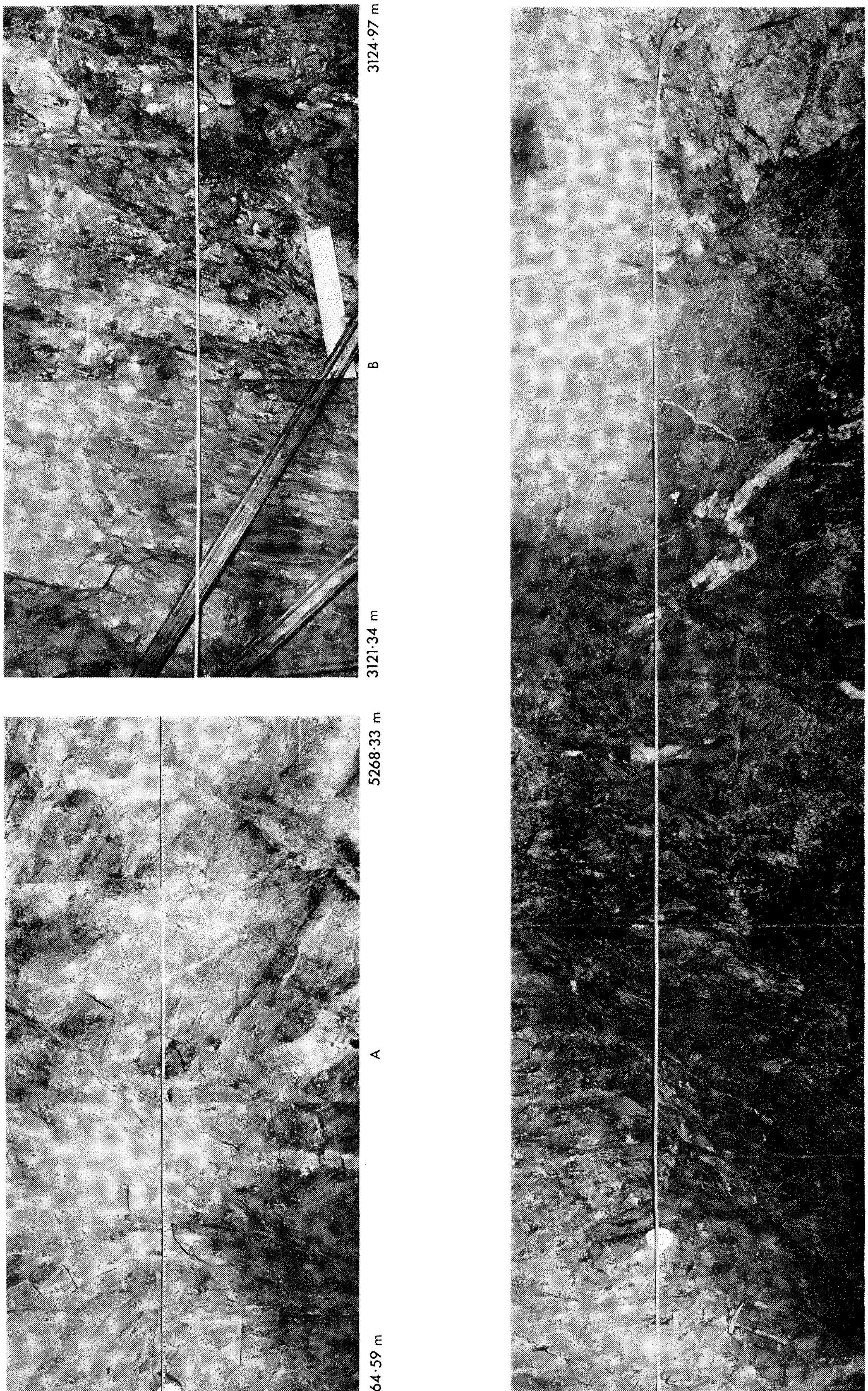

Figure 16. Canning Tunne

A. Thin, sheared, easterly dipping metadolerite dyke. West-block down movement is indicated by dragging of gneissic foliation in adjacent country rock.
B. Part of metadolerite dyke sheared to chloritic schist. This zone required temporary rib support during excavation, and later, reinforced concrete lining.
C. Extensively sheared metadolerite dyke margin which required pneumatically applied mortar.

Note: All Canning Tunnel wall photographs are of the south wall, and distances are from the Canning portal.

veins, and rare slickensiding. One set of shear zones occurs in the margins of the metadolerite dykes and in the adjacent country rock, the movement being generally strike-slip, with some NW blocks having moved northward and others southward. In a second set trending NW, the NE blocks moved northward, and some dykes are offset.

PETROLOGY

Rocks occurring in shear zones are known as metamorphic tectonites. A tectonite is a deformed rock the fabric of which is due to the systematic movement of the individual components under a common external force (Spencer, 1969, p. 137). Various aspects of deformational processes and textures have been discussed by writers such as Spry, 1963; Turner and Weiss, 1963; Spencer, 1969 and Stauffer, 1970.

Deformation by applied stress occurs in two ways (Williams and others, 1954, p. 199). Direct (cataclastic) componental movements are favoured by rapid deformation at low temperatures, and relatively low confining pressures. Indirect (crystalloblastic) componental movements are most effective at high temperatures, under prolonged stress with available chemically active pore fluids, and where stress-unstable minerals occur in the parent rock.

Stauffer (1969) has divided deformational processes into fracture (low temperature), recrystallization (high temperature), intergranular dislocation (low-intergranular cohesion) and crystallographic glide (high-intergranular cohesion). Each process produces distinctive structures and textures.

Tectonites formed in shear zones along the Darling Range are divisible into deformed dolerites and deformed country rock. Ideally the margins of dolerite dykes would be expected to have a higher shear strength than the gneissic country rock. This is supported by uniaxial compressive strength tests done by the Snowy Mountains Engineering Corporation (1972). However, in the Canning Tunnel the metadolerite is more intensely sheared. It appears that the deformation was accompanied by high hydrothermal activity, producing uralitization of pyroxene in the dolerite, concomitant quartz-epidote veining and sulphide mineralization. Some shear zones contain abundant epidote.

Around Burekup hydrothermal activity in the dyke rock was less than in the Canning Tunnel, and more intense shearing occurred in the country rock (Figs. 15A and B). The rocks of this area appear to have been subjected to the physical conditions of the upper amphibolite or lower granulite facies. The gneisses have been recrystallized in this facies, and recrystallization has penetrated part way into the dykes. This is shown by garnet porphyroblasts in the fine-grained rock at dyke margins, and by recrystallized pyroxene. Recrystallization is also indicated by granofelsic transition zones which are coarser than primary dolerite, and have an increasingly doleritic texture and mafic composition towards the centres of dykes. The country rock is a pyroxene bearing, porphyroblastic, microcline gneiss, often with large pseudomorphs of myrmekitic plagioclase after the microcline. The formation of the shear zones appears to have accompanied the metamorphism.

Around North Dandalup the physical conditions affecting deformational processes were between those of the Canning Tunnel and Burekup areas. Quartz mylonites are well developed in several shear zones.

TECTONITES DERIVED FROM DEFORMATION OF DOLERITES

Petrologically the dolerites of the Darling Range area are metadolerites, as shown by alteration of the original texture and mineralogy. The dolerite deformed under shear cleavage with strong indirect componental movements. In the Canning Tunnel there are two general tectonite sequences from the centres of dykes towards the contacts:

(1) Metadolerite → lepidoblastic hornblende schist → lepidoblastic biotite schist → chloritic schist.

(2) Metadolerite → nematoblastic actinolite schist → chloritic schist.

Deformational mechanisms in the first sequence included fracture, recrystallization to more stress-stable mineral assemblages and crystallographic glide. In the actinolite-schist stage, of the second sequence, a strong intergranular dislocation component produced extensive mylonitization of the plagioclase. The chloritic schist generally forms a thin veneer at the contacts.

Around Burekup shearing reached several metres into dyke margins. The tectonite formed is a lepidoblastic hornblende schist which becomes distinctly more leucocratic towards the contacts with the country rock.

TECTONITES DERIVED FROM DEFORMATION OF COUNTRY ROCK

Strong deformation of country rock occurred in the Burekup area under both direct and indirect componental movements. The general tectonite sequence towards the contacts is:

Porphyroblastic gneiss → porphyroclastic augen gneiss → augen schist → lepidoblastic mica schist.

Deformation mechanisms included fracture, intergranular dislocation, recrystallization and crystallographic glide. Goatee texture, caused by intergranular dislocation of microcline porphyroblasts, is well defined. This texture results when material is plucked from the ends of competent granules and incorporated into the strain shadows.

At North Dandalup the country rock is a microcline bearing granitic gneiss, and fracture and intergranular dislocation mechanisms have predominated in rock deformation. Shearing is not as extensive in the metadolerite as around the Canning Tunnel area, nor as extensive in the country rock as around Burekup. Shear zones not adjacent to dykes are common, and occur as intensely fractured zones up to a metre in width, whereas at Burekup they have strong mylonitic lamination or strong alignment of microcline porphyroclasts.

CONCLUSIONS

The general northerly trend of the metadolerite dykes suggests strong east-west tensional forces of a regional scale during intrusion. In the Canning Tunnel, which trends at 292° for most of its length, 28 per cent of excavated rock was metadolerite. Most of the dykes trend NNW and therefore volumetric dilation caused by magmatic intrusion would appear to have been close to this percentage.

Intrusion was followed by metamorphism and tectonism. Textural and mineralogical changes in the dolerite and country rock indicate increasing metamorphic grade southwards from the Canning Tunnel area to the Burekup area.

Tectonism is recognized by the shear zones. In the Canning Tunnel area the intense shearing of dolerite dyke margins was accompanied by high prevailing hydrothermal activity. Southwards to Burekup the more intense shearing of the country rock than the dolerite was accompanied by an increasing grade of metamorphism, and decreasing effect of hydrothermal activity. In zones not adjacent to contacts between metadolerite and country rocks shearing increases in intensity southwards to Burekup. In the Canning Tunnel area, the dip-slip, west-block down movements, indicate east-west tensional forces. A secondary strike-slip component also occurs. Around Burekup strong transcurrent forces resulted in strike-slip movement. Although some west blocks show northward and others show southward movements, more information is required from this area, and farther southwards, to clarify the tectonic trends.

This metamorphism and tectonism, which occurred in the late Precambrian, could have provided the impetus for the development of the Perth Basin in the Palaeozoic.

ENGINEERING SIGNIFICANCE

Rock weakened by shearing, requires structural support in tunnels, may lead to differential settlement in dam sites, and to rapid erosion in spillways.

Immediate grouting is needed to prevent rapid leakage caused by the downward percolation of water in tunnels. Piping caused by percolation under dams is prevented by constructing cut-offs and grout curtains. Deeply weathered shear zones may require chemical grouting, which is more penetrative in weathered material than is cement grout. Shear zones extending from reservoirs to spillways require special measures to prevent foundation uplift caused by build up of pore pressures.

Shear zones directly assist in differential weathering by forming pathways for the downward percolation of water, and extend deep weathering into the country rock along joints and foliation planes. Sheet joints, which are common in country rock along the Darling Range, actively extend weathering. Penetration of water along gneissic foliation planes causes selective weathering of dark bands followed by the decay of feldspars in light bands.

Metadolerite dykes and shear zones have had a strong influence on the topography of the Darling Range area. Dykes often form ridges with gully development at contacts. This process is assisted by the presence of sheared margins. Completely sheared dykes may form saddles. Variations in topographic expression, caused by numerous factors, occur. These include gullies eroded along thin dykes, regardless of degree of shearing, deflection of water-courses along resistant dykes, terracing formed by dykes parallel to the slopes. Dykes with clay-filled joints form barriers to underground water flow, resulting in deeper weathering on the upslope sides of dykes.

Mechanical weathering of metadolerite dykes has formed bouldery metadolerite outcrops, and where chemical weathering is acute also forms reddish doleritic soil. Chemical weathering reduces the surface exposure of metadolerite. The end product is the laterite cap, covering both the metadolerite and the country rock. The localized weathering product of sheared dolerite is often greenish chloritic clay. Micaceous clay results from weathering of sheared country rock.

Shear zones which required remedial work were encountered in the construction of the South Dandalup Dam and the Canning Tunnel.

SOUTH DANDALUP DAM

Geological investigation of the excavated foundation area for the South Dandalup Dam was done by Marcos (1971). Irregular weathering observed during excavation is related to geological structures. Shear zones are common in the granitic gneiss, and vary in width from 2.5 mm to 0.6 m. Shearing of metadolerite dyke margins also occurs. The exposure of shears, faults, and joints during excavation meant more excavation and remedial work, including grouting, than was expected. A double line of curtain grout holes were necessary in several zones of weakness. Faulting accompanied by shearing and hydrothermal activity in a zone about 3 m wide, required special grouting and concrete work.

CANNING TUNNEL

The 5.5 km long Canning Tunnel was constructed to increase the rate of delivery of water from the Canning Dam to the Perth metropolitan area.

Weathered rock generally requires temporary support during excavation. Steel ribbing with timber lagging and cribbing was used at both ends of the tunnel. Ribbing was extended 56 m into the tunnel at the Canning Dam end, and 18 m at the Roleystone end. The greater distance of weathered rock at the Canning heading is due to the steeply dipping gneissic foliation (60° to 80° E), and the sheared metadolerite dyke margin 44 m in from the portal. These structures have facilitated deeper percolation of water. At the Roleystone heading the more gently dipping gneissic foliation (24° W), and the less sheared metadolerite margin 16 m into the tunnel, have resulted in less weathering of both the metadolerite and the gneiss.

Leaking shear zones and joints in the tunnel did not warrant immediate grouting. Although the degree of weathering in shear zones is variable, temporary rib support was required in only one shear zone.

Because water flows through the tunnel steel liners surrounded by concrete were extended, from the portals into the tunnel, to where the weight of vertical ground cover approximately equals the maximum hydrostatic head. The length was 152.70 m at the Canning end (115.82 m of steel liners and 36.88 m of reinforced concrete) and 275.84 m at the Roleystone end. Elsewhere in the tunnel most of the lining treatment was needed for sheared dolerite (Fig. 16B and C). Lining treatments, excluding portal areas, and distances covered are given below:

Rock Type	Pinned mesh and pneumatically applied mortar	Concrete lining	Concrete lining reinforced with steel sets
Granitic complex (includes shear zones, cavities and completely altered zones)	14·02 m	6·10 m	....
Metadolerite (shear zones)	100·58 m	39·01 m	14·63 m

REFERENCES

Compston, W., and Arriens, P.A., 1968, The Precambrian geochronology of Australia: Canadian Jour. of Earth Sciences, v. 5, p. 561-583.

Klenowski, G., 1973, The geology of the Canning Dam-Roleystone Tunnel, Western Australia: Univ. West. Australia Hons. thesis (unpublished).

——— 1974, Burekup proposed dam site, Collie River. Geological investigation progress report: West. Australia Geol. Survey Rec. 1974/21 (unpublished).

——— in prep., North Dandalup proposed dam site, North Dandalup River. Geological report: West. Australia Geol. Survey Rec.

Marcos, G., 1971, South Dandalup Dam: report on geological conditions as exposed by excavation during construction: West. Australia Geol. Survey. Rec. 1971/20 (unpublished).

Snowy Mountains Engineering Corporation, 1972, Canning Tunnel: report on geology. Contract No. 1745: Metropolitan Water Supply, Sewerage and Drainage Board, Perth, W.A., p. 14 (unpublished).

Spencer, E. W., 1969, Introduction to the structure of the earth: McGraw-Hill, New York.

Spry, A., 1963, The chronological analysis of crystallization and deformation of some Tasmanian Precambrian rocks: Geol. Soc. Australia Jour., v. 10, p. 193-208.

Stauffer, M. R., 1970, Deformation textures in tectonites: Canadian Jour. of Earth Sciences, v. 7, p. 498-511.

Turner, F. J., and Weiss, L. E., 1963, Structural analysis of metamorphic tectonites: McGraw-Hill, New York.

Williams, H., Turner, F. J., and Gilbert, C. M., 1954, Petrography: W. H. Freeman and Co., San Francisco.

Wilson, A. F., Compston, W., Jeffery, P. M. and Riley, G. H., 1958, Radioactive ages from the Precambrian rocks in Australia: Geol. Soc Australia Journ., v. 6, p. 179-195.

PETROLEUM EXPLORATION IN WESTERN AUSTRALIA IN 1974

by G. H. Low

ABSTRACT

The downward trend in petroleum exploration activity in Western Australia which has been evident since 1972 continued in 1974. The number of test wells completed was 20 per cent less, and land seismic and marine seismic activity was 69 per cent and 21 per cent respectively, less than the 1973 figure.

Most drilling activity was in the offshore Carnarvon and Canning Basins. A few offshore wells were drilled in the Bremer, Perth, Carnarvon and Canning Basins.

Twenty-one wells of all types were completed during the year (excluding Hilda No. 1 which was abandoned above the objective formations, at a total depth of 1 546 m, because of unsatisfactory hole conditions) for a total of 46 626 m of drilling. Geophysical activity consisted of land and marine seismic surveys, one aeromagnetic survey, and limited gravity and surface geological surveys.

During the year onshore tenements in the Officer, Canning, Carnarvon, and Perth Basins, and offshore areas in the Eucla, Perth, Carnarvon and Canning Basins were surrendered, relinquished or cancelled. Surrender was pending in several other offshore and onshore areas at the end of the year.

INTRODUCTION

Exploratory drilling carried out in the search for petroleum in Western Australia over the past two years is shown in the following tabulation:

	Wells completed 1973	Wells completed 1974	Wells drilling on 31st December 1973	Wells drilling on 31st December 1974
New field wildcat wells	16	15*	2	0
Extension test wells	3	1	0	0
Deeper pool test wells	1	0	0	0
Development wells	0	1	0	0
Stratigraphic wells	2	4	1	0
	22	21	3	0

Total effective drilling : 1973—63 612 m
1974—46 626 m*

* The aborted new field wildcat well Hilda No. 1, which reached a total depth of 1 546 m, is not included in these figures.

Three successful wells were completed during 1974. Lambert No. 1 was a successful test of a new structure in the offshore Carnarvon Basin and is classified as a gas and condensate discovery. West Tryal Rocks No. 2, an extension test step-out located 3.6 km northeast of the discovery well, encountered the same gas-bearing sands about 130 m higher than the first well. Dongara No. 20 was successfully completed as a development well, in the Dongara gas field, located in the northern Perth Basin.

Geophysical survey and surface geological survey activity also declined compared with 1973. The totals for 1974 are as follows (with the 1973 figures in brackets):

Type of Survey	Line km	Party months or geologist month
Land seismic	559 (1 776)	....
Marine seismic	11 815 (14 904)	....
Gravity (land)	....	1·0 (7·0)
Aeromagnetic	6 373 (Nil)	....
Geological	....	3·0 (3·5)

PETROLEUM TENEMENTS

During the year two offshore tenements in the Eucla Basin were cancelled, and partial relinquishments of tenements were made in the offshore Perth, Carnarvon and Canning Basins. Surrenders of other offshore tenements in the Perth, Carnarvon, Canning and Officer Basins have either been completed or are pending. Large areas are currently available for application.

Petroleum tenements current on December 31st 1974 are shown in Figure 17, and the following tabulation lists details of the various holdings:

(3)—46009

PETROLEUM TENEMENTS UNDER THE PETROLEUM (SUBMERGED LANDS) ACT, 1967

Exploration Permits

Number	No. of graticular sections	Expiry date of current term	Registered holder or applicant
WA- 1-P	....	....	Woodside Oil N.L., Shell Development (Aust.) Pty. Ltd., B.O.C. of Australia Ltd.
R1	178	14/11/79	
*WA -2-P	....	....	,, ,, ,, ,,
*WA- 7-P	....	....	,, ,, ,, ,,
WA-13-P	....	....	West Australian Petroleum Pty. Ltd.
R1 Part 1 110 / R1 Part 2 84	194	29/8/79	
WA-14-P	....	....	
R1 Part 1 77 / R1 Part 2 121	198	29/8/79	,, ,, ,, ,,
WA-15-P	352	20/3/75	Arco Aust. Ltd., Australian Aquitaine Petroleum Pty. Ltd. Esso Exploration & Production Aust. Inc. Alliance Oil Development Aust. N.L.
WA-16-P	354	16/4/75	
WA-17-P	378	22/4/75	
WA-18-P	322	16/4/75	
WA-19-P	142	20/3/75	
WA-20-P	....	....	West Australian Petroleum Pty. Ltd.
R1	15	10/10/79	
*WA-21-P	....	....	
WA-23-P	....	....	
R1	199	3/10/79	
WA-24-P	....	....	
R1	104	17/10/79	
WA-25-P	....	....	
R1	128	16/10/79	
WA-26-P	400	22/12/74	Canadian Superior Oil (Aust.) Pty., Ltd., Australian Superior Oil Co. Ltd., Phillips Australian Oil Co., Sunray Australian Oil Co. Inc., Genoa Oil N.L., Pexa Oil N.L., Hartog Oil N.L., Flinders Petroleum N.L., Crusader Oil N.L.
WA-27-P	294	18/5/75	
WA-28-P	375	24/3/75	Woodside Oil N.L., Shell Development (Aust.) Pty. Ltd., B.O.C. of Australia Ltd.
WA-29-P	400	18/5/75	Woodside Oil N.L., Shell Development (Aust.) Pty. Ltd., B.O.C. of Australia Ltd.
WA-30-P	400	2/7/75	Woodside Oil N.L., Shell Development (Aust.) Pty. Ltd., B.O.C. of Australia Ltd.
WA-31-P	400	18/5/75	Woodside Oil N.L., Shell Development (Aust.) Pty. Ltd., B.O.C. of Australia Ltd.
WA-32-P	395	2/7/75	Woodside Oil N.L., Shell Development (Aust.) Pty. Ltd., B.O.C. of Australia Ltd.
WA-33-P	389	18/5/75	Woodside Oil N.L., Shell Development (Aust.) Pty. Ltd., B.O.C. of Australia Ltd.
WA-34-P	397	2/7/75	
WA-35-P	400	2/7/75	
WA-36-P	57	18/5/75	
WA-37-P	118	2/6/75	,, ,, ,, ,,
*WA-39-P			
WA-40-P	102	12/3/75	BP Petroleum Development Aust. Pty. Ltd., Abrolhos Oil N.L.
*WA-50-P	....	....	....
*WA-51-P	....	....	....

* Surrender Pending.

PETROLEUM TENEMENTS UNDER THE PETROLEUM ACT, 1936

Petroleum Leases

Number	Area (square miles)	Expiry date of current term	Holders
1H	100	9/2/88	West Australian Petroleum Pty. Ltd.
H2	100	9/2/88	West Australian Petroleum Pty. Ltd.

PETROLEUM TENEMENTS UNDER THE PETROLEUM ACT, 1967

Exploration Permits

Number	No. of graticular sections	Expiry date of current term	Registered holder or applicant
*EP 3	....	....	....
*EP 5	....	....	West Australian Petroleum Pty. Ltd.
EP 6	199	27/8/75	
EP 7	200	27/8/75	,, ,, ,, ,,
*EP 8	....	....	,, ,, ,, ,,
*EP 9	....	....	,, ,, ,, ,,
EP 13	200	27/8/75	,, ,, ,, ,,
*EP 14	....	....	,, ,, ,, ,,
*EP 15	....	....	,, ,, ,, ,,
EP 17	200	27/8/75	,, ,, ,, ,,
EP 18	86	27/8/75	,, ,, ,, ,,
EP 19	200	27/8/75	,, ,, ,, ,,
*EP 20	....	....	,, ,, ,, ,,
EP 21	90	26/7/75	West Australian Petroleum Pty. Ltd.
EP 23	156	6/8/85	West Australian Petroleum Pty. Ltd.
EP 24	163	6/8/75	West Australian Petroleum Pty. Ltd.
EP 25	96	6/8/75	
EP 26	1	27/8/75	BP Petroleum Development (Aust.) Pty. Ltd.
EP 27	2	19/8/75	
EP 28	4	19/8/75	Abrolhos Oil N.L.
EP 29	7	19/8/75	,, ,, ,, ,,
*EP 31			
EP 32	200	15/4/76	Beach-General Exploration Pty. Ltd., Australian Aquitaine Petroleum Pty. Ltd.
EP 34	1	15/4/76	Woodside Oil N.L., Shell Development (Aust.) Pty. Ltd., B.O.C. of Australia Ltd.
EP 35	1	15/4/76	
EP 36	1	15/4/76	
*EP 37	....	....	....
*EP 38	....	....	....
EP 40	67	26/7/76	West Australian Petroleum Pty. Ltd.
EP 41	180	18/7/76	West Australian Petroleum Pty. Ltd.
EP 42	200	1/9/75	
EP 43	163	1/9/75	,, ,, ,, ,,
EP 44	113	1/9/75	,, ,, ,, ,,
EP 50	110	1/9/75	West Australian Petroleum Pty. Ltd.
EP 54	123	22/9/75	Alliance Oil Development Aust. N.L.
EP 58	200	20/7/76	Associated Australian Resources N.L., Australian Aquitaine Petroleum Pty. Ltd., Abrolhos Oil N.L., Ashburton Oil N.L., Flinders Petroleum N.L., Longreach Oil Ltd., Pursuit Oil N.L.
EP 59	186	18/7/76	
EP 60	2	Appn.	West Australian Petroleum Pty. Ltd.
EP 61	4	19/9/76	
EP 62	8	19/9/76	,, ,, ,, ,,
EP 63	4	19/9/76	,, ,, ,, ,,
EP 64	1	Appn.	,, ,, ,, ,,
EP 65	2	19/9/76	,, ,, ,, ,,
EP 66	1	19/9/76	,, ,, ,, ,,
EP 67	29	25/10/76	,, ,, ,, ,,
EP 68	175	27/7/77	W. I. Robinson
*EP 69	....	....	....
EP 70	71	25/9/77	Associated Australian Resources N.L., Australian Aquitaine Petroleum Pty. Ltd., Abrolhos Oil N.L., Ashburton Oil N.L., Flinders Petroleum N.L., Longreach Oil Ltd., Pursuit Oil N.L.
EP 71	81	6/7/77	Coastal Petroleum N.L.
EP 85	4	Appn.	Endeavour Oil Co. N.L., Target Minerals Pty. Ltd., Beaver Exploration N.L., Tricentrol (Aust.) Ltd.
EP 86	118	Appn.	XLX N.L.

* Surrender Pending.

Production Licences

PL 1	5	24/10/92	West Australian Petroleum Pty. Ltd.
PL 2	4	24/10/92	
*PL 3	....	....	....

* Surrender Pending

PETROLEUM TENEMENTS UNDER THE PETROLEUM PIPELINES ACT, 1969

Pipeline Licenses

Number	Expiry date current term	Registered holder or applicant
1	1/12/91	California Asiatic Oil Co., Texaco Overseas Petroleum Co., Shell Development (Aust.) Pty. Ltd., Ampol Exploration Ltd.
2	1/12/91	,, ,, ,, ,, ,,
3	1/12/91	,, ,, ,, ,, ,,
4	1/12/91	,, ,, ,, ,, ,,
5	1/12/91	,, ,, ,, ,, ,,

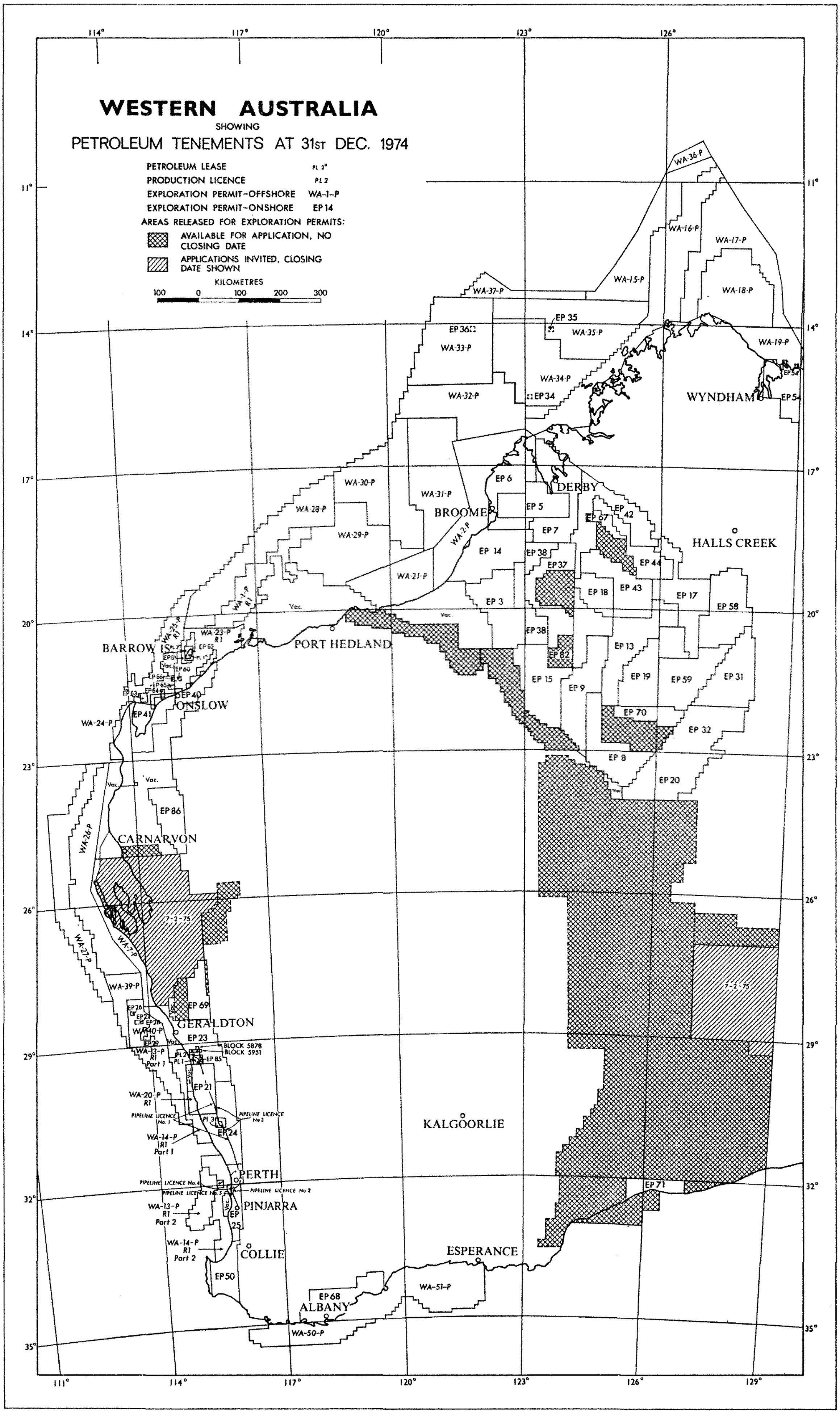

Figure 17. Petroleum tenements at 31st December, 1974.

DRILLING

The positions of wells drilled for petroleum exploration in Western Australia during 1974 are shown in Figures 18 and 19. Details relating to the wells drilled during the year are given in Table 7. All the petroleum exploration wells drilled in Western Australia up to the end of 1974 are listed in Geological Survey Record 1975/1. A summary of the principal results of the drilling in each basin during the year is as follows:

PERTH BASIN

Barragoon No. 1 was located in the central onshore Perth Basin to test an anticlinal closure indicated by seismic data, and to investigate the stratigraphy of a possible onshore extension of a high structural trend from the offshore Vlaming Sub-basin. The well was abandoned as a dry hole after reaching a total depth of 2 335 m in Upper Jurassic Yarragadee Formation. No shows of oil or gas were encountered.

Coomallo No. 1 was drilled to test the potential of an anticlinal fault block on the west flank of the Dandaragan Trough. The well bottomed in the Cattamarra Coal Measures Member of the Lower Jurassic Cockleshell Gully Formation at a total depth of 3 520 m and was abandoned as a dry hole. The small gas shows obtained were confined to coal seams (Fig. 18).

Dongara No. 20 was successfully completed as an in-fill development gas well in the onshore Dongara gas field.

CARNARVON BASIN

Three wells were completed by the B.O.C. group in the Carnarvon Basin during 1974. Lowendal No. 1 and Hampton No. 1 were new-field wildcat tests on the southwestern extension of the Rankin Platform and on the Enderby Trend in the Dampier Sub-basin respectively. No significant hydrocarbon shows were recorded in Lowendal No. 1. A drill-stem test of a gas show in Hampton No. 1, over the interval 535 to 565 m, gave an average flow rate of 3 410 m^3/day accompanied by 46.7 barrels of water per day. Both wells were plugged and abandoned.

Lambert No. 1 was drilled by the B.O.C. group in the northern part of the Dampier Sub-basin, about 17 km west of the Angel gas field and about 32 km northeast of the North Rankin gas field. A drill-stem test conducted over the interval 3 101 to 3 106 m flowed 51° A.P.I. gravity oil, at an average rate of 374 barrels per day, and gas at an average rate of 2 577 m^3/day. The test was carried out through a $\frac{3}{4}$ inch bottom-hole choke. The well is classified as an abandoned oil and gas discovery.

WAPET completed two offshore tests and two onshore stratigraphic wells in 1974. Hilda No. 1A completed the test of a faulted anticlinal structure, about 75 km southwest of the Barrow Island oil field, after the Hilda No. 1 well was abandoned above the target depth because of bad hold conditions. A minor show of oil (A.P.I. gravity 55°) and gas in the basal sand of the Lower Cretaceous Muredong Shale was tested by a formation interval test at 2 669 m. The hole was subsequently plugged and abandoned.

West Tryal Rocks No. 2 was a successful extension test, drilled on the structure discovered in 1973 in the No. 1 well. Two gas and condensate sands were successfully tested by drill-stem tests. The first test over the interval 3 435 to 3 450 m, in a sand that extends between 3 411 and 3 473 m, flowed gas at rates ranging from approximately 255 to 311 x 10^3 m^3/day, with 150 barrels of condensate per day. The second test covered the interval 3 295 to 3 305 m in a sand extending from 3 274 to 3 320 m, and flowed gas at a rate of approximately 436 x 10^3 m^3/day with 221 barrels of condensate per day on a $\frac{1}{2}$ inch choke. The well has been plugged and abandoned.

Onshore in the Robe River area, overlying the Peedamullah Shelf, WAPET drilled twin wells alongside Windoo No. 1 and Mardie No. 1 to obtain cores for more detailed study of gas and oil showings obtained from Lower Cretaceous reservoirs. Both of the twin wells flowed small amounts of gas. Reservoir studies to evaluate the liquid hydrocarbon potential of the area are continuing.

CANNING BASIN

The B.O.C. group drilled three offshore wells in the Canning Basin in 1974, Depuch No. 1, Minilya No. 1 and Poissonnier No. 1. No significant hydrocarbon shows were encountered and the three wells were abandoned as dry holes.

Jones Range No. 1, drilled by WAPET to test an onshore structure on the southwestern flank of the Fitzroy Trough near the edge of the Broome Platform, was also dry and was abandoned.

BROWSE BASIN

The B.O.C. group tested the Heywood, Lombardina, and Prudhoe structures in the Browse Basin with new field wildcat wells during 1974. Heywood No. 1 had minor gas and oil showings but the other two wells were dry. All three wells were abandoned.

BREMER BASIN

Silfar Pty. Ltd. completed two stratigraphic wells (both dry), Kendenup No. 1 and Sunday Swamp No. 1, in the onshore Bremer Basin. Kendenup No. 1 was abandoned and Sunday Swamp No. 1 was completed as a water well.

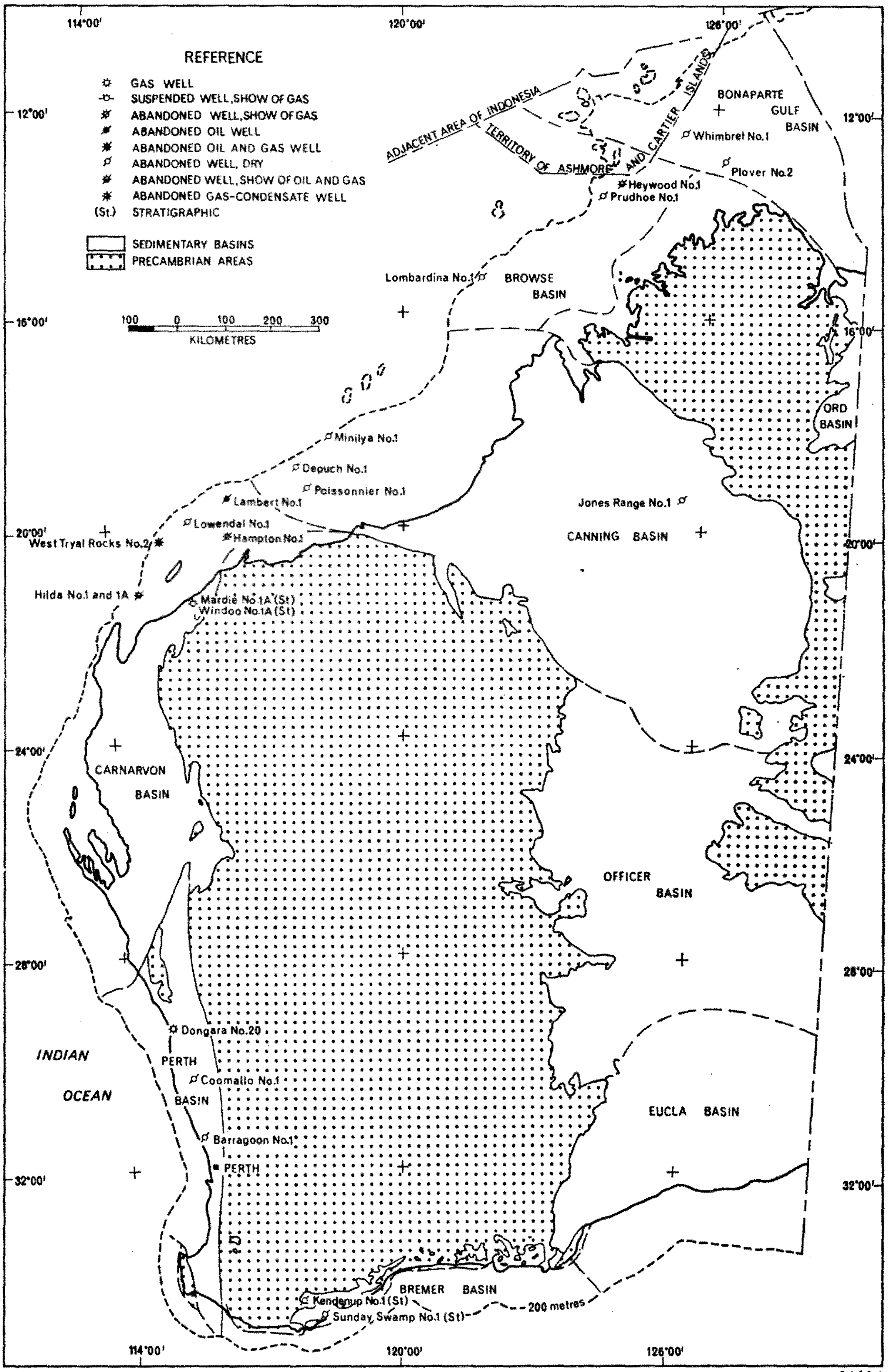

Figure 18. Wells drilled for petroleum exploration in Western Australia during 1974.

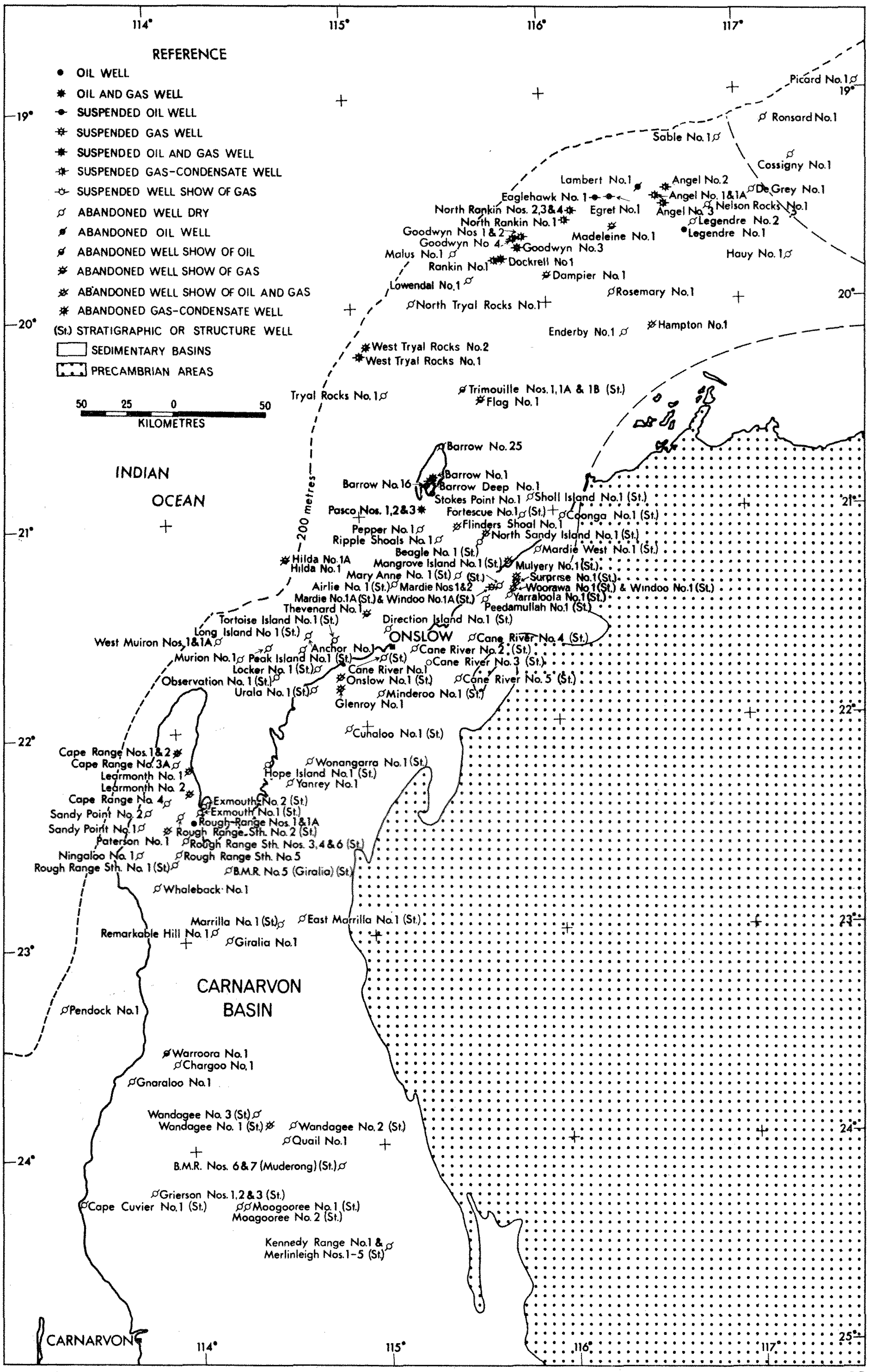

14685

Figure 19. Northern Carnarvon and southwestern Canning Basins showing wells drilled for petroleum to 31st December, 1974.

TABLE 7. WELLS DRILLED FOR PETROLEUM EXPLORATION IN WESTERN AUSTRALIA DURING 1974

Basin	Well	*Subsidized	Concession	Operating Company	Type	Position: Latitude South ° ′ ″	Position: Longitude East ° ′ ″	Elevation and water depth (metres): G.L.	Elevation and water depth (metres): R.T.	Elevation and water depth (metres): W.D.	Dates: Commenced	Dates: Reached T.D.	Dates: Rig released	Total depth (or depth reached) m	Bottomed in	Status on 31 Dec., 1974
PERTH	Barragoon No. 1	*	EP–24	WAPET	NFW	31 21 40	115 35 09	35·8	39·8	....	31/3/74	20/4/74	22/4/74	2 335	U. Jurassic	Dry, P & A
	Coomallo No. 1	*	EP–21	WAPET	NFW	30 14 55	115 24 57	253·0	258·0	....	17/1/74	25/2/74	28/2/74	3 526	L. Jurassic	Dry, P & A
	Dongara No. 20	....	P.L.1	WAPET	DEV	29 16 03	115 01 18	76·3	80·9	....	7/6/74	12/7/74	20/7/74	1 939	....	Gas well
CARNARVON	Hampton No. 1	....	WA–1–P	B.O.C.	NFW	20 07 04	116 32 47	....	30·0	53·0	22/3/74	17/4/74	24/4/74	2 584	....	Gas show, P & A
	Hilda No. 1	*	WA–25–P	WAPET	NFW	21 12 01	114 38 12	....	12·0	145·0	10/3/74	22/3/74	28/4/74	1 546	Tertiary	Dry, P & A
	Hilda No. 1A	*	WA–25–P	WAPET	NFW	21 11 59	114 38 13	....	12·0	145·0	29/4/74	20/9/74	28/9/74	3 466	U. Triassic	Gas and oil show, P & A
	Lambert No. 1	....	W.A.–28–P	B.O.C.	NFW	19 27 23	116 29 23	....	10·0	125·0	13/11/73	24/1/74	3/2/74	3 700	....	Oil & gas well, P & A
	Lowendal No. 1	....	WA–28–P	B.O.C.	NFW	19 52 48	115 38 02	....	30·0	85·0	31/1/74	15/3/74	21/3/74	3 642	....	Dry, P & A
	Mardie No. 1A	....	EP–40	WAPET	STR	21 21 18	115 14 43	6·8	9·4	....	21/11/74	3/12/74	4/12/74	164	....	Gas show suspended
	West Tryal Rocks No. 2	....	WA–25–P	WAPET	EXT	20 12 56	115 03 56	....	12·0	126·0	1/10/74	24/11/74	18/12/74	3 825	....	G & C well, P & A
	Windoo No. 1A	....	EP–40	WAPET	STR	21 21 20	115 40 55	5·2	7·9	....	7/12/74	15/12/74	15/12/74	174	....	Gas show suspended
CANNING	Depuch No. 1	*	W.A.–29–P	B.O.C.	NFW	18 50 07	117 55 19	....	10·0	143·0	4/2/74	30/3/74	3/4/74	4 300	L. Jurassic	Dry, P & A
	Jones Range No. 1	....	EP–43	WAPET	NFW	19 21 43	125 40 09	227·3	231·9	....	30/8/74	2/11/74	6/11/74	2 540	....	Dry, P & A
	Minilya No. 1	....	WA–29–P	B.O.C.	NFW	18 19 29	118 43 57	....	30·0	146·0	4/8/74	30/8/74	5/9/74	2 400	....	Dry, P & A
	Poissonnier No. 1	....	WA–1–P	B.O.C.	NFW	19 18 34	118 09 19	....	30·0	83·0	20/12/73	20/1/74	25/1/74	1 962	....	Dry, P & A
BONAPARTE GULF	Plover No. 2	....	WA–16–P	ARCO	NFW	12 57 29	126 10 28	....	25·3	59·1	10/5/74	19/5/74	23/5/74	1 524	....	Dry, P & A
	Whimbrel No. 1	....	WA–15–P	ARCO	NFW	12 28 59	125 22 40	....	25·3	76·8	5/4/74	4/5/74	8/5/74	2 059	....	Dry, P & A
BREMER	Kendenup No. 1	....	EP–68	SILFAR	STR	34 29 35	117 45 22	159·1	159·4	....	19/12/73	15/1/74	27/1/74	111	....	Dry, P & A
	Sunday Swamp No. 1	....	EP–68	SILFAR	STR	34 45 07	118 17 37	99·0	100·3	....	7/2/74	7/3/74	22/3/74	175	....	Dry; completed as a water well
BROWSE	Heywood No. 1	....	WA–37–P	B.O.C.	NFW	13 27 46	124 04 00	....	10·0	35·0	7/4/74	27/6/74	14/7/74	4 572	....	Gas & oil show, P & A
	Lombardina No. 1	....	WA–32–P	B.O.C.	NFW	15 17 20	121 32 14	....	30·0	175·0	15/5/74	16/7/74	21/7/74	2 855	....	Dry, P & A
	Prudhoe No. 1	....	WA–35–P	B.O.C.	NFW	13 44 56	123 51 51	....	30·0	175·0	13/9/74	1/11/74	12/11/74	3 322	....	Dry, P & A
											Total			52 721		
											Less drilling done in 1973			4 549		
											Total drilling done in 1974			48 172		

ARCO = Arco Australia Ltd.
B.O.C. = B.O.C. of Australia Ltd.
WAPET = West Australian Petroleum Pty. Ltd.
SILFAR = Silfar Pty. Ltd.
DEV = Development well
EXT = Extension test well
G. & C. = Gas and condensate
NFW = New field wildcat well
P. & A. = Plugged and abandoned
STR = Stratigraphic well

GEOPHYSICAL SURVEYS

SEISMIC

During 1974 seismic surveys were conducted in the Perth, Carnarvon, Canning, Browse, and Bonaparte Gulf Basins. Details are as follows:

SEISMIC SURVEYS

Basin	Tenement	Company	Line kilometres	
			Marine	Land
Perth	EP-23	West Australian Petroleum Pty. Ltd.	....	89
,,	EP-24	,, ,, ,,	....	1
,,	PL-1	,, ,, ,,	....	12
,,	WA-12-P	,, ,, ,,	144	....
,,	WA-14-P	,, ,, ,,	268	....
Carnarvon	EP-41	West Australian Petroleum Pty. Ltd.	164	16
,,	PL-1H	,, ,, ,,	....	45
,,	WA-23-P	,, ,, ,,	1 193	....
,,	WA-24-P	,, ,, ,,	588	....
,,	WA-25-P	,, ,, ,,	681	....
,,	PL-2H	,, ,, ,,	12	....
Carnarvon/ Canning	WA-1-P	B.O.C. of Australia Ltd.	1 265	....
	WA-28-P	,, ,, ,,	838	....
Canning	EP-5	West Australian Petroleum Pty. Ltd.	....	11
,,	EP-6	,, ,, ,,	....	142
,,	EP-7	,, ,, ,,	....	8
,,	EP-13	,, ,, ,,	....	81
,,	EP-18	,, ,, ,,	....	54
,,	EP-19	,, ,, ,,	....	81
,,	EP-43	,, ,, ,,	....	2
,,	EP-58/59	Associated Australian Resources N.L.	....	17
,,	WA-29-P	B.O.C. of Australia Ltd.	938	....
,,	WA-30-P	,, ,, ,,	119	....
,,	WA-29-P	Hematite Petroleum Pty. Ltd. (farm-in operator)	683	....
,,	WA-31-P	Amax Petroleum (Aust) Inc. (farm-in operator)	498	....
Browse	WA-32-P	B.O.C. of Australia Ltd.	465	....
,,	WA-33-P	,, ,, ,,	333	....
,,	WA-34-P	,, ,, ,,	1 543	....
,,	WA-35-P	,, ,, ,,	1 010	....
,,	WA-37-P	,, ,, ,,	158	....
Bonaparte Gulf	WA-15-P	Arco Australia Ltd.	213	....
	WA-16-P	,, ,, ,,	247	....
,,	WA-17-P	,, ,, ,,	45	....
,,	WA-19-P	,, ,, ,,	410	....
		Totals	11 815	559

GRAVITY

Gravity surveys were carried out during the year in the Perth and Canning Basins. Details are as follows:

GRAVITY SURVEYS

Basin	Tenement	Company	Party months
Perth	EP-23	West Australian Petroleum Pty. Ltd.	0·2
,,	PL-1	,, ,, ,, ,,	0·1
Canning	EP-6	West Australian Petroleum Pty. Ltd.	0·3
,,	EP-13	,, ,, ,, ,,	0·1
,,	EP-18	,, ,, ,, ,,	0·1
,,	EP-19	,, ,, ,, ,,	0·2
		Total	1·0

MAGNETOMETER

Amax Petroleum (Aust) Inc. conducted 6 373 line kilometres of aeromagnetic survey over part of WA-31-P during 1974.

GEOLOGICAL SURVEYS

West Australia Petroleum Pty. Ltd. carried out surface geological surveys consisting of two geologist-months in the Canning Basin, and one geologist-month in the Carnarvon Basin.

TERTIARY EPEIROGENY IN THE SOUTHERN PART OF WESTERN AUSTRALIA

by R. N. Cope

ABSTRACT

The suggestion that the Darling Plateau has been uplifted since the Eocene was first made 60 years ago, but the relationship of the plateau to surrounding geomorphic units has since received little consideration. It now seems likely that the Darling Plateau surface and its basic drainage pattern were formed during the Cretaceous Period. Evidence from the Blackwood Plateau and the Eucla Basin suggests that uplift took place in at least two main phases, that is, in the Oligocene and the Miocene-Pliocene. There is some evidence that uplift continued into the Quaternary. South of the Darling Plateau the old surface falls regularly to the south coast, and the term Ravensthorpe Ramp is suggested for this geomorphic unit. The hinge line between the two units appears to be a continuation of the Jarrahwood Axis previously described on the Blackwood Plateau; the extension of this term eastwards to cover both areas is therefore proposed. Uplift of the continental interior was accompanied by sagging of the continental margin to form the continental slope. The continental shelf was formed simultaneously by sediment progradation. These events immediately followed the separation of Australia and Antarctica by ocean-floor spreading. A similar history of epeirogenic uplift, development of marginal hinge lines, and peripheral sagging has been reported from South Africa and eastern South America. It is concluded that Cainozoic epeirogeny resulted from forces generated by ocean-floor spreading, although the mechanism is not known.

INTRODUCTION

The hypothesis that the Darling Plateau was uplifted during the Tertiary has been firmly established in the literature for many years (for example, Jutson, 1914, p. 95). However, little consideration has been given to relating the Tertiary tectonic history of the plateau to that of surrounding physiographic provinces such as the Eucla Basin, the south coast area and the Perth Basin. On the west, the Darling Plateau is bounded by the scarp of the Darling Fault. West of the Darling Fault differential erosion has removed all but the youngest geomorphic features so that interpretation of the Tertiary structural history is difficult. To the south, however, there is a gradual transition from the plateau to the continental shelf through the Eucla Basin and what is here termed the Ravensthorpe Ramp.

Interpretation of Western Australian land forms in terms of epeirogeny has been handicapped in the past by the sparsity of elevation control. In recent years, however, partial contoured map coverage has become available at a scale of 1 : 250 000, and since 1970, Royal Australian Survey Corps 1 : 100 000 metric contoured sheets have been published for the western portion of the area under review between Bunbury and Katanning. These data have been assembled to make a generalized contour map representing the plateau surface, if dissection simultaneous with and subsequent to uplift is disregarded (Fig. 20). In compiling this map, use has also been made of the spot heights recorded during the recent B.M.R. helicopter gravity survey (Australia B.M.R., 1969-1972).

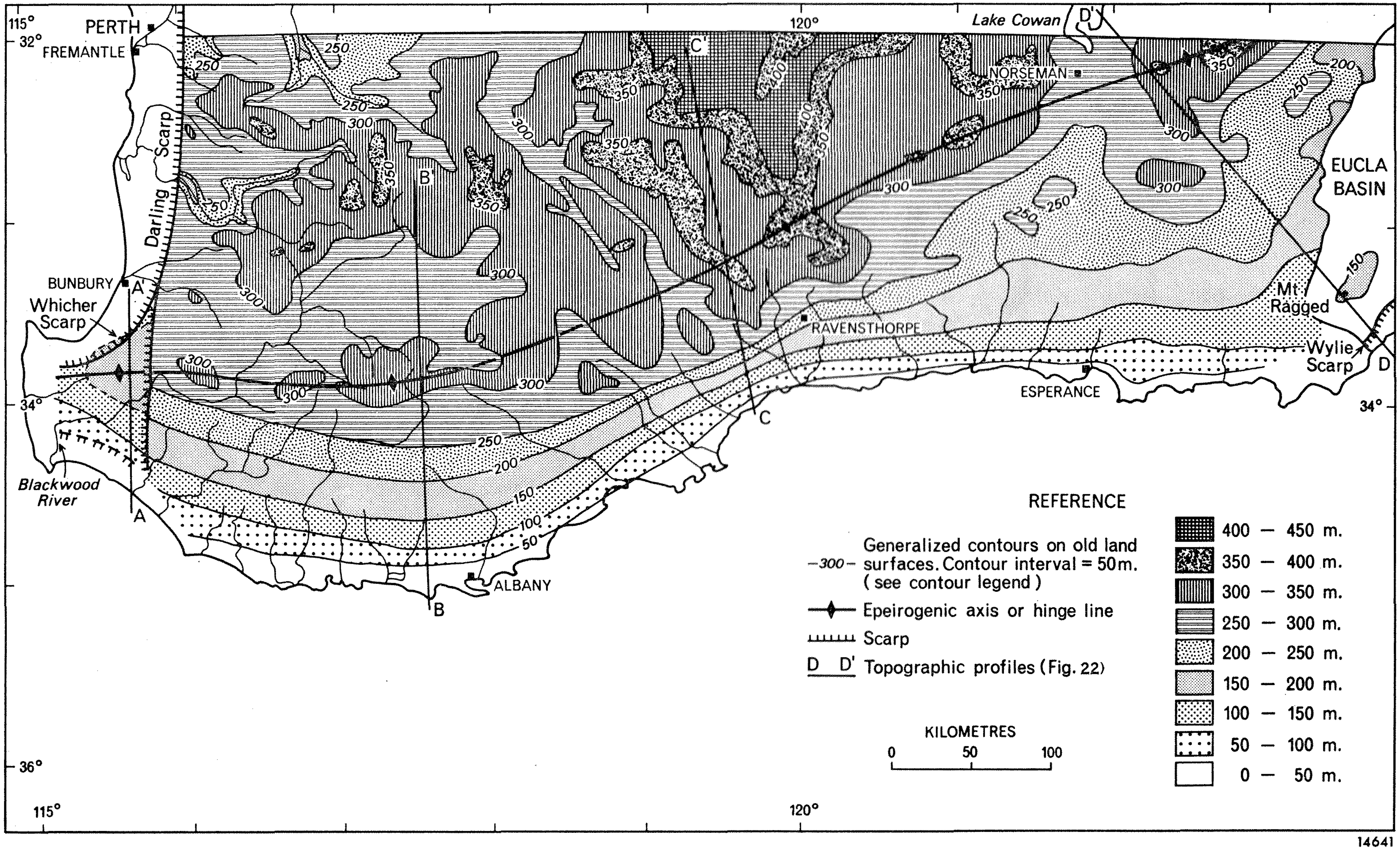

Figure 20. Topographic relief of old land surfaces in the southern part of Western Australia.

The sea floor of the Southern and Indian Oceans has been investigated in recent years. From the magnetic striping and application of the hypothesis of sea-floor spreading it has been suggested that the Antarctic and Australian continents drifted apart in the early Tertiary (McKenzie and Sclater, 1971). In this paper the possible relationship of Tertiary plate movement to epeirogenic uplift is discussed after the evidence from each of the onshore and offshore geomorphic divisions has been reviewed.

ONSHORE GEOMORPHIC SUBDIVISIONS

DARLING PLATEAU

The Darling Plateau in this area and to the north is characterized by a high average elevation, rising from about 300 m in the west to about 400 m in the Eastern Goldfields area (Fig. 20). The highest, and oldest, level is seen in scattered residuals bounded by breakaways (Mount Dale level of Woolnough, 1918) while a somewhat lower level forms an extensive undulating plateau (Jutson, 1914). In the southwestern portion of the Darling Plateau, corresponding with an annual rainfall of over 380 mm, the drainage is incised and this becomes marked on the western margin along the Darling Range.

The ages of the uplifted land surfaces forming the Darling Plateau are not known with certainty. Marine Upper Eocene carbonate sediments are present on the plateau around Lake Cowan, near Norseman (Cockbain, 1968a) and Upper Eocene to Oligocene fluviatile and lacustrine sediments have been encountered in a channel 60 m deep at Coolgardie (Balme and Churchill, 1959). Similar sediments of Eocene age have been encountered at Darkan Swamp, 80 km east-southeast of Perth (Playford and others, in press). Fluviatile clastic sediments are also present in the western part of the area as the Kojonup Sandstone (McWhae and others, 1958), the Nakina Formation (Playford and others, in press) and as un-named deposits in the Newlands area (Lowry, 1965). These sediments are not dated, but an Eocene to Oligocene age appears probable by comparison with the Coolgardie and Darkan Swamp occurrences.

The evidence indicates that the Darling Plateau formed prior to the Early Eocene when it was a semi-mature to mature landscape falling and draining to the south and west (Bunting and others, 1974). Johnstone and others (1973) suggest that the present salt lake system is a relic of the Late Jurassic-Early Cretaceous drainage, the good development of which is said to be attested to by the voluminous sediments of that age in the Perth Basin. However, Late Jurassic to earliest Cretaceous rapid sedimentation in the Perth Basin was followed by major intra-Neocomian uplift of the basin and the long period of tectonic stability lasting some 70 million years between the Late Neocomian and the Early Eocene would seem to be a more likely time during which a mature landscape was developed. Subsequently it was lifted by epeirogenic movement to its present position.

RAVENSTHORPE RAMP

The southern boundary of the Darling Plateau can for the most part conveniently be taken along the major divide parallel to the south coast (Fig. 21). This is illustrated in profiles B-B′ and C-C′ of Figure 22, which ignore later dissection of the old land surface corresponding to the main level of the Darling Plateau. The maximum and minimum regional southerly slopes are about 1 in 150 near Ravensthorpe and about 1 in 600 north of Esperance. There are numerous residual hills and mountain masses rising high above the main surface, the highest of which is the Stirling Range (up to 1 097 m). Marine Eocene rocks occupy depressions on the old land surface and are preserved at elevations of 105 m at Neridup and at about 300 m at Ravensthorpe (Cockbain, 1968b). The rivers draining to the south coast are relatively short and are incised into the tilted surface. At the coast the surface is commonly terminated by cliffs, and in the Esperance area it is modified by a series of erosion benches thought to have been formed during the Pleistocene (Morgan and Peers, 1973).

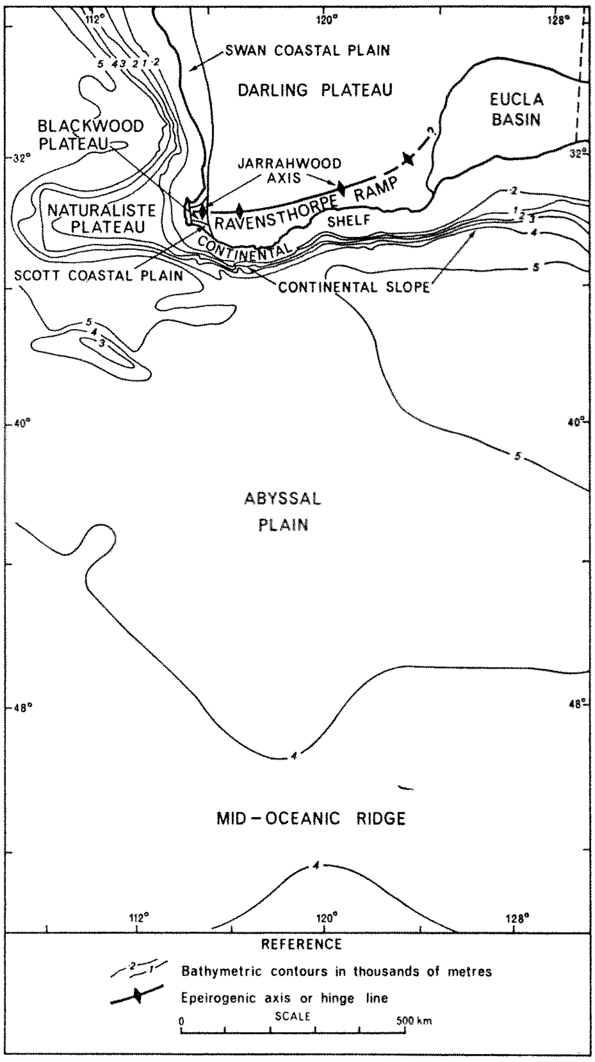

14642

Figure 21. Geomorphic divisions of the southern part of Western Australia and adjacent offshore areas (after Australia, Bureau of Mineral Resources, 1965).

As can be seen from Figures 20 and 22 the boundary between the Darling Plateau and the Ravensthorpe Ramp is a hinge line or epeirogenic axis. There appears to be a slight reversal of dip to the north of the axis, but the available information is not sufficiently detailed to illustrate this clearly.

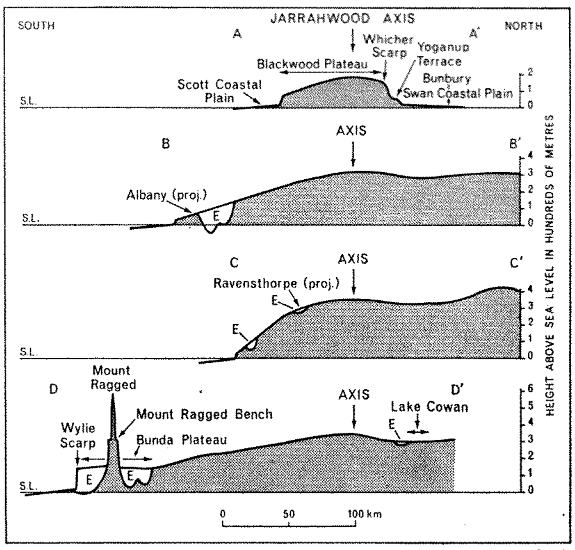

14643

Figure 22. Generalized topographic profiles approximately perpendicular to the south coast. Vertical exaggeration = x 125. E=Eocene marine deposits. For location of profiles see Figure 20.

EUCLA BASIN

The Eucla Basin contains a relatively thick sequence of dated marine Tertiary rocks and thus may be expected to provide important clues to Tertiary tectonic history (Lowry, 1970). Although the present uplifted land surface (the Bunda Plateau) lies at about 100 to 250 m, the basement surface on which the Eocene rests and with which the Darling Plateau and the Ravensthorpe Ramp are thought to be equivalent, lies between —300 m and +150 m beneath the mainland portion of the basin in Western Australia (Lowry, 1970, p. 17 and 145). Allowing for the depth of deposition below sea level of the Eocene formations, clearly there was subsidence during the Early Miocene to accommodate the Abrakurrie Limestone and later epeirogenic uplift to bring it to the level of the Bunda Plateau.

The approximate history of epeirogenic movement has been suggested by Lowry (1970, Fig. 51), who infers two main phases of uplift, in the Oligocene and Middle Miocene. There is no evidence of Miocene subsidence in the Ravensthorpe Ramp, but the Eucla Basin stratigraphy could be duplicated beneath the continental shelf to the south. By analogy with the Eucla Basin epeirogenic uplift of the Darling Plateau may have taken place in the Oligocene or Middle Miocene or in part during each of these times.

The relationship of the southeastern corner of the Darling Plateau and the Ravensthorpe Ramp to the Eocene sediments of the Eucla Basin is shown in Figure 22, D-D′. This illustrates that Tertiary deposition took place on a highly irregular surface, that uplift is post-Eocene and that the pre-Eocene land surface has been modified by post-Eocene planing, probably during the earlier stages of uplift.

The Mount Ragged Bench at about 300 m is thought by Lowry (1970, p. 156) to mark the Late Eocene sea level. However, the relative elevations would thereby imply deposition of the Toolinna Limestone at Wylie Scarp in water depths of about 150 to 275 m rather than in the range of 46 to 92 m Lowry suggests as being appropriate (p. 76). The Mount Ragged Bench is considered here to be a remnant of an earlier erosion cycle, possibly corresponding to the Mount Dale Level in the Eastern Goldfields.

BLACKWOOD PLATEAU

The nature of the Blackwood Plateau has been outlined in a previous paper (Cope, 1972) where it was concluded that an old semi-mature land surface was uplifted along the east-trending Jarrahwood Axis in the middle to late Tertiary. The southern flank is distinct, with a regional slope of about 1 in 300, but the northern flank is truncated by the Whicher Scarp, formed by Pleistocene erosion. The axis forming the boundary between the Darling Plateau and the Ravensthorpe Ramp appears to be the continuation of the uplift axis on the Blackwood Plateau. It is therefore suggested that the term Jarrahwood Axis might be used for both (Figs. 20 and 21).

Between the Blackwood Plateau on the west and the Darling Plateau and the Ravensthorpe Ramp on the east a dissected scarp 50 m high runs roughly along the line of the Darling Fault. This could have resulted either from movement on the fault after the old land surface was formed, for instance during Tertiary uplift, or by differential erosion during a pause in the uplift of the Darling Plateau.

The major movement on the Darling Fault took place between the Triassic (or earlier) and the Neocomian, when, as discussed under "Darling Plateau", there was a marked phase of uplift. Following this, more stable tectonic conditions prevailed. The intra-Neocomian uplift appears to mark a change in tectonic style from a rift phase preceding continental break-up to a drift phase, when India began to drift northwards (Johnstone and others, 1973, p. 11). Following the intra-Neocomian tectonic event, compaction of the thick Phanerozoic sedimentary column is thought to have accommodated additional Cretaceous sediments in a major portion of the Perth Basin, and some Eocene deposits at Perth (Kings Park Shale). This implies compaction faulting along the Darling Fault and the known faults cutting post-Neocomian sediments may similarly have resulted from differential compaction over quiescent major basement faults. However, the intra-Neocomian unconformity forms a north-south syncline in the Perth area which at its deepest point lies some 650 m below sea level (Allen, A. D., pers. comm.). This depth appears to be rather great to be accounted for by compaction alone and the possibility of movement at basement level on the Darling Fault in this area therefore cannot be ruled out.

The Blackwood Plateau is a distinct geomorphic feature, although now strongly dissected, intermediate in height between the Darling Plateau and the Swan Coastal Plain. If, as already discussed, uplift of the Darling Plateau has taken place since the Eocene, the difference in height of the two surfaces must also have originated since then. Compaction during the Middle and Late Tertiary no doubt resulted in some downward movement of the Blackwood Plateau and basement movement on the Darling Fault at this time is also possible. However, it is thought that the Blackwood Plateau may most reasonably be interpreted as an erosional bench formed during a pause in the uplift of the Darling Plateau and itself later undergoing uplift.

The presence of the scarp between the Darling and Blackwood Plateaux is taken to indicate that the Darling Plateau was uplifted by about 50 m prior to the period of tectonic stillstand. The present elevated position of the Blackwood Plateau and the presence of the Whicher Scarp show that the remainder of the uplift of the Darling Plateau has taken place during a second phase of epeirogenic uplift since the Blackwood Plateau semi-mature surface was formed close to sea level.

SWAN AND SCOTT COASTAL PLAINS

The Swan and Scott Coastal Plains lie relatively close to sea level (generally between 0 and 50 m), and they are still in process of formation today. The superficial deposits covering the plains are of Quaternary age.

One of the most striking geomorphic features of the southern Swan Coastal Plain is the Yoganup Terrace south of Bunbury. It is associated with beach deposits which have been exploited for the heavy minerals contained in them and accurate elevations of the base of the deposits are therefore available. The average level of the terrace falls from about 47 m in the south near Yoganup to about 37 m in the north near Dardanup (Sofoulis, J., written comm.). This represents a northward grade of about 1 : 2 500 compared with an estimated northward slope of 1 : 700 on the northern flank of the Blackwood Plateau to the southeast. No reliable dating of the Yoganup Terrace exists but from regional evidence it is believed to be of early Pleistocene or late Tertiary age. The low northerly gradient may indicate the extent of epeirogenic warping along the Jarrahwood Axis since that time.

The question arises as to why there is no equivalent geomorphic feature to the Ravensthorpe Ramp on the western side of the Darling Plateau. The explanation appears to be that the soft Cretaceous sediments of the Perth Basin were easily bevelled by differential erosion to form the Swan Coastal Plain and the 300 m high Darling Scarp. Although the Darling Plateau land surface is not preserved west of the Darling Fault, down-to-the-west tilting during the Tertiary is demonstrated by the westerly plunge of the Jarrahwood Axis on the Blackwood Plateau (Cope, 1972).

OFFSHORE GEOMORPHIC FEATURES

CONTINENTAL SHELF

The continental shelf is narrowest south of the Ravensthorpe Ramp, with an average grade of 1 : 200, and widest south of the Eucla Basin (average grade, 1 : 400). It is fairly narrow west of the Swan Coastal Plain (average grade, 1 : 225). Recent seismic work in various parts of the world has shown that the continental shelf is built from a sequence of prograded sediments of Tertiary to Recent age (Falvey, 1974; Beck, 1972).

CONTINENTAL SLOPE

As with the continental shelf, there are distinct differences in the average grade of the continental slope which are roughly as follows:

south of Eucla Basin	1 : 20
south of Ravensthorpe Ramp	1 : 10
west of Swan Coastal Plain	1 : 15

The continental slope is formed from the prograded fore-sets of the sediment wedge deposited since continental drift began. The margin of the continental plate has sagged several thousand metres. The base of the continental slope has been taken arbitrarily as about 4 000 m. To the west of Cape Leeuwin the slope is interrupted by the Naturaliste Plateau, which forms a terrace projecting westwards, exactly in line with the Jarrahwood Axis. This feature has apparently been formed from a continental fragment which has foundered to its present level after being left behind by the northward drift of India in the Early Cretaceous and by the relative southward drift of Antarctica in the Early Tertiary.

The lower part of the continental slope is sometimes called the continental rise. This term has not been used here, however, as it is so difficult to define with precision.

ABYSSAL PLAIN AND MID-OCEANIC RIDGE

The abyssal plain in this area lies between 4 000 m and 5 500 m, and the mid-oceanic ridge rises above 4 000 m. According to the theory of ocean-floor spreading, the abyssal plains are floored by new oceanic crust which is created along the mid-oceanic ridge and progressively spreads outwards from it. It has been established that on the western side of the Perth Basin the rift phase was followed by the onset of the drift phase in the Neocomian (Johnstone and others, 1973). To the south, however, Australia and Antarctica did not start to drift apart until the late Eocene (Falvey, 1974). Because drift appears to have been synchronous with the sagging of the southern continental margin and the epeirogenic uplift of the interior, it would seem likely that they are genetically related.

STRUCTURAL HISTORY OF THE CRETACEOUS AND TERTIARY

CONTINENTAL RIFTING OF THE PERTH BASIN

Rifting, which formed the Perth Basin, took place between the Triassic, or earlier, and the early Neocomian. Sediments up to at least 20 000 m thick accumulated in the Perth Basin, but no deposits of this age are known along the southern coast of the State.

NEOCOMIAN UPLIFT

A phase of uplift accompanied by normal faulting affected the Perth Basin in the middle Neocomian. The erosion which followed uplift must have been rapid, because the unconformably overlying basal sediments of the Warnbro Group are also of Neocomian age.

EARLY TO LATE CRETACEOUS DEPOSITION

Upper Neocomian to Upper Senonian sediments were deposited as the Warnbro and Coolyena Groups in the Perth Basin (Cockbain and Playford, 1973). The subsidence which provided space for these sediments in the Dandaragan and Bunbury Troughs is thought to have resulted from compaction of the thick earlier Mesozoic sequence but the possibility of some basement-level continued movement on the Darling Fault cannot be excluded. It was probably during this 50 to 60 million year time interval that the land surface now represented by the Darling Plateau was formed. Sediments of roughly equivalent age were deposited in the Eucla Basin as the Loongana Sandstone and the Madura Formation.

LATE CRETACEOUS TO EARLY TERTIARY EMERGENCE

The Maastrichtian to Paleocene was a time of emergence and erosion in the southern part of the State. This may represent the first pulse of epeirogenic uplift, although it was relatively small.

EARLY TERTIARY SUBSIDENCE AND DEPOSITION

In the Perth Basin late Paleocene to early Eocene subsidence is indicated by the Kings Park Shale which rests in a channel cut into Cretaceous rocks. In the Eucla Basin, the Middle Eocene Hampton Sandstone was laid down on a very irregular surface of Madura Formation (Lowry, 1970). Subsidence continued in the Late Eocene in the Eucla Basin. At this time deposition was initiated along the south coast to the west, where the Plantagenet Group was laid down as a shallow-water marine facies in depressions and valleys of a surface with high relief (Cockbain, 1968b). A shallow-water arm of the sea extended northwards from Esperance towards Kalgoorlie, as is shown by the distribution of the Norseman Limestone, Cowan Dolomite and Princess Royal Sponglite (Cockbain, 1968a).

OLIGOCENE UPLIFT

In the Eucla Basin, the Oligocene was a time of uplift, together with erosion and weathering of the underlying rocks (Lowry, 1970, p. 82). By analogy it is deduced that the Darling Plateau land surface underwent its first appreciable uplift (of about 50 m) at this time and that the Blackwood Plateau was then formed close to Oligocene sea level by differential erosion west of the Darling Fault. The pre-existing drainage system was initially incised also at this time.

EARLY MIOCENE SUBSIDENCE IN THE EUCLA BASIN

Very gentle downwarping in the Eucla Basin was renewed in the Early Miocene with deposition of the shallow-water Abrakurrie Limestone, followed disconformably by the Nullarbor Limestone and its lateral equivalent in the north, the Colville Sandstone. In the Bremer Basin along the south coast Miocene sediments do not occur onshore. The offshore portion of the basin has not, as yet, been tested by drilling. In the Perth Basin, Miocene sediments are known only in offshore wells. These sediments, like the Cretaceous sequence, are thick, and this demonstrates the marked downwarping of the western edge of the continental crust in the Cretaceous and the Miocene (Quilty, 1974).

MIOCENE-PLIOCENE UPLIFT

The only area where post-Early Miocene uplift can be clearly demonstrated is the Eucla Basin, where the top of the Nullarbor Limestone now lies at elevations of up to 250 m above sea level. The total epeirogenic uplift of this horizon comprises the present height above sea level of the eroded top of the formation, plus the thickness removed by erosion and the depth of deposition below sea level. The aggregate of these three figures ranges up to about 280 m in the Eucla Basin. This is roughly the amount of vertical uplift, in addition to the inferred approximately 50 m in the Oligocene, that would be required to bring the Darling

Plateau surface to its present position. It therefore seems reasonable to deduce that the epeirogenic uplift of the Darling Plateau took place mainly between the Middle Miocene and the Late Pliocene. However, uplift apparently continued into the Quaternary. The Perth Basin was also uplifted, decreasing from east to west from a north-south hinge line near the Darling Fault. Differential erosion and compaction have reduced the level of the onshore Perth Basin simultaneously with uplift to near sea level, leaving as erosional remnants the Blackwood Plateau in the south, the Dandaragan Plateau in the central Perth Basin and the Victoria Plateau northeast of Geraldton.

PLIOCENE-QUATERNARY EROSION

Incision of the river systems, which was started in the Late Cretaceous, Oligocene and Late Miocene, took place during the major uplift. The Swan and Scott Coastal Plains were formed by differential erosion of the soft Cretaceous sediments during this time interval. The Blackwood Plateau partly survived erosion owing to its relatively high position, but incision of the lower Blackwood River and its tributaries dissected the central portion of the plateau. During the Pleistocene there were marked climatic variations which resulted in major sea level fluctuations. These resulted in the formation of wave-cut benches at various heights both above and below present sea level, and the covering of the onshore Perth Basin with Quaternary sediments.

COMPARATIVE TECTONICS

The structural history of the area as reconstructed above shows interesting comparisons with that of the continental break-up of Gondwanaland and with certain other segments of the ancient super-continent.

The original formation of the Darling Plateau surface appears to date back to the time immediately following the drift of the Indian plate northwards in the Early Cretaceous (Falvey, 1972). The drifting apart of Australia and Antarctica started in the late Paleocene (Falvey, 1974, p. 105). Following this, phases of subsidence along the south coast in the Late Eocene and Early Miocene alternated with phases of uplift in the Oligocene and the Miocene-Pliocene. Following the latest uplift the Darling Plateau lies at an average height of about 350 m with a hinge line or axis (the Jarrahwood Axis) lying parallel to the south coast.

A very similar geomorphic situation and structural history has been reconstructed for southern Africa and for South America east of the Andes (King, 1956). In southern Africa an upwarped middle Cainozoic surface lies at about 1 000 m and a distinct coastal flexure has been eroded to a scarp by the succeeding denudation cycle (King, 1956, Fig. 1, and p. 463). In eastern Brazil, also, a base-level plain, formed between Late Cretaceous and middle Cainozoic, was lifted up to form tablelands at about 1 000 m which are bent down towards the ocean along the eastern margin of the continent (King, 1956, p. 461).

It appears likely that uplift of the interior plateau in eastern South America, southern Africa and Western Australia is related to the drifting apart of these continents from each other and from Antarctica. It is also now known that the edge of the continental plates have sagged to lie below the offshore continental slope. However, the mechanism by which ocean-floor spreading may have produced these features is not known at present.

CONCLUSIONS

1. The ancient land surface of the Darling Plateau was originally formed during the Cretaceous following an intra-Neocomian uplift. The Cretaceous drainage has, in the main, survived to the present; it is seen in the high-rainfall area of the southwest as an incised river system and as a relict drainage pattern in the arid interior.

2. The Darling Plateau was uplifted during the Cainozoic by several epeirogenic phases, the chief two of which occurred in the Oligocene and the Miocene-Pliocene.

3. Between the Darling Plateau and the south coast a distinct slope can be recognized and for this subdivision a new geomorphic term is proposed, the Ravensthorpe Ramp.

4. Slight warping of the old land surface is recognized as variation in elevation of the Darling Plateau and the Eucla Basin, and as the axis or hinge line between the Darling Plateau and the Ravensthorpe Ramp.

5. It is proposed that the term Jarrahwood Axis be extended from the Blackwood Plateau to cover the Darling Plateau-Ravensthorpe Ramp hinge line.

6. The start of epeirogenic uplift coincided with the separation of Australia and Antarctica by ocean-floor spreading. Simultaneously the margin of the continental plate sagged to form the foundation of the upper continental slope. A fragment of the continental-plate margin foundered to form the Naturaliste Plateau.

7. The continental shelf was formed by the later accumulation of sediments on the upper continental slope.

REFERENCES

Australia. Bureau of Mineral Resources, 1965, Geological map of the World, Australia and Oceania, Sheet 11, 1st edn.: Commission for the Geological Map of the World (International Geological Congress, Paris).

Australia. Bureau of Mineral Resources, Reconnaissance 1 : 250 000 gravity maps of W.A., 1969-1972.

Balme, B. E., and Churchill, D. M., 1959, Tertiary sediments at Coolgardie, Western Australia: Royal Soc. West. Australia Jour., v. 42, p. 37-43.

Beck, R. H., 1972, The oceans, the new frontier in exploration: Australia Petrol. Expl. Assoc. Jour., v. 12, pt. 2, p. 5-28.

Bunting, J. A., van de Graaff, W. J. E., and Jackson, M. J., 1974, Palaeodrainages and Cainozoic palaeogeography of the Eastern Goldfields, Gibson Desert and Great Victoria Desert: West. Australia Geol. Survey Ann. Rept. 1973, p. 45-50.

Cockbain, A. E., 1968a, Eocene Foraminifera from the Norseman Limestone of Lake Cowan, Western Australia: West. Australia Geol. Survey Ann. Rept. 1967, p. 59-60.

——— 1968b, The stratigraphy of the Plantagenet Group, Western Australia: West. Australia Geol. Survey Ann. Rept. 1967, p. 61-63.

Cockbain, A. E., and Playford, P. E., 1973, Stratigraphic nomenclature of Cretaceous rocks in the Perth Basin: West. Australia Geol. Survey Ann. Rept. 1972, p. 26-31.

Cope, R. N., 1972, Tectonic style in the southern Perth Basin: West. Australia Geol. Survey Ann. Rept. 1971, p. 46-50.

Falvey, D. A., 1972, Sea-floor spreading in the Wharton Basin (northeast Indian Ocean) and the breakup of eastern Gondwanaland: Australia Petrol. Expl. Assoc. Jour., v. 12, pt. 2, p. 86-88.

——— 1974, The development of continental margins in plate tectonic theory: Australia Petrol. Expl. Assoc. Jour., v. 14, pt. 1, p. 95-106.

Johnstone, M. H., Lowry, D. C., and Quilty, P. G., 1973, The geology of southwestern Australia—a review: Royal Soc. West. Australia Jour., v. 56, p. 5-15.

Jutson, J. T., 1914, An outline of the physiographical geology (physiography) of Western Australia: West. Australia Geol. Survey Bull. 61, 240 pp.

King, L. C., 1956, A geomorphological comparison between eastern Brazil and Africa (central and southern): Geol. Soc. London Quart. Jour., v. 112, pt. 4, p. 445-470.

Lowry, D. C., 1965, Geology of the southern Perth Basin: West. Australia Geol. Survey Rec. 1965/17 (unpublished).

——— 1970, Geology of the Western Australian part of the Eucla Basin: West. Australia Geol. Survey Bull. 122, 201 pp.

McKenzie, D., and Sclater, J. G., 1971, The evolution of the Indian Ocean since the Late Cretaceous: Royal Astron. Soc. Geophys. Jour., v. 24, p. 437-528.

McWhae, J. R. H., Playford, P. E., Lindner, A. W., Glenister, B. F., and Balme, B. E., 1958, The stratigraphy of Western Australia: Geol. Soc. Australia Jour. v. 4, pt. 2, 161 pp.

Morgan, K. H., and Peers, R., 1973, Esperance-Mondrain Island, W.A.: West. Australia Geol. Survey 1 : 250 000 Geol. Series Explan. Notes

Playford, P. E., Cope, R. N., Low, G. H., Lowry, D. C., and Cockbain, A. E., in press, Phanerozoic *in* Geology of Western Australia: West. Australia Geol. Survey, Mem. 2.

Quilty, P. G., 1974, Cainozoic stratigraphy in the Perth area: Royal Soc. West. Australia Jour., v. 57, p. 16-31.

Royal Australian Survey Corps, 1970, 1 : 100 000 topographic survey, Sheets 2130 (Bridgetown), 2131 (Collie), 2230 (Dinninup), 2231 (Darkan), 2330 (Kojonup) and 2430 (Katanning).

Woolnough, W. G., 1918, The Darling peneplain of Western Australia: Royal Soc. New South Wales Jour. and Proc., v. 52, p. 385-396.

THE CLASSIFICATION, GENESIS AND EVOLUTION OF SAND DUNES IN THE GREAT SANDY DESERT

by R. W. A. Crowe

ABSTRACT

Three types of sand dune occur in the Great Sandy Desert, Western Australia: simple and chain longitudinal types and a net-like type. Helicoidal air flow is believed to be responsible for the development of longitudinal dunes in this area. It is postulated that the three types of dune represent stages in an evolutionary sequence that occurs where there is an adequate supply of sand. The most complex (net-like) dunes are shown to occur in depressions and it is suggested that these represent the most evolved type.

INTRODUCTION

The Great Sandy Desert in Western Australia is one of the largest deserts in the world, with an area of approximately 400 000 km^2. It is covered by a remarkable pattern of longitudinal dunes that are now fixed by sparse vegetation. During the last three years, field work in the northeastern part of this area has prompted further study of variations in the dune pattern that cannot always be easily explained. This has involved study of aerial photographs and topographic maps over the rest of the desert and this paper proposes a classification and a theory on the origin of these variations.

CLASSIFICATION

Veevers and Wells (1961, p. 201) classified the longitudinal dunes of the Great Sandy Desert into five categories which they named types A-E, but no attempt was made to explain the significance of the different types. In this report Veevers and Wells' classification is simplified to three types (Figs. 23, 24 and 25) as their types A, B and D are morphologically similar. They are as follows:

Simple longitudinal dunes. Single crest, mainly straight. Wave length 100 m - 2 km (Fig. 23).

Chain longitudinal dunes. Multiple crested, mainly straight. Wave length 400-900 m (Fig. 24).

Net-like dunes. Net-like crest pattern. Not strictly longitudinal dunes although they are elongated parallel to the main wind direction. Wave length <300 m (Fig. 25).

Figure 27 shows the distribution of the different dune types on a topographic map of a representative part of the Great Sandy Desert. The most noticeable trend is that the dunes become increasingly complex towards the centres of depressions. This indicates that the depressions have acted as traps for moving sand, allowing more complex dunes to form in such areas. Thus the morphology of the dunes is related to their topographic position.

The fact that the three categories differentiated are completely gradational from one to another (see Fig. 26) strongly indicates that they have a related origin. Although similar observations on the distribution of dune type have been made by Mabbut (1968) among others, the genesis of these different categories of dunes has not yet been satisfactorily explained.

FORMATION OF LONGITUDINAL DUNES

Bagnold (1952) proposed the theory of helicoidal (Langmuir) air flow for the formation of longitudinal dunes. The theory is that as strong prevailing winds move horizontally across the land surface a thin boundary layer of turbulence develops in response to shearing stresses between the air and the land surface. Within this layer paired vortices form above the land surface, with their axes parallel to the main wind direction. These primary vortices propagate further paired vortices next to them and so on (see Fig. 28).

Other work concerning this subject has been reviewed by Folk (1971a), and Glennie (1970) and Wilson (1973) have described longitudinal dunes on a broader basis with particular reference to Africa and Arabia.

Hanna (1969) has reviewed the literature which shows that helicoidal air flow is restricted to the lowermost atmospheric boundary layer (Fig. 28).

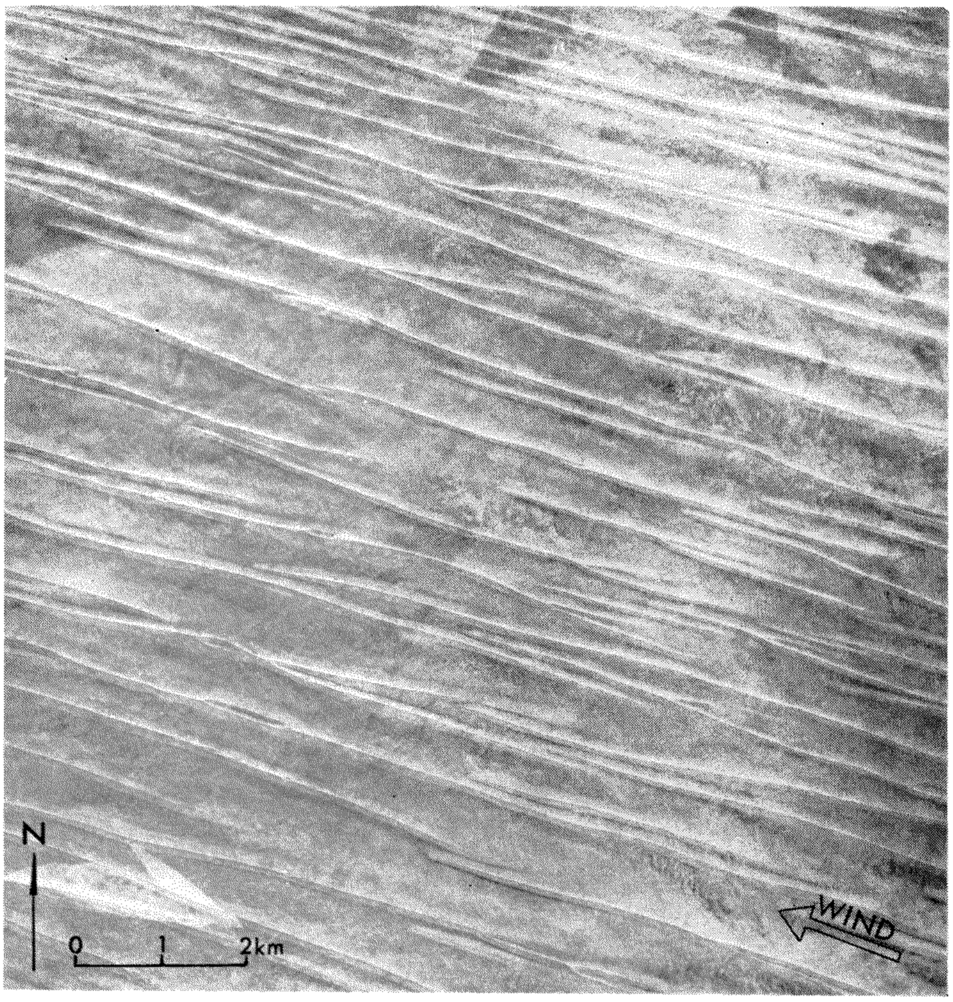

Figure 23. Simple longitudinal dunes. Mount Anderson, Run 6, No. 2132, 1967 photography.

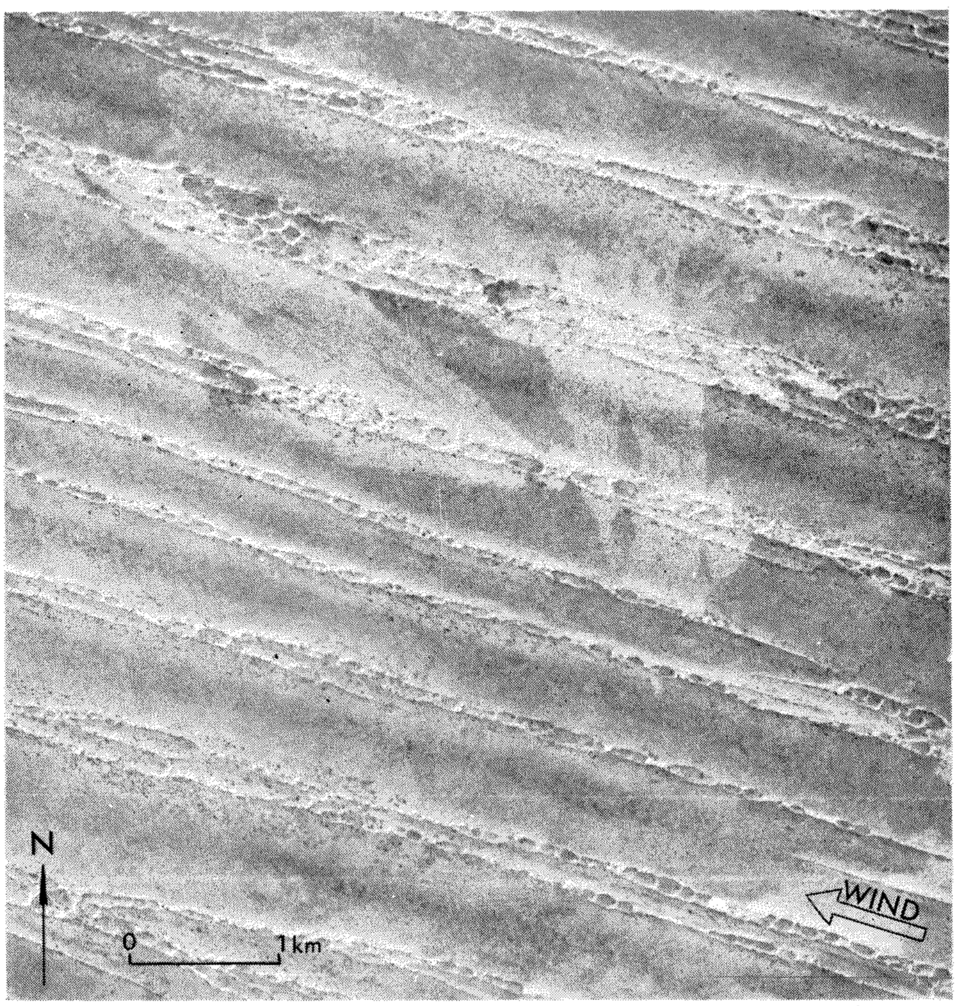

Figure 24. Chain longitudinal dunes. Crossland, Run 14, No. 5955, 1960 photography.

Figure 25. Net-like dunes. Cobb, Run 1, No. 5955, 1960 photography.

Figure 26. Gradation from simple longitudinal dunes to net-like dunes moving into a depression. Cobb, Run 1, No. 121, 1970 photography

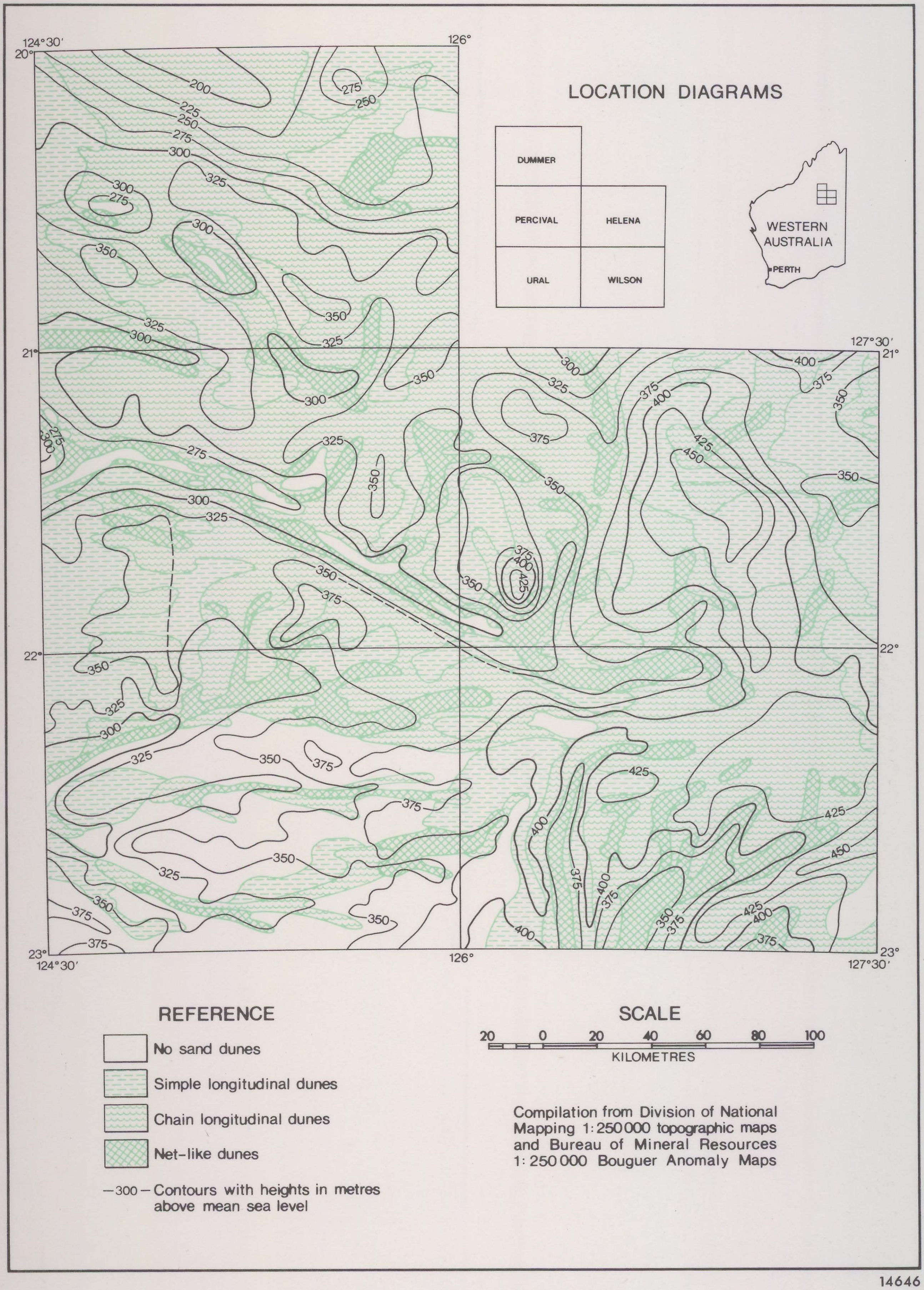

14646

Fig. 27 Topographic position of sand dune types.

The map shows how the net-like dunes generally occur in depressions. Chain dunes are the predominant type in this part of the desert.

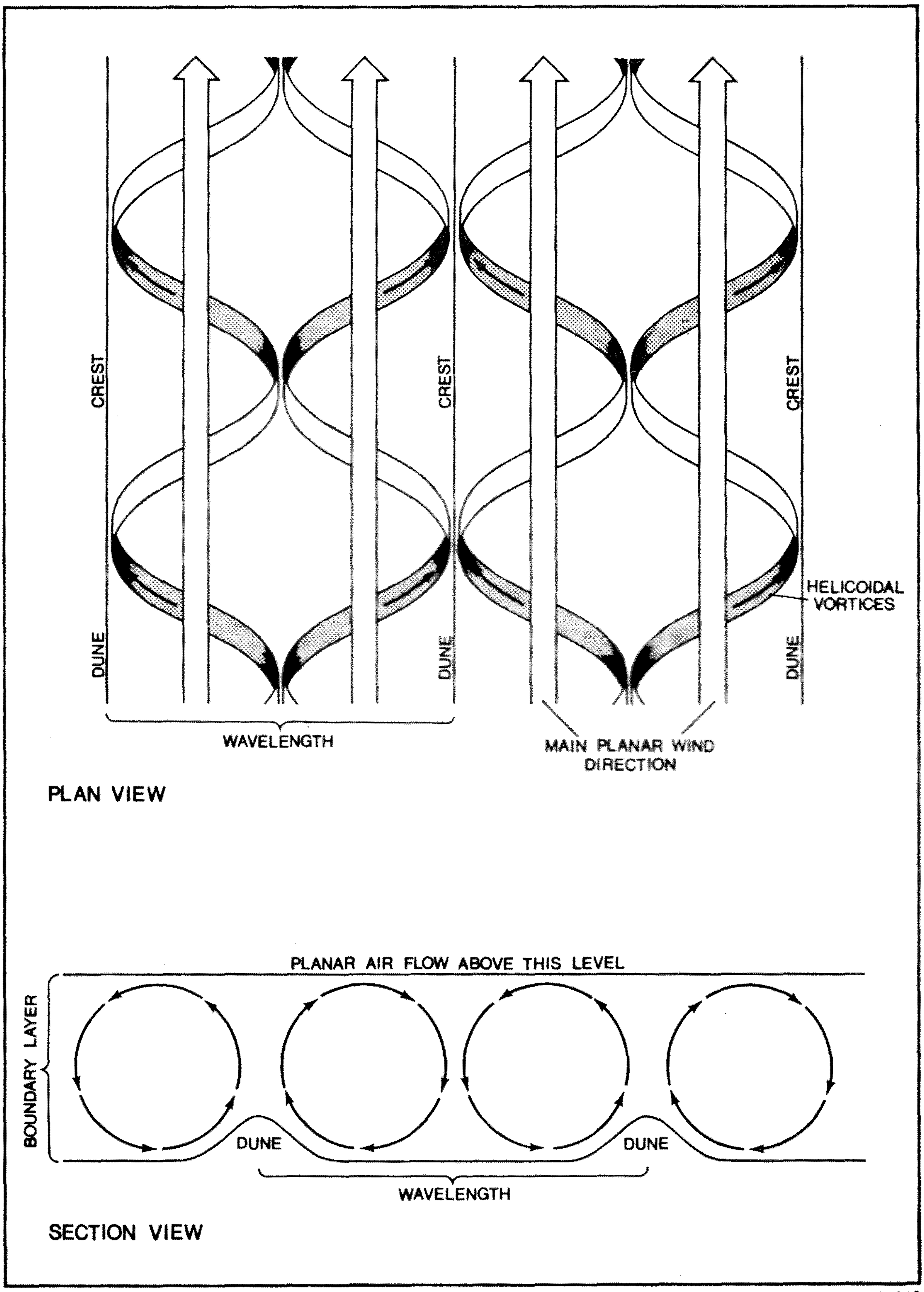

Figure 28. Diagram showing character of helicoidal air flow in dune areas. Note that wave length is related to thickness of boundary layer (adapted from Folk, 1971a).

The helicoidal vortices flow parallel to the main wind direction and produce long ripples or dunes. Above the boundary layer the air flow is essentially planar. It can be seen that the thickness of the boundary layer will govern the size of the vortices and thus the wave lengths of the ripples or dunes. Hanna has also shown that certain conditions are conducive to the formation of such a boundary layer. They are:

(1) Flat underlying terrain

(2) Little direction variation of the wind with height

(3) Wind speed higher than normal

(4) Strong curvature of the wind profile

(5) Unstable lapse rate of temperature near the surface.

He has demonstrated that these conditions are frequently found in desert areas.

Folk (1971b) was the first to find a diagnostic characteristic for this type of air flow. By rolling a cylinder on a greased planar surface he produced patterns identical with longitudinal dune patterns. In both cases "tuning fork junctions", opening upwind or away from the direction of roller movement are present (see Figs. 23 and 24) and Folk believes these are diagnostic features of dunes formed by helicoidal flow. Veevers and Wells (1961, p. 209) showed that the main winds capable of eolian transport in the Great Sandy Desert are winds from the south-southeast to east, in other words the prevailing winds. The tuning-fork junctions opening towards the east indicate that these dunes were formed by helicoidal air flow produced by the prevailing winds.

Application of this information to the variations of dunes, described above, demonstrates that the simple longitudinal dunes have been formed by helicoidal vortices (Fig. 28). The chain-type dunes are more complex and as they grade into simple longitudinal dunes, helicoidal air flow is considered to have also formed the multiple crests of the chain dunes. When the dunes exceed a certain width, a secondary pair of vortices is believed to come into operation, causing a split in the crest. This mechanism is shown in Figure 29.

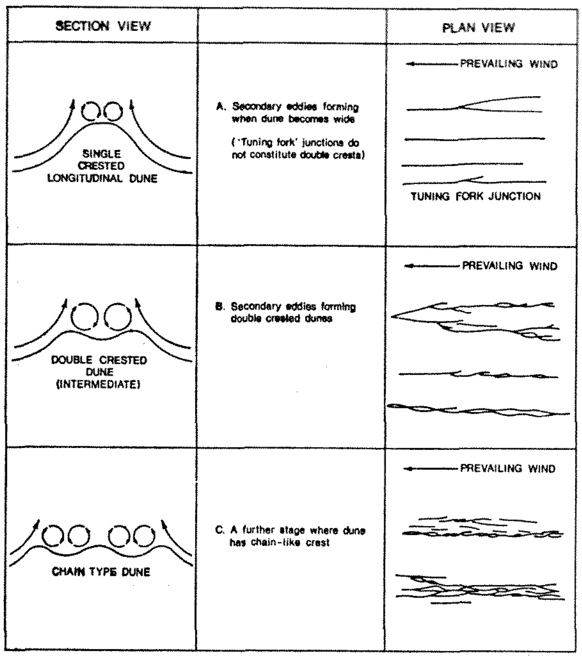

14647

Figure 29. Diagram showing proposed genesis of chain longitudinal dunes. Once secondary eddies form they become self-perpetuating convection eddies as the double crests are constructed.

The next stage is reached when the chain dunes become still wider. The interdune areas then become too narrow to support the original vortices, and these vortices break down. When this happens the chain dunes coalesce to form the net-like pattern.

One of the critical points about the hypothesis is whether the dunes become wider with time. If the wind was strong enough then the dunes would simply become higher. However, if the climate (wind) is stable, then once the dunes reach their maximum height, and additional sand is available, the dunes can only became wider.

The graduation between the simple longitudinal dunes and the net-like dunes (Fig. 26) shows how the more complex dunes are situated in depressions and, therefore, are in areas where more sand is available. This strongly suggests that the dunes have, in fact, become wider and have coalesced in the way described above.

An alternative hypothesis is that the air flow is modified by topographic highs and lows, and that these modifications cause the variations in dune pattern and are not related to sand supply. However, the increase in complexity of the dunes in depressions cannot be easily explained by this theory because the atmospheric boundary layer would be thicker over depressions, causing wider spaced dunes. Clearly this is not the case (Fig. 28), so it is felt that the increase in complexity is mainly dependent on the supply of sand and is best explained by the theory of dune coalescence where unfiorm helicoidal air flow ceases to have a major effect.

CONCLUSIONS

Over a flat plain, with consistent winds in predominantly one direction, and where high temperatures are conducive to turbulent wind action, helicoidal air flow occurs. This forms simple longitudinal dunes where there is an ample supply of sand suitable for eolian transport. As the dunes get older and the supply of sand is maintained these dunes become wider until they form the chain type. In depressions with still further sand available, the chain longitudinal dunes coalesce to form net-like dunes. In such a situation, convection takes over as the main dune-forming mechanism and helicoidal air flow has a reduced effect. If the supply of sand slows, or ceases, then the increase in complexity will stop. Thus, each of the three variations represents a stage in evolution of longitudinal dunes.

ACKNOWLEDGEMENTS

The aerial photograph of Cobb (Fig. 25) is published with permission of the Surveyor General, Department of Lands and Surveys, Perth. The photographs of Crossland (Fig. 24) Cobb (Fig. 26) and Mount Anderson (Fig. 23) have been made available by courtesy of the Director, Division of National Mapping, Department of Minerals and Energy, Canberra.

REFERENCES

Bagnold, R. A., 1952, The surface movement of blown sand in relation to meteorology; *in* Desert Research: UNESCO, Jerusalem, p. 89-96.

Folk, R. L., 1971a, Longitudinal dunes of the northwestern edge of the Simpson Desert, Northern Territory, Australia; 1. Geomorpholgy and grain size relationships: Sedimentology, v. 16, nos. 1 and 2, p. 5-55.

——— 1971b, Genesis of longitudinal and Oghurd dunes elucitated by rolling upon grease: Geol. Soc. America Bull., v. 82, p. 3461-3468.

Glennie, K. W., 1970, Desert sedimentary environments, *in* Developments in Sedimentology, no. 14: Elsevier, Amsterdam.

Hanna, S. R., 1969, The formation of longitudinal sand dunes by large helical eddies in the atmosphere: Jour. Applied Meteorology, v. 8, p. 874-883.

Mabbutt, J. A., 1968, Aeolian landforms in central Australia: Australian Geographical Studies, v. 6, no. 2, p. 139-150.

Veevers, J. J., and Wells, A. T., 1961, The geology of the Canning Basin, Western Australia: Australia Bur. Mineral Resources Bull. 60.

Wilson, I. G., 1973, Ergs: Sedimentary Geol., v. 10, no. 2, p. 77-106.

NEW AND REVISED STRATIGRAPHIC NOMENCLATURE, NORTHEAST CANNING BASIN

by A. N. Yeates†, R. W. A. Crowe*, V. L. Passmore†, R. R. Towner†, and L. I. A. Wyborn†

ABSTRACT

It is proposed that the terms Hardman, Condren Sandstone, and Lightjack, previously defined as members of the Liveringa Formation, be given formation status and that the term "Liveringa" be upgraded to group status to include the Hardman Formation, Condren Sandstone, and Lightjack Formation.

New names proposed are:

(1) Knobby Sandstone: Upper Devonian quartzose sandstone, previously recognized and informally named.

(2) Kirkby Range Member, Hicks Range Sandstone Member, and Cherrabun Member for three mappable units comprising the Hardman Formation on the Crossland Sheet area.

(3) Lake Gregory Beds: Cainozoic mud, silt and sand in the Lake Gregory area.

It is also proposed that the term Wolf Gravel be discarded.

For details of the type sections described below see Yeates and others, 1974.

REVISION OF THE LIVERINGA FORMATION

The Liveringa Formation in the Fitzroy Trough was subdivided into the Lightjack, the Middle and the Hardman Members by Guppy and others (1958). The members, however, were not differentiated on their maps. In the Gregory Sub-basin, the southeastern continuation of the Fitzroy Trough (Yeates and others, in prep.), the Liveringa Formation was subdivided into the Balgo, Condren Sandstone, and Hardman Members (Veevers and Wells, 1961; Casey and Wells, 1964). The Balgo Member was recognized as a lateral equivalent of the Lightjack Member, but, at the time, continuity of the units could not be demonstrated between the two widely separated type sections, and two separate names were retained. The term Balgo Member was subsequently discarded by Playford and others (in press. The Condren Sandstone Member is equivalent to the Middle Member of Guppy and others (1958). Casey and Wells (1964) recognized the Hardman Member in the northwestern part of the Mount Bannerman Sheet area. Its only known stratigraphic equivalent to the southeast is probably the Godfrey Beds (Yeates and others, in prep.), which were previously thought to be Lower Cretaceous (Casey and Wells, 1964).

The type sections of the Hardman Formation, Condren Sandstone, and Lightjack Formation remain those described for these units when they were originally assigned member status. The type sections (locations shown in Fig. 30) are at Mount Hardman (Noonkanbah Sheet area), Condren Pinnacles (Lucas Sheet area), and at Lightjack Hill (Noonkanbah Sheet area), and none of them is complete.

* Geological Survey of Western Australia.

† Bureau of Mineral Resources, Geology and Geophysics, Canberra.

(4)—46009

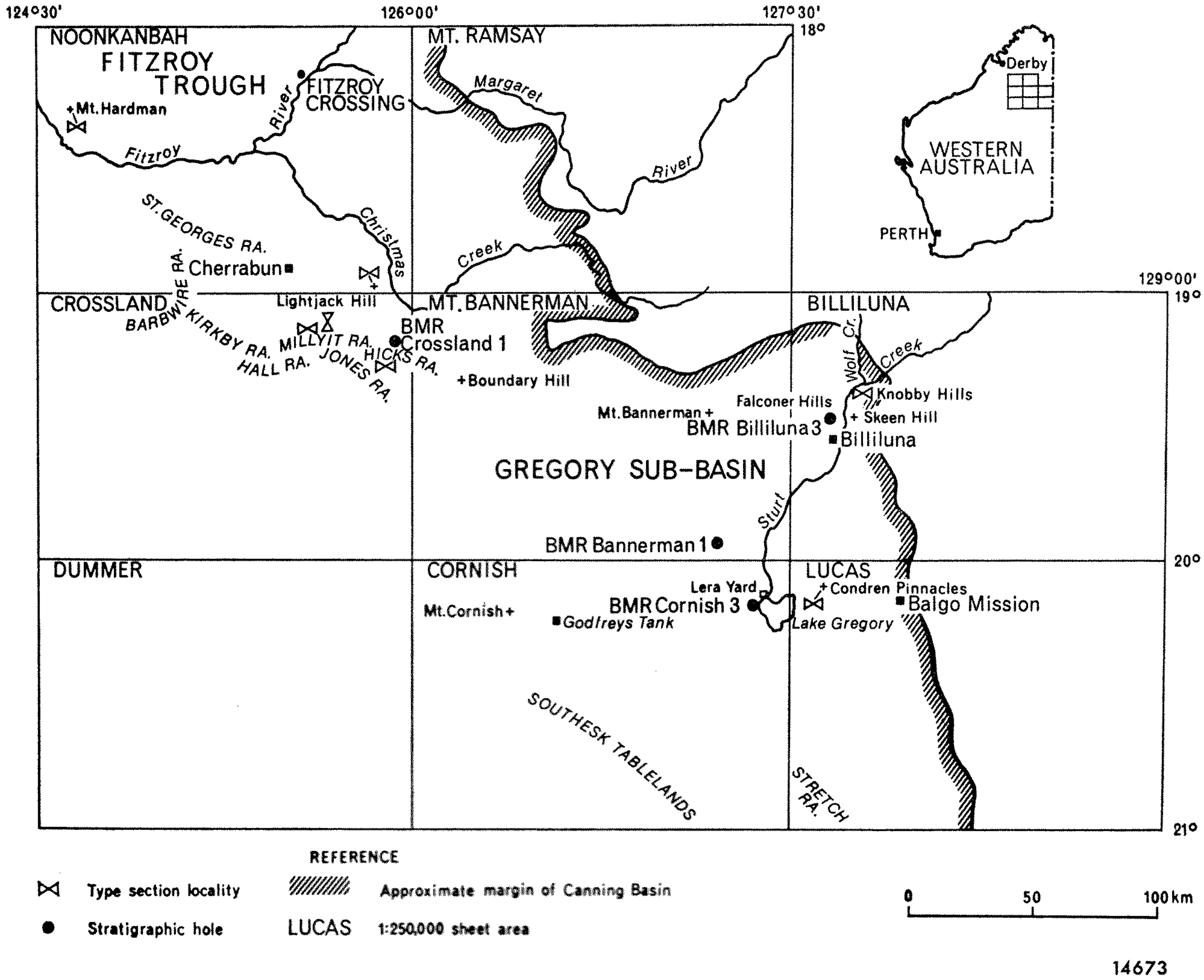

Figure 30. Northeast Canning Basin showing stratigraphic units.

PROPOSED NAME : KNOBBY SANDSTONE

Derivation of name: Knobby Hills, lat. 19° 23′ S, long. 127° 43′ E (Billiluna Sheet area).

Distribution: Crops out in an area of 40 km radius around Knobby Hills.

Lithology: Medium to coarse-grained, cross-bedded quartzose sandstone containing abundant intraformational claystone clasts; quartz granule conglomerate, thin beds of quartz-pebble conglomerate, and rare siltstone.

Type section locality: Lat. 19° 24′ 24″ S, long. 127° 45′ 44″ E, about 2 km east of Sturt Creek and 7 km north of Skeen Hill (Billiluna Sheet area).

Thickness: At the type section (Yeates and others, 1974), 13 m; at Falconer Hills (Billiluna Sheet area), 14.4 m is exposed. A shallow stratigraphic drill hole, BMR Billiluna No. 3, penetrated 170 m at Falconer Hills. The maximum thickness is estimated to be 350 m.

Age: Late Devonian; based on fish fossils.

Fossils: The lycopod *Leptophloem australe* (McCoy, 1874) and placoderm fishes, including undetermined arthrodires (Gilbert-Tomlinson, 1968, p. 210) *Bothriolepis*, *Asterolepis*, and crossopterygian remains (Young, G. C., pers. comm.). The fish plates, though fragmentary, are widespread, but *Leptophloem* specimens are rarer.

Relationships: The Knobby Sandstone lies unconformably on the Proterozoic Peterson Beds and is probably also unconformable on the Lower Ordovician Carranya Beds. The formation may conformably overlie rocks of possible Silurian-Devonian age in the subsurface. No upper contact is exposed. In the subsurface, the Knobby Sandstone is probably overlain by the Lower Permian Grant Formation in the Billiluna area, and possibly by Carboniferous rocks farther southwest away from the margin of the Canning Basin.

Synonomy or modification of previous nomenclature: Casey and Wells (1964) described the sandstone in the Knobby Hills area but did not formally name it. A Late Devonian to Early Carboniferous age was assigned to it on plant fossil evidence.

Veevers and others (1967) have referred to the "Knobby Sandstone" informally.

PROPOSED NEW MEMBERS OF THE HARDMAN FORMATION

KIRKBY RANGE MEMBER

Derivation of Name: Kirkby Range, lat. 19° 07′ S, long. 125° 13′ E (Crossland Sheet area).

Distribution: The Member occurs in the Millyit Range and Kirkby Range (Crossland Sheet area).

Lithology: Argillaceous siltstone, argillaceous sandstone, minor shale, and calcareous sandstone.

Type section locality: Lat. 19° 09′ 39″ S, long. 125° 34′ 24″ E, 1.5 km west of Spring Creek on the northern scarp of the Millyit Range.

Thickness: At least 52 m at the type section (Yeates and others, 1974), at least 22 m in the southern part of the Millyit Range, at least 75 m in Kirkby Range, and at least 70 m in BMR Crossland No. 1.

Age: Late Permian, based on brachiopods, pelecypods, and a microfloral assemblage.

Relationships: A conformable and gradational contact with the underlying Condren Sandstone; apparent conformity with the overlying Hicks Range Sandstone Member (new name).

Synonomy or modification of previous nomenclature: The member was previously recognized as part of the Hardman Formation.

HICKS RANGE SANDSTONE MEMBER

Derivation of name: Hicks Range, lat. 19° 14′ S, long. 125° 54′ E (Crossland Sheet area).

Distribution: Crops out in a narrow belt extending from Barbwire Range to Hicks Range (Crossland Sheet area).

Lithology: Quartzose sandstone, fine to coarse-grained, cross-bedded; minor quartz granule conglomerate.

Type section locality: The type section is a scarp in the central part of Hicks Range at lat. 19° 13′ 46″ S, long. 125° 53′ 42″ E.

Thickness: 27.9 m at the type section (Yeates and others, 1974), 14.8 m at Spring Creek in the Millyit Range, and at least 10 m in the Kirkby Range.

Age: Late Permian; based on marine faunas above and below the member.

Relationships: Rests with apparent conformity on the Kirkby Range Member (new name) and is conformable beneath the Cherrabun Member (new name).

Synonomy or modification of previous nomenclature: The member was previously recognized as part of the Hardman Formation.

CHERRABUN MEMBER

Derivation of Name: Cherrabun Homestead, lat. 18° 54′ 42″ S, long. 125° 31′ 24″ E (Noonkanbah Sheet area).

Distribution: Millyit Range, Jones Range, and Hicks Range (Crossland Sheet area).

Lithology: Fine-grained micaceous sandstone, fossiliferous sandstone, micaceous and ferruginous siltstone, and shale.

Type section locality: At the source of a tributary of Spring Creek at lat. 19° 11′ 00″ S, long. 125° 33′ 06″ E (Crossland Sheet area).

Thickness: At least 22.2 m at the type section (Yeates and others, 1974) at least 24.6 m in the Hicks Range.

Age: Late Permian based on brachiopods, pelecypods, and gastropods.

Fossils: Brachiopods, pelecypods, gastropods, trace fossils, and a microfloral assemblage.

Relationships: In the Crossland Sheet area the member is conformable on the Hicks Range Sandstone Member (new name) and is overlain with slight angular unconformity by the Lower Triassic Millyit Sandstone.

Synonomy or modification of previous nomenclature: The member was previously recognised as part of the Hardman Formation.

PROPOSED NAME: LAKE GREGORY BEDS

Derivation of name: Lake Gregory, lat. 20 ° 12′ S, long. 127″ 30′ E (Lucas and Cornish Sheet areas).

Distribution: Subcrops beneath eolian sand in the terminal reaches of Sturt Creek. A few exposures occur along the margin of Lake Gregory.

Lithology: Green, brown, and red clay, silt, and fine-grained sand, minor marl and calcrete and rare gravel.

Type section locality: The type section is in BMR Cornish No. 3, a continuously cored hole located at lat. 20° 11′ 05″ S, long. 127° 24′ 15″ E at Lera Yard (Cornish Sheet area).

Thickness: 99.1 m in BMR Cornish No. 3 (Yeates and others, 1974), 64.3 m in BMR Mount Bannerman No. 1.

Age: Cainozoic, based on regional relationships.

Fossils: Indeterminate gastropods; possible plant root casts; indeterminate fish bones.

Relationships: Unconformable on Permian formations; conformable beneath eolian sand.

VALIDITY OF THE TERM WOLF GRAVEL

The Wolf Gravel (Casey and Wells, 1964) was the name given to unconsolidated gravel, conglomerate, and sand of unknown thickness along the banks of Wolf Creek in the Billiluna Sheet area. It is recommended the term be discarded as these deposits are indistinguishable from other alluvial deposits of both Wolf Creek and Sturt Creek.

REFERENCES

Casey, J. N., and Wells, A. T., 1964, The geology of the north-east Canning Basin, Western Australia: Australia Bur. Mineral Resources Rept. 49.

Gilbert-Tomlinson, J., 1968, A new record of *Bothriolepis* in the Northern Territory of Australia: Australia Bur. Mineral Resources Bull. 80, p. 191-226.

Guppy, D. J., Lindner, A. W., Rattigan, J. H., and Casey, J. N., 1958, The geology of the Fitzroy Basin, Western Australia: Australia Bur. Mineral Resources Bull. 36.

McCoy, F., 1874, Prodromus of the Palaeontology of Victoria: Victoria Geol. Survey, v. 1, p. 37.

Playford, P. E., Cope, R. N., Low, G. H., Lowry, D. C., and Cockbain, A. E., in press, Phanerozoic, *in* Geology of Western Australia: West. Australia Geol. Survey, Mem. 2.

Veevers, J. J., and Wells, A. T., 1961, The geology of the Canning Basin, Western Australia: Australia Bur. Mineral Resources Bull. 60.

Veevers, J. J., Roberts, J., White, M. E., and Gemuts, I., 1967, Sandstone of probable Lower Carboniferous age in the north-eastern Canning Basin, Western Australia: Australian Jour. Sci., v. 29, p. 330-331.

Yeates, A. N., Crowe, R. W. A., Towner, R. R., Wyborn, L. A. I., and Passmore, V. L., 1974, New and revised stratigraphic nomenclature, northeast Canning Basin, Western Australia: Australia Bur. Mineral Resources Rec. 1974/183 (unpublished).

Yeates, A. N., Crowe, R. W. A., Towner, R. R., Wyborn, L. A. I., and Passmore, V. L., in prep., Notes on the geology of the Gregory Sub-basin and adjacent areas of the Canning Basin, Western Australia: Australia Bur. Mineral Resources Rec. (unpublished).

SOME PROBABLE LOWER PROTEROZOIC SEDIMENTS IN THE MOUNT PADBURY AREA

by J. C. Barnett

ABSTRACT

A thick sequence of folded sediments on the northern edge of the Yilgarn Block is bounded by the Bangemall Basin to the north, of gneiss and schist, to the west; the gneiss and schist are probably related to the Gascoyne Province. The sediments are of low metamorphic grade and consist mainly of alternating hematite shale and banded iron formation (BIF); some of the BIF in the upper part of the sequence has clastic texture. The sequence includes a thick conglomerate section and there are dolomite beds in the upper part.

The succession is named the Padbury Group: it incorporates three formations, named in descending order the Millidie Creek, Robison Range and Labouchere Formations, and also includes the conformably underlying units, namely the Horseshoe Range and Peak Hill Beds, although these are not yet given formation status.

The boundaries of the Padbury Group are all either faulted or concealed, but the evidence indicates that the sediments are of Lower Proterozoic age; they are possibly contemporaneous with part of the Mount Bruce Supergroup.

INTRODUCTION

This paper discusses a sequence, delineated in the course of regional mapping, on the east side of the Robinson Range 1 : 250 000 Sheet. The area described is between latitudes 25° 05′ S and 25° 50′ S and longitudes 118° 00′ E and 118° 30′ E, about 750 km NNE of Perth, and 100 km north of Meekatharra.

The sequence was mapped on the adjoining Peak Hill 1 : 250 000 Sheet by MacLeod (1970a). The BIF on the Peak Hill and Robinson Range Sheets were subsequently investigated by Sofoulis (1970), and some carbonate intrusions within the sediments were examined by MacLeod (1970b), Lewis (1971) and Lewis and Williams (1971).

MacLeod (1970a) considered that the sequence was probably of Archaean age, but present evidence suggests that it is more likely to be Lower Proterozoic.

The purpose of this paper is to revise the stratigraphic nomenclature, to advocate a Lower Proterozoic age for the sequence, and to describe its lithology.

REGIONAL SETTING

The Padbury Group forms a sequence on the northern edge of the Yilgarn Block. It is unconformably overlain by the Bangemall Basin to the north, and to the west abuts a metamorphic complex of gneiss and schist which is probably related to the Gascoyne Province, a Lower Proterozoic mobile belt. The sequence is strongly deformed but lacks metamorphism; the arenaceous rocks are cleaved, and the finer-grained beds vary from shale to phyllite.

The gneiss and schist contain intrusions of granite and highly metamorphosed remnants of BIF and pelitic and psammitic sediments. The contact is probably faulted; there are air-photo lineaments along the contact and the foliation of the gneiss is discordant with the strike of the sediments. The contact therefore provides no conclusive stratigraphic evidence for the age of the Padbury Group.

It is noteworthy that the metamorphic complex appears to be related to the Gascoyne Province; this suggests that the Province extends farther east than is shown on the 1973 edition of the State Geological Map.

The sediments wrap around the southeastern margin of the gneiss. Between the sediments and gneiss in this area are mafic and ultramafic volcanics which are faulted against the gneiss. The boundary between the volcanics and the Padbury Group is concealed by superficial deposits.

On the north the boundary with the Bangemall Basin is a complex of established faults and probable faults shown by air-photo lineaments, although regionally this can be shown to be an unconformity (MacLeod, 1970a).

To the south the alluvial plain of the Murchison River covers the boundary with the Archaean Yilgarn Block.

Within the sediments in the southeast are a number of carbonate intrusions and a few easterly trending unmetamorphosed dolerite dykes. Laterite in the extreme southeast has a remnant texture suggestive of dolerite which was probably a large stock or sill.

The Padbury Group is folded and faulted. The major fold axes parallel the boundaries of the metamorphic complex, and swing in a broad arc around its convex southeastern margin. Minor folding on several scales is common, and dips are generally steep, vertical or slightly overturned. Faults, and probable faults indicated by air-photo lineaments, are common; the most common trends are north and east, parallel to the fold axes, and there is a subsidiary northwest trend. There is apparently a faulted slice of Labouchere Formation against the eastern margin of the metamorphic complex. Major folds, faults and air-photo lineaments are shown on Figure 31.

STRATIGRAPHY OF THE PADBURY GROUP

MacLeod (1970a) divided the succession into four units, named in ascending order the Peak Hill Beds, Horseshoe Range Beds, Labouchere Beds and Robinson Range Beds. This fourfold division is retained together with the addition of an upper, fifth, unit—the Millidie Creek Formation. The Labouchere and Robinson Range Beds are upgraded to formation status; the Horseshoe Range and Peak Hill Beds, which do not crop out well on the Robinson Range Sheet, are retained at this stage as "Beds".

The Padbury Group is defined as the sequence of BIF, hematitic shale, wacke, siltstone conglomerate and dolomite which occurs in the Mount Padubry (lat. 25° 38′ 30″ S, long. 118° 16′ 30″ E)—Robinson Range—Mount Fraser area, and consists of the Millidie Creek Formation (top), the Robinson Range Formation, the Labouchere Formation, and those units that conformably or disconformably underlie the Labouchere Formation. By implication this includes the Horseshoe Range Beds and the Peak Hill Beds. The Padubry Group is at least 12 500 m thick, and is probably Lower Proterozoic in age.

The sequence on the Robinson Range Sheet is summarized in Table 8.

PEAK HILL BEDS

These are not well exposed on the Robinson Range Sheet, and are not discussed further.

HORSESHOE RANGE BEDS

MacLeod reports that the Horseshoe Range Beds overlie the Peak Hill Beds. These beds crop out in the northeast part of the Robinson Range Sheet, where they consist of siltstone and phyllite with subsidiary BIF, minor wacke, and chert bands up to 150 mm thick. MacLeod (1970a) estimated a thickness of 1 000 m.

The BIF consists of laminated quartz and hematite, with silty and jasper bands. Laminations are 5-10 mm thick, and individual bands of BIF are generally 3-4 m thick. The siliceous

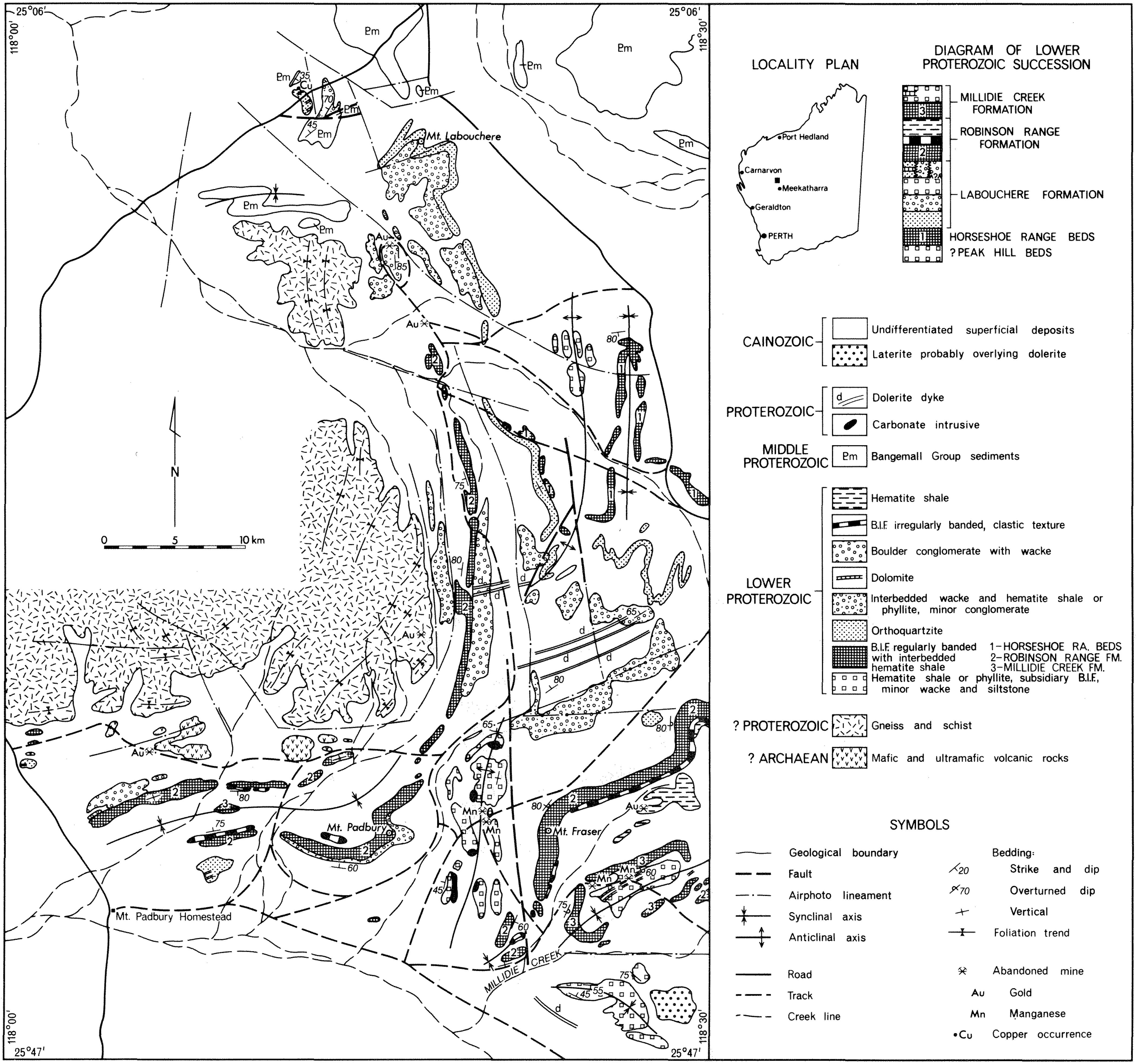

Fig. 31. Geological map of the Mt Padbury area, Robinson Range sheet.

14680

TABLE 8. PADBURY GROUP

MILLIDIE CREEK FORMATION	*Hematite shale* or *slate* with minor BIF, chert, and feldspathic wacke. Two thin bands of dolomite. *BIF* and *hematite shale*, interbanded. BIF has clastic texture.
ROBINSON RANGE FORMATION	*Hematite shale*, laminated. BIF, irregularly banded, clastic texture. *Hematite shale*, minor BIF increasing towards top. *BIF* and *hematite shale* interbedded. *Hematite shale*; laminated, BIF and chert bands towards top.
LABOUCHERE FORMATION	*Wacke, grit, conglomerate, shale, silstone* and *chert*. Three thin dolomite beds in west. Large lenticular boulder conglomerate in places.
	TYPE AREA
	Feldspathic wacke and *hematite shale* or *phyllite*. Alternating bands; wacke predominants in lower part, hematite shale becomes predominant in top part. *Orthoquartzite.*
	SOUTHERN AREA
	Hematite shale with thin BIF horizons, minor wacke and siltstone.
HORSESHOE RANGE BEDS	*Siltstone, phyllite* and *BIF*, interbanded. Minor wacke.
PEAK HILL BEDS	*Hematite phyllite* with *BIF*. Not well exposed.

laminae are composed of a mosaic of polygonal grains about 0.1 m across, and the hematite laminae are of anhedral to wispy hematite intergrown with minor quartz. In some BIF layers the hematite is more evenly distributed, but lamination is still evident.

The phyllite is usually reddish-purple and hematitic, but more chloritic varieties are dark green. Wacke bands contain quartz and feldspar clasts and some flakes of shale; individual beds are 3-4 m thick. The BIF is manganese stained.

The top portion of the beds is a succession of wacke and siltstone.

LABOUCHERE FORMATION

The Labouchere Formation is defined as that formation of feldspathic wacke, hematitic shale, conglomerate and orthoquartzite which occurs at its type area 5 km south of Mount Labouchere (lat. 25° 11′ 45″ S, long. 118° 17′ 30″ E), and that conformably overlies the Horseshoe Range Beds and underlies the Robinson Range Formation. It is about 5 000 m in thickness.

The base of the formation on the Robinson Range Sheet is an orthoquartzite or silicified arenite, which weathers to a pinkish grey colour. This bed has a distinctive air-photo pattern, and is a useful marker horizon. It forms the prominent strike ridge which includes Mount Labouchere. It is poorly sorted, medium to coarse grained, with small pebbles in places. Feldspar and muscovite clasts are rare.

This orthoquartzite is overlain by a sequence of alternating wacke and phyllitic shale with rare bands of siltstone. The shale proportion is minor at the bottom, but increases through the sequence, to predominant at the top, and the wacke beds are progressively better sorted up the sequence. Minor microconglomerate beds occur, and a coarser conglomerate bed in the north of the area contains pebbles and cobbles of white quartz, purple quartzite and jasper.

The wacke is quartzo-feldspathic with minor muscovite. It is generally red-brown in colour and weathers to pale yellow. Individual beds are usually a few metres thick. Graded bedding and ripple marks are present.

In the southern part of the area, between Mount Fraser and Mount Padbury, and southeast of Mount Fraser, is a sequence of hematite shale with BIF layers, some arkose and wacke, and a little siltstone. The BIF layers are 1-2 m thick and are commonly coated with manganese. This southern sequence is probably a facies change. A less likely possibility is that it is a higher part of the succession, which in the north has been cut out by disconformity.

The top 1 000 metres of the formation is a lithologically variable sequence containing conglomerate. The top beds, in the central and western part of the area, are of thick lenticular boulder, cobble and pebble conglomerate with wacke and shale interbeds. The rudite clasts are well rounded, and are of white quartz and quartzite, with rare black, red and freen fuchsitic quartzite, and reddish sandstone. These clasts have been tectonically elongated and flattened, and are up to 60 cm long; the median size is about 5 cm. The matrix is composed of poorly sorted quartz, feldspar and muscovite sand.

Elswhere the top beds consist of conglomeratic orthoquartzite with pebbles and cobbles up to 8 cm long, interbedded with phyllite or shale, grey chert, and, in the west, three dolomite layers. Each of the dolomite layers is a few metres in thickness.

This is succeeded by interbedded feldspathic wacke, grit, conglomerate, siltstone and shale, each bed being from 0.5-3 m in thickness. The coarser beds are generally graded. Thin white chert beds occur towards the top.

ROBINSON RANGE FORMATION

The Robinson Range Formation is defined as that formation of BIF, hematite shale and chert which occurs at its type section along the range north and west of Mount Padbury. It conformably overlies the Labouchere Formation and conformably underlies the Millidie Creek Formation. It is about 3 500 m thick and is named after the Robinson Range, which runs easterly at about latitude 25° 40′ S, between longitudes 118° 00′ E and 119° 15′ E. The base of the formation is taken as the first appearance of hematite shale with BIF layers.

The basal unit is hematite shale, with bands of BIF up to 15 cm thick, and laminated and nodular chert. The BIF bands become increasingly common up the succession, which passes into interbedded shale and BIF. This main BIF section is shaley in the middle. The BIF is commonly enriched by supergene iron.

Of three samples of BIF examined in thin section, two were of hematite-chert BIF, and one of hematite-quartz BIF. The hematite-chert BIF contains regular bands of massive hematite alternating with chert bands, which include martite octahedra up to 3 mm across. The hematite-quartz BIF is composed of alternating bands, 3-5 mm thick, of fine hematite with martite octahedra, and bands 7-10 mm thick, of quartz grains up to 0.1 mm in diameter.

Above the main BIF section is hematite shale, with minor BIF layers towards the top, and then another BIF unit which is distinguished in the field by irregular and indistinct banding. This higher BIF unit is a quartz-magnetite-hematite rock containing scattered martite or magnetite octahedra, up to 0.3 mm across, with few regular bands of quartz or iron oxide. It may have formed in a higher energy environment than the more regularly banded BIF as it has clastic textures.

Above this horizon is laminated red hematite and green chlorite shale, which is the topmost unit of the formation.

MILLIDIE CREEK FORMATION

The Millidie Creek Formation is defined as that formation of BIF, hematitic shale, feldspathic wacke, chert and dolomite which occurs at its type section 5 km SE of Mount Fraser; it conformably overlies the Robinson Range Formation.

It is at least 1 500 m thick and is named after Millidie Creek, which drains the area south and east of Mount Fraser, and joins the Murchison River at lat. 25° 46′ 00″ S, long. 118° 19′ 00″ E.

The Millidie Creek Formation is the youngest known formation of the Padbury Group and is found in two synclinal cores in the south of the area.

The formation consists of a basal unit of BIF about 300 m thick, succeeded by a shale or slate unit with interbedded feldspathic wacke, BIF, dolomite and chert.

The basal BIF contains thin interbedded hematite shale layers, which become more common higher in the unit. In the lower part, the individual BIF layers have lenticular bands of jasper and white chert. The upper and more shaley section contains chert bands up to 10 cm thick.

The BIF consists of alternating fine-grained quartz-magnetite bands, and coarser clastic textured quartz-magnetite-hematite bands. In thin section one of these coarser bands was seen to contain a lens or nodule of quartzite, which consists of a mosaic of polygonal quartz grains, about 0.05 mm across, with trails of fine-grained iron oxide outlining rounded or irregular to angular shard-like shapes 0.5-1.0 mm across. This BIF has a clastic texture and some of the rounded shapes suggest an original oolitic texture, which was later fragmented. Crystal casts after pyrite occur on some bedding planes.

Above the basal BIF unit is a succession of manganese-stained slate and minor feldspathic wacke, containing two dolomite horizons less than one metre thick near the base. Thin BIF and rare chert horizons occur in the upper part.

The dolomites consist of dolomitic layers and laminae of manganese dioxide. The dolomitic layers are composed of brown dolomite rhombs, about 0.1 mm across, in a matrix of finer-grained quartz, sericite and chlorite.

ECONOMIC GEOLOGY

There are a few small abandoned gold mines in the area, mostly in the sediments within 3 km of the gneiss. They are in or near quartz reefs, and are associated with minor amounts of copper, and less commonly lead. The two largest mines are in a conglomeratic portion of the Labouchere Formation. A costean in the northwest of the area has exposed a quartz vein in dolomite of the Labouchere Formation; the vein contains bornite and malachite.

Manganese has been worked at several localities near Mount Fraser. The ore has formed by replacement in old drainage channels and at the base of scree slopes. Only erosonial remnants of originally more widespread superficial deposits are preserved. The source of the manganese was the nearby BIF and dolomite which are generally stained by manganese.

The BIFs of the Robinson Range Formation contain local concentrations of hematite and goethite, formed by supergene enrichment. No mining has been undertaken but Sofoulis (1970) indicates reserves of 36.6×10^6 tonnes of average grade, ranging from 45 to over 60 per cent iron, for the combined Robinson Range and Peak Hill areas. This estimate assumes an average ore depth of 15.2 m.

The conglomerate at the top of the Labouchere Formation is a potential host for placer gold or uranium, but there has been no reported exploration work on it.

DEPOSITIONAL ENVIRONMENT OF SEDIMENTS

With the exception of the Labouchere Formation the Padbury Group is largely composed of alternating hematite shale and BIF, with lesser amounts of wacke and siltstone. The general pattern is therefore an alternation of chemical and fine clastic sedimentation with occasional contributions of coarser sediment.

The iron in the BIF was originally magnetite so that it was deposited in a mildly oxidising environment. In the upper part of the sequence the BIF often has clastic texture, and one sample suggests a possible oolitic texture. This indicates a higher energy environment than for most chemical sediments. The fine lamination in the associated hematite shale may be non-glacial varves. A possible environment is a shallow marine basin; the chemical sediments and lack of coarser sediments may indicate that adjacent land masses were of low relief.

The Labouchere Formation is coarser grained than the rest of the Padbury Group. The sequence is alternating wacke and shale with conglomerate, common graded bedding, some current bedding and rare ripple marking; it might indicate deposition on the distal margin of a large delta. However, the very coarse conglomerate at the top of the formation suggests a short period of near-shore sedimentation.

AGE OF THE PADBURY GROUP

MacLeod (1970a) assigned these sediments to the Archaean, because of the gold mineralization, presence of BIF, and lithological and structural similarity to Yilgarn Block clastic-volcanic sequences. He mentioned the possibility of a Lower Proterozoic age, perhaps equivalent to the Mount Bruce Supergroup.

The author considers that the sediments are of Lower Proterozoic age, because the succession is more like the Lower Proterozoic sequences of the Hamersley Basin than the Archaean rocks of the Yilgarn Block. The gold and BIF is not diagnostic of Archaean assemblages.

The evidence for a Proterozoic rather than an Archaean age is as follows:

(1) Different structural style to the Archaean of the Yilgarn Block.

(2) Layers of dolomite in upper part of succession.

(3) Common presence of manganese in BIFs and dolomite.

(4) Low grade of metamorphism.

Between the Padbury Group and the metamorphic complex in the southwest are volcanic rocks in faulted contact with the gneiss. The volcanics are mostly metamorphosed mafic rocks with possible pillow structures, but include some altered high-magnesium basalts with quench textures; the high-magnesian basalt implies that the volcanics are more likely to be Archaean rather than Proterozoic. Unfortunately the relationship between the volcanics and the sediments of the Padbury Group is unknown.

The evidence therefore supports a Lower Proterozoic age for the Padbury Group: it is possibly equivalent to part of the Mount Bruce Supergroup in the Hamersley Basin. When mapping of the area across the northern margin of the Yilgarn Block is complete, the relation of the Padbury Group to other Precambrian lithostratigraphic units may be revealed with more clarity.

REFERENCES

Lewis, J. D., 1971, The geology of some carbonate intrusions in the Mount Fraser area, Peak Hill Goldfield, Western Australia: West Australia Geol. Survey Ann. Rept., 1970, p. 50-56.

Lewis, J. D., and Williams, X. L., 1971, The geology and geochemistry of some carbonate intrusions in the Mount Fraser area, Peak Hill Goldfield, Western Australia: West. Australia Geol. Survey Rec. 1970/8 (unpublished).

MacLeod, W. N., 1970a, Peak Hill, W.A.: West. Australia Geol. Survey 1 : 250 000 Geol. Series Explan. Notes.

———1970b, Intrusive carbonate rocks of the Mount Fraser area, Peak Hill Goldfield: West. Australia Geol. Survey Ann. Rept., 1969, p. 26-29.

Sofoulis, J., 1970, Iron deposits of the Robinson Range, Peak Hill Goldfield, W.A.: West. Australia Geol. Survey Rec. 1970/6 (unpublished).

THE APPLICATION OF ERTS IMAGERY TO GEOLOGICAL MAPPING IN THE KALGOORLIE AREA

by R. D. Gee and I. R. Williams

ABSTRACT

A comparison of ERTS imagery with both factual and interpretation geological maps of the Kalgoorlie and Kurnalpi 1:250 000 Sheets demonstrates that the greatest potential of the imagery lies in the recognition of faults and lineaments. Strike dislocations, recognizable on the imagery, correspond closely with major strike faults that have been postulated on hitherto negative evidence. Conspicuous imagery lineaments probably represent fracturing late in the crustal evolution. The broad disposition of greenstone belts and granite batholiths is recognizable, although granite is identified mainly by the overlying superficial Cainozoic sediments. The imagery provides a poor guide to lithology. In most cases the imagery strike trends in the greenstone belts relate to gross lithological layering, but in the more structurally isotropic rocks (e.g. metabasalt) dissection along joints gives spurious strike trends. No routine use of ERTS imagery can be envisaged for the systematic production of 1 : 250 000 geological sheets, however, it is a useful data source during the interpretative stage of regional geological studies.

INTRODUCTION

The Earth Resources Technology Satellite (ERTS) programme is an experimental multidisciplinary study, sponsored by the United States National Aeronautics and Space Administration and the United States Geological Survey, to assess the management of earth resources by remote sensing from spacecraft. The Geological Survey of Western Australia joined the Australian appraisal effort through the Australian Committee for ERTS (ACERTS), and elected to study the "applicability of ERTS imagery to the problems of regional mapping and structural interpretation in poorly exposed Archaean greenstones and metasediments, intruded by granite batholiths and basic dykes". This paper is a modification of a type-III Report of that study, the abstract of which was forwarded via ACERTS to NASA in July, 1974.

The original proposal was to study the area of the main greenstone belt between Kalgoorlie and Norseman. However the lack of coverage in the vicinity of Kambalda, and the cloud covered imagery of the Norseman region required the selection of the Kurnalpi (SH/51-10) and Kalgoorlie (SH/51-9) 1 : 250 000 Sheets. This area is bounded by latitudes 30° S and 31° S, and longitudes 120° E and 123° E.

OBJECTIVES

The broad objective is to evaluate the use of ERTS imagery in the production and interpretation of 1 : 250 000 geological maps. This involves a comparison of the imagery with both "ground truths" and pre-ERTS interpretations. In this study, emphasis is given more to major geological features that relate to Archaean plutonism, vulcanism and crustal deformation, and less to late fracture patterns. Little emphasis is given to Cainozoic weathering sedimentation.

The objective outlined above should be considered in the light of the basic problem of regional geology in the Archaean Yilgarn Block of Western Australia, namely, the difficulty of establishing continuity between small and widely scattered outcrops in strongly lateritized areas.

The objectives that relate to the process of regional mapping present no special problems, because the primary purpose is to systematically document the position and nature of all areas of outcrop. This process should always require ground observation. A related problem involves the attempt to extract the maximum information from areas of laterite. The laterite in this area was an *in situ* blanket development that is now partially dissected and removed by erosion. Commonly vague relict structural patterns can be seen on the ERTS imagery. This investigation also considers whether the multi-spectral overview can "see through" the laterite.

However it is in the interpretive stage where the greatest problem lies. Realistic structural and stratigraphic reconstructions over distance of tens of kilometres are often difficult, and generally require the postulation of large dislocations or faults in areas that are inherently complex. Evidence for these faults is often apparent only after completion of 1 : 250 000 scale mapping or even after synthesis at a scale of 1 : 1 000 000. Mostly these structures have no obvious surface expression, and in many cases the evidence for their existence is based upon the postulate that best fits the data.

IMAGERY AND METHODS

The imagery used is identified by the numbers E-1109-9133 and E-1092-01190. Each ERTS frame covers an area of about 34 000 km^2, compared with about 16 000 km^2 for a 1 : 250 000 sheet. The imagery is not meridionally oriented because the satellite has a heading of 190°. For convenience the imagery analyses are presented here in the standard 1 : 250 000 meridional sheet format, which accounts for the gaps in the Figures 32A and 33A. Coverage is available for the gaps but it is not considered necessary to mosaic the prints for this presentation.

The imagery is available in four spectral bands, namely Multi-spectral Scan (MSS) 4 (0.5-0.6 micrometers, blue-green), MSS 5 (0.6-0.7μ, green-yellow), MSS 6 (0.7-0.8μ, visible red), MSS 7 (0.8-1.1μ, reflected solar infrared). In this study 70 mm negatives, at a scale of 1 : 3.369 million of MSS 4, 5, 6 and 7, were obtained and enlarged to 1 million scale. Preliminary work involved a comparison of the four spectral bands at a scale of 1 : 1 000 000 using annotated transparent overlays. Enlarged prints at a scale of 1 : 250 000 were then made of MSS 7. This enlarged scale provides more data without loss of resolution, enabling the imagery to be directly compared with published 1 : 250 000 maps. However for the purpose of presentation in this paper, the figures have been reduced to 1 : 1 000 000 scale.

The ERTS overlays are reproduced here by superimposed printing on the imagery (Figures 32A and 33A). Three morphological elements are presented on the ERTS overlays:

(1) Major boundaries between contrasting tonal patterns that are not obviously related to drainage features. These boundaries may represent lithological boundaries.

(2) Trends of structural or morphological elements. These may represent traces of planar or curvi-planar structural elements in the bedrock.

(3) Lineaments in excess of 5 km in length, of any morphological expression. These may represent faults, late fractures or master joints.

COMPARISON OF SPECTRAL BANDS

The MSS bands 4 and 5 are totally inadequate for bedrock geological studies. However it is notable that only MSS 4 gives a clear contrast between the Cainozoic sandplain marked by a scrub heath vegetation and the Quaternary alluvial and colluvial sands marked by eucalypt vegetation. In areas of undulating and partly dissected sandplain the Quaternary units mark the small drainage lines that lie on the sandplain unit. Therefore some possible ERTS application for the broader aspects of superficial geology, geomorphology and terrain evaluation are suggested.

Because of the strong reflection near the red end of the visible spectrum, MSS 7 and 6 give a tonal contrast between areas of outcrop (including laterite) and areas of no outcrop.

These two bands are of equal value in bedrock studies, however on MSS 7 the strongly lateritized areas show out more conspicuously as darker grey. Also the intricate dark grey tonal patterns on the surface of the salt lakes, which are well displayed on all spectral bands, are more conspicuous on MSS 7. Black areas, due to the greater reflection (i.e. less penetration) of the layer-wave length, indicate bodies of standing water. For example, the King of the West Lake is represented by the black spot displayed midway on the eastern margin of Figure 32A.

COMPARISON WITH GEOLOGICAL MAPS

Kalgoorlie (Kriewaldt, 1969) and Kurnalpi (Williams, 1970) sheets have been published and are not presented here. Both these are outcrop maps and can reliably be considered as "ground truth" at this scale.

GRANITIC AREAS

The major areas of tonal contrast reflect the gross disposition of the greenstone belts and major granite bodies. Two main tonal patterns are recognized. Firstly, isotropic areas of light grey colour generally represent areas underlain by granite; and secondly, structurally anisotropic areas of dark grey colour generally represent the intervening greenstone belts. Boundaries between the two types have considerable strike extent, and these are shown in Figures 32A and 33A.

However, in detail, the correlation is poor. Many substantial outcrops of granite lie outside the boundary inferred from the overlays. The peripheral portions of the granite masses are, in places, foliated lit-par-lit zones that appear as structurally anisotropic areas and therefore appear as part of the succession. The discrepancy between the ERTS-indicated granite contact and the observed outcrop is particularly evident in the Bulyairdie Dome (Fig. 33B). Usually discrepancies are of the order of 5 km. It is noteworthy that some well-exposed mafic sequences occur within areas of ERTS-indicated granite. Some examples are the greenstone belts at Yangan Hill (location 1, Fig. 33A) and Carr Boyd Mine (location 2, Fig. 33A).

The ERTS imagery does not appear to have provided information on the internal structure of the granite batholiths. Rechecking of imagery in areas of well-exposed granite fail to show any indication of structure. In fact these large areas of outcrop cannot even be distinguished from Cainozoic sand. Very diffuse imagery patterns in the Bulyairdie Dome (location 3, Fig. 33A), having forms remarkably similar to flow-fold geometry, are seen to merge with known lithological traces in the layered sequence around the margin of the dome. Yet these internal traces cannot be matched with any known internal structure, and in fact, occur on large areas of Cainozoic sand. They are the expression of sinuous vegetation patterns that reflect arcuate drainage lines on Quaternary alluvium which is reworked from the older sandplain deposits. Field observations cleary show they are unrelated to bedrock geology.

Similar patterns are apparent in an area of granite on the southern extension of the Bulyardie Anticline (location 4, Fig. 33A). This feature resembles the product of giant-scale strain-slip cleavage, although it is expressed on the ground as arcuate drainage patterns. The area of granite itself is confined by two linear structures that are discussed later. There is no evidence to relate this imagery pattern to bedrock structures.

A distinct imagery pattern is visible in the western part of the granite mass at Lake Owen (location 5, Fig. 32A). Three sets of dark traces seem to indicate remnants of mafic-volcanic rocks within the granite body. Ground inspection has shown these traces are due to sheets of transported ironstone gravel originally derived from the lateritized mafic rocks immediately to the west. These traces probably mark an old sheetwash surface which has now been partly dissected by linear creeks. Although the possibility that mafic-volcanic rocks underlie these traces cannot be discounted, the best evidence is that the underlying rock is granite.

A number of light grey, tonally isotropic, areas on the imagery are not granite. Ground examination demonstrates that they are discrete areas of felsic-volcanic or sedimentary rock within the greenstone sequence. For example the area 3 km east of Kanowna (location 6, Fig. 33A), is a mass of felsic agglomerate and that at Gordons (location 7, Fig. 33A) is an intrusive porphyritic rock. The large area in the Randalls-Mount Belches area (location 8, Fig. 33A) is underlain by greywacke and shale.

Within the greenstone belts at least five small (2-5 km diameter) well exposed granitic plutons, whose presence has been established by ground mapping, are not recognizable on the imagery. These examples include Credo and Mungari on the Kalgoorlie Sheet and Cowarna, Cardunia and Juglah Rocks on the Kurnalpi Sheet. However the outline of one body of granite on the northern extension of the Kunnunalling Anticline has been defined more precisely from the ERTS imagery.

GREENSTONE BELTS

Most imagery trends in the greenstone belts can be related to known geological features. However the individual lithological components, such as conglomerate layers in arenaceous sequences, gabbro sills in metabasalts and interlayering of sediments and volcanics, cannot be distinguished. In fact it is not possible to confidently distinguish between mafic-volcanic, felsic-volcanic and sedimentary rocks. The only possibility of correlation lies in the fact that the mafic-volcanic areas are darker, and are enhanced by the presence of scattered laterite caps.

Structurally anisotropic patterns occur over areas of ferruginous laterite from which no previous structural grain had been recognized. Herein lies a potential use for the imagery. The imagery appears to pick out morphological trends of laterite, having lengths of about 2 km. These trends in many cases correspond with the major structural grain. However in one area of basalt north of the Bulong Anticline (location 9, Fig. 33A), imagery trends are consistently perpendicular to arcuate layering which is defined by gabbro sills recognizable on the ground. This feature may be due to dissection of the laterite along joints, and consequently casts doubts on the general usefulness of using the imagery to determine primary structural trends within the greenstone belts.

The suite of ENE-trending mafic dykes that are clearly represented on aeromagnetic maps and commonly seen in outcrop (Figs. 32B and 33B) are not recognizable on the imagery of this area.

COMPARISON WITH PREVIOUS INTERPRETATION

The pre-ERTS interpretation of Kurnalpi (Fig. 33B) is a modification of one previously published (Williams, 1970), whereas the interpretation for Kalgoorlie (Fig. 32B) is new.

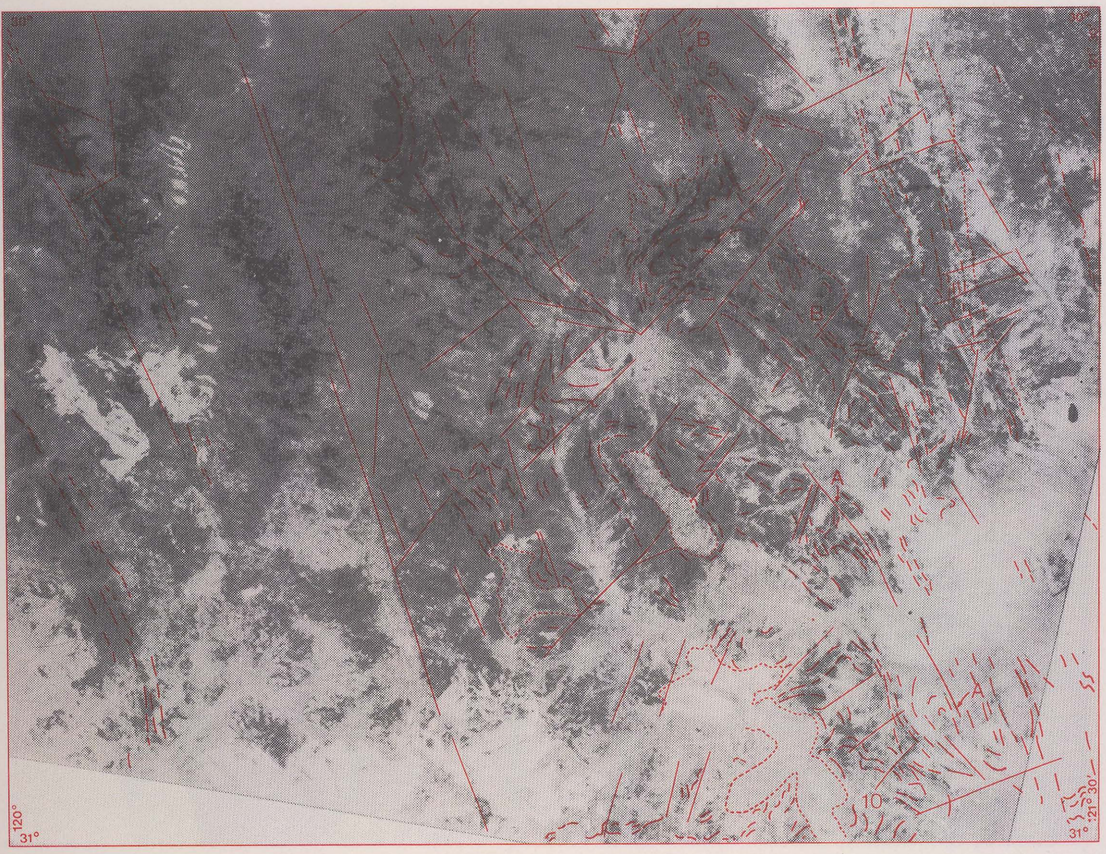

A

------------ Boundary between major tonal patterns
– – – – – Trends in outcrop areas
———— Imagery lineament
Letters refer to dislocation structures ; numerals refer to location cited in text

0 10 20 30 40 km

ERTS image of Kalgoorlie Sheet area, at a scale of 1:1 000 000.

B Ag Archaean granitic rocks ; Ab Mafic rocks ; As Sediments ; Ac Conglomerate ; Af Felsic volcanics ;
Ai B.I.F. ; ---- Postulated strike fault ; ‡‡ Fold traces ; —— Lithological trend ;

Pre-ERTS interpretation of Kalgoorlie Sheet.

Figure 32.

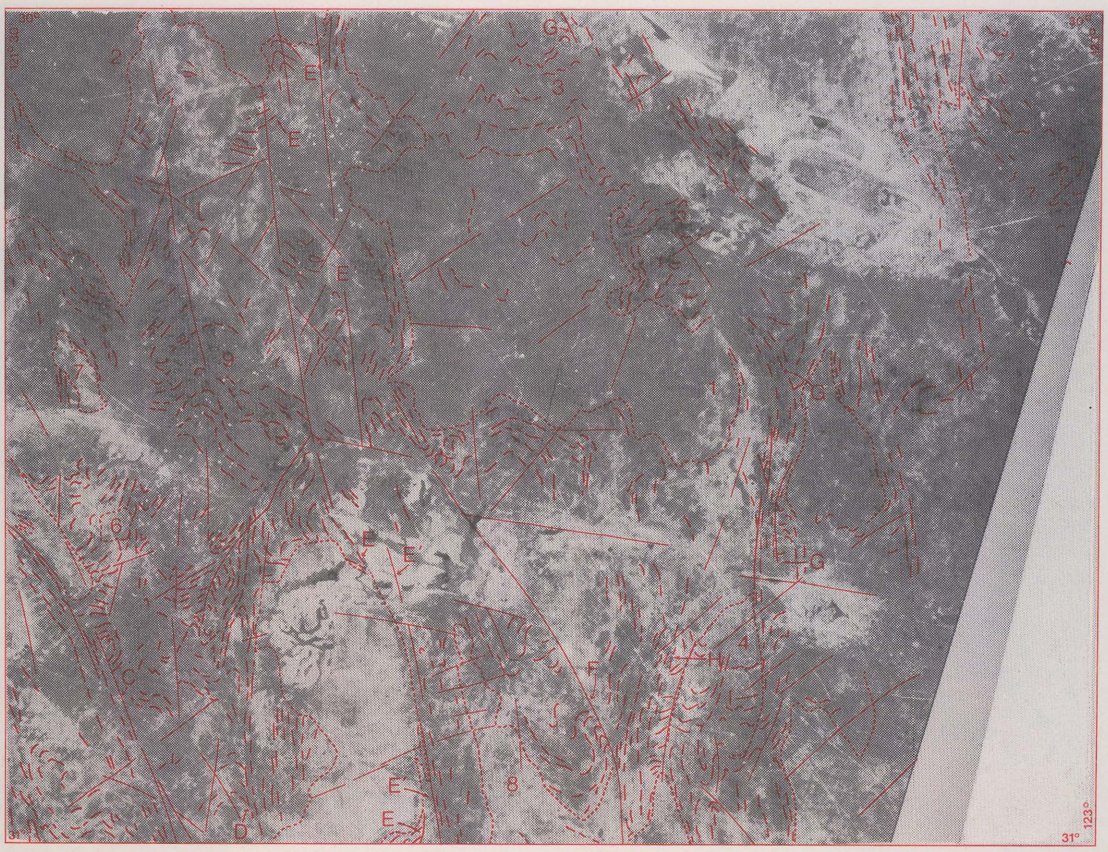

A

------------ Boundary between major tonal patterns
— — — — Trends in outcrop areas
———— Imagery lineament
Letters refer to dislocation structure ; numerals refer to locations cited in text

0 0 20 30 40 km

ERTS image of Kurnalpi Sheet area, at a scale of 1:1 000 000.

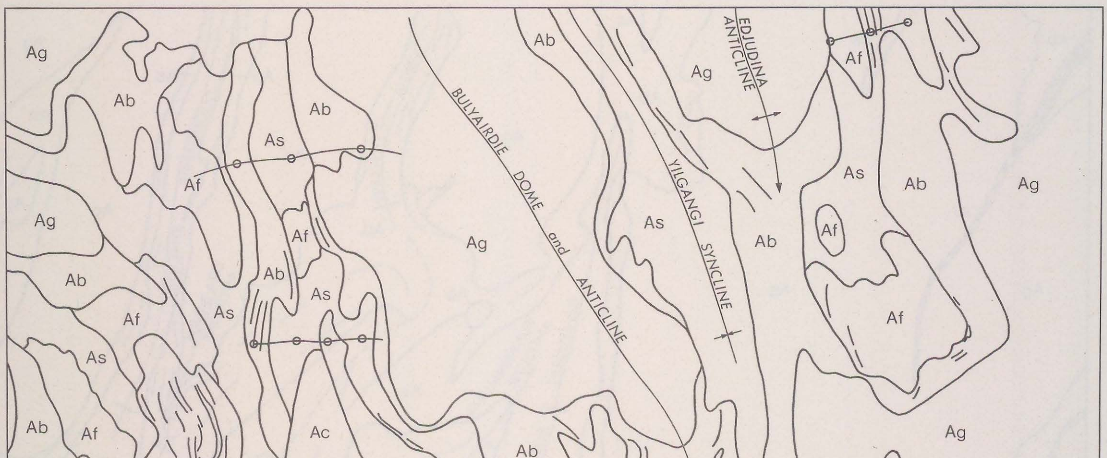

B

Ag Archaean granitic rocks ; Ab Mafic rocks ; As Sediments ; Ac Conglomerate ;
Af Felsic volcanics ; Ai B.I.F. ; ---- Postulated strike fault ; Fold traces ;
—— Lithological trend : o—o Proterozoic mafic dyke

Pre-ERTS interpretation of Kurnalpi Sheet.

Figure 33.

On interpretation maps, it is convenient to represent the Archaean succession by four main units. These are:

(1) A mafic and ultramafic association.

(2) Discrete complexes of felsic volcanic rock.

(3) Fine or medium-grained argillaceous volcanogenic sedimentary rock.

(4) Arenaceous and conglomeratic clastic rock.

Unit 3 occurs peripherally to Unit 2. Unit 1 is thought to form thick sequences that are persistent for long distances along strike. Multi-layering of the mafic-felsic volcanic cycle has previously been demonstrated in the Kalgoorlie region (Williams, 1970). Unit 4 occurs mainly at stratigraphically high levels. Current concepts involve large ovate composite granitic batholiths that intrude the Archaean succession. The interbatholithic areas are in general crumpled synclinal belts.

STRIKE DISLOCATIONS

On the ERTS imagery these features are recognized as the loci of structural discordance that extend for distances of the order of tens of kilometres. They are *not* the most conspicuous features of the imagery and are best revealed once the overlays are made.

They may, or may not, be enhanced by an imagery lineament. Nine strike dislocations are shown on the overlays (labelled A and B on Fig. 32A and C to I on Fig. 33A) and there is evidence for several more. The correlation of these dislocations with previously inferred strike faults is good; several extensions to suspected structures are made, and some new structures are evident. The term "strike fault" is used for a fault that trends parallel with the gross regional strike of the sequence. Strike-slip movement is not implied. Some previously postulated strike faults are shown in Figures 32B and 33B.

Structure A. This structure, which is enhanced by a lineament, relates precisely to a postulated strike fault that lies immediately west of the Kurrawang Syncline. It is manifest on the interpretation map (Fig. 32B) as a line of lithological and structural miss-match, and is known to extend at least 40 km to the south into the Spargoville area. Its northwesterly extension is uncertain, however it may splay into two faults, one into the Siberia Syncline and the other into the Davyhurst Syncline.

Structure B. The nature and significance of this structure is uncertain. In the northern part of the Kalgoorlie sheet it corresponds with the western margin of the major granite body, and has been pointed out previously, the strike discordance may well be related to superficial ferruginous material. However this line of discordance persists to the south-southeast along the western margin of the Ora Banda Anticline and appears to pass to the east of the Kurrawang Syncline, where it can be related to another postulated strike fault.

Structure C. This is the locus of a marked strike discordance that separates northwesterly striking trends to the southwest, from a complex, but generally northerly striking terrain, to the northeast. It nearly fits a line of discordance that Williams (1970) has interpreted as an unconformity. The correlation is not precise and the ERTS-indicated locus disagrees with some ground observations. In view of the possible spurious nature of some of the ERTS trends, this correlation could be considered as significant and supports the interpretation of an unconformity.

Structure D. This corresponds precisely with the Mount Monger Fault which has been recognized in the field as a locus strike discordance, shearing and quartz veining.

Structure E. This structure, which actually consists of two closely adjacent lines of discordance (E and E′), lies immediately to the east of the Bulong Anticline. A major structure has been suspected in this area because it lies between the Bulong and the Belches Anticlines. There is no known syncline separating these two anticlines and a major structural problem exists here.

It is possible that this structure marks a completely faulted out syncline. Structure E can be followed to the northern boundary of Kurnalpi sheet and in fact the aeromagnetic coverage indicates that it extends for hundreds of kilometres to the north and joins with the Keith-Kilkenny Lineament. The Keith-Kilkenny Lineament is very conspicuous on aeromagnetic maps of the Eastern Goldfields and has been shown to be one of the most important tectonic structures of the area (Williams, 1974).

Structure F. This structure appears to dislocate the eastern limb of the Yindalgooda Syncline and does not coincide with any previously recognized strike fault. The imagery gives no indication of its northerly extension. If it continues on the north-northwesterly trend it may merge with Structure E′, as shown on the ERTS overlay. However this would conflict with the position of the trace of the Yindalgooda Syncline which is established from facing evidence in the metabasalts. Alternatively, it could swing to the northeast and join with structures G, H, and I. Known lithological trends support this latter alternative.

The significance of structure F remains uncertain, however it appears to be related to a major system of splay faults that merges into the Keith-Kilkenny Lineament.

Structure G. This relates closely to the southeasterly continuation of the Keith-Kilkenny Lineament. On the geological map (Fig. 33B) it follows closely the Yilgangi Syncline and has a considerable strike extent. To the south it appears to swing from a southeasterly to a southerly direction and becomes involved in a possible splay fault system incorporating structures H and I.

FOLDS

The arcute traces correspond in most cases to previously interpreted folds. The arc around the Ora Banda Anticline between the Siberia and Goongarrie Synclines and the Kurrawang Syncline (Fig. 32A) is clearly depicted on the imagery. Smaller areas of more local crumpling are also recognizable e.g. at Mount Burges (location 10, Fig. 32A). However it has been pointed out that spurious fold patterns can result in areas of lateritized mafic rock due to dissection along cross fractures rather than the bedding. As a qualitative estimate, approximately 60 per cent of the apparent fold traces have geological validity. The balance is either clearly spurious or enigmatic and cannot be resolved with the present data.

In this category is the form of the Yindalgooda Syncline. On the ERTS imagery the Yindalgooda Syncline appears to be a half structure whose eastern limb is completely faulted out by the dislocation F (Fig. 33A).

On the ERTS imagery it apperas that the mafic rocks in the Yindalgooda Syncline are linked over the Belches Anticline to the mafic belt to the west. This reconstruction, however, conflicts with the ground observations because the inferred connecting "mafic rocks" are actually lateritized sedimentary rocks.

IMAGERY LINEAMENTS

Lineaments form two main sets. The most prominent is northeasterly trending, which is roughly perpendicular to the north-northwesterly trending structural grain of the greenstone belts. The second is a set of north-northwesterly trending lineaments that in places enhance known major structural dislocations. Apart from a secondary relationship (for example, following joints that may in some way relate to folds or faults) the lineaments do not appear to show any relationship to the processes of crustal deformation. They appear to be late fractures that are related to master joint patterns or faults. The most conspicuous lineament is that north-northwest trending structure that extends continuously from the southern to the northern edge in the western part of the Kalgoorlie sheet area (Fig. 32A). It lies entirely within granite and has no obvious relationship to bedrock structure.

DISCUSSION AND CONCLUSIONS

The main attributes of ERTS imagery are:

(1) They are small-scale

(2) They approximate closely to orthophotos

(3) The imagery is multispectral

(4) They present repetitive coverage under constant sun angle and constant image processing.

Factors 1 and 4 enable very large tracts of the earth's surface to be viewed under constant conditions, without the patchwork quilt effect of conventional mosaics. Factor 2 enables imagery to be compared directly with geological maps. However, it should be pointed out that at smaller scales, involving larger areas, projection problems will arise. Factor 3 in itself is not of any advantage for the type of application envisaged here, although it has been noted that certain bands have their individual uses. It is acknowledged here that no attempt has been made to adequately assess the value of the multi-spectral factor by using colour composites. It is concluded that the greatest value of ERTS lies in the overview that the satellite coverage allows.

The most significant contribution lies in demonstrating large strike faults. These structures have previously been postulated, mainly on negative evidence, and only in a few cases has their presence been established. Strike trends which serve to outline these faults are more perceptible on MSS 6 and 7, than on the other two bands. In the context of regional fault and lineament analysis the ERTS data are more useful than conventional photomosaics, especially at the continental scale. In this respect it would be an extra tool of the regional geologist that would complement, rather than replace, photogeology and other forms of remote sensing such as aeromagnetics. The imagery gives only a broad guide to first-order block distribution and at the reconnaissance stage has little to recommend it over the more conventional methods employing areal photomosaics and aeromagnetic maps. No routine day to day use of ERTS imagery can be envisaged at this stage.

These conclusions are intended to apply only to the Kalgoorlie test area; however they do accord with other ACERTS investigations, and other studies, reported in the Weekly Abstracts of the National Technical Information Service of the U.S. Department of Commerce. Examination of other parts of the State indicates a varying potential use for ERTS imagery. For example, in the forested and cultivated areas of the southwestern portion of the Yilgarn Block, no lithological and very little structural information is extractable, whereas in the Pilbara Block the patterns of post-granite mafic dykes, and the shape of the granite domes with their delicately scalloped edges is depicted with superior clarity on the imagery than on small-scale mosaics.

REFERENCES

Kriewaldt, M. J. B., 1969, Kalgoorlie, W.A.: West. Australia Geol. Survey 1 : 250 000 Geol. Series Explan. Notes.

Williams, I. R., 1970, Kurnalpi, W.A.: West. Australia Geol. Survey 1 : 250 000 Geol. Series Explan. Notes.

——— 1974, Structural subdivision of the Eastern Goldfields Province, Yilgarn Block: West. Australia Geol. Survey Ann. Rept. 1973, p. 53-59.

DEFINITIONS OF NEW AND REVISED STRATIGRAPHIC UNITS OF THE EASTERN PILBARA REGION

by S. L. Lipple

ABSTRACT

New and revised stratigraphic units of the eastern Pilbara region, Western Australia, are formally defined. They are the Archaean Warrawoona Group (mainly a volcanic sequence), its two principal divisions the Talga Talga and Salgash Subgroups, and its formations (Duffer Formation, Marble Bar Chert, Kelly, Panorama and Wyman Formations), the Boobina Porphyry, and the Gorge Creek Group (dominantly a sedimentary sequence) the Soansville Subgroup, and five of the Group's formations (Corboy and Paddy Market Formations, Honeyeater Basalt, Budjan Creek Formation and Lalla Rookh Sandstone); the Lower Proterozoic Tumbiana Formation (Fortescue Group) and two members (Mingah Tuff and Meentheena Carbonate) and the Lower Proterozoic Spinaway Porphyry.

INTRODUCTION

This report describes and formally defines new and revised stratigraphic units in the Archaean and Lower Proterozoic rocks of the eastern Pilbara region, made necessary as a result of regional mapping of the Marble Bar 1 : 250 000 Sheet area. Descriptions of the regional geology, including that of various Archaean granitic plutons named during mapping, but omitted from this report, are given by Hickman and Lipple (1974, see particularly Fig. 3). Although initially defined for the Marble Bar 1 : 250 000 Sheet area, the units are applicable to the eastern Pilbara region generally. Additional stratigraphic and plutonic units occurring only in the Nullagine 1 : 250 000 Sheet area are described by Hickman (in prep.).

Discussion of earlier Archaean stratigraphic nomenclature in the Pilbara region is given by Ryan (1964, 1965). Development of the stratigraphic subdivision of the Pilbara region may be seen by comparison of the earliest scheme presented by Maitland (1908, frontispiece), the subdivision of Noldart and Wyatt (1962, 1 : 500 000 geological structure map of the Pilbara region), and that of this report.

The Archaean layered succession is divided into a lower, dominantly volcanic suite, the Warrawoona Group and an Upper (locally unconformable), mainly clastic sedimentary suite, the Gorge Creek Group. The constituent subdivisions, together with some previous stratigraphic schemes, are given in Table 9. For convenience, an intrusive metamorphosed Archaean porphyry, the Boobina Porphyry, is described with the Warrawoona Group.

TABLE 9. GENERALIZED STRATIGRAPHY OF THE ARCHAEAN LAYERED SUCCESSION

Group	Subgroup	Formation	Maximum Thickness (km)	Lithology	Former Stratigraphic Divisions
Gorge Creek Group		1 Lalla Rookh Sandstone ? ; 2 Budjan Creek Formation ? ; 3 Mosquito Creek Formation*	2–3 5–10	1 and 2. Sandstone and conglomerate 3. Mainly turbidities, generally schistose, local conglomerate and sandstone near the base	Gorge Creek Formation of Low (1965) = Lalla Rookh Sandstone and Paddy Market Formation (jaspilites) Series (Maitland, 1908; David, 1950, p. 4; Finucane, 1953; Ryan, 1964). 'Series' (Low, 1965) System (Fairbridge, 1953, Chap. I, p. 33, Ryan, 1964) Succession/succession (Noldart and Wyatt, 1962, p. 14, 47, 100–101, 105–107; Ryan, 1964–1965)—Middle Creek Formation; Eastern Creek Formation = Gorge Creek Formation (Low, 1965, Ryan, 1964, 1965) = Dromedary conglomerate; Budjan Creek Formation.
		Honeyeater Basalt	0–1	Pillow Basalt	
	Soanesville Subgroup	Paddy Market Formation	1	Banded Iron Formation and ferruginous clastic sedimentary rocks	Cleaverville Formation of Ryan (1964, 1965) = jaspilite unit (Paddy Market Formation) in Gorge Creek Formation of Low (1965).
		Charteris Basalt*	0–1	Pillow Basalt	
		Corboy Formation	1–2	Quartzite, sandstone and psammopelitic sedimentary rocks	
—V—	—V—	Wyman Formation	1	Porphyritic, columnar-jointed rhyolite	
Warrawoona Group	Salgash Subgroup	—V—V— — —	2–3	Pillow basalt and chert	
		Panorama Formation ⋮ Kelly Formation	1	Dacitic lava tuff and agglomerate and chert with local sandstone and conglomerate	
		— — —	3–5	Pillow basalt and chert	Warrawoona Beds (Maitland, 1908—see frontispiece for best illustration of his stratigraphic divisions) 'Series' (Maitland, 1908; Finucane, 1953) 'Series' (Low, 1965) System (Fairbridge, 1953, Chap. I, p. 33) Succession/succession (Noldart and Wyatt, 1962; Ryan, 1964, 1965)
		Marble Bar Chert	0·1	Banded Chert	
		— — —	0–0·3	Pillow Basalt	
		Duffer Formation	5–8	Dacitic agglomerate	
	Talga Talga Subgroup	— — —	5–8	Basalt with subordinate ultramafic and chert units	

Former divisions shown by vertical arrows (range indicated by arrows beside the table):

- Pilbara System (Noldart and Wyatt, 1962) (Ryan, 1964, 1965 included granitic rocks also) — whole succession
- Mosquito Creek Beds (Maitland 1905) — uppermost formations (1, 2, 3)
- Roebourne Group (Ryan, 1964, 1965) — Honeyeater Basalt to base
- Warrawoona Beds (Maitland, 1905, 1908) — Honeyeater Basalt to base
- Cleaverville Formation (Ryan, 1964, 1965) — Paddy Market Formation to Corboy Formation
- Regal Formation (Ryan, 1964, 1965): — Wyman Formation to base

* Not present in Marble Bar Sheet area. — — — unnamed units —V—V— unconformity ⁞?⁞ relationship uncertain

Partly overlying the Warrawoona Group, with a moderate angular unconformity, is the Mosquito Creek Formation which at present is considered to be part of the Gorge Creek Group.

Within the Lower Proterozoic Fortescue Group, the Tumbiana Formation and two members are formally defined. An intrusive Lower Proterozoic porphyry, the Spinaway Porphyry, is described with the other Fortescue Group units because it occurs at a particular stratigraphic level in the group.

ARCHAEAN LAYERED SUCCESSION

A summary of the Archaean stratigraphic units is given in Table 9.

The Charteris Basalt and Mosquito Creek Formation are included in Table 9 for completeness, but are not defined here as they are restricted to the Nullagine Sheet area, and will be described by Hickman (in prep.).

It will be noted that the Talga Talga Subgroup is not divided into formations. Although units of formational status are present in the type area, more work is required to determine whether these can be extrapolated to other parts of the region.

For convenience cosanguinous igneous rocks, within the volcanic piles, are included as part of the units in which they occur.

WARRAWOONA GROUP

Derivation of name: Warrawoona mining centre (latitude South—S, longitude East—E), (21° 20′ 05″ S, 119° 54′ 25″ E), 1 : 250 000 Marble Bar Sheet area.

Definition: The Warrawoona Group consists of the Talga Talga Subgroup; Duffer Formation; Salgash Subgroup includes Marble Bar Chert, Kelly and Panorama Formation; and the Wyman Formation (youngest).

Lithology: It consists mainly of volcanic rocks with subordinate ultramafic rocks, chert and clastic sedimentary rocks.

Thickness: Range, 5-20 km.

Stratigraphic relations: Lower margin intruded by, or faulted against, Archaean granitic rocks. Overlain both conformably and unconformably by the Gorge Creek Group.

Age: Archaean, as intruded by Archaean granitic rocks (dated in the Mooyella area by de Laeter and Blockley (1972) at 3 125 ± 366 m.y.). Felsic porphyry, from Copper Hills mine, dated by de Laeter and Trendall (1970) at 2 880 ± 66 m.y.

Synonymy: The term, Warrawoona Group, supercedes "Warrawoona Succession" of Noldart and Wyatt (1962, p. 14, 47, 100-101, 107-117) and "Warrawoona Beds" of Maitland (1908, p. 155, 156, 161, 162, 284, 286, 287) and "Warrawoona Series" of Maitland (1908, p. 156), Finucane (1953), and Ryan (1964, 1965).

Talga Talga Subgroup

Derivation of name: Talga Talga mining centre (21° 0′ 10″ S, 119° 48′ 15″ E), Marble Bar 1 : 250 000 Sheet area.

Type area: Near Talga Talga mining centre, from the granite contact westwards through the mining centre almost to the Coongan River.

Lithology: In the type area, the Talga Talga Subgroup consists of a lower pillow basalt sequence containing some stratiform and some lensoid ultramafic units, overlain by a thin sequence of intercalated basalt, siltstone and chert. The chert is overlain by a stratiform, ?vesicular brecciated ultramafic layer, then a thick monotonous sequence of pillow basalt with minor thin chert horizons. The basalt may be quite vesicular, even scoriaceous. The upper margin is marked locally by a thin siltstone. Elsewhere the subgroup consists essentially of pillow basalt with associated minor felsic volcanic, ultramafic and sedimentary rocks.

Thickness: Maximum, 5-8 km.

Stratigraphic relations: The Talga Talga Subgroup is the lowest exposed portion of the Warrawoona Group. It is intruded by Archaean granitic rocks along the lower margins and conformably overlain by lavas and pyroclastic rocks of the Duffer Formation.

Duffer Formation

Derivation of name: Duffer Creek (21° 7′ 20″ S, 119° 45′ 35″ E) Marble Bar 1 : 250 000 Sheet area.

Type area: The area north of Marble Bar townsite, extending westwards from the lower reaches of the Duffer Creek, across the Coongan River to the base of the ranges west of the river. The formation is well exposed around Marble Bar townsite and along the banks of the Coongan River.

Lithology: A volcanic pile of predominantly dacite lava, tuff and agglomerate. Pyroclastic rocks are a feature of this formation. Dacite lava is massive to schistose and may be vesicular or porphyritic. Intercalations of pillow basalt, tuff and agglomerate are also present, particularly in the northern portion of the Marble Bar Belt, and some sedimentary rocks are common throughout the sequence. Minor porphyritic intrusions also occur. Thin cherts are present in the upper part of the succession.

Thickness: Maximum, 5-8 km.

Stratigraphic relations: The Duffer Formation conformably overlies pillow basalt of the Talga Talga Subgroup and conformably underlies the pillow basalt and cherts of the Salgash Subgroup. The Marble Bar Chert or Chinaman Pool chert locally form the stratigraphic unit overlying the Duffer Formation.

Synonymy: Noldart and Wyatt (1962, p. 88-89) refer without definition to a series of feldspar porphyry dykes as the "Duffer's Creek Porphyry". They mapped the steeply-dipping Archaean volcanic rocks to the north of the Coongan River—Duffer Creek junction as Proterozoic porphyry flows, suggested that the dykes were feeders, and implied that the flows were also part of the Duffer Creek Porphyry. The porhpyry dykes were noted by Maitland (1908, p. 7, 19 and 205) as intruding Archaean basalt but were not named by him. He described the area west of the Coongan River as agglomerate, not porphyry as shown by Noldart and Wyatt (1962). The nature of rocks on the adjacent Port Hedland 1 : 250 000 Sheet (Low, 1965, p. 10), also mapped as Proterozoic porphyry, is uncertain. These may actually be partly an extension of the Archaean volcanic rocks in the Marble Bar Sheet area, herein defined as belonging to the Duffer Formation, or, more probably, are equivalent to the Lower Proterozoic Bamboo Creek Porphyry exposed on the Nullagine 1 : 250 000 Sheet (Noldart and Wyatt, 1962; and Hickman, in prep.). De la Hunty (1963, p. 26-27, 32; and 1964, p. 13) also used the name for rocks on the Balfour Downs 1 : 250 000 Sheet area.

As the name "Duffer" was previously used without adequate description or definition, it is reapplied to the suite of Archaean volcanic rocks which dominate the area that Noldart and Wyatt incorrectly show as Proterozoic porphyry, and which they imply is the main outcrop area of the "Duffer Creek Porphyry".

Hickman and Lipple (1974) have shown that the rocks in the Copper Hills area referred to, but not strictly defined, by Noldart and Wyatt (1962, p. 108, 192-193, Plate V) as "Copper Hills Porphyry", are actually Archaean felsic rocks of the Duffer Formation.

Salgash Subgroup

Derivation of name: Salgash mining centre (21° 16′ 45″ S, 119° 47′ 35″ E), Marble Bar 1 : 250 000 Sheet area.

Definition: The Salgash Subgroup consists of the Marble Bar Chert, the Chinaman Pool chert (an informal name), the Panorama and Kelly Formations (lithostratigraphically equivalent) and other unassigned volcanic rocks.

Type area: The type area is between Camel Creek and Salgash. The subgroup is also well exposed along Chinaman Creek, west of Marble Bar and in the North Pole Dome, southwest of North Pole.

Lithology: The unit consists of approximately 2 km of lower basalt lavas, commonly pillowed with intercalated chert horizons; 1 km of dacite lava tuff and agglomerate with local sedimentary rocks (Panorama Formation and Kelly Formation); and about 0.5-1 km of upper basalt lavas, commonly pillowed with intercalated chert horizons; and minor felsic volcanic and ultramafic units.

Thickness: The unit has variable thickness, between 1-8 km, due partly to variation in original depositional thickness, and partly to tectonic thinning.

Stratigraphic relations: The subgroup conformably overlies the Duffer Formation and underlies the Wyman Formation. The upper margin is locally unconformable, as in the Kelly Belt. A distinctive association of closely spaced, thick chert units, including the Marble Bar Chert and Chinaman Pool chert within the pillow basalt, occurs at the base of the subgroup. This association has been recognised from the Pilgangoora Syncline to McPhee Dome.

Marble Bar Chert

Derivation of name: The Marble Bar (21° 8′ 50″ S, 119° 42′ 40″ E), Marble Bar 1 : 250 000 Sheet area. This is the popular name given to the chert where it crops out in the Coongan River, and from which the adjacent pool and nearby township derive their names.

Type area: The Marble Bar, in the Coongan River, 5 km southwest of the Marble Bar township.

Lithology: The Marble Bar Chert is a colourful red and white banded chert exhibiting local hydroplastic brecciation with injection veins of massive dark grey chert. The chert is illustrated by Maitland (1908, Figs. 45-48) and Noldart and Wyatt (1962, p. 108-109).

Thickness: 100 m.

Stratigraphic relations: The unit occurs conformably within the Salgash Subgroup at, or near, the contact with the underlying Duffer Formation.

Synonymy: The same unit was referred to by Noldart and Wyatt (1962, p. 114-116) as the Marble Bar Jaspillite. It was also described by Maitland (1908, p. 19, 204).

Panorama Formation

Derivation of name: Panorama Ridge, which is a prominent ridge extending about 22 km west from 21° 15′ 10″ S, 119° 30′ 10″ E to 21° 16′ 0″ S, 119° 17′ 30″ E, Marble Bar 1 : 250 000 Sheet area.

Type area: Panorama ridge, in the area 6 km northeast from North Shaw mining centre.

Lithology: Dacite lava, tuff and agglomerate are dominant in the western portion. The lava is generally massive but may be vesicular or porphyritic. Minor sedimentary rocks including shale, sandstone and conglomerate, are intercalated within the volcanic sequence. Banded cherts including red and white, grey and white, black and white, and green varieties are prominent. In the eastern portion of the formation, sandstone, grit and conglomerate become dominant. The conglomerate contains abundant clasts of chert, dacite, vein quartz and rare basalt. Current stratification is common in the sandstone and grit units.

Thickness: Maximum 1 km.

Stratigraphic relations: The Panorama Formation is a lenticular volcanic-sedimentary rock sequence occurring conformably within unassigned pillow basalt of the Salgash Subgroup. The volcanic and sedimentary rocks exhibit an interfingering contemporary facies relationship with some contribution from the volcanic pile to the adjacent sedimentary deposits. A similar felsic volcanic-conglomerate unit in the North Shaw Belt is correlated with the Panorama Formation. The Panorama and the Kelly Formations are equivalent.

Kelly Formation

Derivation of name: Kelly copper mine (21° 47′ 30″ S, 119° 52′05″ E), Marble Bar 1 : 250 000 Sheet area.

Type area: Three km southwest of Kelly copper mine.

Lithology: The Kelly Formation consists of porphyritic and vesicular dacite lavas, tuff and agglomerate with some porphyritic dacite sills and minor chert horizons. Some of the dacite lavas exhibit columnar jointing.

Thickness: Maximum 1 km.

Stratigraphic relations: The Kelly Formation is a felsic volcanic pile interfingering with the conformably surrounding unassigned pillow basalts of the Salgash Subgroup. It is equivalent to the Panorama Formation, and is overlain unconformably by the Wyman Formation

Wyman Formation

Derivation of name: Wymans Well (21° 17′ 45″ S, 119° 47′ 05″ E), Marble Bar 1 : 250 000 Sheet area.

Type area: The type area is along Camel Creek, south of Wymans Well where the Formation occurs in rugged orange coloured hills, and near Fieldings Gully. The unit is also well exposed in the upper reaches of Budjan Creek.

Lithology: The formation typically consists of massive to schistose, flow banded, porphyritic rhyolite, locally with notable columnar jointing. It also contains felsic tuff and agglomerate and minor basalt lava and agglomerate in the Soanesville Belt. The columnar jointing is well illustrated by photographs in Noldart and Wyatt (1962, p. 108-109).

Thickness: Maximum, about 1 km.

Stratigraphic relations: Conformably overlies the Salgash Subgroup in the Warrawoona Syncline.

Unconformably overlies the Salgash Subgroup in the Kelly Belt and is there unconformably overlain by the Budjan Creek Formation. It is unconformably overlain by the Soanesville Subgroup in the Soanesville Belt.

Synonymy: Rocks of this unit in the Wymans Well and Upper Budjan Creek areas were described by Noldart and Wyatt (1962, p. 108-109, 192 and Fig. 43, 44) as belonging to the "Copper Hills Porphyry".

Boobina Porphyry

Derivation of name: Boobina Creek (21° 41′ 35″ S, 119° 56′ 55″ E), Marble Bar 1 : 250 000 Sheet area.

Type area: The Boobina Porphyry and its relationships with surrounding rocks may be readily observed along the Corunna Downs road 2-3 km Northwest from Copper Hills. It is also well exposed along the road between Copper Hills and Kelly, near 21° 41′ 35″ S, 119° 56′ 55″ E.

Lithology: A weakly metamorphosed dacite porphyry with a dark grey-green, purple or black aphanitic groundmass. Euhedral to subhedral phenocrysts constitute about sixty percent of the rock and are principally plagioclase (An_{30}) and quartz with lesser amounts of biotite. Plagioclase laths often form glomeroporphyritic groups. The larger phenocrysts are the more altered. In the area south of Kelly, instead of biotite, the porphyry contains altered hornblende. The colourless matrix of the rock is too fine for microscopic identification, but is probably a quartzo-feldspathic aggregate. The texture is consistent with devitrification of glass or metamorphic recrystallization of an extremely fine groundmass.

Rock relationships: The Boobina Porphyry intrudes the Talga Talga Subgroup and Duffer and Kelly Formations. It is intruded by the probably late Archaean Mondana Adamellite which contains abundant xenoliths of the porphyry. The porphyry exhibits a low grade regional metamorphism similar to adjacent Archaean layered succession. In the Kelly area the porphyry is intruded by several white, fine-grained, quartz-feldspar porphyry dykes. The unit is faulted against the Duffer Formation and some faults and shears within the porphyry are quartz-filled and contain copper mineralization.

Structure: The two masses cropping out northwest and southwest of Copper Hills may be connected in depth.

Synonymy: The "coarse-grained feldspar porphyry . . . to fine-grained black feldspar porphyry" of Noldart and Wyatt (1962, p. 193 and Plate V), corresponds to the mass herein defined as the Boobina Porphyry.

The material dated at 2 880 ± 66 m.y., by de Laeter and Trendall, 1970, as Copper Hills Porphyry, in thin section closely resembles the Boobina Porphyry.

GORGE CREEK GROUP

Derivation of name: Gorge Creek (20° 51′ 25″ S, 119° 30′ 55″ E) which crosses the Great Northern Highway, about 1 km west of Farrell Well, Port Hedland 1 : 250 000 Sheet area.

Definition: The Gorge Creek Group consists of the Soanesville Subgroup (Corboy Formation, Charteris Basalt and Paddy Market Formations), Honeyeater Basalt, the coequivalent Lalla Rookh Sandstone and Budjan Creek Formation and the Mosquito Creek Formation.

Lithology: It consists mainly of sandstone, grit, conglomerate, argillaceous sedimentary rock, banded iron formation and minor basalt.

Thickness: Maximum, 5-8 km.

Stratigraphic Relations: Conformably (locally unconformably) overlies and folded with the Warrawoona Group. Relationships with the Warrawoona Group often obscured by regional slides. Unconformably overlain by the Lower Proterozoic Fortescue Group. Intruded by Archaean granitic rocks.

Synonymy: The term, Gorge Creek Group, supersedes "Gorge Creek Formation" of Low (1965, p. 8), Kriewaldt and Ryan (1967, Table 2), Noldart and Wyatt (1962, p. 105-106), and Ryan (1964 and 1965).

Soanesville Subgroup

Derivation of name: Soanesville mining centre (21° 31′ 50″ S, 119° 10′ 55″ E), Marble Bar 1 : 250 000 Sheet area.

Definition: The Soanesville Subgroup consists of the Paddy Market Formation (youngest) and the Corboy Formation, and unassigned sedimentary and volcanic rocks in the Soanesville Belt. Southwest of Yandicoogina mining centre, basaltic volcanic rocks (Charteris Basalt) occur between the Paddy Market Formation and the Corboy Formation.

Lithology: The subgroup includes sandstone, siltstone, ferruginous shale, banded iron formation and pillow basalt. Ultramafic and gabbroic sills intrude the formation.

Thickness: Maximum, 5-8 km.

Stratigraphic relations: Conformably overlain by Honeyeater Basalt, and both conformably and unconformably overlies the Wyman Formation, Salgash Subgroup and Talga Talga Subgroup.

In the Soanesville Belt unassigned rocks of the subgroup are unconformably overlain by a thin, flatlying sequence of felsic lavas, centred on 21° 22′ 53″ S, 119° 07′ 20″ E, which have not been assigned to any named unit. The connection of the unassigned Soanesville Subgroup sedimentary rocks with the Corboy Formation, farther north, is obscured by structural complexity and further study is required to elucidate its nature.

Corboy Formation

Derivation of name: Corboy mining centre (21° 44′ 30″ S, 119° 39′ 25″ E), Marble Bar 1 : 250 000 Sheet area.

Type area: Around the Corboy mining centre in the Coongan Syncline.

Lithology: The unit consists mostly of quartzite, sandstone and psammopelitic sedimentary rocks. There are minor felsic volcanics and ultramafic rocks in the southern portion of the formation, and basalt, usually pillowed, in the northern portion.

Thickness: 1-2 km.

Stratigraphic relations: The relationships of the Corboy Formation to the surrounding units is in many places obscured by regional slides. It conformably overlies the Wyman Formation and conformably underlies the Paddy Market Formation.

Paddy Market Formation

Derivation of name: Paddy Market Creek (21° 22′ 55″ S, 119° 15′ 15″ E), Marble Bar 1 : 250 000 Sheet area.

Type area: The unit is well exposed in a gorge cut by Paddy Market Creek through a prominent ridge at 21° 22′ 55″ S, 119° 15′ 15″ E. It is also well exposed east of Split Rock homestead and north of Honeyeater Creek (21° 13′ 30″ S, 119° 14′ 50″ E). Ferruginous shale is prominent in the area north of Honeyeater Creek.

Lithology: Banded iron formation, shale and ferruginous sandstone and siltstone.

Thickness: Maximum, about 1 km.

Stratigraphic relations: Conformably underlies the Honeyeater Basalt and conformably overlies the Corboy Formation.

Synonymy: The Cleaverville Formation of Ryan (1964, 1965) is equivalent to jaspilites of the Gorge Creek Formation of Low (1965) and these are synonymous with the Paddy Market Formation.

Honeyeater Basalt

Derivation of name: Honeyeater Creek (which crosses the unit at 21° 14′ 00″ S, 119° 15′ 55″ E) Marble Bar 1 : 250 000 Sheet area.

Type area: Adjacent to Honeyeater Creek.

Lithology: The Honeyeater Basalt consists of a monetonous sequence of variolitic, amydaloidal and pillowed basalt.

Thickness: 0.5 km.

Stratigraphic relations: Conformably overlies the sedimentary rocks of the Soanesville Syncline and the Paddy Market Formation in the Lalla Rookh Syncline. Conformably overlain by the Lalla Rookh Sandstone.

Lalla Rookh Sandstone

Derivation of name: Lalla Rookh mining centre (21° 03′ 10″ S, 119° 16′ 35″ E), Marble Bar 1 : 250 000 Sheet area.

Type area: In the Lalla Rookh Syncline, southeastwards from near the Lalla Rookh mining centre.

Lithology: Sandstone and conglomerate, usually well bedded and locally showing cross-stratification and ripple marks.

Thickness: Maximum 2-3 km.

Stratigraphic relations: The Lalla Rookh Sandstone conformably overlies the Honeyeater Basalt. Some local unconformities with the other Warrawoona Group are notable. Equivalent to the Budjan Creek Formation.

Budjan Creek Formation

Derivation of name: Budjan Creek (21° 50′ 30″ S, 119° 52′ 05″ E), Marble Bar 1 : 250 000 Sheet area.

Type area: The unit is well exposed in gorges cut by the upper reaches of Budjan Creek.

Lithology: The basal conglomerate, containing chert, vein quartz and dacite clasts, is overlain by shale, siltstone and sandstone units and capped by a thick conglomerate containing angular chert clasts.

Thickness: Exposed thickness is between 1-1.5 km.

Stratigraphic relations: Unconformably overlies Wyman Formation and Salgash Subgroup. Upper margin partly concealed by unconformable cover of Lower Proterozoic Fortescue Group, and partly faulted against divisions of the Warrawoona Group. Equivalent to Lalla Rookh Sandstone.

References: Noldart and Wyatt (1962), Kriewaldt (1964), Low (1965), Ryan (1964, 1965, 1966), Ryan and Kriewaldt, (1964).

LOWER PROTEROZOIC FORTESCUE GROUP

Tumbiana Formation

Derivation of name: Tumbiana Pool in the Nullagine River (21° 14′ 30″ S, 120° 29′ 20″ E), Nullagine 1 : 250 000 Sheet area.

Type area: From Pelican Pool (21° 20′ 25″ S, 120° 21′ 25″ E) to 3 km northeast on the Nullagine River.

Lithology: Upper carbonate member lower tuff member.

Thickness: At Meentheena, about 200 m. In Marble Bar Sheet area about 50 m.

Stratigraphic relations: Part of Lower Proterozoic Fortescue Group. Conformably overlies Kylena Basalt. Conformably overlain by Nymerina Basalt. Subdivided into Meentheena Carbonate Member and Mingah Tuff Member.

Synonymy: Original name, "Tumbiana Pisolite" (Noldart and Wyatt, 1962, p. 80).

Mingah Tuff Member

Derivation of name: Mingah Well, Meentheena Station (21° 18′ 30″ S, 120° 25′ 05″ E), Nullagine 1 : 250 000 Sheet area.

Type area: Pelican Pool (21° 20′ 25″ S, 120° 21′ 25″ E) on the Nullagine River.

Lithology: Basaltic to intermediate tuff. Minor siltstone, mudstone and basalt. Has characteristic pisolitic texture in places, and ripple marks locally. Thin carbonate overlain by basalt (30 m thick) occur near the middle of the sequence.

Thickness: 150 m at Pelican Pool.

Stratigraphic relations: Underlies Meentheena Carbonate Member, conformable overlies Kylena Basalt.

Structure: Sheet-like.

Meentheena Carbonate Member

Derivation of name: Meentheena homestead (21° 18′ 23″ S, 120° 26′ 03″E), Nullagine 1 : 250 000 Sheet area.

Type area: 3 km northeast of Pelican Pool (21° 20′ 25″ S, 120° 21′ 25″ E).

Lithology: Ripple-bedded dark grey siliceous carbonate rocks, containing algal stromatolites and syndepositional slump structures.

Thickness: 20 m.

Stratigraphic relations: Underlies Nymerina Basalt, overlies Mingah Tuff Member.

Structure: Sheet-like (Krynine's classification, 1948). Member extends from the Gregory Range into the Pyramid 1 : 250 000 Sheet area.

Spinaway Porphyry

Derivation of name: Spinaway Well, Nullagine 1 : 250 000 Sheet area (21° 36′ 45″ S, 120° 3′ 20″ E).

Type area: The Spinaway Porphyry is well exposed 18 km south of Spinaway Well near the Great Northern Highway.

Lithology: It is a coarse-grained plagioclase quartz dacite porphyry with abundant euhedral calcic oligoclase phenocrysts and quartz phenocrysts set in a dark blue-black quartzo-feldspathic groundmass. Opaque minerals, secondary sphene and numerous small apatite crystals are associated with chlorite pseudomorphing original pyroxene. There are pleochroic haloes due to ?allanite and zircon. Secondary sericite, calcite and epidote are common. Further description of the Spinaway Porphyry is given by Hickman (in prep.).

Stratigraphic relations: Intrusive sill into the Hardey Sandstone of the Fortescue Group.

Age: Lower Proterozoic, as preliminary geochronological studies indicate an age of 2 124 ± 195 m.y. (Trendall, 1975).

Synonymy: Correlated with the Bamboo Creek Porphyry by Noldart and Wyatt (1962, p. 89).

REFERENCES

David, T. W. Edgeworth, 1950, The geology of the Commonwealth of Australia, v. 1: London, Arnold and Co., 747 p.

Fairbridge, R. W., 1953, Australian Stratigraphy (2nd edn.): Perth, University of West. Australia Press.

Finucane, K. J., 1953, The geological structure of northwestern and central Western Australia in relation to mineralization: Empire Mining Metall. Australia and New Zealand Cong. 5th Pub., v. 1, p. 188-194.

Hickman, A. H., 1975, Precambrian structural geology of part of the Pilbara region: West. Australia Geol. Survey Ann. Rept. 1974, p. 68.

———in prep., Explanatory notes on the Nullagine 1 : 250 000 geological sheet, W.A.: West. Australia Geol. Survey Rec. 1975/5.

Hickman, A. H., and Lipple, S. L., 1974, Explanatory notes on the Marble Bar 1 : 250 000 geological sheet, W.A.: West. Australia Geol. Survey Rec. 1974/20.

de la Hunty, L. E., 1963, The geology of the manganese deposits of Western Australia: West. Australia Geol. Survey Bull. 116, p. 26-27, 32.

———1964, Balfour Downs, W.A.: Geol. Survey 1 :250 000 Geol. Series Explan. Notes, p. 13.

Kriewaldt, M. G. B., 1964, Dampier and Barrow Island, W.A.: Geol. Survey 1 : 250 000 Geol. Series Explan. Notes.

Kriewaldt, M. G. B., and Ryan, G. R., 1967, Pyramid, W.A.: West. Australia Geol. Survey 1 : 250 000 Geol. Series Explan. Notes.

Krynine, P. D., 1948, The megascopic study and field classification of sedimentary rocks: Jour. Geol., v. 56, p. 130-165.

de Laeter, J. R., and Blockley, J. G., 1972, Granite ages within the Pilbara Block, Western Australia: Geol. Soc. Australia Jour., v. 19, p. 363-370.

de Laeter, J. R., Lewis, J. D., and Blockley, J. G., 1975, Granite ages within the Shaw Batholith of the Pilbara Block: West. Australia Geol. Survey Ann. Rept. 1974, p. 73-79.

de Laeter, J. R., and Trendall, A. F., 1970, The age of the Copper Hills porphyry: West. Australia Geol. Survey Ann. Rept. 1969, p. 54-59.

Low, G. H., 1965, Port Hedland, W.A.: West. Australia Geol. Survey 1 : 250 000 Geol. Series Explan. Notes.

Maitland, A. G., 1905, Further report on the geological features and mineral resources of the Pilbara Goldfield: West. Australia Geol. Survey Bull. 20, 127 p.

———1908, The geological features and mineral resources of the Pilbara Goldfield: West. Australia Geol. Survey Bull. 40, 309 p.

Noldart, A. J., and Wyatt, J. D., 1958, Summary progress report on reconnaissance survey of portion of the Pilbara Goldfield, Western Australia: West. Australia Geol. Survey Bull. 113, p. 35-44.

——— 1962, The geology of portion of the Pilbara Goldfield: West. Australia Geol. Survey Bull. 115, p. 199.

Ryan, G. R., 1964, A reappraisal of the Archaean of the Pilbara Block: West. Australian Geol. Survey Ann. Rept. 1963, p. 25-28.

——— 1965, The geology of the Pilbara Block, Western Australia: Australasian Inst. Mining Metall. Proc. 214, p. 61-94.

——— 1966, Roebourne, W.A.: West. Australian Geol. Survey 1 : 250 000 Geol. Series Explan. Notes.

Ryan, G. R. and Kriewaldt, M. G. B., 1964, Facies changes in the Archaean of the West Pilbara Goldfield: West. Australia Geol. Survey Ann. Rept. 1963, p. 28-30.

Trendall, A. F., 1975, Preliminary geochronological results from two porphyry bodies: West. Australia Geol. Survey Ann. Rept. 1974, p. 103-106.

LIME RESOURCES OF THE COASTAL LIMESTONE BETWEEN LANCELIN AND MANDURAH

by J. L. Baxter

ABSTRACT

Limestone for industry in the Perth metropolitan area is obtained from quarries in the Coastal Limestone at Spearwood, Coogee, Fremantle and Wanneroo. The resources of high quality limestone (containing more than 75 per cent $CaCO_3$) in the Lancelin-Mandurah area are estimated to be about five hundred million tonnes. Most of this material is within 5 km of the coast and contained on land which is considered prime for urban development. To protect the limestone resources for future industrial purposes steps should be taken immediately to rationalize land development and utilization of the limestone bearing country in the vicinity of the metropolitan area.

INTRODUCTION

The limestone resources in the vicinity of the Perth metropolitan area were first reviewed by the Geological Survey of Western Australia during 1951 and 1952 (McMath, 1952). The present survey was undertaken to assess the current resources of limestone and provide data to assist in planning development in the vicinity of the metropolitan area.

It is apparent that limestone between Wanneroo and Fremantle is effectively sterilized, as most limestone ridges here are subdivided for urban development, and consequently high grade limestone deposits, such as those at Reabold Hill and Mosman Park, are excluded from this survey. This report is a summary of the results presented by Baxter and Rexilius (1974).

GEOLOGY

Coastal limestone is exposed in ridges parallel to the coast and up to 5 km inland. The exposures form reefs and wave cut benches in several places along the coast, e.g. Yanchep, Lancelin, Singleton.

The Coastal Limestone ranges in composition from a calcareous sandstone to a limestone with a quartz component of 1 or 2 per cent, to more than 50 per cent. Variation in composition occurs, both locally and regionally, throughout the unit. The MgO content of limestone in all areas decreases from about 2 per cent along the coast to about 0.5 per cent on the inland margin.

The Coastal Limestone is essentially a series of dunes, but locally beach ridges, lacustrine deposits and reef facies occur. For example reef facies limestone is exposed at Peppermint Grove, Trigg and Cottesloe, while 1 km east of Singleton a cocquina, thought to be a beach deposit, has formed.

The petrography of the Coastal Limestone has been reviewed by Baxter and Rexilius (1974). The calcareous fraction of the unit contains foraminifers and rotaliids with fragments of calcareous algae, echinoids and molluscs, while the terrigenous fraction consists almost entirely of well rounded quartz sand grains with minor feldspar and very rare heavy minerals. Typical chemical analyses of the higher grade areas of limestone are given in **Table 10.**

LIMESTONE RESOURCES

Five zones of high-grade limestone (greater than 75 per cent $CaCO_3$) outlined by the survey are shown in Figure 34. They are north of Mandurah, between Coogee and Spearwood, west of Lake Pinjar, northwest of Yanchep and south of Ledge Point. The high-grade material is a skeletal grainstone which is usually white, chalky, fine to medium grained and moderately to slightly coherent.

TABLE 10. CHEMICAL ANALYSES OF COASTAL LIMESTONE FROM QUARRIES BETWEEN MANDURAH AND LANCELIN.

Locality	Manduarh	Coogee-Spearwood Thomson Lake	Lake Pinjar		Yanchep Smokebush Hill	Ledge Point		Breton Bay
						Coast	Inland	
G.S.W.A. No.	41320	41197	41107	41176	41113	41159	41160	41152
SiO_2	14·4	7·23	13·1	13·6	8·08	31·0	15·0	9·85
CaO	45·3	49·9	46·8	46·6	49·4	35·0	45·8	49·2
$\equiv CaCO_3$	*80·0*	*89·0*	*83·5*	*83·2*	*88·2*	*62·5*	*81·7*	*87·8*
MgO	0·65	0·75	0·56	0·72	0·67	2·00	0·58	0·56
$\equiv MgCO_3$	*1·36*	*1·57*	*1·17*	*1·51*	*1·40*	*4·18*	*1·21*	*1·17*
Fe_2O_3	0·14	0·18	0·20	0·16	0·14	0·11	0·21	0·07
FeO	0·06	<0·05	<0·05	<0·05	<0·05	0·12	<0·05	0·10
Al_2O_3	0·81	0·53	0·79	0·62	0·48	0·21	0·73	0·12
TiO_2	0·05	0·02	<0·01	0·02	0·03	0·07	0·02	0·07
P_2O_5	0·07	0·08	0·07	0·06	0·07	0·08	0·06	0·05
MnO	<0·005	<0·005	<0·005	<0·005	<0·005	<0·005	<0·005	<0·005
Na_2O	0·10	0·11	0·08	0·11	0·06	0·16	0·15	0·08
K_2O	0·51	0·36	0·39	0·30	0·28	0·23	0·54	0·12
S	0·018	0·045	0·015	0·011	0·009	0·089	0·016	0·017
H_2O^+	1·12	1·05	0·99	0·88	1·05	1·57	0·84	1·14
Total	99·4	100·2	100·3	100·5	99·8	100·3	100·5	100·6

Trace elements (ppm)

Cr_2O_3	20	10	10	15	15	15	15	15
V_2O_5	<10	<10	<10	<10	<10	<10	<10	<10

Analyst: Government Chemical Laboratories.
Note: Analyses percentage on dry basis
≡equivalent to

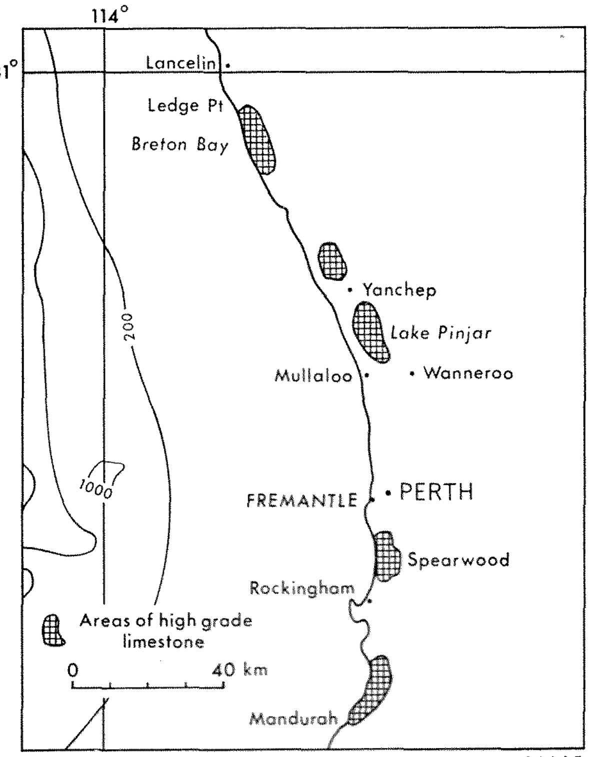

Figure 34. High grade limestone in the vicinity of the Perth metropolitan area.

The deposit north of Mandurah is essentially untested. The limestone occurs east of beach resorts along the coast and contains several zones with greater than 80 per cent $CaCO_3$.

Limestone quarries in the Coogee-Spearwood area have been established for some time, and currently provide most of the lime utilized in the metropolitan area. Large areas are held under various agreements by Swan Portland Cement Ltd and Cockburn Cement Ltd, but smaller areas of high grade limestone are being mined by contractors and government departments for road construction.

West of Lake Pinjar limestone reserves, established by the two portland cement manufacturers, are being held by them to supply their future needs. Several operators are mining in the area to supply lime burning and road construction needs. Most of the limestone here contains more than 80 per cent $CaCO_3$ and less than 1 per cent MgO.

Northwest of Yanchep, adjacent to the Yanchep National Park and within State Forest No. 65, an area of high grade limestone assaying in excess of 85 per cent $CaCO_3$ has been sampled. Isolated areas of this deposit have been quarried to provide material for road construction. This area contains the largest unsecured resources of limestone in the metropolitan area and, if protected, will ensure continued supplies of limestone for industrial purposes for some time.

South of Ledge Point an ill-defined zone of limestone, some of which assays more than 80 per cent $CaCO_3$, has been sampled. The grades of surface exposure vary over short distances and drilling will be required to assess the full potential of this zone.

The inferred resources of these five areas, assuming a mineable depth of ten metres in high-grade limestone, is five hundred million tonnes.

In planning future development of metropolitan Perth the distribution of these important resources should be taken into account and appropriate provision made for their application in the best interests of the community (Baxter and Rexilius, 1974).

REFERENCES

Baxter, J. L. and Rexilius, J. P., 1974, Lime Resources between Lancelin and Mandurah, W.A.: West. Australian Geol. Survey Rec. 1974/24 (unpublished).

McMath, J. C., 1952, Perth and Environs Limestone Resources: West. Australia Geol. Survey, Map Sheets 1-3.

THE MOUNT SEABROOK TALC DEPOSIT

by S. L. Lipple

ABSTRACT

Near Mount Seabrook a white talc deposit, containing 6.8×10^6 t indicated reserves, occurs as a lens within Precambrian metasedimentary schists. The talc was formed at the locus of intense deformation by metamorphism of sandy dolomite. The talc and nearby dolomite have very similar major oxide and trace element compositions. Westside Mines N.L. established a mine in 1972 and total production to the end of 1974 was 14 100 t of lump talc.

INTRODUCTION

The Mount Seabrook talc deposit is located at Trillbar Station, 174 km by road northwest from Meekatharra, lat 25° 36′ 00″ S and long 117° 43′ 17″ E (Fig. 35). The talc was first noted in 1965 by prospector Mr. M. Lalor in the company of an Aboriginal. Mr. Arthur Doust pegged M.C. 190P over the deposit in May, 1969. Adjacent claims were pegged in June, 1969, by Lalor Prospectors Syndicate who later purchased M.C. 190P and carried out geological mapping of the deposit. By May, 1971, Westside Mines N.L., a small public Western Australian company had acquired the whole deposit.

Exploration was concentrated on the northern part of the deposit and included costeaning, diamond and percussion drilling, and shaft-sinking. Following various technical assessments of the talc and market studies, a pilot plant was installed in June, 1972. In August, 1973, a commercial treatment plant was brought into production. By December 1974, 14 000 t of talc had been produced. Of this, 5 062 t were sold realising about $200 000 f.o.b. value.

The mapping on which this report is based was conducted during five days in May, 1974, using 1969, 1 : 40 000 scale air-photographs.

Brief descriptions of the talc deposit were published by Mining Journal (1972, 1973).

REGIONAL GEOLOGY

The Mount Seabrook talc deposit lies near the boundary between the Archaean Yilgarn Block and the Gascoyne Province of Proterozoic metamorphism. The area was mapped by Johnson (1950).

The area about the mine is underlain by metasedimentary rocks with minor gabbro and ultramafic intrusions, metamorphosed generally to greenschist facies, but grading into schists and gneisses. This sequence is probably a continuation of Archaean volcanic and sedimentary rocks, respectively at Mount Maitland (trending northerly) and Mount Taylor-Mount Gould (trending northeasterly), in the adjacent Yilgarn Block. Alternatively, they could be relics of Proterozoic rocks (Pre-Bangemall Group) within gneisses and migmatites of the Gascoyne Province.

In the vicinity of Mount Seabrook (Fig. 35), the metasedimentary rocks strike east-northeast and dip steeply. Evidence provided by a conglomerate, locally truncating and incorporating BIF, suggests that the sequence faces northwards in the vicinity of the mine.

The local base of the succession is a medium-grained granitic gneiss of uncertain origin. This grades northwards through schistose rocks into a

(5)—46009

sequence which is composed mainly of sandstone, grit and conglomerate, but also includes a useful marker horizon of BIF that makes up the spine of the prominent ridge called Mount Seabrook.

Above these predominantly clastic rocks the sequence contains a large dolomite lens. This is poorly exposed, except near Three Corners Well, and obscured by calcrete and transported soil. The dolomite may be locally unconformable over sandstones 1 km west of the talc mine. The rock is grey, fine grained, poorly bedded, and well crystallized. It consists of interlocking polygonal dolomite, minor quartz and chlorite, all of which are strongly oriented, and traces of intergranular talc. Problematic concentric structures in dolomite north of the talc mine have a poorly defined banding resembling stromatolites, but are probably of liesegang origin. The larger dolomite lens appears to wedge out to the east and to grade into clastic sediments to the west.

Several medium-grained massive to schistose gabbro bodies which intrude the metasedimentary sequence (Fig. 35) have had their igneous texture and mineralogy almost completely destroyed. Some of the gabbro masses are intensely sheared to form dark green mafic schists. Decreasing grain size and increasing feldspar content suggests southward facing of a gabbro sill north of Livingstones. Some ultramafic intrusions occur 2 km west of Four Corner Well.

STRUCTURE AND METAMORPHISM

The metasedimentary rocks are steeply dipping with local overturning. The structural interpretation is shown on Figure 35. The broad symmetry of the sequence, together with scant facing evidence suggest that a synclinal fold trace extends east southwards through the Livingstones Find area, bisecting the dolomite and continuing eastwards through sandstones between Bullock Well and Winga Well. Isoclinal folding probably occurs within the gneisses and schists southwest of Mount Seabrook and in the Four Corner Well-Thomson NE Well area. Mesoscopic folding within individual beds is common throughout the metasedimentary sequence.

Metamorphic grade and degree of schistosity, or gneissosity, diminish from the northern and southern areas towards the central dolomite unit, with concomitant increase in preservation of primary mineralogy and textures, although all rocks exhibit some degree of schistosity and cleavage. Metamorphic assemblages observed, variously including biotite, muscovite, chlorite, albite, talc, chloritoid, tourmaline and dolomite, are all consistent with greenschist or lower greenschist facies metamorphism (Turner, 1968, p. 268-270).

Near Mount Seabrook the metasedimentary rocks are moderately to intensely schistose with the development of talc schist in the mine area.

MINE GEOLOGY

The geology of the mine area, together with the positions of the quarry and the various mine buildings, are shown in the inset to Figure 35.

Near the talc mine the rocks consist of metamorphosed sandstone (local current structures), quartzite, pebble conglomerate, quartz-muscovite (biotite-chlorite) schist, and some psammopelitic schist. Schists exhibit vertical lineation along bedding or schistosity planes. A contorted (steeply plunging chevron folds) schist, containing quartz, green muscovite, and magnetite has a distinctive aerial-photo pattern south of the mine. It may represent a fault or northward-thrust zone extending east-northeast from the truncated end of the Mount Seabrook BIF. The schist passes westwards along strike into well laminated sandstone with green muscovite, and grit.

The talc body is a lens of contorted, steeply dipping, white to light green schist with abundant iron and manganese oxide stained fracture partings. The surface talc weathers to an orange or creamy colour. Small quartz pods and grains are present throughout. In thin section the rock is massive, to weakly foliated, fine-grained (a.g.d. 0.05 mm) talc, with minor rounded or anhedral quartz and tiny (0.02 mm) accessory ?apatite. Veinlets of fine opal, probably formed by wheatering, discolour some talc. Rounded strained quartz, with relatively coarse (0.3 mm) talc wrapped around the grains, form an ocellar texture. Talc has partially replaced the quartz. It is difficult to determine petrographically whether the rounded grains represent original detritial quartz, or whether they have undergone perhaps several phases fo recrystallization accompanied by talc replacement. Discontinuous shear zones of very fine talc are deflected around quartz grains. These zones are partly embayed by coarse talc. Minor subhedral quartz bipyramids (0.2 mm) and plagioclase crystals are also embayed by talc. Fresh talc schist, exposed within the quarry, exhibits a light green vanadate staining along fracture and schistosity planes.

The talc has a lenticular interfingering relationship with surrounding quartzose sediments (Fig. 35, inset). Bands and lenses of sandstone are enclosed by talc, particularly near the margins of the ore body, and individual horizons can be traced from schistose sandstone or quartz-muscovite schist via talcose quartz-muscovite schist into talc schist over short distances.

The relationships between the talc schist and enclosing metasedimentary rocks and schists is further complicated by local folding, possible caused by faulting. Near the mine the strike is markedly discordant to the regional strike (as shown by the Mount Seabrook BIF), but changes direction rapidly along strike towards the northwest and merges north of Mount Seabrook with the regional strike (Fig. 35).

The sequence around the mine is locally obscured by 1-2 m of consolidated scree and colluvium. The talc schist, in particular, is covered by colluvium and by minor development of siliceous breccia capping.

The talc quarry is located on the northern part of the talc schist, excavated into a north-sloping ridge with three production benches each about 4 m high and 5-10 m wide. South of the quarry a quartz band projects into the talc lens and will affect quarry extensions. The quarry is rectilinear in design with surface dimensions of 55 m by 65 m. The floor is about 10 m below the north rim.

ORIGIN OF THE TALC SCHIST

The talc schists were produced by greenschist facies metamorphism of sandy dolomite intercalated with enclosing siliceous metasidementary rocks. Turner (1968, p. 131-151 and p. 282-286) discusses greenschist facies metamorphism of carbonate rocks in detail.

The original sediment at Mount Seabrook probably contained 40 per cent silica if none was added from outside the system. Hydrous metamorphism resulted in the formation of talc at low to moderate temperatures since further recrystallization of talc to actinolite or diopside did not occur. Quartz, in excess of that required to form talc, has recrystallized as lenses and granules of coarse quartz throughout the talc schist. Some siliceous metasedimentary bands are preserved within the talc schist. The margins are transitional and contain sandstone and quartz-muscovite schist which presumably reflect decrease in original carbonate content.

Chemical analyses of several talc schist samples (29627A-D) from Mount Seabrook quarry, dolomite (29626B) from 1.6 km west of the quarry, and a sample of Three Springs talc (29643) are listed in Table 11. The Mount Seabrook talc samples show little variation and their average corresponds closely with the analysis of Three Springs talc, which is derived from the metamorphism of stromatolitic dolomite (Wenham, in press). The trace element content, particularly Ni, V, and Cr, show that formation from one of the igneous ultramafic rocks of the area is improbable. Comparison of the talc analyses, with the nearby dolomite sample, shows that derivation from dolomite is likely.

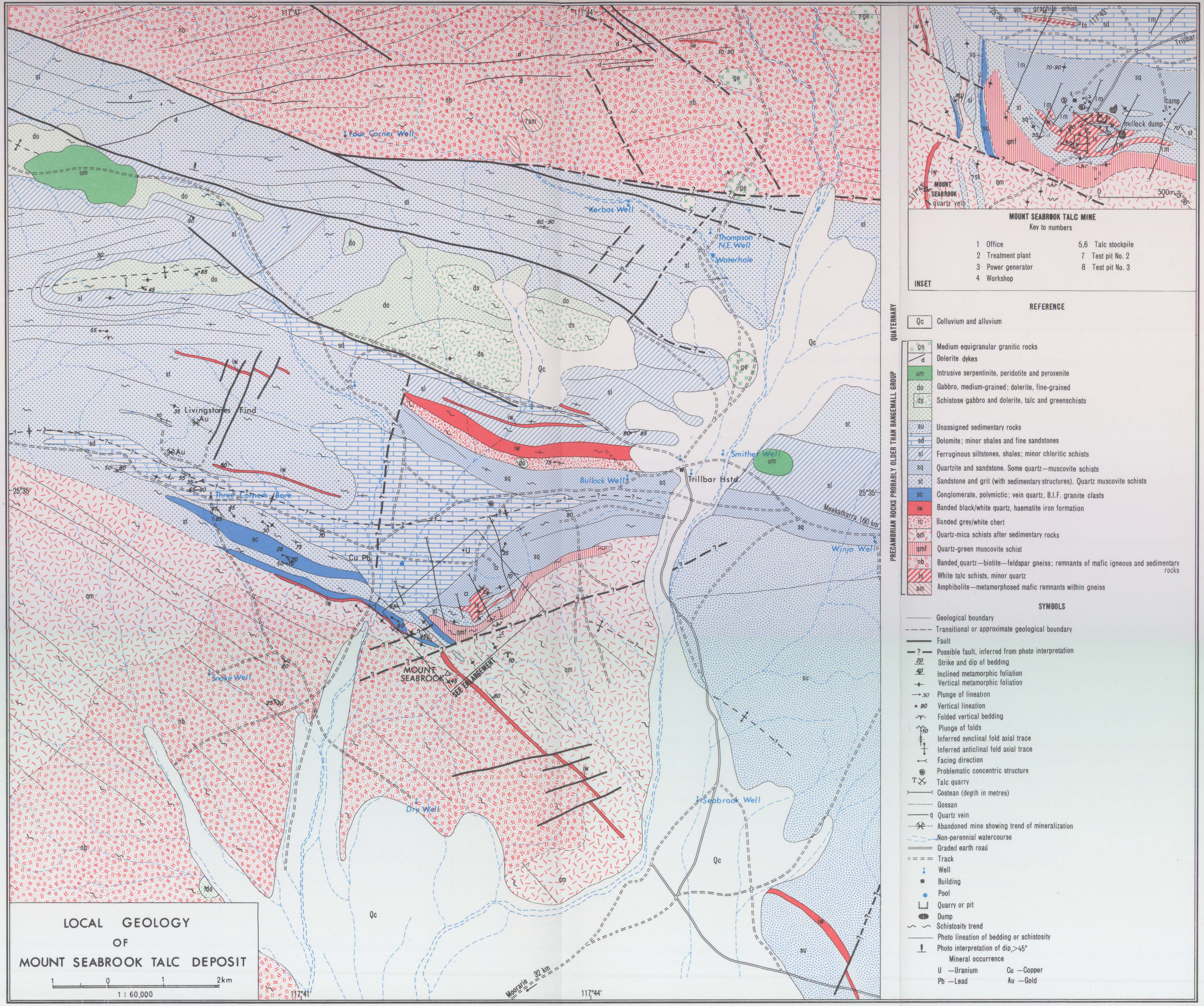
LOCAL GEOLOGY
OF
MOUNT SEABROOK TALC DEPOSIT
1 : 60,000
2km
MOUNT SEABROOK TALC MINE
Key to numbers
1 Office
2 Treatment plant
3 Power generator
4 Workshop
5,6 Talc stockpile
7 Test pit No. 2
8 Test pit No. 3
INSET
REFERENCE
QUATERNARY
Qc Colluvium and alluvium
PRECAMBRIAN ROCKS PROBABLY OLDER THAN BANGEMALL GROUP
ge Medium equigranular granitic rocks
d Dolerite dykes
um Intrusive serpentinite, peridotite and pyroxenite
do Gabbro, medium-grained; dolerite, fine-grained
ds Schistose gabbro and dolerite, talc and greenschists
su Unassigned sedimentary rocks
sd Dolomite; minor shales and fine sandstones
sl Ferruginous siltstones, shales; minor chloritic schists
sq Quartzite and sandstone. Some quartz—muscovite schists
st Sandstone and grit (with sedimentary structures). Quartz muscovite schists
sc Conglomerate, polymictic; vein quartz, B.I.F. granite clasts
iw Banded black/white quartz, haematite iron formation
ic Banded grey/white chert
qm Quartz-mica schists after sedimentary rocks
qmf Quartz-green muscovite schist
nb Banded quartz—biotite—feldspar gneiss; remnants of mafic igneous and sedimentary rocks
lm White talc schists, minor quartz
am Amphibolite—metamorphosed mafic remnants within gneiss
SYMBOLS
Geological boundary
Transitional or approximate geological boundary
Fault
Possible fault, inferred from photo interpretation
Strike and dip of bedding
Inclined metamorphic foliation
Vertical metamorphic foliation
Plunge of lineation
Vertical lineation
Folded vertical bedding
Plunge of folds
Inferred synclinal fold axial trace
Inferred anticlinal fold axial trace
Facing direction
Problematic concentric structure
Talc quarry
Costean (depth in metres)
Gossan
Quartz vein
Abandoned mine showing trend of mineralization
Non-perennial watercourse
Graded earth road
Track
Well
Building
Pool
Quarry or pit
Dump
Schistosity trend
Photo lineation of bedding or schistosity
Photo interpretation of dip >45°
Mineral occurrence
U —Uranium
Pb —Lead
Cu —Copper
Au —Gold
Four Corner Well
Kerbas Well
Thompson N.E. Well
Waterhole
Livingstones Find
Three Corners Bore
Bullock Well
Smither Well
Trillbar Hstd.
Meekatharra 160 km
Winja Well
MOUNT SEABROOK
SEE ENLARGEMENT
Snake Well
Dry Well
Seabrook Well
Moorarie 32 km
Trillbar
camp
mullock dump
graphite schist
quartz vein
25°35'
117°41'
117°44'

Fig. 35.

14687

TABLE 11. CHEMICAL ANALYSES OF MT. SEABROOK TALC AND DOLOMITE AND THREE SPRINGS TALC

Sample No.	29626B	29627A	29627B	29627C	29627D	Average 29627A–D	29643
Major oxides per cent							
SiO_2	1·49	63·6	64·3	63·4	64·3	63·9	62·0
Al_2O_3	0·87	0·24	0·25	0·22	0·28	0·25	0·21
FeO	0·44	0·46	0·46	0·57	0·57	0·51	0·75
Fe_2O_3	<0·05	<0·05	<0·05	<0·05	<0·05	<0·05	<0·05
CaO	28·9	0·36	0·26	0·09	0·02	0·18	0·01
MgO	21·3	30·5	30·1	31·3	30·6	30·6	32·3
Na_2O	0·04	0·01	0·02	0·01	0·01	0·01	0·01
K_2O	0·01	0·01	0·01	0·01	0·01	0·01	0·01
MnO	0·05	0·01	0·01	0·01	0·01	0·01	0·01
CO_2	45·0	0·01	0·01	0·01	0·01	0·01	0·01
P_2O_5	0·19	0·01	0·05	0·02	0·02	0·03	0·01
H_2O^+	1·45	4·81	4·58	4·50	4·50	4·59	4·68
H_2O^-	0·02	0·07	0·07	0·26	0·22	0·15	0·23
TiO_2	0·02	0·01	0·01	0·02	0·02	0·02	0·01
Total	99·78	100·05	100·09	100·38	100·53	100·21	100·20
Trace elements ppm							
Cr	24	28	20	54	35	34	57
V	20	<10	<10	<10	<10	<10	<10
Zn	12	13	5	10	7	9	37
Pb	25	11	14	37	19	20	25
Cu	10	16	6	18	11	12	11
Co	5	3	3	14	14	8	12
Ba	340	90	110	120	110	107	130
Zr	<5	<5	<5	<5	<5	<5	<5
Rb	<5	<5	<5	<1	<1	<3	<1
Sr	49	4	5	<1	9	<5	<1
Li	<1	<1	3	<1	<1	<1	<1
Ga	1·1	0·5	0·2	0·2	0·3	0·3	0·3
B	2	2	9	7	7	6	22
Mn	350	14	18	15	14	15	32
Ni	18	19	24	13	21	19	11

Analyses: W.A. Govt. Chem. Labs., Mineral Divison: E. J. Tovey and R. S. Pepper.
29626B: Dolomite 1·6 km west of quarry
29627A–D: Talc from Mt. Seabrook quarry
29643: Talc from Coodawa, 8 km ENE of Three Springs

The main variation, in major oxide content of the dolomite and talc schist, is in silica and lime. The silica differences probably reflect original composition. The silica poor dolomite has only minor chlorite and traces of talc because it contains low silica, together with a much lower degree of deformation. Small pods of talc are reported to occur along its northern margin. The high lime content of dolomite contrasts with that of the talc. This is a problem if the original dolomitic parent, suggested for the talc schist, had similar lime/magnesia ratio to the dolomite analysed. No carbonate veins occur in the fresh talc schists exposed in the quarry. Hence, either the parent rock of the talc schist was low in lime, or calcium carbonate was expelled during recrystallization.

PROPERTIES AND APPLICATIONS OF TALC

The talc is white, platey with a variable hardness between 1.2 and 1.5 (Moh scale). It contains course quartz inclusions. Near surface talc has been silicified by incorporation of excess silica within the crystal lattice. Average brightness of 29627A-D is about 89 (Elrepho, 457μ) and yellowness is 3.7. In general, it is a high grade micaceous talc suitable for paper coating, paint extender, cosmetics and as an industrial filler. About 70 per cent of recent production has been used in paper applications. The talc has been used in Japan as a paint extender and for coating high quality paper. Application in the U.K. and U.S.A. is mostly in cosmetic and pharmaceutical products. In eastern Australia and New Zealand, the talc is used in cosmetics and as a filler in fibro glass, plastics, paints, dusting powders etc.

ORE RESERVES

Total inferred ore reserves for the whole talc deposit are estimated to be 6.8 x 10^6 t to a depth of 35 m. The depth assessment is supported by diamond drilling, proving the presence of good quality talc to a depth of at least 22 m (locally to 35 m) in the northern part of the deposit. The talc is compact and the ore is assumed to have a density of 2.6 t per cubic metre.

In the more closely drilled portion of the deposit, next to the mine, there are 508 000 t measured ore reserves and 356 000 t indicated ore reserves (*Commerce*, July, 1974, p. 9, 11) to a depth of 15 m, lying beneath 2-3 m of overburden. Inferred reserves between 15-30 m are about two million tonnes. Allowing for waste rock, loss during mining, and inferior talc rejected during treatment, the saleable talc present is probably half the reserves given above.

CONCLUSIONS

The talc deposit is a white schistose rock suitable for various commerical applications. It has formed, in a site of strong deformation, by greenschist facies metamorphism of a sandy dolomite intercalated with ?Archaean siliceous metasedimentary rocks. The main dolomite unit overlying the talc schist has been less deformed and less metamorphosed and, because of its low silica content, has only traces of talc. Although chemical analyses support a dolomitic origin of the talc, comparison should also be made with schists formed from mafic and ultramafic intrusions in the region.

ACKNOWLEDGEMENT

The author thanks Westside Mines N.L. for providing detailed drilling information and plans of the quarry site.

REFERENCES

Johnson, W., 1950, A geological reconnaissance survey of part of the area included between the limits lat. 24° 0′ S and lat. 29° 0′ S and between long. 115° 30′ E and long. 118° 30′ E including parts of the Yalgoo, Murchison, Peak Hill and Gascoyne Goldfields: West. Australia Geol. Survey Bull. 106. p. 103.

Mining Journal, 1972, v. 278, No. 7136, p. 431.

——— 1973, v. 280, No. 7192, p. 514.

Turner, F. J., 1968, Metamorphic petrology, mineralogical and field aspects: McGraw Hill, New York.

Wenham, M., in press, Talc in Western Australia *in* Knight C. L. (Ed.), Economic Geology of Australia and Papua New Guinea, v. 2: Australasian Inst. Mining and Metallurgy, Melbourne.

PRECAMBRIAN STRUCTURAL GEOLOGY OF PART OF THE PILBARA REGION

by A. H. Hickman

ABSTRACT

The structural geology of granite-greenstone and Proterozoic terrain in the eastern part of the Pilbara craton is reinterpreted. Regional mapping of 36 000 km^2 of country around the towns of Marble Bar and Nullagine has revealed Archaean and Proterozoic structures belonging to five periods of deformation:

D1: Interfolding of greenstone and granitic material, granitic intrusion and migmatization. Crustal reworking to produce a granodioritic, partly gneissic, protocrust.

Deposition of a 15-30 km-thick layered succession.

D2: Diapiric movement (solid-state) of protocrust forming 30-100 km-wide granitic domes and intervening greenstone synclinoria. Greenschist to amphibolite facies metamorphism.

D3: Conjugate folding and faulting. Dyke intrusion.

D4: Open recumbent folding. Relations to D3 uncertain.

D5 (Proterozoic): Open upright folding about northerly trending axes. Tight folding and associated strike faulting on the eastern margin of the craton.

INTRODUCTION

The chief structures of the Pilbara craton are its large granitic domes and intervening greenstone synclinoria, deeply eroded before the deposition of an overlying Lower Proterozoic cover. Between Roebourne and Nullagine the latter has been largely stripped off exposing a 60 000 km^2 area of typical Archaean geology.

This paper describes the structural geology of 36 000 km^2 in the eastern part of the craton and its surrounds using information gained during remapping of the Marble Bar and Nullagine areas (Hickman and Lipple, 1974; Hickman, in prep.). The structural geology of this area was first described by Noldart and Wyatt (1962) who recognized the existence of dome and basin structures but attributed them to cross-folding of an early fold system. Late orogenic granitic batholiths were said to have "tightened the existing fold patterns, further compressing the synclinal belts and accentuating the domal patterns".

STRATIGRAPHY

The Precambrian stratigraphy of the area has been described by Hickman and Lipple (1974) and Hickman (in prep.). Its major subdivisions are:

Middle Proterozoic—conglomerate, sandstone, shale and carbonate.

Unconformity

Lower Proterozoic —dolomite, shale and chert over a predominantly volcanic assemblage.

Unconformity

Archaean—

Gorge Creek Group: sandstone, shale, chert, banded iron formation, conglomerate, turbidites with minor pillow basalt.

Unconformity

Warrawoona Group: pillow basalt, andesite, chert, dacite, ultramafic rocks, pyroclastic rocks and minor clastic sedimentary rocks.

Faulted or intrusive contact

Foliated granodiorite to adamellite complex.

In an accompanying paper Lipple (1975) formally defines the Gorge Creek and Warrawoona Groups, and tabulates the Archaean succession of the Marble Bar area.

Certain evolutionary models proposed by previous workers to explain Archaean greenstone belt developement (e.g. Anhaeusser and others, 1968) postulate deposition of the layered succession (in this case the Warrawoona and Gorge Creek Groups) within isolated elongate basins positioned along the present belts. Such restricted deposition did not take place in the Marble Bar-Nullagine area where stratigraphic sequences can be traced between belts and across major greenstone domes (e.g. the North Pole Dome and McPhee Dome). The Archaean stratigraphic pile of this area is broadly tabular over lateral distances of at least 200 km.

GEOCHRONOLOGY

Table 12 summarizes geochronological data from rocks of the area.

TABLE 12. GEOCHRONOLOGICAL SUMMARY OF THE MARBLE BAR AND NULLAGINE SHEETS

	Rock type and relations	Locality	Age m.y.	Initial Sr^{87}/Sr^{86}	Method and reference
PROTEROZOIC	Spinaway Porphyry. Felsic sill in Fortescue Group	W side Great Northern Highway, 15 km N of Nullagine 21° 46′ S, 120° 05′ E	2 124 ± 195	0·712 6 ± 0·013 9	Rb-Sr Trendall, 1975
PROTEROZOIC	Bamboo Creek Porphyry. Felsic sill in Fortescue Group	Bamboo Creek Mining Centre, 20° 55′ S, 120° 13′ E	2 820 ± 516	0·701 0 ± 0·020 0	Rb-Sr Trendall, 1975
PROTEROZOIC	Black Range Dyke	Cooglegong Creek, 21° 35′ S, 119° 28′ E	2 329 ± 89	0·726 2 ± 0·012	Rb-Sr Lewis, Rosman and de Laeter, 1975
ARCHAEAN	Moolyella Adamellite	Moolyella 20 km east of Marble Bar	2 670 ± 95	0·739 7 ± 0·041 9	Rb-Sr de Laeter and Blockley, 1972
ARCHAEAN	Cooglegong Adamellite	Shaw River 50 km SE of Marble Bar, 21° 30′ S, 119° 00′ E	2 602 ± 132	0·731 0 ± 0·029	Rb-Sr de Laeter, Lewis and Blockley, 1975
ARCHAEAN	Cookes Creek Granite	45 km ENE of Nullagine	2 750*		Rb-Sr Trendall (pers. comm.)
ARCHAEAN	MAIN PERIOD OF DEFORMATION, D2				
ARCHAEAN	Copper Hills "Porphyry". Felsic tuff in Warrawoona Group	Copper Hills Mine, 21° 39′ S, 119° 58′ E	2 880 ± 66	0·730 3 ± 0·011 9	Rb-Sr de Laeter and Trendall, 1969
ARCHAEAN	Foliated migmatitic granite	Moolyella, 20 km east of Marble Bar	3 125 ± 366	0·701 6 ± 0·004 7	Rb-Sr de Laeter and Blockley, 1972
ARCHAEAN	Foliated migmatitic granite	Shaw River, Spear Hill, 21° 30′ S, 119° 00′ E	2 951 ± 83	0·702 0 ± 0·001 0	Rb-Sr de Laeter, Lewis and Blockley, 1975
ARCHAEAN	Granitic Rock	Pilbara Block	3 050 ± 180		Rb-Sr Compston and Arriens, 1968

* Unpublished provisional value subject to revision by further analyses planned at time of writing.

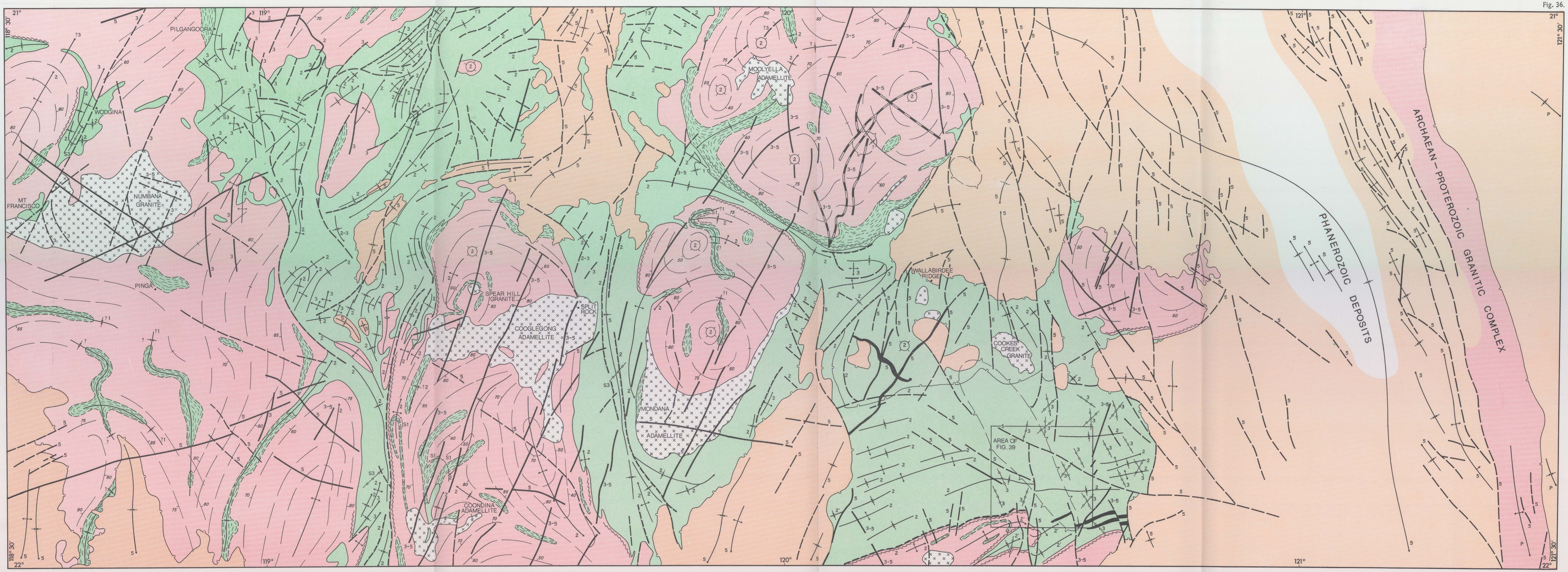

MAJOR STRUCTURAL DIVISIONS

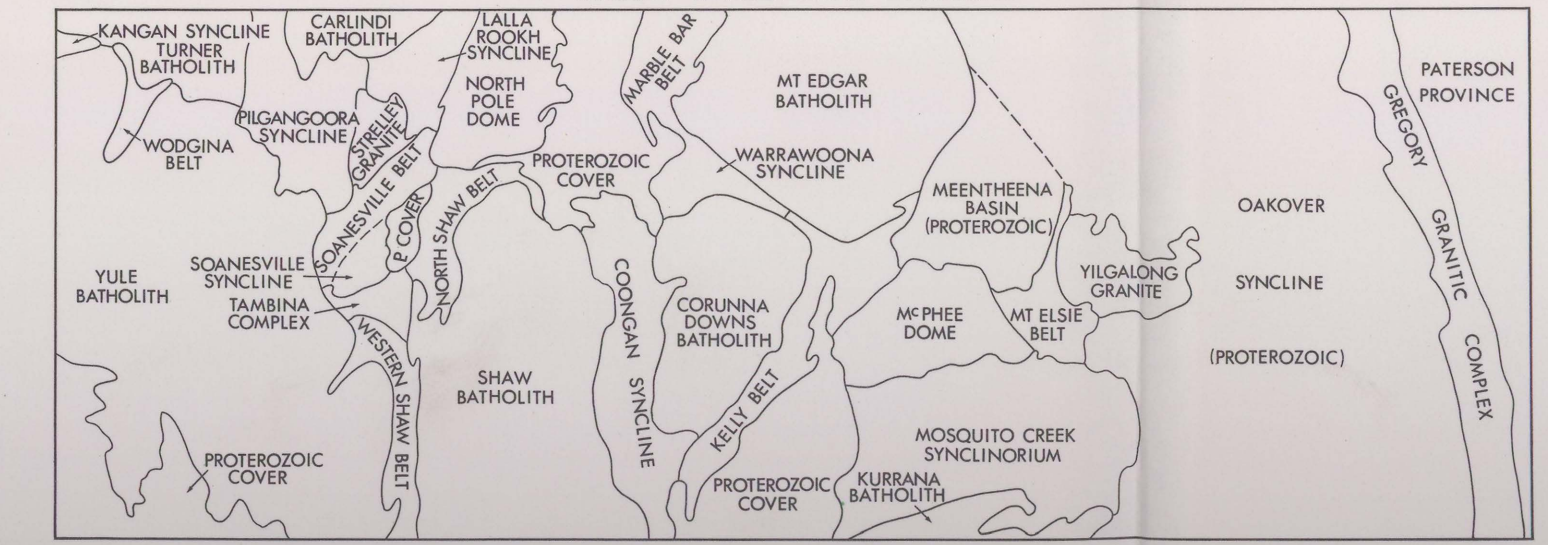

REFERENCE

- Mafic to ultramafic dyke
- Felsic dyke
- Proterozoic rocks
- Unconformity
- Post-tectonic Archaean granite
- Intrusive contact
- Archaean greenstones and metasediments
- Archaean granitic rocks with numerous greenstone xenoliths
- Archaean granitic rocks

SYMBOLS

- 1, 2, 3, 4, 5, P — First, second, third, fourth, fifth and Paterson Province deformation structures
- S1 — D1 foliation (schistosity)
- S2 — D2 foliation (schistosity) with dip locally indicated
- S3 — D3 foliation (strain-slip cleavage)
- Synclinal fold axis
- Anticlinal fold axis
- Synformal anticlinal axis
- Dome
- Tectonic slide
- Shear belt
- Fault
- Unconformity
- Zone of Proterozoic granite stocks

GEOLOGICAL SURVEY OF WESTERN AUSTRALIA

STRUCTURAL GEOLOGY OF THE MARBLE BAR AND NULLAGINE SHEET AREAS

SCALE

10 0 10 20 30 KILOMETRES

Perhaps the most significant point revealed by Table 12 is that rocks deformed by D2, in effect the greenstones and most of the area's granitic rocks, appear to be aged between 3.2 and 2.8 b.y. whereas the post-tectonic, non-deformed granites ("younger granites") are 2.7-2.6 b.y. old. For reasons advanced by de Laeter and Blockley (1972) it seems probable that the 2.7-2.6 b.y. granites are derived by partial remelting of the migmatitic granites. Such cross-cutting massive granites are commonly generated and emplaced during the later stages of major orogenic episodes; the last such episode in the region was D2. Accordingly it is believed that D2 culminated at about 2.7 b.y.

STRUCTURAL FORMS

Figure 36 shows the position and geological relationships of individual structures and the distribution of major structural units.

GRANITIC DOMES AND GRANITIC SYNCLINES

The granitic domes are broad, steep-sided structures, generally round to ovoid in plan and measuring 30-100 km in diameter. Surface geology and Bouguer anamoly patterns indicate that at depth the domes merge to form a predominantly granitic basement. Each mass typically contains several plutons; composition and texture are extremely varied.

Most of the rocks are foliated. Often, as in marginal areas near the enveloping greenstones, the foliation is extremely pronounced and schistose granitic rocks are common. Towards the centre of each dome this foliation becomes less conspicuous and often only a weak biotite alignment can be detected. Indeed, it is not uncommon to observe what appear to be primary flow structures in such areas. The predominant foliation of the domes is mechanical, a strain effect of vertical shear stress during diapiric movement. On Figure 36 its strong geometrical relationship to the shape of these domes is obvious, and it is superimposed across all internal plutonic boundaries except those of the 2.6-2.7 b.y. granites.

Few of the domes are simple structures; most, especially the larger ones, contain synclines in which the foliation referred to above converges downwards. These intra-domal synclines are characterized by broken trails of greenstone material and, in some cases, by shear belts along their length. Their rocks and structures are similar to those found near contacts with the major greenstone belts and the probability is that many are root zones of now eroded overlying greenstone synclines. This is certainly true at Warrery Gap (Corunna Downs Batholith) and Tambourah (Yule Batholith) where tapering greenstone protuberances pass progressively into intra-domal synclines as deeper structural levels are exposed. Less commonly, greenstone xenolith belts, within the domes, do not lie in D2 synclinal cores and these may represent pre-D2 fold remnants within the plutonic complex (c.f. pre-dome structures of Rhodesian Basement Complex, Stowe, 1968). Alternatively they may mark past granite-greenstone contacts forced apart by later plutons. An example of this type of contact is the northern margin of the Bamboo Springs Adamellite (Hickman and Lipple, 1974).

POST-TECTONIC GRANITES

Unlike the foliated granitic complex, which has been deformed during doming, the post-tectonic granites (Fig. 36) are massive discordant intrusions with sharply defined contacts. The granite and adamellite which comprises them is equigranular unfoliated to poorly foliated, and contains much more microcline, quartz and muscovite than the older granitic rocks. Many of the post-tectonic granites are fringed by associated late-stage pegmatite veins containing economically important minerals, especially cassiterite and tantocolumbite.

The post-tectonic granites form irregular stocks. An absence of marginal disruption of the intruded country rocks and the occurrence of roof pendants and xenoliths of host rock within the bodies suggests "permitted" rather than "forceful" intrusion, probably by a process of magmatic stoping.

The recent mapping has revealed a significant degree of structural control over the emplacement of the post-tectonic granites. The recognition of synclines within the domes has shown that the intrusions tend to occupy D2 synclines, whether these be in granitic or greenstone areas (Fig. 36). Partial remelting of the pre-D2 granitic complex, probably in the high temperature, low confining pressure environment beneath the synclines, must have been followed by upward magmatic intrusion along lithological contacts and shear planes (Fig. 37). High pressure rigid-dome cores were not invaded.

The post-tectonic granites are now exposed at three structural levels:

High level: Granite enclosed by greenstones, e.g. Cookes Creek, Wallabirdee Ridge. Economic minerals of W, Mo, Cu, F, Li and Ba.

Intermediate: Granite at or near greenstone-older granite contacts e.g. Wodgina, Mount Fancisco, Split Rock, Mondana and ?Pilgangoora. Economic minerals of Sn, Ta, Li, Be, and W.

Low level: Granite enclosed by older granite e.g. Moolyella, Spear Hill, Cooglegong, Coondina and ?Pinga (not exposed). Economic minerals of Sn and Ta; others rare.

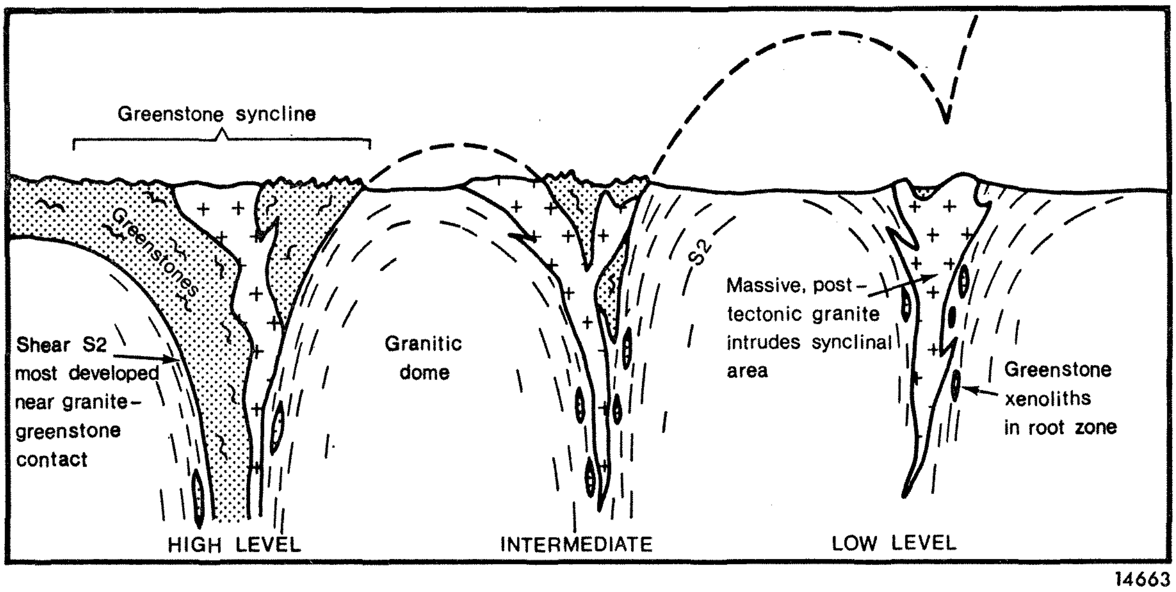

Figure 37. Diagrammatic cross-section showing various structural environments of the post-tectonic granites.

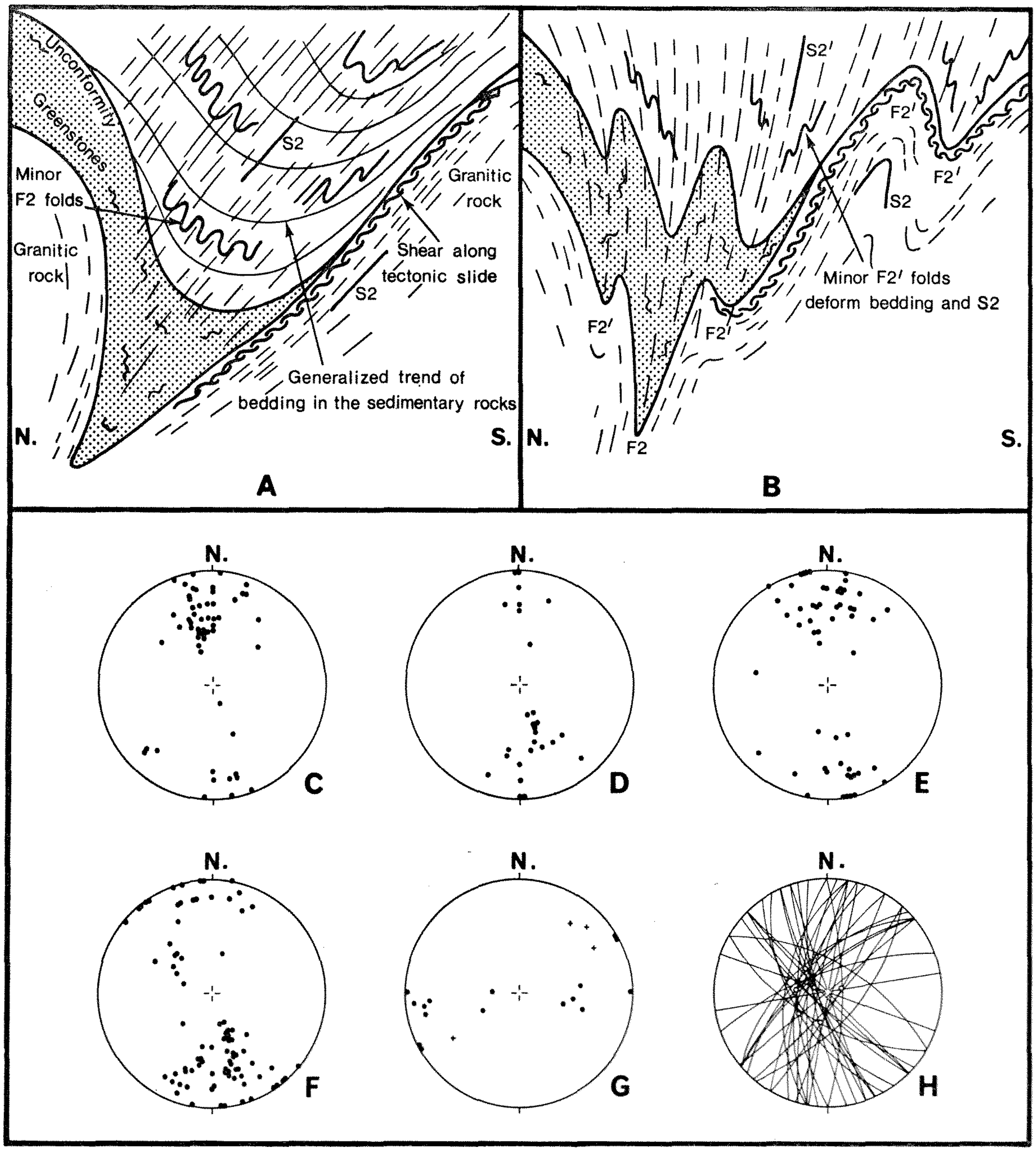

Figure 38. Structural interpretation of the Mosquito Creek Synclinorium. A. Initial form of synclinorium after main D2 folding. B. D2 synclinorium modified by late D2 movements. Includes F2′ folding. C–H: Stereograms of structures in the eastern part of the synclinorium; C, poles to bedding in the northern half of the synclinorium (note prevailing dip is approximately 50° at 170°); D, poles to bedding in the southern half of the synclinorium (prevailing dip is approximately 45° at 350°); E, poles to S2 and S2′ in the northern half of the synclinorium (prevailing steep southerly dip); F, poles to S2 and S2′ in the southern half of the synclinorium (prevailing moderate to steep northerly dip); G, dots, β-points at S:S2 intersection where both measured (approximates to F2 plunge); crosses, F2 plunge measurement; H, S3 great circles. Area of maximum intersection corresponds to regional b-tectonic axis; dots, β-points to conjugate S3 planes.

GRANITE-GREENSTONE CONTACTS

Granite-greenstone contacts are either intrusive or tectonic; in no case has an unconformity been discovered. This situation appears very common in similar terrain elsewhere in the world and has often been cited as evidence that the granite domes are intrusive.

Marginal intrusive relationships do not of course prove that an entire granitic dome is a magmatic intrusion. As excellently demonstrated by the post-tectonic Mondana Adamellite, granite-greenstone contacts are very susceptible to magmatic intrusion. Moreover, without exception, the migmatites of the contact zones are sheared in harmony with neighbouring greenstones. Tectonic foliation can often be traced along strike from greenstone rocks across invading granitic bodies and back into greenstone rocks. Clearly these intrusive structures generally pre-date the marginal shear around the domes. It is possible that the foliated marginal intrusive bodies are syn-orogenic granites generated during deformation of the older granitic complex. Such rocks could have originated as intrusions into the mechanically active contact zone during doming, consolidated and then been sheared by continued deformation. Alternatively, some of the migmatites may have been formed before doming by granitic intrusion along the granitic basement-greenstone boundary.

Sheared contacts commonly accompany steeply dipping, attenuated marginal greenstone units. Attenuation and faulting may be so intense as to tectonically condense or slide out many kilometres of rock at the base of the greenstone succession. In many cases the granites themselves are converted to schist, often with complete destruction of all igneous textures. Such strongly deformed contacts are typical of fairly deep structural levels.

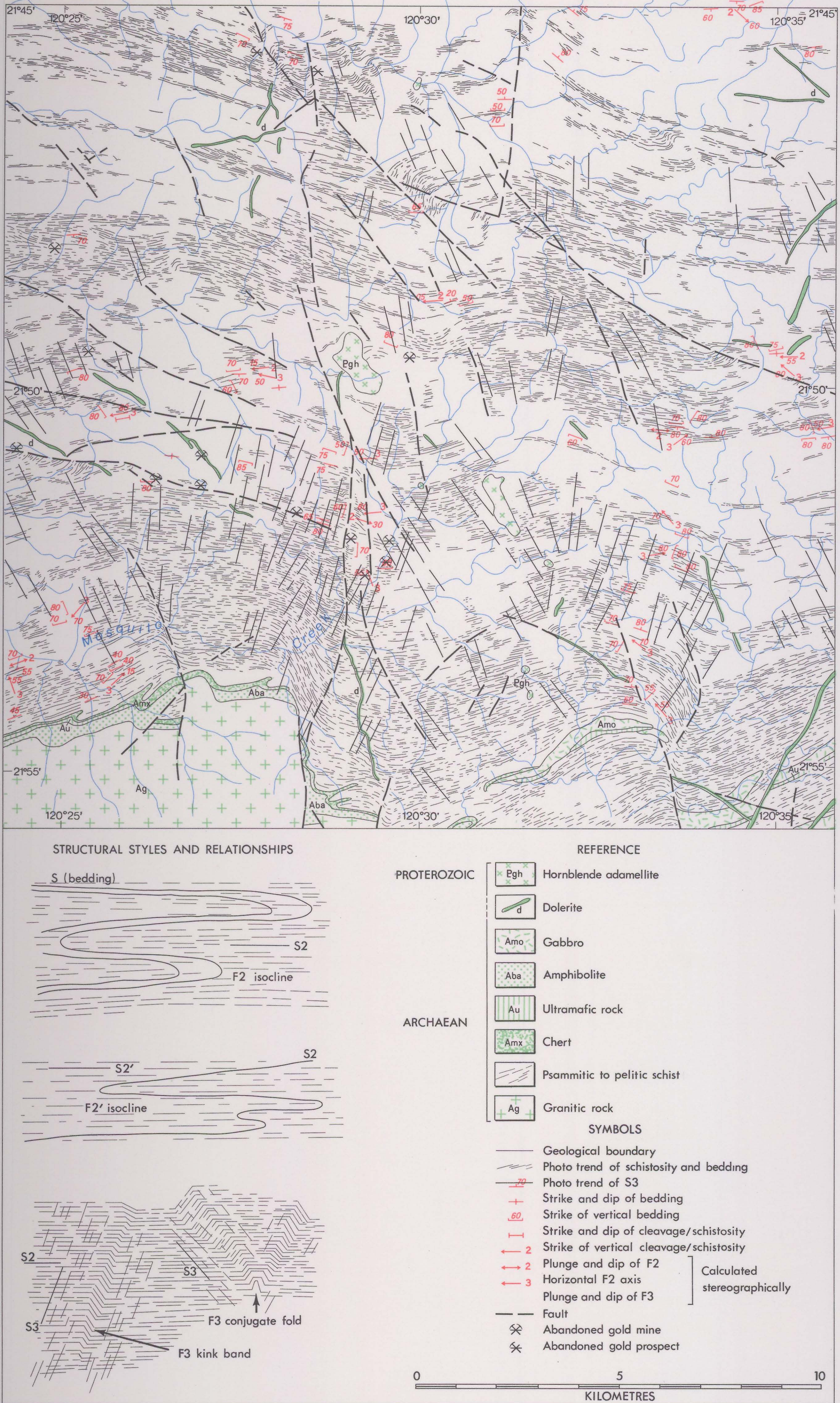

Fig. 39. Structural geology of the Mosquito Creek area.

14661

GREENSTONE SYNCLINORIA AND GREENSTONE DOMES

Major synclines containing volcanic and sedimentary rocks metamorphosed to greenschist facies lie between the granitic domes. These regionally extensive structures crop out as the "greenstone belts" of the area. Their shapes are controlled by those of adjacent domes, so that not only linear belts but also triangular and four-sided patterns occur. Extrapolations of surface geology indicate that the depth of the synclines ranges to about 30 or 40 km, that is to levels approaching the base of the crust. Dome crestal levels also vary; some of the granitic masses can be projected to about 15 km a.s.l. whereas others culminate at or below present ground level (0.3 km a.s.l.). Examples of the latter type are the North Pole and McPhee Domes where domed greenstone cover is preserved.

It has often been suggested that the arcuate nature of greenstone belts, and their varied orientation within a given region, is the result of cross-folding. In this area there is no evidence of superimposed cross-folding and no interference of minor structures where belts merge. The synclines and their associated second-order folds were produced by differential vertical movements. They complement the domes and are primarily non-cylindrical nonplane folds. Their associated schistosity rims the domes and is continuous between belts of different orientation.

Most of the greenstone belts are composed of upright tight to isoclinal similar folds. Individual limbs of these folds are extremely attenuated in places and slides (longitudinal strike thrusts) are common. One such slide occurs on the eastern margin of the Western Shaw Belt where the normal eastern limb of this major overturned syncline has been completely sheared out against the diapiric Shaw Batholith. In many areas vertically stretched and flattened pillow structures, conglomerate pebbles and agglomerate clasts testify to the degree of strain.

Vertical shear, often parallel or sub-parallel to bedding, has produced a widespread, steeply inclined schistosity in the greenstones. This schistosity is of the same age and origin as the main foliation of the granitic rocks. At relatively high structural levels, in low dipping sequences, such schistosity is very weak or completely absent and primary structures such as pillows, clasts and cross-bedding are not visibly deformed.

At North Pole and McPhee Creek two major greenstone domes occur. The North Pole Dome is 35 km in diameter. Across it a 15 km-thick greenstone succession of pillow basalts, chert and felsic volcanics are inclined at attitudes of 15-45°. Only in the centre is a small core of underlying adamellite exposed. Tensional faults radiate from the centre of the dome but the rocks show no evidence of internal deformation (Hickman, 1973).

About 100 km to the south-east of North Pole lies the McPhee Dome. Some 40 km long and 25 km across, this structure exposes a 7 km-thick succession of pillow basalt, chert and felsic agglomerate. Bedding inclination is very low in the centre of the structure although dips of 40-60° occur in its outer flanks. No granitic core is exposed.

THE MOSQUITO CREEK SYNCLINORIUM

The east-northeast trending Mosquito Creek Synclinorium is about 30 km wide and 60 km long and is unique in the eastern part of the Pilbara craton. Its great thickness of schistose flysch-type sediments and its persistantly east-northeasterly trending sub-isoclinal folds are not repeated elsewhere. Bounded to the north by greenstones, to the south by granite and unconformably overlain by Proterozoic rocks to the east and west, the unit presents interesting stratigraphic and structural problems.

At both the northern and southern contacts the base of the succession includes chert, peridotite, amphibolite, dolerite and gabbro; rock types which are not present at higher stratigraphic levels. Although the igneous rocks could all be interpreted as intrusive the isolated occurrence of chert at this position implies a real stratigraphic equivalence of the two sequences. The northern contact is a locally faulted unconformity inclined southwards at about 60°. The southern contact is a tectonic slide inclined northwards at 30° to 50° and overlies extensively sheared granite. Deformation is greatest in the central and southern parts of the synclinorium and its core lies relatively close to the southern contact. All these features indicate most shear and attenuation on the synclinorium's southern limb.

Graded bedding provides excellent facing evidence across the unit and although fold structures are generally not visible from the air, repeated reversals of facing across strike reveal the existence of major upright isoclines. In all but the most psammitic and psephitic beds the dominant foliation of the rocks is schistosity and it is this, rather than bedding, which is visible on aerial photographs. The synclinorium contains two generations of similarly orientated isoclines, the schistosity being parallel to axial planes to the first folds and folded by the second. The second generation folds possess a steeply inclined axial-plane cleaveage which is quite commonly observed to cross-out both the bedding and the earlier schistosity. As can be seen in Figure 36 an anticline and a syncline of the second generation deform the southern contact of the synclinorium. Figures 38 A and B presents a cross-section through the unit.

Superimposed on the foliations just mentioned are structures belonging to a later phase of deformation. Kink folds, conjugate folds and related strain-slip cleaveage are more conspicuous in this structural unit than elsewhere in the eastern part of the craton. Figure 39 shows that in the vicinity of the Mosquito Creek Mining Centre all these structures are visible from the air. Orientation and plunge of the conjugate kink folds is partly governed by pre-existing structural fabric but the intersection of their axial planes is the b-tectonic axis (Fig. 38H). Micro- and mesoscopic kink bands or joint-drags (Dewey, 1965) are common in the more pelitic beds, especially in the vicinity of northerly striking wrench faults. They are invariably angular in style and generally plunge steeply. The bands commonly occur in conjugate systems where two sets of kink zones, inclined at about 90° to each other, show opposite senses of rotation.

PROTEROZOIC BASINS

As noted elsewhere in the Pilbara (Kriewaldt, 1964; Ryan, 1966) synclines and structural basins in Proterozoic rocks tend to be positioned over Archaean synclines. Four of the five major basins in this area conform to this pattern and the nature of the rocks underlying the fifth, the Oakover Syncline, is largely unknown.

The Proterozoic succession unconformably overlies both Archaean granitic rocks and greenstones but only above the latter are its lower-most formations, the Mount Roe Basalt and Hardey Sandstone, ever present. Over large areas a systematic Proterozoic overlap can be traced from depositional basins underlain by greenstones onto granitic rocks (Hickman and Lipple, 1974; Hickman, in prep.). It may never be known whether the position of these basins was structurally or lithologically controlled. Structural control would have been chiefly responsible had either erosion of Archaean structures been incomplete or had Archaean domes and synclines been reactivated shortly before Proterozoic deposition. Lithological control might have been effective under certain weathering conditions during the late Archaean.

Because synclinal folds in the Proterozoic rocks tend to coincide with those in the basement it has been suggested that the Proterozoic structures may have been formed by slight tightening of the Archaean folds. Proterozoic synclines and structural basins may also have originated partly by gravitational downwarping within depositional basins. It should be noted, however, that anticlines to the northwest and southeast of the Yilgalong Granite deform basin sequences deposited over greenstones and that in the southwestern part of the Marble Bar Sheet area northerly trending synclines and anticlines (very open) occur over granite. It is concluded that structure and topography of the Archaean basement influenced but did not control fully the development of Proterozoic folds. The general northerly axial trend of these structures suggest deformation at least partly in response to a maximum east-west compressive stress.

STRUCTURAL HISTORY

The structural geology of the area is the product of several periods of deformation. Style, orientation and interference of major and minor structures reveal a long and complex history of folding, faulting and dyke intrusion. Mapping at 1 : 250 000 scale does not permit detailed structural analysis. Consequently, certain of the deformation phases may be further subdivided in the future.

In the following account D1, D2 ... refers to first deformation, second deformation ..., F1, F2 ... to folds produced during D1, D2 ..., S to bedding, and S1, S2 ... to foliations produced during D1, D2 ... .

FIRST DEFORMATION D1

All structures formed before the main episode of deformation, D2, are classed as D1 structures. They include early isoclinal folds of greenstone material forming detached structures within the granitic rocks, displaced granite-greenstone contacts, schistose dykes, deformed pegmatite veins, gneissic banding and, on a regional scale, all granitic plutons across which S2 is superimposed. It seems certain that such diverse structures represent deformations of several tectonic and intrusive episodes, but their relationships are generally obscured by D2 structures.

Certain of the megascopic greenstone masses occurring within the granitic domes are deformed by D2 folding and cross-cut by S2. Their contained schistosity, S1, is likewise deformed. Mafic dykes within the granites include folded and foliated bodies which may represent feeders of the greenstone succession. Gneissic banding in the granitic complex is locally deformed by pre-D2 structures, such as interfolial pegmatite veins. The banding was formed by attenuation of migmatite, lit-par-lit injection or possibly by metamorphic differentiation.

MAIN DEFORMATION D2

The dominant structural elements of the area, the granitic domes and greenstone syncliniria, were formed during the main episode of deformation. The Mosquito Creek Synclinorium is also a D2 structure, although this preserves evidence of two generations of folding during the same tectonic episode.

Differing competence of the greenstones and granitic rocks has established a regional fold pattern of broad domes and narrow cuspate synclines. Such a pattern is typical of a buckled basement—supracrustal contact in which the basement material is most viscous (Ramsay, 1967, p. 383-386). Internal deformation styles within the two types of rock are, as might be expected, very different. The greenstone synclinoria contain numerous upright tight to isoclinal noncylindrical, nonplane and often conical similar folds. Shearing-out of fold limbs along tectonic slides is quite common.

The granitic domes, on the other hand, are characterized by folding closer to the concentric model with flexural slip along shear planes parallel to the granite-greenstone contacts. Vertical shear, often parallel or sub-parallel to bedding and granite-greenstone contacts has produced the regional schistosity, S2, of the area. Late D2 folds and their associated axial-plane cleavage in the Mosquito Creek Synclinorium are referred to as F2′ and S2′ respectively.

Vertical movement is clearly predominant in the formation of diapiric structures, such as the granitic domes, but the cause of such movement, and the physical state of the material moving is debatable. D1 and D2 structures in the granitic rocks show that these were at least partly domed in the solid-state while preservation of depositional structures in the greenstones leaves no doubt that they were solid. The tabular nature of the greenstone succession rules out down-warping under narrow elongate geosynclinal basins (a model adopted by Anhaeusser and others, 1968, in the Barberton Mountain Land of South Africa). Dome and syncline development was probably a response to "inverted density stratification" (Ramberg, 1967), a low density layer (granitic complex) being overlain by a 15-30 km-thick high density layer (greenstones). Upward movement of the broad viscous granitic domes, over relatively large areas, was complemented by more rapid downward movement of less viscous greenstone material in narrow belts. Ramberg's certifuged models use "low" viscosity, low density bottom layers and consequently produce intrusive salt dome-like diapirs. In model S226 (Ramberg, 1967, p. 174), however, equal viscosities are used to produce structures more closely resembling those of the granitic domes and greenstone synclines.

THIRD DEFORMATION D3

In many areas D2 structures are visibly deformed by folds, faults and cleavage belonging to a later episode of deformation. Structures of this type have been described in the Mosquito Creek Synclinorium, but they also occur in many other areas (Fig. 36). Good examples of D3 folding occur in the Pilgangoora Belt where major F2 axes are deflected several times over a distance of 30 km.

Northeasterly striking, steeply inclined, strain-slip or "crenulation" cleavage, S3, is widespread in schist and phyllite of the greenstone belts. It bears an axial relationship to F3 folds and often produces a steeply plunging microscopic crenulation of S2.

Faults, commonly veined by quartz, are an extremely common D3 structure and fall into two sets, one striking northeast, the other northwest. Most of these faults are wrenches with a tendency for northeast striking fractures to involve sinistral movement, and northwest wrenches to be dextral. This implies a sub-horizontal north-south maximum compressive stress during their formation.

Dolerite dykes have intruded many D3 fractures and are little deformed by later movement. They cross-cut the post-tectonic granites and were probably feeders for the Lower Proterozoic basalt lava succession of the Fortescue Group. Structures grouped under "D3" probably range in age from late Archaean to early Proterozoic.

FOURTH DEFORMATION D4

Sub-horizontal micro and mesoscopic recumbent open crenulations of S2 are tentatively referred to a fourth period of deformation. Their style is distinctive but their relations to D3 have not been established. Axial trend is generally westerly.

FIFTH DEFORMATION D5

Major open folds with northeasterly to northwesterly trending axes deform the area's Proterozoic succession. Although much of the latter once covered the entire area extensive Phanerozoic peneplanation in the centre and west has generally preserved only synclines in shallow basement depressions.

A noteable exception to this D5 style of folding is found in the Gregory Range. Here upright tight to isoclinal folding about north to northwest trending axes is accompanied by a strong steep axial-plane cleavage, S5, and related high angle faults. This belt of deformation is situated on the eastern margin of the craton. It includes Middle Proterozoic rocks (Waltha Woora Formation) and consequently must have formed less than 1 000 m.y. ago.

A conjugate system of wrench faults is developed in the Proterozoic rocks. East-northeasterly striking dextral wrenches, and west-northwesterly sinistral wrenches, testify to a motive east-west maximum compressive stress. Such a stress field is in accord with the regional D5 fold trend. Vertical movement is present on some faults and predominates in the Gregory Range.

It is likely that D5 includes two deformations, an early phase of open folding, perhaps partly syndepositional, followed by wrench faulting and a later phase of predominantly vertical movements.

CONCLUSIONS

The area's Archaean greenstones were deposited as a 15-30 km-thick tabular succession on a granitic crust. Diapiric movements, culminating at about 2.7 b.y., produced major granitic domes and intervening greenstone synclinoria. Shortly after the culmination of this deformation post-tectonic granites were intruded, chiefly in synclinal areas. Subsequent erosion and minor brittle deformation was followed by the deposition of a thick Proterozoic succession. The final major stage in the structural development of the area was one of widespread open folding about northerly trending axes.

REFERENCES

Anhaeusser, C. R., Roering, C., Viljoen, M. J., and Viljoen, R. P., 1968, The Barberton Mountain Land: A model of the elements and evolution of an Archaean fold belt: Geol. Soc. South Africa Trans., v. 71, Annex, p. 225-254.

Compston, W., and Arriens, P. A., 1968, The Precambrian geochronology of Australia: Canadian Jour. of Earth Sciences, v. 5, p. 561-583.

Dewey, J. F., 1965, Nature and Origin of Kinkbands: Tectonophysics, v. 1, p. 459-494.

Hickman, A. H., 1973, The North Pole Barite Deposits, Pilbara Goldfield: West. Australia Geol. Survey Ann. Rept. 1972, p. 57-60.

——— in prep., Explanatory notes on the Nullagine 1 : 250 000 Geological Sheet: W.A.: West. Australia Geol. Survey Rec. 1975/5.

——— and Lipple, S. L., 1974, Explanatory notes on the Marble Bar 1 : 250 000 Geological Sheet: W.A.: West. Australia Geol. Survey Rec. 1974/20 (unpublished).

Kriewaldt, M. J. B., 1964, The Fortescue Group of the Roebourne region Northwest Division: West. Australia Geol. Survey Ann. Rept. 1963, p. 30-34.

de Laeter, J. R., and Trendall, A. F., 1970, The age of the Copper Hills Porphyry: West. Australia Geol. Survey Ann. Rept. 1969, p. 54-59.

de Laeter, J. R., and Blockely, J. G., 1972, Granite ages within the Pilbara Block, Western Australia: Geol. Soc. Australia. Journ., v. 19, p. 363-370.

de Laeter J. R., Lewis, J. D., and Blockley, J. G., 1975, Granite ages within the Shaw Batholith of the Pilbara Block: West. Australia Geol. Survey Ann. Rept. 1974, p. 73-79.

Lewis, J. D., Rosman, K. J. R., and de Laeter, J. R., 1975, The age and metamorphic effects of the Black Range dolerite dyke: West. Australia Geol. Survey Ann. Rept. 1974, p. 80-88.

Lipple, S. L., 1975, Definitions of new and revised stratigraphic units of the Eastern Pilbara Region; West. Australia Geol. Survey Ann. Rept. 1974, p. 58-63.

Noldart, A. J., and Wyatt, J. D., 1962, The geology of portion of the Pilbara Goldfield: West. Australia Geol. Survey Bull. 115.

Ramberg, H., 1967, Gravity, Deformation and the Earth's Crust (as studied by centrifuged models): Academic Press, London.

Ramsay, J. G., 1967, Folding and fracturing of rocks: International Series in the Earth and Planetary Sciences, McGraw-Hill, New York.

Ryan, G. R., 1966, Roebourne, W.A.: West. Australia Geol. Survey 1 : 250 000 Geol. Series Explan. Notes.

Stowe, C. W., 1968, Intersecting fold trends in the Rhodesian Basement Complex south and west of Selukwe: Geol. Soc. South Africa Trans., v. 71, Annex., p. 53-78.

Trendall, A. F., 1975, Preliminary geochronological results from two Pilbara porphyry bodies: West. Australia Geol. Survey Ann. Rept. 1974, p. 103-706.

GRANITE AGES WITHIN THE SHAW BATHOLITH OF THE PILBARA BLOCK

by J. R. de Laeter*, J. D. Lewis and J. G. Blockley

ABSTRACT

Two radiometric ages have been obtained by the Rb-Sr method from granites of the Shaw Batholith, southwest of Marble Bar. The older age, from migmatites and gneissic and foliated, granites of the main portion of the batholith, is 2951 ± 83 m.y., with an initial Sr^{87}/Sr^{86} ratio of 0.7020 ± 0.0010. This is probably a metamorphic age and the low initial ratio suggests a derivation from primary crustal material. The post-tectonic Cooglegong Adamellite, which intrudes the older granite and is associated with a swarm of tin bearing pegmatites, gives an age of 2606 ± 128 m.y. with an initial Sr^{87}/Sr^{86} ratio of $0.730\,3 \pm 0.028$. The initial ratio suggests that the Cooglegong Adamellite consists of reworked material and is probably derived from partial melting of the older granite.

* Department of Physics, Western Australian Institute of Technology.

INTRODUCTION

This paper forms a continuation of work initiated by de Laeter and Blockley (1972) on the geochronology of individual granite batholiths within the Archaean Pilbara block of Western Australia. The earlier paper was concerned with the Moolyella Granite, and its envelope of older gneissic granites, which lies to the east of Marble Bar. The present paper deals with the Shaw Batholith, to the southwest of Marble Bar.

NOMENCLATURE

Certain stratigraphic and structural names are used in this paper concurrently with their first formal definition, revision or appearance, and for clarity these are listed below:

(1) Hickman and Lipple (1974) first define the Moolyella, Cooglegong, Spear Hill and Mulgandinnah Adamellites.

(2) The stratigraphic units Warrawoona Group and Gorge Creek Group are formally revised in Lipple (1975).

(3) The structural names Shaw Batholith and Mount Edgar Batholith first appear in Hickman and Lipple (1974).

In their paper of 1972 de Laeter and Blockley referred to the Moolyella Granite. This intrusion has now been formally defined as the Moolyella Adamellite by Hickman and Lipple (1974). The Moolyella Adamellite and the surrounding older gneissic granites together make up the Mount Edgar Batholith.

PREVIOUS GEOCHRONOLOGICAL WORK

A review of Archaean geochronology in Western Australia has been made by Arriens (1971), and with respect to the Pilbara granites by de Laeter and Blockley (1972). Briefly an age of 3050 ± 180 m.y. was obtained by Compston and Arriens (1968) for 12 samples of gneissic granite collected from localities throughout the Pilbara, and a U-Pb age of 2400 to 2600 m.y. by Greenhalgh and Jeffery (1959) from a pegmatite at Woodstock. For the Mount Edgar Batholith, which is similar to the Shaw Batholith, de Laeter and Blockley (1972) obtained an age of 3125 ± 366 m.y. for the older gneissic granite and 2670 ± 95 m.y. for the Moolyella Adamallite which intrudes it. A younger age limit for igneous activity in the granite batholiths of the Pilbara is provided by an age of 2329 ± 89 m.y., obtained by Lewis and others (1975) for the Black Range dolerite dyke, a member of a dyke swarm which intrudes most units of the Archaean granites.

REGIONAL SETTING

Granitic rocks occupy the greater part of the Pilbara Block (Prider, 1965; Daniels and Horwitz, 1969) and form large dome-like bodies intruded into an older layered series. On a broad scale, however, the granites are concordant with the layered rocks which consist of a lower volcanic sequence, the Warrawoona Group, overlain by sediments of the Gorge Creek Group (Hickman and Lipple, 1974). The layered sequences are now preserved in tight synclines which wrap round and separate the granitic batholiths.

Noldart and Wyatt (1962) noted that the granite batholiths were variable, grading from a central core of homogeneous magmatic granite through an intermediate zone of gneissic granite with pegmatites to a marginal migmatitic granite. Ryan (1965) suggested that the large domes had been intruded by younger granites and Blockley (1970) mapped out several such intrusions and related them to tin mineralization in the Marble Bar area. The most recent mapping by Hickman and Lipple (1974) has shown that the older gneissic granite batholiths are composite, and consist of several mappable units ranging in composition from tonalite to granite.

The present study is confined to the granites of a single gneissic dome, the Shaw Batholith, which is situated 30 km southwest of Marble Bar. For the purpose of this study the dome has been divided into two units only, the younger intrusive Cooglegong Adamellite, one of the "tin" granites of Blockley (1970), and the older gneisses and migmatites which make up the bulk of the batholith.

THE SHAW BATHOLITH

The Shaw Batholith (Fig. 40) is a large oval granitic dome, approximately 80 by 40 km in size, extending southwards from about 30 km southwest of Marble Bar into the northern portion of the adjacent Roy Hill map sheet. The greater part of the dome consists of leucocratic gneissic granite which becomes migmatitic within a few kilometres of the margin. This portion of the batholith forms a flat featureless plain covered by a thin veneer of residual sand and gravel, and only a few isolated outcrops of granite. Intruded into the older granites are the younger "tin" granites which form low rounded hills with large expanses of bare rock.

Older granite

Detailed mapping by Hickman and Lipple (1974) has shown that the older granites of the Shaw Batholith include a number of discreet bodies which form mappable units. The main part of the mass, however, is a medium to coarse-grained, equigranular biotite adamellite gneiss with some granodiorite and tonalite. Foliation throughout the mass is characterized by orientation of feldspar, micas, quartz and hornblende. Towards the margin of the batholith migmatitic varieties become prominent and include nebulitic, stromatic, vein and banded migmatites. For the outermost few kilometres the batholith consists of approximately equal proportions of injected granite and metamorphosed country rock.

Intrusive bodies within the older granites of the Shaw Batholith include tonalite, adamellite and porphyritic adamellite. Some of the major bodies are shown on Figure 40. The Mulgandinnah Adamellite is a fine to medium-grained, well foliated biotite adamellite which occurs as small stocks, having cross-cutting contacts with the enclosing gneisses. The rocks contain xenoliths of the country rock and are thought to be derived by remobilization of the surrounding gneisses. The most prominent of the intrusions, within the older granites of the Shaw Batholith, are the two large irregular masses of porphyritic biotite adamellite. The rocks are easily distinguished by the presence of phenocrysts and although generally well foliated some portions are massive.

The age relationships between the various older granite types present in the Shaw Batholith are uncertain, but for the purposes of this study the various rock units have not been distinguished.

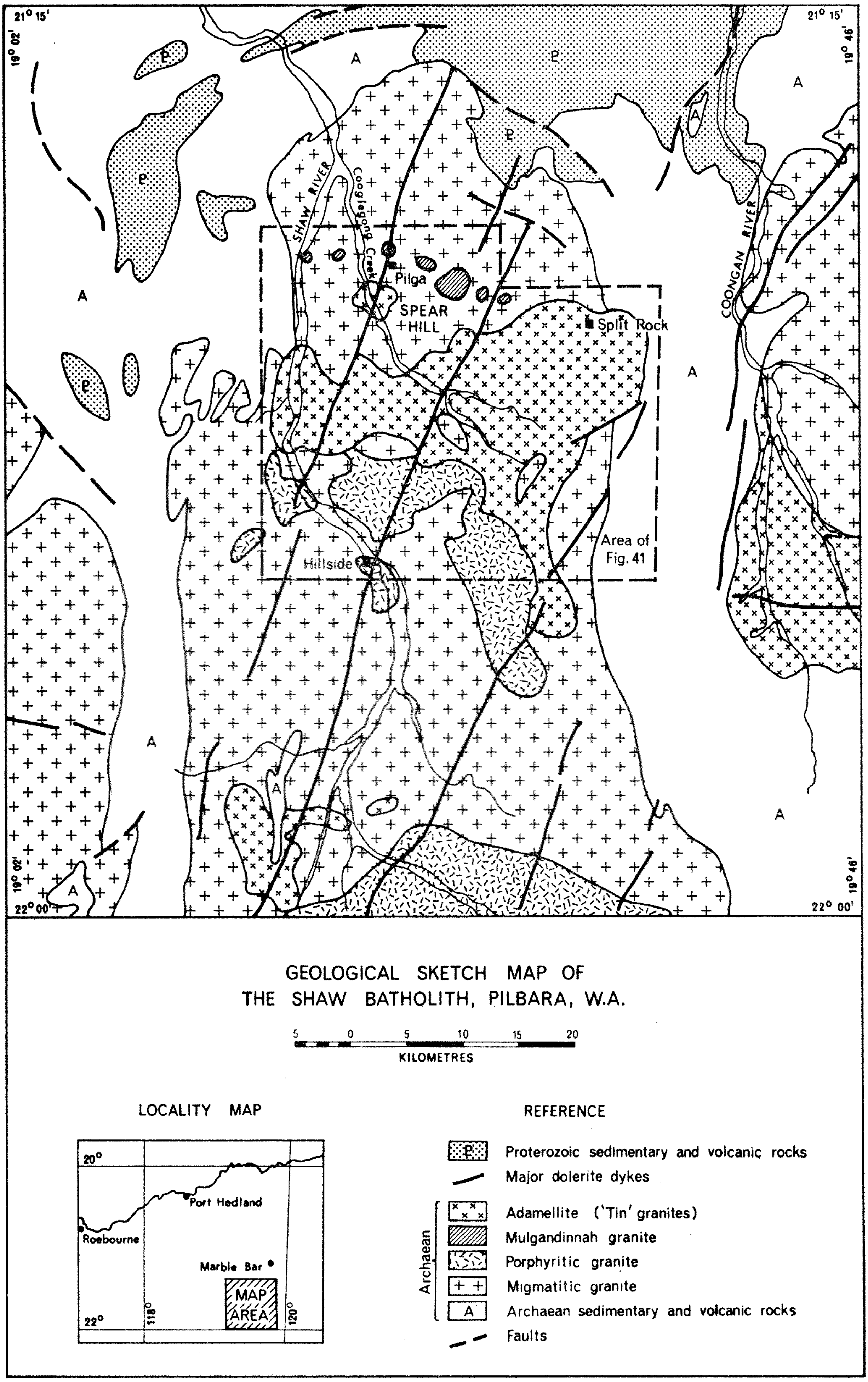

21° 15'
19° 02'
19° 46'
22° 00'
A
P
SHAW RIVER
Coogiegong Creek
Pilga
SPEAR HILL
Split Rock
COONGAN RIVER
Hillside
Area of Fig. 41
GEOLOGICAL SKETCH MAP OF THE SHAW BATHOLITH, PILBARA, W.A.
5 0 5 10 15 20
KILOMETRES
LOCALITY MAP
20°
22°
118°
120°
Port Hedland
Roebourne
Marble Bar
MAP AREA
REFERENCE
Proterozoic sedimentary and volcanic rocks
Major dolerite dykes
Archaean
Adamellite ('Tin' granites)
Mulgandinnah granite
Porphyritic granite
Migmatitic granite
Archaean sedimentary and volcanic rocks
Faults
14669

Figure 40.

Younger granites—the Cooglegong Adamellite

Three stocks of medium to coarse-grained, poorly foliated biotite adamellite intrude the Shaw Batholith (Fig. 40) and constitute the younger, or "tin" granites of Blockley (1970). These granites are associated with cassiterite bearing pegmatites which intrude the older granites and have given rise to extensive tin workings in the district. The largest of the younger granites, named after the Cooglegong tin mining centre, is the Cooglegong Adamellite, which forms an irregular arcuate intrusion with an area of about 400 km^2 (Fig. 41). The Cooglegong Adamellite outcrops mainly as low tors and boulder fields, but in the area east of the Black Range outcrop is almost continuous over large areas.

The Cooglegong Adamellite intrudes the migmatitic, gneissic and foliated rocks of the older complex and where contacts are seen the relationship is intrusive, with the younger granite clearly transecting foliation and banding in the older rocks. Locally the Cooglegong Adamellite contain xenoliths of the older granite. Along its eastern margin the adamellite intrudes mafic and ultramafic rocks of the Warrawoona Group and the contact zone is marked by extensive pegmatites.

The Cooglegong Adamellite is cut by rhyolite and dolerite dykes and by quartz veins. The rhyolite dykes are restricted to the general vicinity of the Cooglegong and Spear Hill Adamellites and are probably related to the younger granite magma.

MATERIAL USED

Most of the samples of both older and younger granites used in this study were originally collected for geochemical work by J. G. Blockley. The samples proved inadequate to define an isochron for the older granite, and further sampling of the marginal migmatite complex was undertaken. The final choice of samples for geochronology was made on the results of preliminary XRF determination of Rb and Sr. Ten samples of older granite and seven of younger granite were selected and analysed. The location of each specimen is shown on Figure 41.

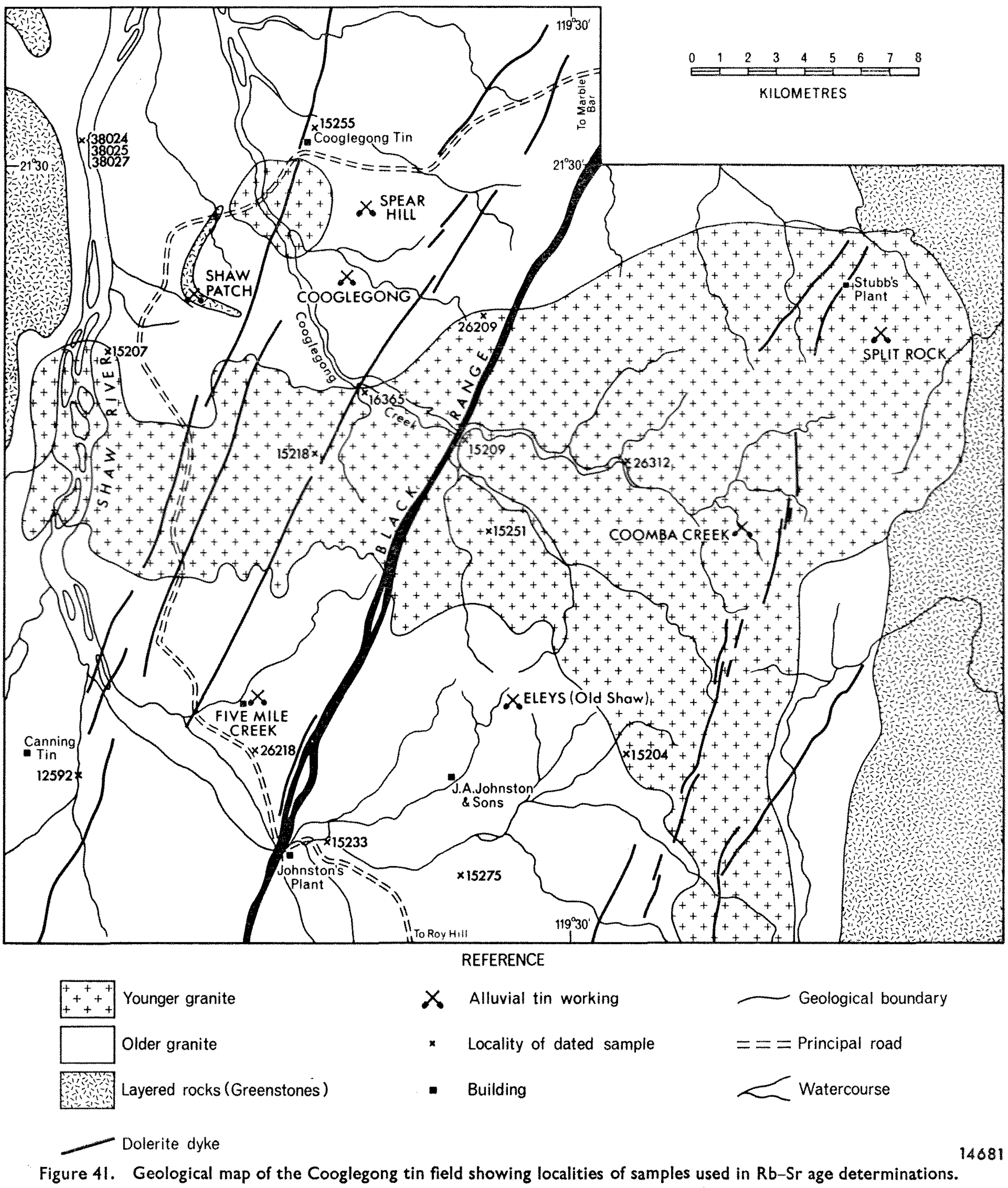

Figure 41. Geological map of the Cooglegong tin field showing localities of samples used in Rb–Sr age determinations.

Older granite

For descriptive purposes the samples can be divided into three groups, five samples of migmatite, three of gneissic granite and two specimens from discreet intrusions within the older granites.

The samples of migmatite were collected from an outcrop measuring about 100 by 200 m in the bed of the Shaw River, to the west of Spear Hill and less than one kilometre from the margin of the Shaw Batholith. The migmatite is a banded complex consisting of a granitic neosome and an amphibolitic palaesome. The amphibolites are the metamorphosed equivalents of the basaltic country rocks.

Specimens 38024A, 38025A, B and C, and 38027C are all from the granitic portion of the migmatite and are course-grained, strongly foliated mylonitic gneisses. The principal minerals in each specimen are quartz, microline and oligoclase, with minor hornblende or chloritized biotite. Secondary epidote, muscovite and carbonate, and accessory apatite, opaques and sphene are present in most specimens. Microcline is always more plentiful than oligoclase, specimens 38024A and 38025C being leucocratic granite, and the remainder hornblende adamellite. The migmatites appear to be derived from a sheared and partially recrystallized igneous rock. Individual feldspar crystals and elongate patches of mosaic quartz are surrounded by narrow zones of fine-grained recrystallized material and there are narrow veins of partially recrystallized material traversing the rock. It is suggested that at least two periods of deformation produced these mylonite gneisses.

Of the gneissic granites both 15255 and 12592 are granodiorites. Specimen 15255 was collected from a dark band in the gneiss and is a strongly foliated, medium-grained, equigranular granoblastic aggregate of sodic oligoclase, quartz and green hornblende, with subordinate microcline and accessory sphene, apatite, zircon and opaques. Secondary minerals present include epidote and chlorite. Specimen 12592 is a coarse-grained leucocratic granodiorite with large subhedral antiperthitic crystals of oligoclase, up to 1 cm long, set in a medium-grained granoblastic aggregate of quartz and oligoclase. A little chlorite and sphene are present as well as secondary epidote and sericite. Biotite adamellite is represented by specimen 26218 which is a coarse-grained, directionless, granoblastic aggregate of quartz, oligoclase and microcline with minor chloritized biotite, accessory, sphene and secondary epidote and sericite.

Specimens 15233 and 15375 were collected from intrusions which form part of the older granite complex, 15233 from a small stock of foliated adamellite, and 15275 from a large irregular intrusion of porphyritic adamellite. Phenocrysts in 15275 are of subhedral microcline, up to 1 cm long, and are set in a coarse-grained matrix of microline, oligoclase and quartz with minor biotite and accessory sphene, allanite, apatite and zircon. Secondary epidote and chlorite are also present. The overall texture of the rock is granitic with only minor modification due to metamorphism. The texture of 15233, a medium-grained biotite adamellite, also remains igneous in character. The sodic oligoclase of this rock has retained a subhedral crystal form and is often zoned to a narrow albitic rim. There are also relicts of a coarse granophyric intergrowth between microcline and quartz. The rock contains large flakes of secondary muscovite and has none of the small, euhedral brown sphenes that are common in the older granite suite. The possibility that 15233 comes from a small stock of younger granite will be discussed later.

Younger granite

Petrographically the samples of Cooglegong Adamellite form a homogeneous group. The rock is medium to coarse grained, directionless, leucocratic and equigranular. One specimen, 15204, however, is of a porphyritic variety. The rock consists essentially of quartz, microcline and plagioclase with minor biotite and chlorite and accessory apatite, zircon and opaques. Secondary minerals, other than chlorite, include epidote, muscovite, sphene and stilpnomelane and rare carbonate and fluorite. The texture of the rock is typically hypidiomorphic granular.

Slightly saussuritized microcline forms about two thirds of the feldspar present. It is commonly poikilitic, enclosing rounded grains of quartz and plagioclase. Perthitic exsolution lamellae of albite are present in most specimens, as is myrmekitic replacement. The microcline phenocrysts of specimen 15204 are up to 1 cm in length, and are mantled by strongly saussuritized plagioclase.

The plagioclase is a calcic oligoclass ($An_{20\text{-}30}$) and is is usually strongly saussuritized. Alteration is to epidote and sericite but in some specimens (15218, 15207) large flakes of muscovite have developed. Narrow zones of unaltered sodic oligoclase surround many crystals.

Most biotite in the Cooglegong Adamellite is altered partly, or completely, to a green chlorite. The chlorite is usually associated with epidote and colourless granular sphene, and sometimes with a little fluorite and carbonate (15207). In one specimen (26312) the biotite is being replaced by muscovite. Accessory apatite and zircon are also commonly associated with the chlorite and biotite.

EXPERIMENTAL PROCEDURES

All instruments and methods used in this study are the same as those described by Lewis and others (this volume p. 84).

RESULTS

The measured Rb/Sr and Sr^{87}/Sr^{86} ratios, as well as the Rb^{87}/Sr^{86} ratios calculated from them, are given in Table 13. The errors accompanying the data are at the 95 per cent confidence level. The data are also plotted in Figures 42 and 43.

TABLE 13. ANALYTICAL DATA FOR GRANITES FROM THE SHAW BATHOLITH

a. Older gneissic granites

Sample No.	Rb (ppm)	Sr (ppm)	Rb/Sr	Rb^{87}/Sr^{86}	Sr^{87}/Sr^{86}
15255	37	725	0·80 ± 0·002	0·231 ± 0·004	0·711 4 ± 0·000 2
38025A	93	397	0·232 ± 0·003	0·671 ± 0·007	0·730 0 ± 0·000 2
12592	116	306	0·383 ± 0·004	1·110 ± 0·01	0·751 0 ± 0·000 3
38025B	120	296	0·403 ± 0·004	1·168 ± 0·02	0·750 7 ± 0·000 3
26218	158	249	0·637 ± 0·007	1·85 ± 0·02	0·781 3 ± 0·000 3
38027C	183	278	0·654 ± 0·007	1·90 ± 0·02	0·782 8 ± 0·000 2
38025C	197	215	0·90 ± 0·01	2·63 ± 0·03	0·809 7 ± 0·000 4
15275	173	154	1·14 ± 0·01	3·35 ± 0·03	0·339 7 ± 0·000 3
38024A	270	189	1·41 ± 0·02	4·15 ± 0·04	0·869 4 ± 0·000 4
15233	320	73	4·45 ± 0·05	13·5 ± 0·14	1·246 8 ± 0·000 5
b. Younger Cooglegong Adamellite					
26209	326	102	3·22 ± 0·03	0·64 ± 0·1	1·089 2 ± 0·000 4
15204	368	110	3·36 ± 0·04	10·1 ± 0·1	1·106 0 ± 0·000 4
15207	475	82	5·76 ± 0·06	17·7 ± 0·2	1·372 0 ± 0·000 5
15251	574	65	7·87 ± 0·08	24·7 ± 0·2	1·622 5 ± 0·000 5
16365	432	48	9·19 ± 0·1	29·3 ± 0·3	1·780 1 ± 0·000 5
15218	551	50	11·1 ± 0·1	36·4 ± 0·4	2·090 1 ± 0·000 6
26312	638	40	16·2 ± 0·2	56·81 ± 0·6	2·901 2 ± 0·000 6
15209*	480	40	12·0 ± 0·1	39·0 ± 0·4	1·979 1 ± 0·000 5

* This sample not included in the isochron (see text).

Note: The Rb and Sr concentrations have been determined by comparison with a number of standard rocks. Although no assessment of the mass absorption coefficient of individual samples was made we believe the values are accurate to about ±5 per cent. The Rb/Sr ratios do not correspond exactly with the ratios that would be derived from the separate Rb and Sr values shown.

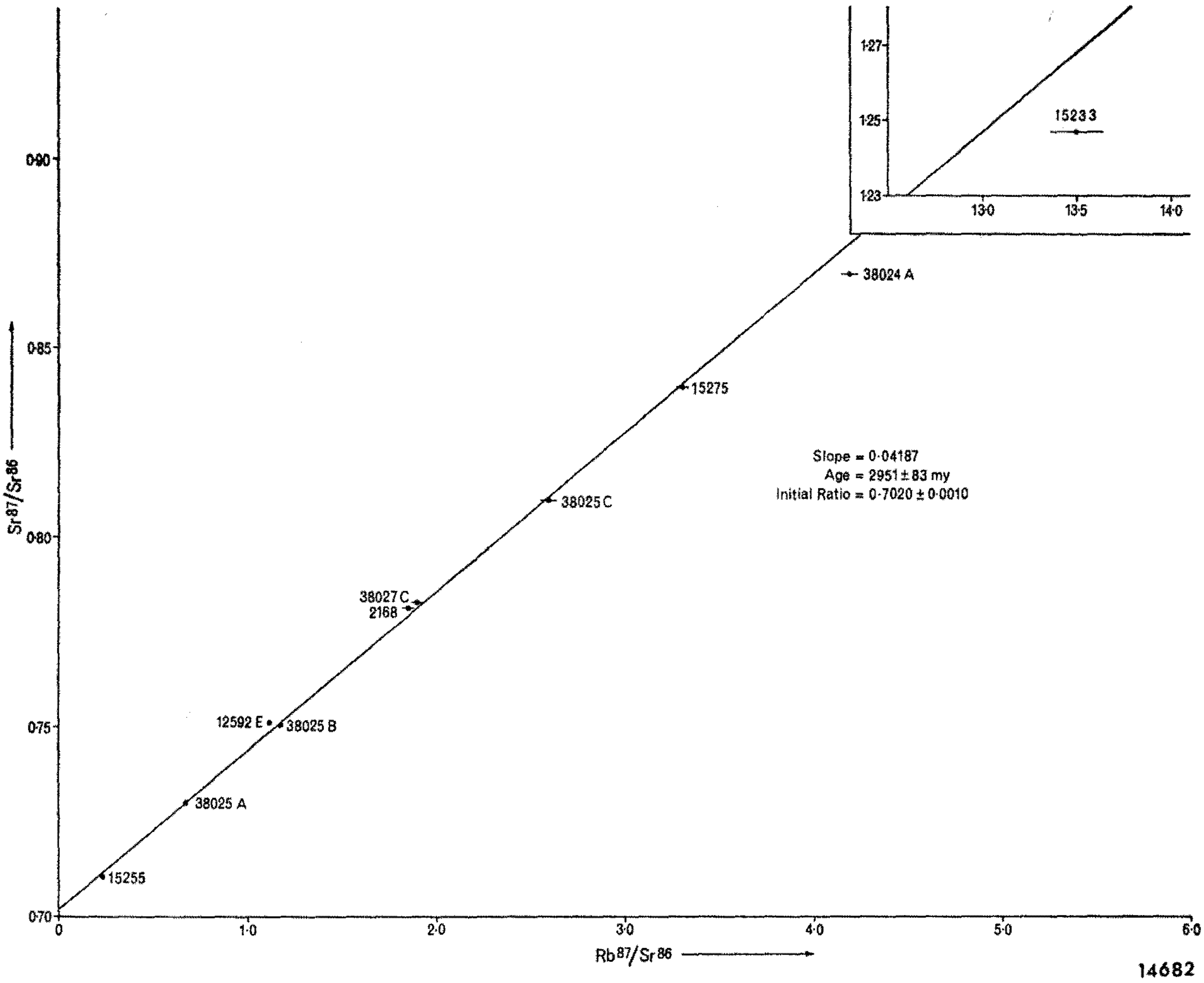

Figure 42. Isochron plot of granite samples from the older gneissic and migmatitic portions of the Shaw Batholith.

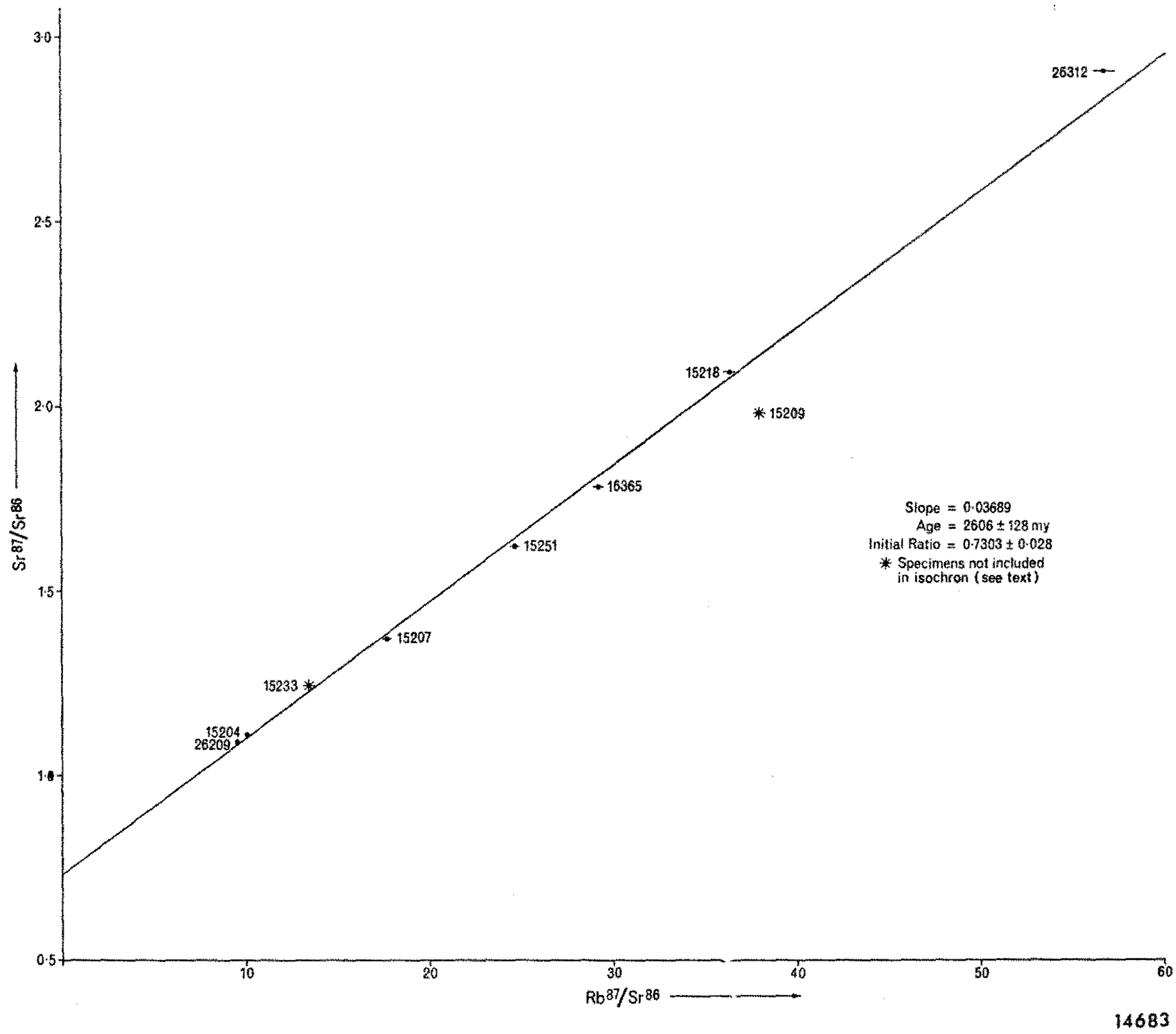

Figure 43. Isochron plot of samples of the Cooglegong Adamellite.

Regression analyses of the Rb^{87}/Sr^{86} and Sr^{87}/Sr^{86} data were carried out using the programme of McIntyre and others (1966). The ages derived from the data are 2951 ± 83 m.y. for the migmatites and gneisses of the older granitic complex of the Shaw Batholith, and 2606 ± 128 m.y. for the younger Cooglegong Adamellite. The initial Sr^{87}/Sr^{86} ratio calculated for the older samples is 0.7020 ± 0.0010, and for the younger samples 0.7303 ± 0.028.

For both isochrons the mean square of the weighted deviates is greater than unity, implying a scatter in the data points greater than can be expected from experimental uncertainties alone. Either or both of the assumptions that the initial Sr^{78}/Sr^{86} ratios were homogeneous, and that all samples were closed to Rb and Sr, therefore, do not hold for these two suites of samples. The programme has examined each set of data for geological variation and indicated that the rocks within the older isochron probably had slightly different initial Sr^{87}/Sr^{86} ratios and ages, whereas the suite of rocks comprising the younger isochron had the same initial ratios but, slightly different ages.

DISCUSSION

The results of the present study confirm and extend the work of de Laeter and Blockley (1972). Two major periods of granite formation are indicated; an early period at about 3 000 m.y. during which the gneissic and migmatitics granites of the Shaw and Mount Edgar Batholiths were formed, and a later one at 2 700-2 600 m.y. during which the Moolyella and Cooglegong 'tin' granites were emplaced.

The radiometric age of the gneissic granites from the Shaw Batholith, 2951 ± 83 m.y., agrees with the 3050 ± 180 m.y. determined by Compston and Arriens (1968) for a composite sample of all the older Pilbara granites, and is within the error limits of the age found by de Laeter and Blockley (1972) for the Mount Edgar gneissic granites. The interpretation of this age, however, is problematic. Hickman and Lipple (1974) have shown that the older granite complex of the Shaw Batholith is a composite mass containing several distinct ages of intrusion. They have also shown that the main phase of deformation and metamorphism, which gave rise to the gneissic texture, affects the whole of the older granite complex. The isochron of Figure 42 includes two specimens from the intrusive bodies (15233 and 15275), as well as eight from the granites and migmatites into which they are intruded, so that the determined age is, strictly speaking, a metamorphic one. Field evidence, however, suggests that granite intrusion and regional deformation were synchronous in which case the separately mapped intrusions may be only the final phase of formation of the complex. If this is true, then the determined age will be related to the final phase of granite intrusion within the older Shaw granites. Small age differences in the samples, suggested by the statistical examination of the data may reflect an extensive period during which the granites were emplaced, and differences in initial Sr^{87}/Sr^{86} ratios are probably due to varying amounts of country rock assimilated by the marginal migmatite specimens.

As stated earlier the geological affinities of specimen 15233 are uncertain. It was collected from a small intrusion which was presumed to be part of the older granite suite, but has certain petrographic affinities with the younger granites. The specimen plots equally well on either isochron (Figures 42 and 43) and its removal from the older suite raises the calculated age only slightly to 2973 ± 86 m.y., with an initial Sr^{87}/Sr^{86} ratio of 0.7018 ± 0.0010.

The age determined for the younger, post-tectonic Cooglegong Adamellite, 2606 ± 128 m.y. agrees well with that determined for the Moolyella Adamellite. Regional mapping has demonstrated the presence of several similar granites (Blockley, 1970; Hickman and Lipple, 1974) and it seems probable that they were all intruded at about the same time. There is no known geological reason for the scatter of points on the isochron being related to slight age differences within the Cooglegong Adamellite but specimen 15209, which has been excluded from the calculations, has obviously been affected by its proximity to the Black Range dyke. Lewis and others (1975) have examined the adamellite within the contact aureole of the dyke and shown that the rock behaved as an open system with respect to Rb and Sr. Perhaps the intrusion of the dyke swarm had a minor effect on samples collected far from any exposed dyke.

As with the Mount Edgar Batholith the initial Sr^{87}/Sr^{86} ratio of 0.7020 ± 0.0010 for the older Shaw granites suggests an immediate mantle derivation. Similarly the ratio of 0.7303 ± 0.028 for the Cooglegong Adamellite is consistent with the remelting of pre-existing crustal rocks. The wide uncertainty of the latter value is due to the fact that none of the analysed specimens had a very low Rb/Sr ratio. The figure is, however, similar to the 0.7397 ± 0.0419 found by de Laeter and Blockley (1972) for the Moolyella Adamellite.

REFERENCES

Arriens, P. A., 1971, The Archaean geochronology of Australia: Geol. Soc. Australia Spec. Pub. no. 3, p. 11-23.

Blockley, J. G., 1970, Preliminary report on tin granite in the Pilbara Goldfield: West. Australia Geol. Surv. Ann. Rept. 1969, p. 34-37.

Compston, W., Arriens, P. A., 1968, The Precambrian geochronology of Australia: Canadian Jour. Earth Sciences, v. 5, p. 561-583.

Daniels, J. L., and Horwitz, R. C., 1969, Precambrian tectonic units of Western Australia: West. Australia Geol. Surv. Ann. Rept. 1968, p. 37-38.

de Laeter, J. R. and Blockley, J. G., 1972, Granite ages within the Archaean Pilbara Block: Geol. Soc. Australia Jour., v. 19, p. 363-370.

Greenhalgh, D., and Jeffery, P. M., 1959, A contribution to the Precambrian chronology of Australia: Geochim. et Cosmochim. Acta, v. 16, p. 39-57.

Hickman, A. H., and Lipple, S. L., 1974, Explanatory Notes on the Marble Bar 1 : 250 000 Geological Sheet, W.A.: West Australia Geol. Survey Rec. 1974/20 (unpublished).

Lewis, J. D., Rosman, K. J. R., and de Laeter, J. R., 1975, The age and metamorphic effects of the Black Range dolerite dyke: West. Australia Geol. Survey Ann. Rept. 1974, p. 80.

Lipple, S. L., 1975, Definitions of new and revised stratigraphic units of the Eastern Pilbara Region: West. Australia Geol. Survey Ann. Rept. 1974, p. 58-63.

McIntyre, G. A., Brooke, C., Compston, W., and Turek, A., 1966, The statistical assessment of Rb-Sr isochrons: Jour. Geophys. Research, v. 71, p. 5459-5468.

Noldart, A. J., and Wyatt, J. D., 1962, The geology of portion of the Pilbara Goldfield: West. Australia Geol. Survey Bull. 115.

Prider, R. T., 1965, Geology and mineralization of the Western Australian Shield: *in* McAndrews, J., (Ed.), Geology of Australian Ore Deposits (2nd edn.): 8th Commonw. Mining Metall. Congr., Melbourne, p. 56-65.

Ryan, G. R., 1965, The geology of the Pilbara Block, Western Australia: Australasian Inst. Mining Metall. Proc. No. 214, p. 61-94.

THE AGE AND METAMORPHIC EFFECTS OF THE BLACK RANGE DOLERITE DYKE

by J. D. Lewis, K. J. R. Rosman* and J. R. de Laeter*

ABSTRACT

The Black Range dyke is a member of a large north-northeasterly trending basic dyke swarm in the Pilbara district of NW Western Australia. The dyke has been dated by the Rb-Sr method at 2 329 ± 89 m.y. and is shown to be a probable feeder for the overlying Mount Roe Basalt. Where studied the dyke is 120 m wide and has remelted the enclosing granite for a distance of 2 m. Chemical analyses of five samples show that apart from a narrow marginal zone of assimilation the dyke has had no effect on the bulk chemistry of the granite. Within the contact aureole however, microcline has been converted to perthitic orthoclase up to 55 m from the dyke. Within 24 m of the dyke a consideration of isotopic ratios shows that the rock behaved as an open system with respect to radiogenic Sr and that within 10 m of the dyke the granite completely lost its radiogenic Sr and has equilibrated with the dyke. From a consideration of the temperatures required to melt granite and convert microcline to orthoclase it is suggested that a temperature of about 530° C was required to bring about an open system with respect to Sr.

INTRODUCTION

The Black Range dolerite dyke is part of a north-northeast trending dyke swarm which gives rise to prominent topographic features in the Marble Bar district of the northwest of Western Australia. The dark ridge of gabbro, up to 60 m high, which marks the course of the Black Range dyke was remarked upon by the earliest exploration party in the area (Gregory, 1861) and by all subsequent geological parties.

Because cross cutting undeformed basic dykes could be found both in the Archaean rock and superincumbent sediments and lavas of the district, Maitland (1906) grouped the Black Range dyke swarm with his "Newer Greenstones" and assigned a post-Nullagine age. Noldart and Wyatt (1962), however, separated the dyke swarm from a few small dykes which undoubtedly cut the Nullagine succession and assigend a Lower Proterozoic, pre-Nullagine, age to the Black Range dyke.

More recent geological work (summarized by Daniels, 1966) has shown that the former Nullagine System probably spans a period of 1 500 m.y. and can be divided into two groups corresponding to Lower and Middle Proterozoic ages. The Lower Proterozoic Mount Bruce Supergroup has itself been separated into three groups, the Fortescue, Hamersley and Wyloo Groups and Daniels suggests an age of about 2 400 m.y. for the lowermost Fortescue Group, to which all the Proterozoic rocks in the vicinity of the Black Range dyke belong.

With respect to the Black Range dyke swarm the result of this recent work in the Pilbara district has been to narrow the time interval during which the dykes could have been emplaced. Another result has been to give rise to speculation that these very large dykes could be the feeders of the Mount Roe Basalt, which is the oldest stratigraphic unit of the Fortescue Group in the Marble Bar-Nullagine area.

The purpose of this paper, then, is to determine the age of the Black Range dyke and investigate the possibility that this may be the age of the Archaean/Proterozoic unconformity in the Pilbara region. The project was initiated after it was noted that a granite sample (15209), collected near the dyke for the age determination of the Cooglegong Adamellite, gave an anomalously low apparent age. This study will also investigate, therefore, the effect of thermal metamorphism on the isotope ratios of the surrounding granite.

REGIONAL SETTING

The regional geology of the Marble Bar area has been described by Noldart and Wyatt (1962) and more recently by Hickman and Lipple (1974). Essentially a layered sequence of Archaean volcanic rocks, the Warrawoona Group, overlain by sediments of the Gorge Creek Group, have been folded between large masses of intruded granite about 3 000 m.y. old. The volcanic and sedimentary sequences are now preserved in tight synclines which wrap round, and separate, the granites. The large migmatitic and gneissose granite batholiths have themselves been intruded by irregular stocks of equigranular adamellite (the "tin" granites of Blockley, 1970) and the whole is traversed by large basic dykes of the Black Range dyke swarm.

Overlying the Archaean rocks, with a strong angular unconformity, are the gently folded Lower Proterozoic rocks of the Fortescue Group. The succession consists of flood basalts and andesites with thick intercalations of tuff, shale, sandstone, grit and conglomerate and it has a maximum total thickness of 2 500 m in the Marble Bar geological map area. Nowhere is the succession complete. In the immediate vicinity of Marble Bar and overlying the northern margin of the Shaw Batholith only the Mount Roe Basalt, the Hardey Sandstone and the Kylena Basalt are present; that is, the three oldest members of the succession. To the south of the batholith, on the Roy Hill Sheet, the succession begins with the Kylena Basalt and continues up through the remainder of the Fortescue Group, to the lowermost member of the Hamersley Group, before the Cainozoic sediments of the Fortescue River are reached.

THE SHAW BATHOLITH

The Shaw Batholith (Fig. 44) is a large oval granitic dome, approximately 80 by 40 km in size, extending from about 30 km southwest of Marble Bar to a few kilometres south of the sheet margin. The greater part of the dome consists of leucocratic gneissic granite which becomes migmatitic within a few kilometres of the margin. The gneissic granite is variable but is commonly a medium to coarse-grained, equigranular biotite adamellite with some biotite grandiorite and a little biotite tonalite. Foliation in this mass is marked by elongate quartz blebs and the alignment of feldspar, biotite, and where present, hornblende. Marginally the Shaw Batholith has incorporated much basaltic country rock and consists of alternating bands of adamellite and amphibolite.

Extensive areas of foliated porphyritic biotite adamellite near the southern margin of the batholith, and to the northeast of Hillside also form part of the Shaw Batholith and the small stocks of the Mulgandinnah granite, a fine-grained biotite adamellite, probably represent remobilized older granite (Hickman and Lipple, 1974).

The youngest portions of the Shaw Batholith are three bodies of intrusive adamellite which constitute the younger "tin" granites of the area (Blockley, 1970). The largest of these bodies is the Cooglegong Adamellite, an irregular intrusion about 35 km long which divides the Shaw Batholith in two.

* Department of Physics, Western Australian Institute of Technology.

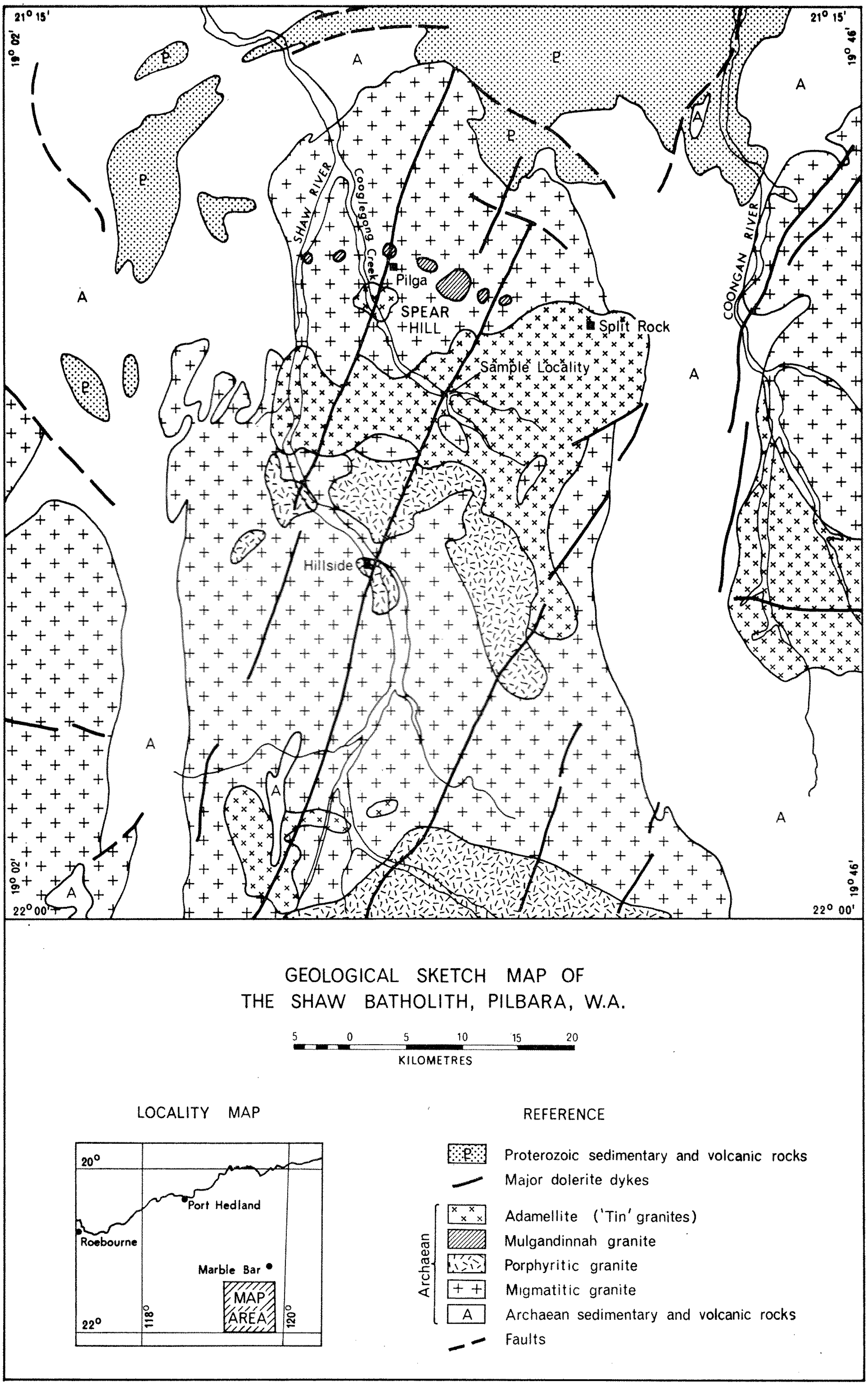

Figure 44.

(6)—46009

Smaller intrusions of similar rock type are found at Spear Hill, to the north of the main mass, and at Coodina to the south of Hillside. These younger granites are poorly foliated, leucocratic, medium to coarse-grained equigranular biotite adamellites.

THE BLACK RANGE DYKE

Throughout most of its area the Shaw Batholith forms a low level plain, with granite covered by a thin veneer of residual sand and gravel. The younger granites, however, form low rounded hills and the Black Range dyke traverses the batholith as a narrow razor-back ridge 60 m high and 70 km long. This ridge is cut at several points by rivers, most notably the Cooglegong Creek and the Shaw River. At these points the relationships between the dyke and the surrounding granites are best displayed, and this report is concerned principally with exposures in the Cooglegong Creek.

The Black Range dyke follows an almost continuous but slightly sinuous course from Coolyia Creek, 15 km northeast of Pilga, to Bootherina Pool on the Western Shaw River, a few kilometres inside the northern boundary of the Roy Hill Sheet. South of Hillside the dyke occupies a series of *en echelon* fractures, with only minor gaps and offsets to the course of the dyke. At Hillside, and again a few kilometres to the north, the dyke occupies a double fracture and encloses slices of granitic country rock a kilometre or so in length and about 100 m wide. The width of the dyke varies up to 150 m and its northern section is usually about 100 m wide. The Black Range dyke is intruded entirely into the granites of the Shaw Batholith; no information is available for its southern termination but at Coolyia Creek the dyke ends abruptly at a west-northwest trending fault. The fault is probably associated with a suite of dacite dykes which are earlier than the Black Range dyke, although movement along the fault continued after the emplacement of the dyke and has led to the preservation of Proterozoic basalts a little to the north.

SAMPLE LOCALITY-COOGLEGONG CREEK

At Cooglegong Creek an excellent section through the Black Range dyke is seen (Fig. 45). The western margin of the dyke is obscured by the same fallen boulders of coarse dolerite which obscure contact relationships throughout much of the dyke length, but it can be seen that the rock texture varies from basaltic near the margin to gabbroic near the centre of the dyke. The dyke is approximately 120 m wide at this point and as it is traversed towards the eastern margin the rock again becomes fine grained and basaltic in character. Whereas the dyke rock is nearly black throughout most of its exposure the marginal metre or so becomes considerably paler, and on examination xenocrysts of quartz and partially digested xenoliths of granite can be seen. This is evidently a zone of contaminated material with a diffuse boundary towards the dyke but with a sharp vertical margin towards a two to three metre wide zone of remelted granite which borders the dyke. Assimilation of granitic material by the basic magma is also well demonstrated by exposures near Hillside Homestead where veins of basalt carrying granitic xenoliths intrude along joints in the granite. Near the dyke margin the vein is of contaminated basalt and the xenoliths are angular and easily distinguished from the enclosing basalt. A few metres away, near the distal end of the vein, the xenoliths have been almost completely assimilated and remain only as ghosts in a porphyry matrix only slightly darker than the granite.

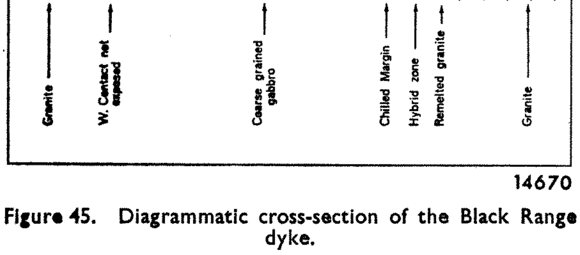

14670

Figure 45. Diagrammatic cross-section of the Black Range dyke.

The zone of remelted granite which borders the dyke is well seen both in the Cooglegong Creek and at Hillside. Elsewhere the scree of gabbro blocks from the dyke effectively obscures this narrow marginal zone.

The remelted granite has the appearance of a coarse grained, pink weathering, quartz feldspar porphyry; towards both dyke and enclosing granite the margin is sharp and vertical but slightly irregular.

The country rock around Cooglegong Creek is the Cooglegong Adamellite, one of the younger "tin" granites of Blockley (1970). In the vicinity of the creek the rock is a medium to coarse grained, pink weathering, directionless granite that is sparsely jointed. A few small pegmatites are present in the granite, including one that carries a small quantity of beryl. Near the margin with the zone of remelted granite the Cooglegong Adamellite has a slightly baked appearance, but elsewhere the rock is uniform and apparently unaltered.

Petrography

Specimens were collected from each of the rock types present but, in particular, a suite of samples was collected from the granite at measured distances from the dyke margin in Cooglegong Creek. The location of each specimen is given in Table 14.

TABLE 14. BLACK RANGE DYKE-SPECIMEN LOCATIONS

Sample No.	Location (distance from dyke margin m)	Rock Type
Dyke Rocks		
15104	Dyke centre	quartz gabbro
15105	6·0	dolerite
15106	0·5	basalt
15107	0·1	contaminated basalt
Country Rocks		
15108	0·22	remelted granite
15109	2·4	partially remelted granite
15135	6·0	
15136	10·5	
15137	24	altered granite
15138	55	
15139	98	
15140	189	fresh granite
15141	305	

The central portion of the dyke is a moderately fresh, medium to coarse-grained gabbro consisting of prismatic labradorite, euhedral to subhedral augite and interstitial micropegmatite. The labradorite prisms are up to 4 mm long and are zoned from a core of composition An_{60-65} to a sodic rim of oligoclase (An_{20}). The plagioclase is fresh except for the development of a little chlorite along some cleavages. Augite crystals up to 3 mm long are commonly rimmed by and sometimes completely altered to a pale green actinolite. The relationship between augite and labradorite crystals indicates that they cristallized simultaneously. A few large patches of chlorite may indicate the former presence of orthopyroxene. The most notable feature of the gabbro is the proportion of interstitial granophyre. Most quartz dolerites contain a small proportion of micropegmatite, but in the Black Range gabbro the proportion rises to about 15 per cent and individual patches can be up to 3 mm across. Labradorite prisms usually form the nucleus about which the granophyre developed and the result is that some plagioclase is almost completely surrounded by granophyric over-growths of quartz and sodic plagioclase. Although the feldspar component of the granophyre is usually a poorly twinned plagioclase there are a few areas of microcline granophyre.

Other minerals present in the gabbro are minor apatite, ilmenite altered to leucoxene and granular sphene, and a little secondary brown hornblende and epidote.

Specimens 15105 and 15106, from the marginal portion of the dyke, are similar to the gabbro from the dyke centre in all except grain size and degree of alteration. In addition, patches of quartz are more common and within the granophyre microcline is more prominent. It is possible that this indicates a small amount of assimilation of granitic rock. In these marginal specimens alteration of pyroxene to actinolite and chlorite is complete and much of the plagioclase is saussuritized.

Hybridization has produced a narrow zone of very variable rock along the dyke margin but essentially the rock is a fine grained hornblende granophyre with corroded xenocrysts of quartz and feldspar. The bulk of the rock consists of saussuritized laths of calcic oligoclase, up to 1 mm long, and acicular actinolite, up to 2 mm long, with an interstitial matrix of very fine-grained granophyre and patches of clear quartz. The granophyre makes up about half the rock and appears to have formed on the oligoclase laths.

Plagioclase xenocrysts are present as ghost crystals and show the effects of assimilation by melt channels which have developed along cleavages, so dividing the original crystal into an orientated group of cleavage rhombs separated by a network of secondary plagioclase. Quartz xenocrysts however, are only attacked at the margins and are found as irregular shaped grains up to 8 mm across with embayed margins. Associated marginally with the quartz xenocrysts are small euhedral prisms of olive green hornblende. Whereas the actinolite of the main mass probably represents altered acicular augite, the green hornblende appears to have developed from mafic minerals associated with the granite xenoliths.

Remelted granite is represented by specimen 15108 which contains about 40 per cent of relict crystals from the original granite and 60 per cent of fine-grained granophyre. The relict material displays all stages of remelting, from patches in which a granitic texture is modified only by highly sutured margins and the development of minor granophyre zones along feldspar/quartz interfaces, through separated relict grains of quartz and feldspar, to ghost crystals of feldspar similar to the xenocrysts of the contaminated dyke margin. The groundmass contains many small prisms, up to 0.5 mm across, of albite and microline and a mass of fine-grained granophyre with larger interstitial quartz patches.

The mineralogy of the rock is similar to the granite mass and includes quartz, microcline and albite in sub-equal proportions, minor biotite and accessory zircon and ilmenite. The biotite, however, forms small olive-brown flakes which crystallized after the remelting and are not relict. Although in the field the boundary between the remelted granite of 15108 and the main mass of the country rock is easily delineated, remelting phenomena can be observed for a further 4 m away from the dyke. Specimen 15109, taken just outside the remelted zone, differs only in degree from 15108. Relict granite makes up about 60 per cent of the rock but granophyre zones up to 0.5 mm wide have developed along grain boundaries and there are large patches of granophyre where all original texture has been destroyed. The biotite in 15109 is the same small olive-brown flakes observed in 15108 but some appear to have recrystallized from larger original flakes. In 15135, 6 m from the dyke margin, granophyre zones between crystals have been developed but chloritized biotite from the original granite remains.

In the zone 10 m to 30 m from the margins of the dyke, the Cooglegong Adamellite has been altered but not reconstituted in any way. The main effects appear to be that microcline has been converted to orthoclase and the margin of some crystals are sutured and granulated.

All feldspars in this zone are slightly turbid and sericitized. These thermal effects diminish noticeably through the zone. Specimen 15136, 10.5 m from the contact, contains only orthoclase and the grain boundaries are highly sutured. Specimen 15137, 24 m from the contact, is similar but 15138, 55 m from the contact, shows no evidence of sutured margins due to contact metamorphism and the microcline is only patchily converted to orthoclase. In contrast to the non-perthitic microcline of the main granite mass in this narrow orthoclase zone, the K-feldspar is perthitic on a very fine scale. As a result of fine scale twinning perpendicular to the length of exsolved albite lamellae, some of the feldspar appears to have a fine microcline twinning pattern but under high power the feldspar is resolved into two components, a slightly sericitized orthoclase, twinned on the Carlsbad law, and exsolved blebs and spindles of plagioclase, twinned on the albite law. In specimen 15138 the conversion to perthitic orthoclase is seen only in zones within the microcline which have close spaced cleaveage. Outside these zones the microcline with normal cross-hatched twinning contains few perthitic lamellae. The granular margins, seen in specimens 15136 and 15137, are observed particularly at the interface of oligoclase and orthoclase crystals and appear to form by small overgrowths on the oligoclase.

In some instances there appears to be a diminution of albite blebs in the perthitic orthoclase over a narrow zone (0.1 mm) adjacent to the oligoclase and it seems that the granular margin has formed by diffusion of albite out of the orthoclase.

At approximately 60 m from the dyke margin, or half the width of the intrusion, the metamorphic effect of the dyke is minimal. Specimens 15139, 40 and 41 collected from 100 to 300 m from the dyke are typical examples of the Cooglegong Adamellite. The rock is coarse grained, leucocratic, directionless, sparsely porphyritic and contains sub-equal amounts of quartz, microcline and plagioclase with minor biotite accessory apatite, zircon and opaques and secondary chlorite, muscovite and epidote. Subhedral phenocrysts of microcline, up to 2 cm across, are sparsely distributed throughout the rock and usually enclose small e/uhedral crystals of sodic oligoclase (An_{16}). Early formed subhedral plagioclase crystals, up to 2 mm across, are also sodic oligoclase but are usually zoned to a narrow rim of albite (An_8). The bulk of the rock, however, is a xenomorphic aggregate of quartz, microcline and albite (An_8), the latter apparently replacing microcline. The plagioclase is usually slightly sericitized and in both feldspars large flakes of muscovite have developed. Small flakes of interstitial brown biotite, usually partially chloritized, are associated with accessory apatite and zircon and secondary epidote.

CHEMISTRY

Table 15 contains analyses and norms of five rocks from the Cooglegong Creek area including the contaminated marginal basalt and the remelted granite.

The gabbro from the dyke centre (15104) is a normal tholeiite except for a higher than usual silica content. The high proportion of micropegmatite in the rock would account for the high silica figure and the 8 per cent quartz of the norm.

Similarly the analysis of 15141 is consistent with the leucocratic adamellite described above, and contact metamorphism of 15135 does not appear to have altered the bulk chemistry of the rock. Almost complete remelting has not changed the major element of chemistry of 15108. This rock, only a few centimetres from the dyke margin, has not lost its more mobile constituents such as Na_2O and K_2O, neither has it assimilated any basaltic material. Assimilation of acid material by the basic dyke, however, is well illustrated by 15107C. Apart from the Al_2O_3 figure, which is inexplicably lower than either the gabbro or the adamellite, a mixture of 60 per cent granitic material and 40 per cent basic gives a good approximation to the actual analysis of the hybrid rock.

TABLE 15. ANALYSES OF SPECIMENS FROM THE BLACK RANGE AND COOGLEGONG GRANITE

Sample No.	15104	15107C	15108	15135	15141
SiO_2	54·19	66·77	75·20	74·56	74·78
Al_2O_3	13·58	12·79	13·21	13·57	13·72
TiO_2	0·62	0·36	0·10	0·05	0·05
Fe_2O_3	1·19	1·09	0·39	0·07	0·16
FeO	8·77	4·59	1·31	0·99	0·99
K_2O	0·64	2·92	4·42	4·69	4·29
Na_2O	1·74	2·34	3·57	3·90	4·00
CaO	9·28	4·44	0·78	0·72	0·77
MgO	7·49	3·24	0·23	0·11	0·14
MnO	0·21	0·10	0·05	0·08	0·05
CO_2	0·04	0·03	0·03	0·04	0·01
P_2O_5	0·09	0·05	0·03	0·02	0·03
H_2O^+	2·15	1·44	0·70	0·45	0·47
H_2O^-	0·07	0·06	0·13	0·12	0·03
Total	100·1	100·2	100·2	99·4	99·5

Trace Elements (ppm)

F	525	545	80	775	825
Li	230	40	40	25	120
Rb	345	165	375	620	510
Sr	130	115	35	20	20
Ba	1 070	800	350	220	200
Zr....	a	a	a	50	90
Sn	b	b	b	b	b
Ni	180	75	15	20	15
Cu	90	55	10	40	40
Zn	110	75	75	50	60
U	b	6	8	6	2

a = less than 10 ppm b = less than 2 ppm

C.I.P.W. Norms

Q	8·34	26·03	34·89	31·59	32·64
C	0·00	0·00	1·29	0·93	1·16
Or	3·55	17·14	26·00	27·78	25·41
Ab	14·72	19·80	30·21	33·00	33·84
An	27·53	15·86	3·48	3·19	3·56
Di	14·50	4·66	0·00	0·00	0·00
Wo	7·38	2·36	0·00	0·00	0·00
En	4·02	1·22	0·00	0·00	0·00
Fs	3·10	1·08	0·00	0·00	0·00
Hy	25·97	12·75	2·48	2·03	1·89
En	14·66	6·75	0·50	0·25	0·25
Fs	11·31	5·99	1·98	1·78	1·64
Mt	1·74	1·59	0·58	0·14	0·29
Il	1·18	0·68	0·19	0·09	0·09
Ap	0·21	0·12	0·07	0·05	0·07
Cc	0·09	0·07	0·07	0·09	0·02

15104: Gabbro, dyke centre.
15107C: Marginal hybrid rock.
15108: Remelted granite.
15135: Partially melted granite 6 m from dyke.
15141: Fresh granite 305 m from dyke.

Analysts: Government Chemical Laboratories; 15104, 15107C, 15108: R.S.Y. Pepper; 15135, 15141: R. W. Lindsey.

Whereas the major element chemistry of these rocks is comparable to normal basic and granitic rocks, the trace elements reveal some striking anomalies when compared with published averages (e.g. Krauskopf, 1967; Vinogradov, 1962). While Ni, Cu and Zn values conform to the published figures Rb is high and Sr low in both gabbro and adamellite. The average Rb/Sr ratio for gabbroic rocks is about 0.1 and for granites about 0.6, but in this study (see Table 16) the ratios are approximately 0.6 and 13 respectively. This suggests that both rocks are highly differentiated and that for the Cooglegong Adamellite the present level of erosion is very near the roof of the intrusion.

The Li values are also high, particularly for the gabbro, but while Ba is high in the gabbro it is low in the adamellite. The low values recorded for Li in the remelted and contact altered adamellite (15108, 15135) might be a reflection of the mobility of this element at an elevated temperature.

EXPERIMENTAL PROCEDURES

About 200 g of each sample was reduced to -200 mesh using a jaw crusher and a Tema mill. Approximately 0.4 g of each powdered sample was then taken into solution using a HF-$HClO_4$ mixture. The solution was then converted to the chloride form with 2.5M HCl. After taking to dryness the residue was dissolved in 1M HCl and centrifuged.

The supernate was transferred to a quartz ion-exchange column containing 2g of Dowex 50W-X8, 200-400 mesh cation-exchange resin. Strontium was eluted using 2.5M HCl and, after being taken to near dryness, each sample was loaded on the side filaments of a conventional rhenium triple filament assembly ready for mass spectrometric analysis.

Blank determinations using the isotope dilution technique showed that the Rb and Sr contamination introduced by the chemical processing was less than 10^{-9}g and 10^{-8}g respectively. Full details of the isotope dilution technique used in this laboratory are given by de Laeter and Abercrombie (1970).

Isotopic analyses were carried out on a 12 inch radius, 90° magnetic sector, solid source mass spectrometer equipped with an electron multiplier. Previously outgassed rhenium filaments were used throughout the analyses. No evidence of Sr contamination from the ion source or filaments was ever observed.

A 1μg sample of $SrCl_2$ produced an ion-beam of approximate strength 10^{-11} amps for many hours of operation. The resulting signals were amplified in a vibrating reed electrometer with a 10^{8} ohm input resistor. A voltage to frequency converter, followed by an electronic counter, allowed digital presentation of the data, which was fed on-line to a small digital computer. The amplifying system was periodically checked for linearity and speed of response.

Mass 85 was monitored on a sensitive scale at intervals during the analysis in order to correct the measured 87 peak for Rb contribution. The isobaric contribution of Rb^{87} to the Sr^{87} ion-beam was always less than 0.01 per cent before data were collected.

The isotopic peaks were scanned magnetically from mass 86 to 88 and then back again, this operation constituting one sweep. Approximately 40 sweeps were taken for each sample.

Replicate analyses of the NBS 987 Sr standard were made, to give a mean value of Sr^{87}/Sr^{86} of $0.710\,2 \pm 0.000\,1$, normalised to a Sr^{88}/Sr^{86} value of 8.375 2. The Sr^{87}/Sr^{86} values listed in Table 16 have been normalised to a Sr^{88}/Sr^{86} value of 8.375 2. A value of 1.39×10^{-11}/yr was used for the decay constant of Rb^{87}.

X-ray fluorescence was used to select rocks with favourable Rb/Sr ratios for mass spectrometric analysis, and also to determine precise values of the Rb/Sr ratio for the selected samples. A Siemen's SRS-1 fluorescence spectrometer equipped with a molybdenum tube, a lithium fluoride (200) crystal and a scintillation detector was used.

RESULTS

The measured Rb/Sr and Sr^{87}/Sr^{86} ratios, as well as the Rb^{87}/Sr^{86} calculated from these, are given in Table 16. The errors accompanying the ratios are at the 95 per cent confidence level. The data are also plotted on Figures 46 and 47.

TABLE 16. ANALYTICAL DATA FOR THE BLACK RANGE DOLERITES AND ASSOCIATED ADAMELLITES

Sample No.	Rb ppm	Sr ppm	Rb/Sr	Rb^{87}/Sr^{86}	Sr^{87}/Sr^{86}
(a) Dyke Rocks					
15104	44	120	0·363 ± 0·004	1·05 ± 0·01	7·752 1 ± 0·000 3
15105	106	161	0·655 ± 0·007	1·91 ± 0·02	0·799 1 ± 0·000 3
15106	75	79	0·907 ± 0·009	2·65 ± 0·03	0·818 2 ± 0·000 3
15107	183	140	1·32 ± 0·01	3·83 ± 0·04	0·846 2 ± 0·000 4
(b) Cooglegong Adamellite					
15108	440	61	7·23 ± 0·07	22·4 ± 0·2	1·466 5 ± 0·000 2
15109	661	45	14·6 ± 0·15	49·4 ± 0·5	2·475 2 ± 0·000 4
15135	684	42	16·4 ± 0·16	56·1 ± 0·6	2·605 8 ± 0·000 4
15136	636	48	13·1 ± 0·13	43·3 ± 0·4	2·191 5 ± 0·000 3
15137	576	43	13·3 ± 0·13	44·4 ± 0·5	2·291 7 ± 0·000 4
15138	608	44	13·7 ± 0·14	46·7 ± 0·5	2·567 4 ± 0·000 5
15139	595	48	12·4 ± 0·12	41·0 ± 0·4	2·202 2 ± 0·000 4
15140	535	54	9·9 ± 0·10	32·1 ± 0·3	1·980 6 ± 0·000 4
15141	590	56	10·6 ± 0·11	34·6 ± 0·4	2·052 5 ± 0·000 4
15209*	480	40	12·0 ± 0·12	39·0 ± 0·4	1·979 1 ± 0·000 4

* This sample was analysed as part of the project on the Shaw Batholith (de Laeter and others, 1975).

NOTE: The Rb and Sr concentrations have been determined by comparison with a number of standard rocks. Although no assessment of the mass absorption coefficient of individual samples was made we believe the values are accurate to about ±5 per cent. The Rb/Sr ratios do not correspond exactly with the ratios that would be derived from the separate Rb and Sr values shown.

Regression analysis of the Rb^{87}/Sr^{86} and Sr^{87}/Sr^{86} data were carried out using the programme of McIntyre and others (1966). The data which were fitted to an isochron (Fig. 46) were the four samples from the dyke itself (15104-15107), the remelted granite 15108 and the partially remelted granites 15209 and 15135. The mean square of the weighted deviates for these samples was greater than unity, implying a scatter in the data points greater than can be expected from experimental uncertainties alone. Either or both of the assumptions that the initial Sr^{87}/Sr^{86} ratio was homogeneous, and that all the samples were subsequently closed to Rb and Sr, therefore do not hold for the suite of samples. The programme has then examined the set of data for geological variation and indicated that the distribution of the residuals suggests that the rocks comprising the isochron probably have slightly different initial Sr^{87}/Sr^{86} ratios and ages. The best estimate of the age of the rocks is 2 329 ± 89 m.y. and the initial Sr^{87}/Sr^{86} ratio 0.7262 ± 0.012.

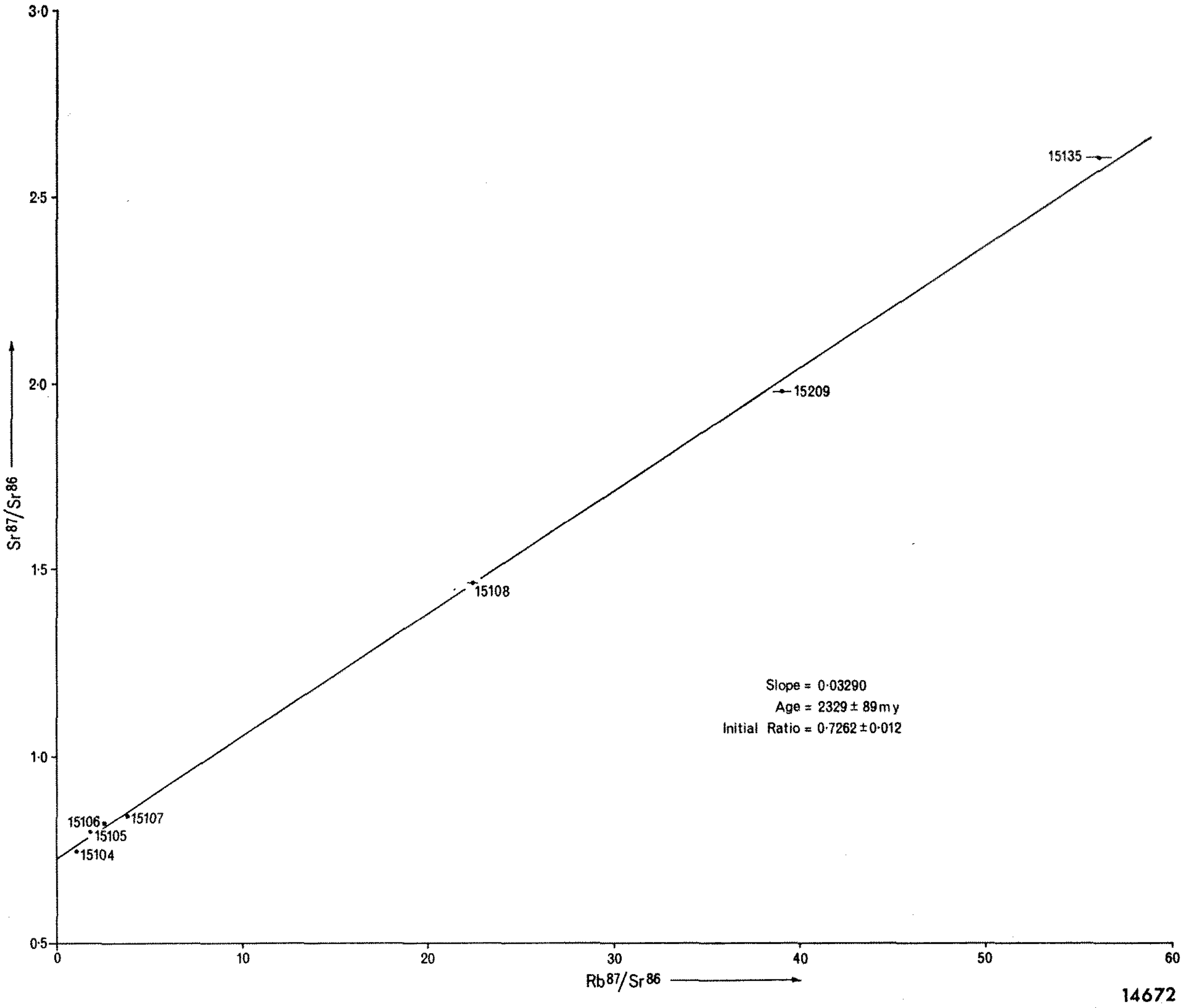

Figure 46. Isochron plot of samples from Black Range dolerite dyke and its metamorphic aureole. 15104–7: dolerite samples; 15108, 15135, 15209: granite samples.

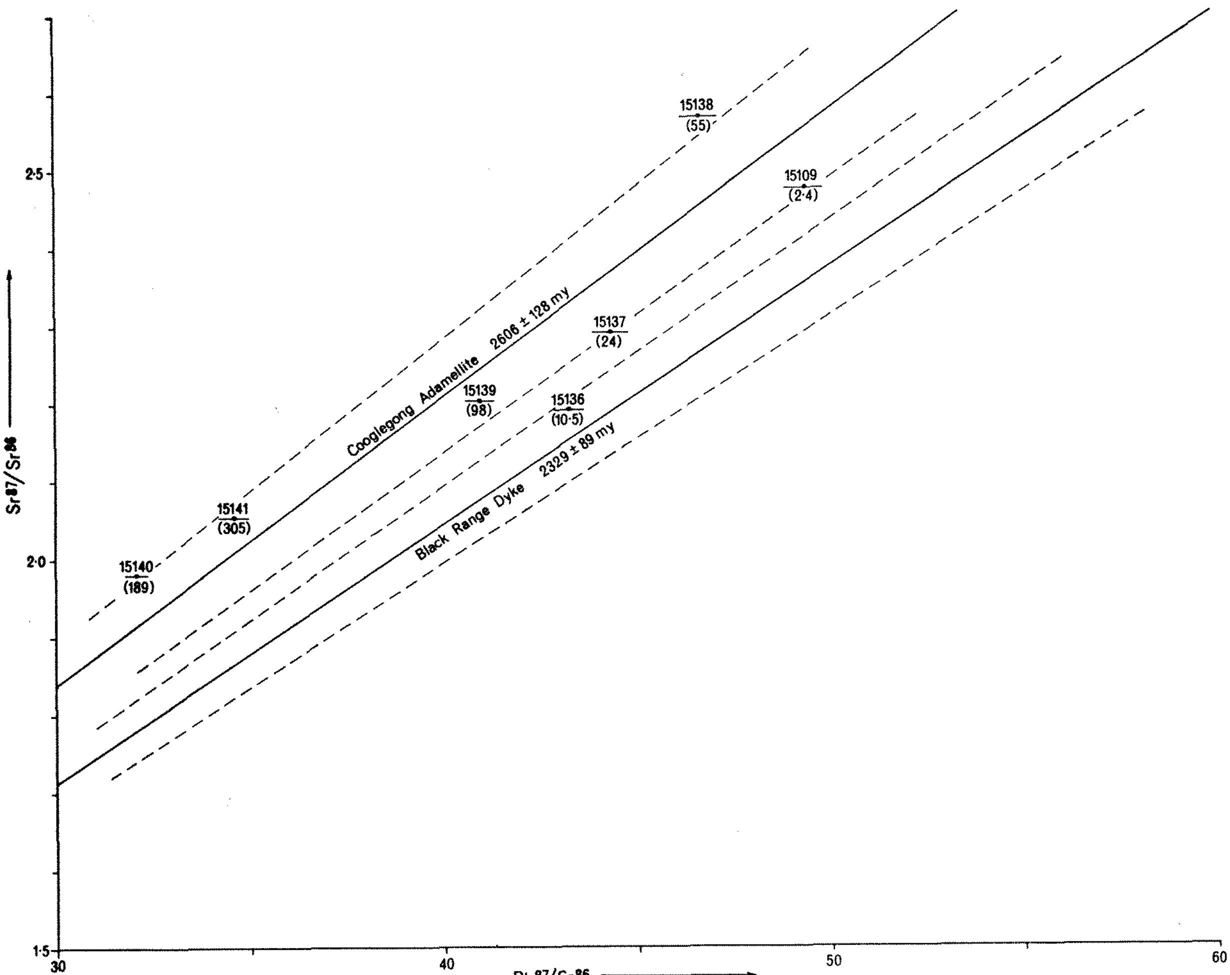

14671

Figure 47. Isochrons of Cooglegong Adamellite (de Laeter and others, 1975) and Black Range dyke, with samples from the contact aureole of the dyke not plotted on Figure 46. Figures in brackets are distance of samples from the dyke in metres.

An isochron comprising only the four samples from within the dyke and the completely remelted granite at the dyke margin (15108) gave an age of 2 340 ± 120 m.y. and an initial $Sr^{87}/^{86}$ ratio of 0.7259 ± 0.016.

DISCUSSION

The age of the Black Range dyke as found in this study is consistent with the geology of the area. The dyke is younger than the Cooglegong Adamellite which has been dated at 2 606 ± 128 m.y. (de Laeter and other, 1975) and is older than the 2 200 m.y. obtained by de Laeter and others (1974) for shales in the Weeli Wolli Formation in the overlying Hamersley Group.

The Mount Roe Basalt, the lowest member of the Fortescue Group, is a highly carbonated and altered basalt and unsuitable for radiometric dating but it is possible that the Black Range dyke at 2 329 ± 89 m.y. could be a feeder for the flows. As stated earlier no direct connection exists between the dyke and the basalt flows as the Fortescue Group, to the north of the Shaw Batholith, is preserved only by the downthrow of the fault against which the dyke terminates. Near the township of Nullagine however, the Cajuput dyke, another member of the Black Range dyke swarm, is overlain by the Hardey Sandstone and cuts basalts believed to be part of the Mount Roe series (Hickman, in prep.).

As the Hardey Sandstone conformably overlies the Mount Roe Basalt it appears reasonable to assume that the age of the Cajuput dyke and the age of the Black Range dyke swarm would be no younger than the age of the youngest flow of the Mount Roe Basalts. The age of these basalts and hence the age of the Archaean/Proterozoic unconformity in the Marble Bar area will, therefore, not be dissimilar to the 2 329 ± 89 m.y. found for the Black Range dyke.

For a dyke as large as the Black Range, part of a swarm covering most of the Pilbara region, it could reasonably be assumed that the magma was derived directly from the mantle. The initial Sr^{87}/Sr^{86} ratio of 0.7262 ± 0.012, however, suggests that the magma was derived by reworking older crustal material. This initial ratio is similar to that found for the Moolyella granite, 0.7397 ± 0.042 and for the Cooglegong Adamellite, 0.7303 ± 0.028 (de Laeter and Blockley, 1972; de Laeter and others, 1975), both of which appear to have been formed by reworking of older granitic material. A possibility exists that the magma has been enriched in radiogenic strontium. Fratta and Shaw (1974) described "residence contamination" of a basic dyke by diffusion of K, Rb, and Li from a granitic country rock but although this might explain the high Rb and Li content of the dyke, the K_2O content has remained normal for a basic magma.

Fratta and Shaw did not find that Sr diffused into the dyke. Neither is contamination a likely source of radiogenic Sr. Various studies have shown that when a basic magma assimilated granitic material potash is preferentially extracted (Lewis, 1970) and again, the potash has remained low in the Black Range dyke. In the absence of an alternative explanation it must be assumed that the Black Range dyke represents reworked Archaean material.

Age determination by the Rb-Sr whole rock method gives the time elapsed since the rock ceased to be an open system. For igneous rocks this will usually be the age of the intrusion. A later period of metamorphism can relatively easily re-equilibrate the minerals within the rock without disturbing the closed system of the whole rock and many examples are available (see Faure and Powell, 1972, p. 98) where, after quite severe metamorphism, the whole rock samples indicate the age of intrusion while mineral separates give the age of metamorphism. The intrusion of a dyke would not normally be considered to cause severe metaporphism of the country rock yet the isochron for the Black Range dyke has been obtained by including several whole-rock analyses of the enclosing Cooglegong Adamellite. It is concluded, therefore, that close to the dyke the adamellite became an open system with respect to Rb and Sr. The adamellite bordering the dyke was almost totally remelted and entirely lost its radiogenic Sr.

It appears that this open system extended into the adamellite at least 24 m from the dyke margin and that for the first 10 m the rock came into nearly complete equilibrium with the dyke. Some portions of the rock closer than 10 m from the dyke, however, did not equilibrate (spec. 15109) and the statistical analysis of the specimens making up the isochron of Figure 46 indicates that the initial Sr^{87}/Sr^{86} ratios were slightly different and probably reflect the diverse origins of the specimens. Beyond 50 m from the dyke, however, the rock appears to retain the age of intrusion of the Cooglegong Adamellite. All specimens from the metamorphic aureole of the dyke not used to calculate the isochron for the dyke are plotted on Figure 47 along with the isochron for the dyke and for the adamellite (from de Laeter and others, 1975). It will be seen from the graph that several specimens lie between the two isochrons, indicating perhaps a partial equilibration, and that the specimens collected furthest from the dyke actually appear to be older than the Cooglegong Adamellite. It is possible that this apparently older age is due to the expulsion of radiogenic Sr^{87} from the aureole of the dyke.

Direct evidence for migration of radiogenic Sr under moderate metamorphic conditions is not common, but Wasserburg and others (1964) have shown that hornblende diorite dykes which intrude augen gneiss, granites and overlying metasediments, all of Precambrian age, have been enriched in Sr^{87} during Mesozoic metamorphism.

In this example, from the Panamint Mountains of California, the dykes have a metamorphic mineral assemblage but the metamorphism has not been sufficient to obliterate the original basaltic textures. Nevertheless, Sr enrichment has occurred on a scale sufficient to give apparent ages which are absurd. The Black Range dyke, in contrast, appears to have caused a depletion of radiogenic Sr within its aureole and to be the first reported example of the open-system behaviour of whole-rock samples due to contact metamorphism.

Several authors, however, have reported the lowering of mineral ages within a contact aureole. Hart (1964) studied the contact zone of the Eldora Stock, Colorado, a small intrusion of adamellite, and found that various minerals responded differently to contact metamorphism but that beyond one intrusion width the ages were unaffected. At distances less than one-tenth the intrusion width, however, the mineral ages of biotite and K-feldspar were severely affected and rapidly approached the age of the intrusive stock. Calk and Naesser (1973) studied the thermal effect of a small basalt intrusion on fission tracks in sphene and apatite from the surrounding adamellite. Again it was shown that beyond one intrusion width there has been no effect and that complete annealing of the apatite took place only within a zone of one-tenth the intrusion width from the basalt.

Despite the difference in methods used the same order of magnitude applies to the metamorphic effect of the Black Range dyke. The dyke is approximately 120 m wide and a sample taken 10.5 m from the dyke has been completely equilibrated while samples beyond 100 m appear to be unaffected.

Insufficient data are available to make an independent estimate of the temperature required to bring about the open-system behaviour of the adamellite with respect to Rb and Sr but, from a consideration of the results of other workers, some estimate of the temperature distribution through the metamorphic aureole can be made.

From regional geological considerations it is unlikely that the present level of erosion is more than 1-2 km below that at the time of intrusion of the dyke. Initial wall rock temperatures, therefore, would be only about 50°C and pH_2O about 500 Kb. Assuming instantaneous injection and an initial temperature of 1 100°C for the basic magma the contact temperature would reach a maximum of 575°C and then decline (Jaeger, 1968). This temperature would be insufficient to melt the adamellite but the presence of a remelted zone 2 m wide, and partial melting up to 6 m from the dyke, indicates that elevated temperatures must have been maintained for a considerable period of time.

Experimental work by Tuttle and Bowen (1958) on the system Q-Or-Ab-H_2O suggests a minimum melting temperature of 770°C at 500 Kb and Piwinskii (1968) obtained a melting temperature of 725°C for granites of the Sierra Nevada Batholith. Such temperatures could be obtained at the margin of the Black Range dyke only by convection or by a flow of magma through the dyke channel. Convection is unlikely because this would lead to homogenization of the contaminated wall rocks with the bulk of the magma. A flow of magma through the dyke channel is consistent with the dyke being a feeder to the Mount Roe Basalts. As partial remelting has affected rocks up to 6 m from the contact, it must be assumed that a temperature of about 750°C was attained for a short while at this distance and that contact temperatures rose somewhat higher.

A second maximum temperature point can be obtained within the contact aureole of the Black Range dyke by considering the transformation of microcline to orthoclase which takes place within 55 m of the dyke. The transition has been investigated by Steiger and Hart (1967) and Wright (1967) for the metamorphic aureole of the Eldora Stock. These authors conclude that the transformation takes place slightly below 400°C, more than 50°C lower than experimental work suggests. (Goldsmith and Laves, 1954; Tomisaka, 1962).

The two temperatures thus obtained for the aureole of the Black Range dyke, 750°C at 6 m and 400°C at 55 m allow an estimation of the temperature at significant points within the aureole. Twenty-four metres from the dyke specimen 15137 has lost a significant proportion of its radiogenic Sr and, assuming an exponential temperature gradient, a temperature of about 530°C is suggested. Similarly 10 m from the dyke, where the Cooglegong Adamellite has behaved as a completely open system with respect to radiogenic Sr, the temperature rose to about 650°C. These temperatures are in agreement with Steiger and Hart (1967), who estimate a temperature of 500-550°C for the regional metamorphism which equilibrated the Sr of the Idaho Springs Formation surrounding the Eldora Stock, and the 500-600°C estimated from Calk and Naesser (1973) to erase fission tracks from apatite and sphene. The temperatures produced in the aureole of the Black Range dyke are also in excess of the 350-400°C required to reset mineral ages in the aureole of the Eldora Stock (Steiger and Hart 1967).

ACKNOWLEDGEMENTS

The autors would like to thank Mr. W. W. Thomas of the Department of Physics, Western Australian Institute of Technology, for technical assistance during this project.

REFERENCES

Blockley, J. G., 1970, Preliminary report on tin granite in the Pilbara Goldfield: West. Australia Geol. Survey Ann. Rept. 1969, p. 34-37.

Calk, L. C., and Naesser, C. W., 1973, The thermal effect of a basalt intrusion on fission tracks in quartz monzonite: Jour. Geology, v. 81, p. 189-198.

Compston, W., and Arriens, P. A., 1968, The Precambrian geochronology of Australia: Canadian Jour. of Earth Sciences, v. 5, p. 561-583.

Daniels, J. L., 1966, The Proterozoic geology of the North-West Division of Western Australia: Australasian Inst. Mining Metall. Proc. No. 219, p. 17-26.

de Laeter, J. R., and Abercrombie, I. D., 1970, Mass spectrometric isotope dilution analyses of rubidium and strontium in standard rocks: Earth and Planetary Science Letters, v. 9, p. 327-330.

de Laeter, J. R., and Blockley, J. G., 1972, Granite ages within the Archaean Pilbara Block, Western Australia: Geol. Soc. Australia Jour. v. 19, p. 363-370.

de Laeter, J. R., Peers, R., and Trendall, A. F., 1974, Petrography, chemical composition, and geochronology of two dolerite sills from the Precambrian Weeli Wolli Formation, Hamersley Group: West. Australia Geol. Survey Ann. Rept. 1973, p. 82-91.

de Laeter J. R., Lewis, J. D., and Blockley, J. G., 1975, Granite ages within the Shaw Batholith of the Pilbara Block: West. Australia Geol. Survey Ann. Rept. 1974, p. 73-79.

Faure, G., and Powell, J. L., 1972, Strontium Isotope Geology: Springer-Verlag, Berlin.

Fratta, M., and Shaw, D. M., 1974, 'Residence' contamination of K, Rb, Li and Tl in diabase dikes: Canadian Jour. of Earth Sciences, v. 11, p. 422-429.

Goldsmith, J. R., and Laves, F., 1954, Potassium feldspars structurally intermediate between microcline and sanidine: Geochim. and Cosmochim. Acta, v. 6, p. 110-118.

Greenhalgh, D., and Jeffery, P. M., 1959, A contribution to the Precambrian chronology of Australia: Geochim. et Cosmochim. Acta, v. 16, p. 39-57.

Gregory, F. T., 1861, Journal of the North-West Exploring Expedition: Gov. Printer, Perth, W.A.

Hart, S. R., 1964, The petrology and isotopic-mineral age relations of a content zone in the Front Range, Colorado: Jour. Geology v. 72, p. 493-525.

Hickman, A. H., in prep., Explanatory Notes on the Nullagine 1 : 250 000 Geological Sheet, W.A.: West Australia Geol. Survey Rec. 1975/5.

——— and Lipple S. L., 1974, Explanatory Notes on the Marble Bar 1 : 250 000 Geological Sheet, W.A.: West. Australia Geol. Survey Rec. 1974/20 (unpublished).

Jaeger, J. C., 1968, Cooling and solidification of igneous rocks *in* H. H. Hess and A. Poldervaart (Eds.), Treatise on rocks of basaltic composition, v. 2: Wiley, New York, p. 503-536.

Krauskopf, K., 1967, Introduction to Geochemistry: McGraw-Hill, New York.

Leggo, P. J., Compston, W., and Trendall, A. F., 1965, Radiometric ages of some Precambrian rocks from the Northwest Division of Western Australia: Geol. Soc. Australia Jour., v. 12, p. 53-65.

Lewis, J. D., 1970, Petrography and significance of some xenolith-bearing basic dykes of the Meckering district, Western Australia: West, Australia Geol. Survey Ann. Rept. 1969, p. 46-54.

McIntyre, G. A., Brooks, C., Compston, W., and Turek, A., 1966, The statistical assessment of Rb-Sr isochrons: Jour. Geophys. Research v. 71, p. 5459-5468.

Maitland, A. G., 1906, Third report on the geological features and mineral resources of the Pilbara Goldfield: West. Australia Geol. Survey Bull. No. 23.

Noldart, A. J., and Wyatt, J. D., 1962, The geology of portion of the Pilbara Goldfield: West. Australian Geol. Survey Bull. No. 115.

Piwinskii, A. J., 1968, Experimental studies of igneous rock series, central Sierra Nevada Batholith, California: Jour. Geology v. 76, p. 548-570.

Steiger, R. H., and Hart, S. R., 1967, The microcline-orthoclase transition within a contact aureole: Am. Mineralogist, v. 52, p. 87-116.

Tomisaka, T., 1962, On order-disorder transformation and stability range of microcline under high vapour pressure: Mineralogical Jour. (Tokyo) v. 3, p. 261-281.

Tuttle, O. F., and Bowen, N. L., 1958, Origin of granite in the light of experimental studies in the system $NaAlSi_3O_8$—$KAlSi_3O_8$—SiO_2—H_2O: Geol. Soc. American Mem. 74, p. 153.

Vinogradov, A. P., 1962, Average contents of chemical elements in the principal types of igneous rocks of the earth's crust: Geochemistry, v. 7, p. 641-664.

Wasserburg, G. J., Albee, A. L., and Lanphere, M. A., 1964, Migration of radiogenic strontium during metamorphism: Jour. Geophys. Research v. 69, p. 4395-4401.

Wright, T. L., 1967, The microcline-orthoclase transformation in the contact aureole of the Eldora Stock, Colorado: Am. Mineralogist v. 52, p. 117-136.

A GEOCHEMICAL STUDY OF A DOLOMITE-BIF TRANSITION IN THE LOWER PART OF THE HAMERSLEY GROUP

by R. Davy

ABSTRACT

Partial chemical analyses are reported on approximately 50 samples taken from the lower part of the Millstream No. 9 drill core to cover the transition between iron formation and the overlying dolomite unit of the Wittenoom Dolomite. The iron formation contains less iron (22.6 per cent Fe) and more calcium (6.6 per cent CaO) than other magnetite-bearing iron formations from Western Australia and other parts of the world. A transition zone, 2.2 m thick, separates the iron formation from the dolomite. This zone has a high iron content with magnetite-rich bands, but otherwise is similar in lithology to the overlying rocks. The dolomite unit is characterized by a mixture of very uniform dolomites, carrying up to 1.1 per cent MnO, with thin bands of intercalated carbonaceous shale. The latter contain up to 11.9 per cent K_2O which occurs as authigenic low-sodium adularia. Origins of the rocks are obscured by diagenesis which, by recrystallization, has destroyed many of the primary features of the rocks. However, the high carbon content and vestigial textures suggest fossil remains at some levels, and the rocks are believed to have been formed as chemical precipitates in shallow water, with relatively rare deposition/superimposition of clastic shales. The feldspar is believed to have been formed from illite with potassium extracted from sea water and, possibly, tuffaceous material.

INTRODUCTION

The central Hamersley Group of the Proterozoic Hamersley Basin of northwest Western Australia is characterized by the presence of numerous banded iron formation units.

Within the Hamersley Group, the Brockman Iron Formation (in particular the Dales Gorge Member) is the locus for the bulk of the known hematite deposits and is the host for all the Precambrian iron ore currently being mined in the Hamersley Range area; its stratigraphy is well known and is thoroughly documented.

Over the last few years intense exploration activity has been focussed on the Marra Mamba Iron Formation, which also occurs within the Hamersley Group, stratigraphically below the Brockman Iron Formation. Ore in the Marra Mamba Iron Formation occurs near the top of the formation, close to its contact with the overlying Wittenoom Dolomite; this part of the Hamersley Group is less well documented stratigraphically.

This paper describes, geochemically and petrographically, a section through the lower part of the Wittenoom Dolomite, intersected in an exploratory hole drilled by the G.S.W.A. in 1972 as part of a programme to test and to evaluate water-bearing potential, in the hope that it will have direct application in current iron ore exploration.

There is still some confusion concerning the passage of Wittenoom Dolomite downwards into Marra Mamba Iron Formation and it is not yet certain that the iron formation discussed in this paper is part of the Marra Mamba Iron Formation. Some geologists consider, that elsewhere in the area, the Wittenoom Dolomite contains iron formation near its base. The problem will only be resolved when additional exposures, or drill intersections, of the contact are found and examined.

The Millstream No. 9 hole, sited in the Fortescue Valley (Pyramid 1 : 250 000 Sheet, SF/50-7; co-ordinates 515.299; lat. 21°37'S, long. 117°01'E) was drilled to test the water-bearing capacity of the surficial calcrete and underlying Wittenoom Dolomite. The geology of the general area is given in MacLeod (1966) and Kriewaldt and Ryan (1967). The hole was extended below its original intended depth and core has been recovered over a distance of 167.75 m in the interval 61.5 m to 229.25 m (the bottom of the hole). The core largely consists of dolomite unit in the lower part of the Wittenoom Dolomite, but, at 223.5 m, a magnetic band is present and the remainder of the core is iron rich and passes into a siliceous iron formation unit. The whole of the core has been logged by geologist W. A. Davidson of the Western Australian Geological Survey (unpublished file report) but this study was restricted to the lower portion of the hole from 177.6 m to the end (approximately 50 m).

The dolomite unit in the core consists of massive to thinly laminated dark grey dolomite with black, carbonaceous partings and thin interbedded zones of black carbonaceous shale. These shale bands are commonly 2 mm to 2 cm thick. A large proportion of the upper and middle (unsampled) portions of the core consists of intraformational dolomite breccia, and minor brecciation (both intraformational and compactional or diagenetic) occurs elsewhere. It was noted that dolomite, with associated shale bands, extends below the first magnetic band to 225.2 m at which point the core becomes noticeably more siliceous. The zone from 223.0 m to 225.2 m is considered a transition zone between iron formation and the dolomite unit. A log of the core is given with Figure 48.

The iron formation found in the Millstream 9 core is a mixture of siliceous material with magnetite-rich bands and with subordinate carbonate. It grades upwards into dolomite and shales as noted earlier. Below this band of siliceous iron formation manganiferous shales are believed to occur (A. F. Trendall, pers. comm.) though these were not reached in this core.

Samples were chosen as far as possible to be representative of the various rock types (Table 17). A disproportionately large number of the shales was sampled, in that the great majority of the shales which exceeded 2 mm were chosen. Dolomite samples were chosen to be as representative of this type of rock as possible. The length of dolomite core selected was a standard 5 cm. The thicknesses of the remaining samples are given in Table 17.

TABLE 17. SAMPLES ANALYSED FROM THE MILLSTREAM 9 DRILL CORE WITH HAND SPECIMEN DESCRIPTION.

GSWA Sample Number	Depth (m)	Description
42301	177·6	Dark grey dolomite with incipient bedding. Two very thin (1 mm) zones of lighter carbonate
42302	177·9	Massive black cavity infilling associated with white carbonate vein, thin (2 mm) layer of shale at bottom
42303	178·5	Dark grey rock ' oozing ' oily hydrocarbons
42304	184·4	Massive dark grey dolomite
42305	186·2	Black shale (5 mm)
42306	190·2	Black shale (2 cm)
42307	190·5	Black shale (2–3 mm)
42308	191·5	Black shale, 5 mm thick, splitting into two sections 2 mm and 3 mm thick with veinlet 0·5–1 mm of intercalated dolomite
42309	191·7	Black shale (4 mm)
42310	192·0	Black shale (4–6 mm)
42311	192·1	Massive dark grey dolomite with indications o bedding
42312	193·5	Black shale (2 cm)
42313	195·7	Black shale with dolomite intercalations (6–7 mm)
42314	198·7	Shaly dolomite
42315	198·8	Massive dark grey dolomite
42316	201·9	Black dolomitic shale (3–4 mm)
42317	204·4	Black dolomitic shale (4–6 mm)
42318	206·6	Finely banded, grey-black dolomitic shale with rare lighter zones
42319	206·9	Dark grey dolomite
42320	207·85	Dark grey-black dolomite with oily smears
42321	208·6	Black shaly dolomite (2-5 mm), irregularly surfaced
42322	209·3	Dark grey, bituminous dolomite
42323	209·6	Dark grey dolomite
42324	210·5	Dark grey, finely banded dolomite
42325	210·7	Brecciated, blotchy dolomite with ' shale ' bands (1–2 mm) and dark streaks
42326	212·5	Black shale (1–2 mm)
42327	213·3	Black shale (2–4 mm)
42328	214·4	Massive dark grey dolomite
42329	216·1	Thinly bedded dark grey dolomite
42330	216·7	Black shale (2 cm)
42331	218·1	Dark grey massive dolomite
42332	218·8	Black shale (1·5 cm)
42333	219·3	Black shale (1 cm)
42334	222·5	Dark grey dolomite
42335	223·0	Black shale (2 cm)
42336	223·35	Dolomite, adjacent to contact with magnetite-rich rock. Dolomite, rather leached-looking, variably dark to light grey
42337	223·4	Black magnetite-rich rock (3 cm)
42338	224·85	Black shale (2–3 cm)
42339	225·1	Dark grey dolomite, with carbonaceous partings
42340A	225·2	Carbonate rock adjacent to first main magnetic band
42340B	225·2	Magnetite-dolomite-silicate rock (2 cm)
42340X		Composite of iron formation from 225·2 m to 229·2 m
42341D	225·7	Magnetite rock (5 mm)
42341L	225·7	Chert dolomite zone (1·5 cm)—8 mm below 42341D Part of swell zone of a pod
42342	225·8	Magnetite-rich zone (4 mm)
42343D	226·3	Magnetite-rich zone (4mm) adjacent to siliceous pod
42343L	226·3	Siliceous pod (2 cm)
42344	226·7	Siliceous zone with carbonate; irregular shape (2 cm)
42345D	226·8	Thinly bedded magnetite-rich rock (3 mm)
42345L	226·8	Chert-carbonate rock (2 cm) immediately above 42345D
42346	227·2	Rather featureless silica-phyllosilicate rock with rare opaques (1 cm)
42347	227·3	Magnetite band (3 mm)
42348D	228·3	Magnetite band (1·2–1·5 cm) with fine, lighter layers
42348L	228·3	Siliceous (chert) zone with rare riebeckite (7 mm), 2·5 mm above 42348D
42349D	228·9	Thinly banded magnetite rock (1·4 cm)
42349L	228·9	Siliceous zone with carbonate (1cm)
42350	229·25	Riebeckite-carbonate rock (1 cm)

N.B. The normal thickness of sample is 5 cm. Other thicknesses used are listed. The fissility of the shales enabled collection of relatively clean shale samples. However, the iron formation zones were less fissile, with, in some cases, gradational zones. As clean zones as possible were chosen by careful selection of the samples

Other samples from the dolomite unit were chosen because of their particular interest, and included a portion of rock which was oozing hydrocarbons (178.4 m, 42303), and one which was a cavity infilling (177.9 m, 42302).

The shale samples were split to give as pure specimens as possible, and their fissibility made separation from adjoining dolomite relatively easy. However thin sections showed, in some cases, that intercalations of dolomite were present. The surfaces of the shales are quite undulatory, and the thicknesses of the shales vary by several millimetres even in the width of the core.

A composite sample was taken from the iron formation. A thin sliver of uniform thickness was cut from the side of the core from 225.2 m to the end of the hole at 229.25 m. This was bulked. Because of the wide variation of rock types, the extreme thinness of some layers, and the presence of pod-like structures in some places it was not possible to choose representative small portions of the rock. Instead, samples were cut from some of the thicker layers (mesobands) to give an indication of the composition of the "purer" members of the various phases. Many zones showing transitional mineral changes were not sampled because of their innate variability.

PREPARATIONAL AND ANALYTICAL TECHNIQUES

The samples were divided into four portions. One part was used for thin section preparation, one part for atomic absorption analysis, one part for wet chemical and X-ray diffraction analysis (where applicable), and one part was retained for reference purposes.

The samples for analysis were passed through a jaw-crusher and then ground in a Tema ring-mill using chrome-steel grinding heads.

Determinations were restricted to the following elements: Na, K, Ca, Mg, Mn, C, Cu, Pb, Zn, Ni, Ba, Sr, and V, together with carbonate (as CO_2) and phosphorus (as P_2O_5). Hydrocarbon or non-carbonate carbon was measured separately from carbonate carbon. All components except C, CO_2 and P_2O_5 were determined by atomic absorption spectrometry and the choice of elements was restricted to those relevant elements for which suitable analytical equipment was available. Three digestion methods were used in the AAS determinations, partly for comparative purposes, but also because of difficulties in the determination of various elements.

A description of the methodology is given in Davy (1975).

The analysis for free (non-carbonate) carbon, carbon dioxide and phosphorus (expressed as the pentoxide) was carried out by the Government Chemical Laboratories.

The thin sections were half-stained with Alizarin-Red-S solution after being dipped into dilute hydrochloric acid. A red stain on grains of carbonate indicated the presence of calcite. No attempt was made to discriminate, by any staining technique, between dolomite and iron-bearing carbonate.

X-ray diffraction analysis was carried out by the Government Chemical Laboratories.

PETROGRAPHY

An approximate mineralogical composition of the samples analysed is given in Figure 48.

DOLOMITE UNIT

The dolomite unit can best be considered in terms of two end phases: dolomite and shale. Mixtures of the two and a few variants containing chert occur in places.

The *dolomite phase* consists, charcteristically, of a mosaic of recrystallized dolomite which shows evidence of its former (primary) structures only in the disposition of some of the contained opaques. The dolomite is dark grey and massive. The bedding is more apparent in hand specimen than in thin section though the thin sections reveal that it is the dispersed trains of opaques which define the bedding. The dolomite shows no sign of lineation and/or foliation, and in many samples, grains of secondary dolomite enclose the trains of opaques. The size of the dolomite grains varies from about 0.03 mm to 0.35 mm with the most common size range being 0.07 to 0.1 mm. There is some small variation in size from specimen to specimen and, in general, late stage veins, wherever found, contain the largest (0.30-0.35 mm) grains.

Primary textures are not easy to deduce. The trains of opaques show slight irregularities and in 42324 (210.5 m)* an overturned fold is indicated. The opaques commonly appear more abundant than the analyses would suggest and consist of carbonaceous material (organic carbon, hydrocarbons or graphite), together with pyrite and possibly hematite. Their grain size (except for pyrite) is of the order of 0.001 mm, though irregular, larger aggregates up to 0.01 mm in diameter are relatively common.

The opaques are commonly collected into diffuse aggregates up to 0.1 mm in diameter, which define the bedding (e.g. 42322). These aggregates may have sufficient lateral width as to suggest former pellets (42311, 42319), and elsewhere similarities with algal structures are possible.

Pyrite occurs in nearly all samples as small cubes or pyritohedra, as well as in irregular grains. All pyrite is of the order of 0.01 to 0.02 mm in diameter. Sample 42302 is unusual in the amount of pyrite present. In this sample it appears as loose aggregates (interspersed with dolomite) of ?framboids with the aggregates reaching 3 to 4 mm in diameter. There is no indication of the time of formation of the greater part of the pyrite except in 42302 where it is clearly secondary.

Post-depositional changes include the recrystallization of dolomite. There is no indication whether dolomite was the primary mineral. In some samples the dolomite has a tendency to form discrete rhombs, which still contain some dispersed opaques, but which, in many cases (e.g. 42303, 21, 25 and 34) appear to have pushed the brownish-black hydrocarbon material into the interstitial zones between the rhombs. Other post-depositional features are shown by the presence of incipient stylolites (42319, 24) or definite stylolites (42328, 29, 31). These are in general parallel with the bedding with the amplitude varying up to 2.5 mm. Late-stage veins of dolomite are present in 42315, 24 and in 42329 where they appear to cement fine cracks.

The mineralogy of *the shales* is very uniform. All are fine grained with only dolomite (or calcite), and traces of quartz, mica, and, rarely pyrite, being readily identified in thin section. The overall grain size is less than 0.01 mm, in many cases less than 0.002 mm. Optical identification is rendered very difficult because of the all-pervasive opaques, which, in thin section, appear to be very abundant (especially in 42312, 30). The opaque grains, however, largely hydrocarbon or graphite, are usually quite small but conceal transparent minerals above or below them. The shales are all thinly laminated with bedding traces no more than 0.01 to 0.1 mm apart.

* Subsequently the G.S.W.A. sample number only is given. The depth from which the sample were taken will be found by referring to either Table 17 or to Figure 48.

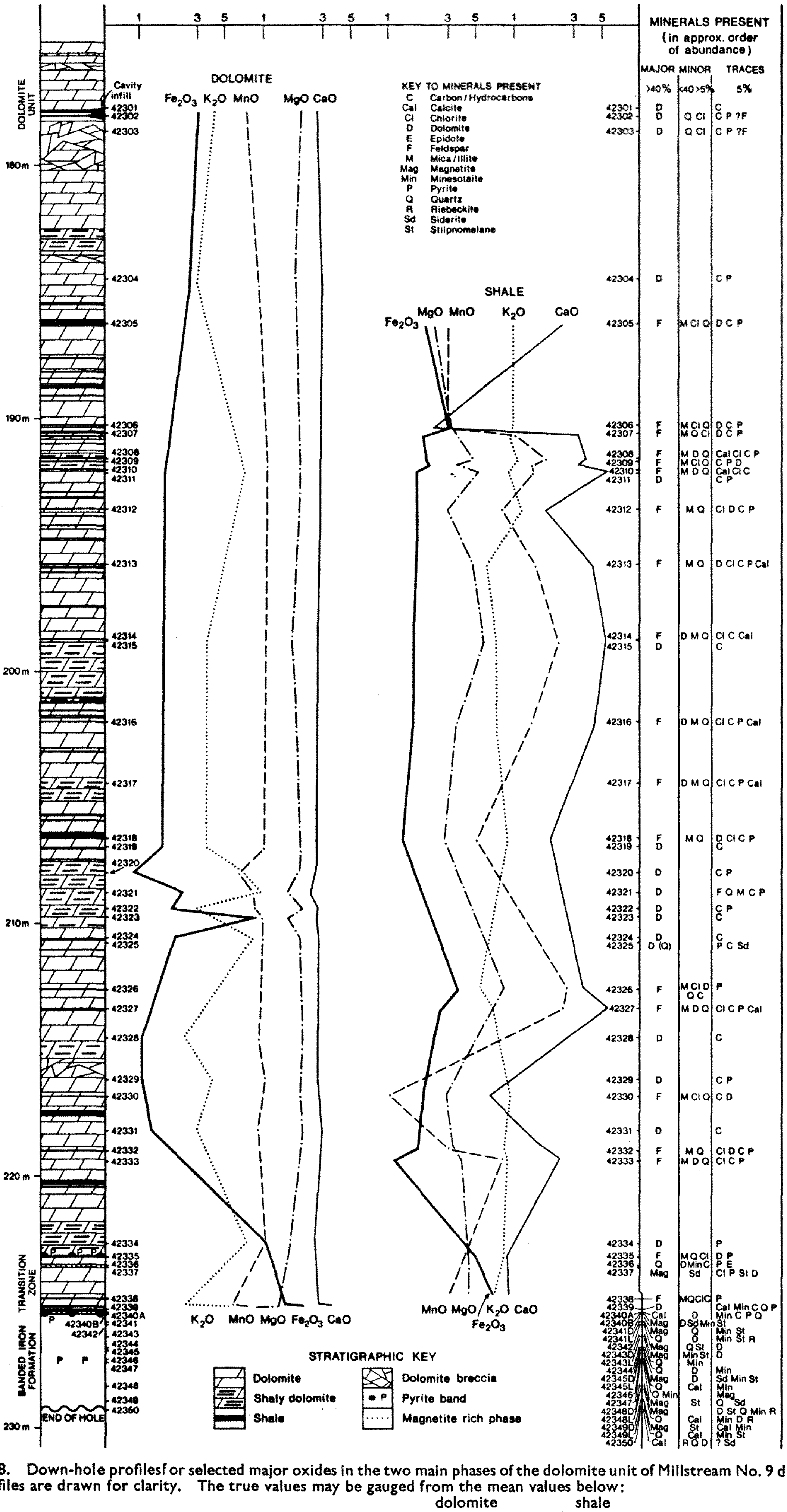

Figure 48. Down-hole profilesf or selected major oxides in the two main phases of the dolomite unit of Millstream No. 9 drill core. The profiles are drawn for clarity. The true values may be gauged from the mean values below:

	dolomite (per cent)	shale (per cent)
CaO	27·7	2·96
MgO	19·1	4·21
MnO	0·95	0·11
K_2O	0·50	8·74
Fe_2O_3	2·9	2·1

Left hand: stratigraphic log. Right hand: essential mineralogy of samples analysed.

The bedding is defined by the parallelism of the phyllosilicates and differences in the opaque content. The mineralogy of the majority of shale samples has been determined by X-ray diffraction analysis which revealed that the bulk of the non-opaque material was a low-temperature, largely monoclinic K-feldspar—considered to be adularia.

Careful examination of the thin sections revealed traces of cross-hatch twinning on two grains only (42333), suggesting the presence of some microcline. A few small (0.05 mm) detrital grains of quartz, including one rutilated quartz grain (42306), and of white mica were noted, the remainder was so fine grained that its origin is in doubt. The shale sections, in particular, were examined for evidence of volcanic material, but none was found.

The shales contain dolomite and/or calcite. Calcite was recognized in thin section by the pink stain taken with Alizarin-Red-S solution. Grains of calcite and dolomite were larger than other components of the shale, ranging up to 0.5 mm in a few grains. Calcite has irregular outlines with no crystal forms, but dolomite occurs both as irregular grains and as "blastic" rhombs.

A few samples contain negligible carbonate (42306, 30, 35, 38). Several contain dolomite which appears to have penetrated into the shale from both above and below (e.g. 42307, 16). Others are impregnated with carbonate throughout (e.g. 42309, 26) but have a tendency for the carbonate to be concentrated in specific layers. A few consist of alternations of shale and dolomitic shale (e.g. 42313, 27).

Quartz is recognizable in the thin section in layers and in veins in 42328.

Several of the samples chosen were found to be breccias. These included 42302, 03, 25 and 33. Of these, the first three are dominantly dolomitic, the last is a shale. Sample 42302 was chosen as a black, apparently massive, cross-cutting cavity infilling (initially suspected of carrying manganese dioxide) whilst 42303 was oozing hydrocarbons. Sample 42325 was chosen because of dark streaks which were considered possibly manganiferous, and 42333 appeared in hand specimen to be a normal shale.

The cavity infilling (42302) is a mixture of chert, dolomite and shale and has components of all three except that no K-feldspar was detected by X-ray diffraction (indicating that less than 5-10 per cent of the mineral was present). The thin section shows several zones with apparent gradational bedding. Dolomite at the base of each zone passes through dolomitic carbonaceous shale to carbonaceous shale in a regular fashion over 5 to 8 mm, with the dolomite grains, even at the base, separated by carbonaceous films. Later dolomite infilling of translayering cracks contains aggregates of pyrite (with interstitial dolomite). The pyrite in aggregate reaches 3 mm in diameter though individual grains are rarely more than 0.03 mm across.

The bituminous rock 42303 proved to be largely dolomite with subordinate shale, small amounts of chert, and again, negligible K-feldspar. The brecciation of 42325 was more obvious in hand specimen than in thin section. In the section all the dolomite occurred as rhombs, in places discrete, with brown interstitial material. Elsewhere the dolomite rhombs were so abundant as to form a mosaic with the interstitial material absent.

TRANSITION ZONE

The first optically recognizable sign of the top of the iron formation is seen in 42336 (223.35 m) which is a rock composed largely of granular chert impregnated with minnesotaite, dolomite and carbon/hydrocarbons. The opaques are unusual in that they are composed of little "rings" of ?carbon 0.01 mm in diameter. These rings have small (0.001 to 0.005 mm) protruberences on them. They occur singly or in aggregate (giving the rock a well marked banding), and appear to be organic in origin. The minnesotaite occurs (as in the iron formation proper) in single arcuate fibres or plates and in sheaves of plates up to 0.15 mm long and, cumulatively, with a similar width.

Immediately below the last sample there is a prominent magnetite-rich band some 3 cm thick but for the next 1.8 m there is a reversion to the dolomite unit type of rock with both dolomite (42339) and shale (42338).

The main features of difference from the corresponding rock above are the presence of calcite with the dolomite in the carbonate facies rock, and the presence of small amounts of minnesotaite in the carbonate. The shale contains visible quartz in thin layers and veins.

IRON FORMATION

At 225.2 m there is a distinct facies change to more siliceous iron formation, with reduction of the carbonate content of the rock. In lower zones carbonate is more variable, with calcite quite prominent, and with siderite accompanying or replacing dolomite. The iron formation contains an abundance of thin bands (mesobands) of quite markedly variable lithology. Some zones are magnetite rich (with accessory siderite, dolomite, or stilpnomelane), some are chert rich (with subordinate carbonate and minnesotaite), others are carbonate rich (with subordinate chert, riebeckite, magnetite) and others are phyllosilicate rich (mainly ferrostilpnomelane). Some of the bands appear homogeneous and have sharp boundaries, others are gradational and merge into a mesoband of different type. In a few places minnesotaite and pale to olive green ferrostilpnomelane occur together, but, for the most part, these minerals seem to be mutually exclusive. Megascopic features of the bands include pod structures, and possible compactional features with tension cracks infilled by overlying layers. The overall grain size of the minerals is small. Opaques reach 0.1 mm, but the greater part of all other minerals except carbonates are much smaller than this. Carbonates, particularly those in veins, or those which have rhombic outlines can be as large as 0.3 mm, and, in one zone 0.6 mm. Quartz in veins can also reach 0.1 to 0.3 mm in diameter, though most approach chert-size grains. Minnesotaite plates and fibres can reach 0.1 to 0.5 mm. There is some suggestion of a later recrystallization of at least part of the carbonate.

On the basis of the chemistry of the rock (see later section) certain of the calcites of the iron formation are considered to be ferroan calcite (or ankerite) though no separation and analysis has been made. The lowest refraction index determined in oil on crushed rock is about 1.52 and the highest about 1.69.

RESULTS

ANALYTICAL

Condensed results of analysis are presented in Table 18. A complete set of results, including values given by both geochemical (HCl/HNO_3) and "total" (HF based) attacks, is given in an unpublished Geological Survey report (Davy, 1975).

The samples have been grouped by lithological type in Table 18 to facilitate comparisons between the groups.

The means and standard deviations of the composition for dolomite and shale (from the dolomite unit), and for the magnetite-rich phases of the iron formation, and iron formation/transition zone, are given in Table 19.

DOLOMITE UNIT

The dolomite unit, with its contained shales, is dark grey to black. In thin section the proportions of minerals in the shales are very hard to estimate for the proportion of opaques appears grossly in excess of those reported in the analyses. The opaque minerals present are pyrite, carbon (or hydrocarbons) and hematite. The organic grains are finely divided, though the iron minerals are slightly larger. Samples were deliberately chosen to get "pure" shales, and typical dolomites. The feature of the samples analysed is the prominence of the "end members" of dolomite and shale (see Fig. 49). Other samples can, for the most part, be considered as simple mixtures of shale material with dolomite. In a few places (42321) there is dilution by silica.

Because of the fundamental difference in composition between the dolomites and the shales separate down-hole profiles have been drawn for selected elements for these phases (see Fig. 48). The close correlation of manganese with calcium ($r = 0.93$) shows that this element is present in the carbonate phase and not in the opaques. The manganese values are exceptionally high for dolomite. Barium is also relatively high in the dolomites, showing close correlation with calcium ($r = 0.87$).

The sodium and potassium values of dolomites are rarely reported. However the sodium values appear about normal whereas the potassium values are slightly elevated (e.g. Pettijohn, 1957, p. 418).

Iron values are approximately the same in both shales and dolomites, away from the contact with the iron formation, with the exception of a dolomitic rock at 209.6 m (42323). With this one possible exception, iron has no particular affinity with carbonate and the prominence of fine opaques suggests that, despite the presence of traces of visible pyrite, some of the iron may be present as finely dispersed hematite.

Comparison with the analyses of dolomites reported by Pettijohn (1957, p. 418) and with dolomites reported by Deer, Howie and Zussman (1962, v. 5, p. 280) shows that most of the dolomites approximate to the composition of pure dolomite, with the molecular ratio of calcium to magnesium approximately 1 : 1. In general the dolomite phase is not calcitic though calcite appears in the carbonate rocks in the transition zone with the iron formation.

Trace element values are low in the dolomite and are comparable with those reported from unmineralized dolomites in other parts of the world. However, barium values are well above those suggested by Turekian and Wedepohl (1961), Hawkes and Webb (1962) and Krauskopf (1967) for carbonate rocks. The base metals all appear marginally higher than the averages given by these authors. There are traces of carbon, and the phosphate content, with the exception of sample 42323, is very low.

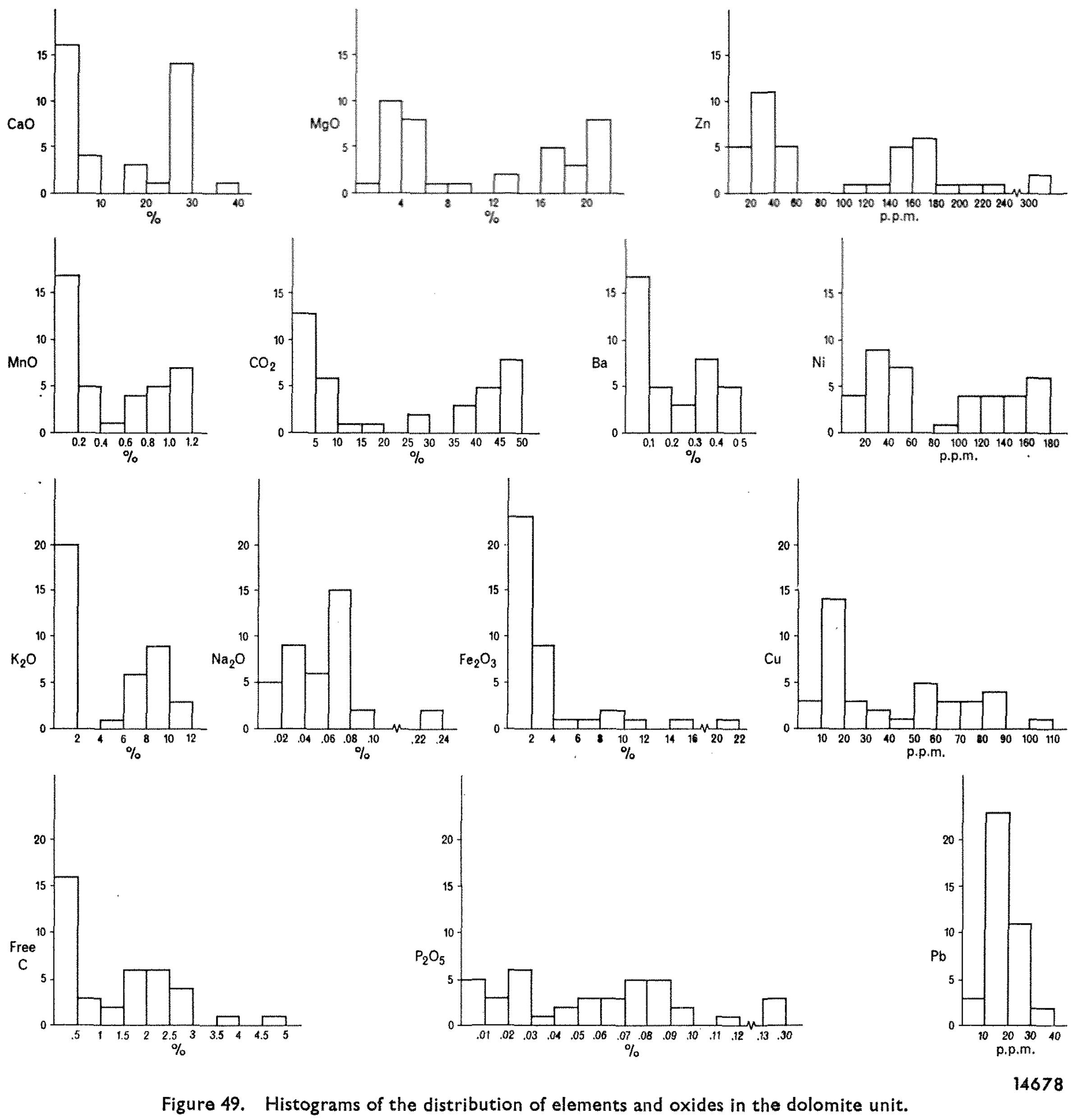

Figure 49. Histograms of the distribution of elements and oxides in the dolomite unit.

TABLE 18. PARTIAL ANALYSIS OF ROCKS FROM MILLSTREAM 9

1. DOLOMITES

Sample		42301	42304	42311	42315	42319	42320	42321	42322	42323	42324	42328	42329	42331	42334	42339 Transition Zone	42340A Transition Zone
Depth (m)		177·6	184·4	192·1	198·8	206·9	207·85	208·6	209·3	209·6	210·5	214·4	216·1	218·1	222·5	225·1	225·2
	Digestion																
Fe_2O_3 %	$HF/HClO_4$	3·0	2·6	1·7	1·7	1·6	0·9	2·3	1·9	8·7	2·0	1·1	1·1	1·3	10·6	14·7	21·7
MnO %	$HF/HClO_4$	0·75	0·93	1·11	1·08	1·05	0·67	0·85	0·88	1·01	1·02	0·94	1·06	0·93	1·08	0·57	0·70
MgO %	$HF/HClO_4$	20·4	18·4	20·1	17·2	20·2	19·7	16·2	20·1	16·4	19·7	21·2	20·1	20·9	16·2	13·3	5·30
CaO %	$HF/HClO_4$	27·1	29·7	29·2	27·4	27·7	26·9	24·8	28·0	27·7	28·1	28·4	27·7	29·5	25·7	27·1	35·3
Na_2O %	$HF/HClO_4$	0·02	0·02	0·03	0·03	0·05	0·02	0·06	0·03	0·05	0·03	0·04	0·04	0·04	0·08	0·08	0·07
K_2O %	HF/H_2SO_4	0·42	0·30	0·72	0·36	0·36	0·72	0·96	0·30	0·42	0·84	0·24	0·39	0·30	0·73	0·24	0·54
Cu ppm	$HF/HCl/HClO_4$	10	10	20	10	20	20	30	20	20	20	20	20	20	30	20	25
Pb ppm	$HF/HCl/HClO_4$	40	20	30	15	20	20	20	20	20	20	20	20	25	25	20	25
Zn ppm	$HF/HCl/HClO_4$	45	40	55	30	60	30	140	30	20	15	20	30	35	30	40	30
Ni ppm	$HF/HCl/HClO_4$	30	15	45	30	60	45	135	30	30	15	15	30	30	60	30	45
V ppm	HCl/HNO_3	<12	12	12	12	100	<12	<12	<12	<12	12	<12	<12	12	40	<12	<12
Ba %	HCl/HNO_3	0·40	0·35	0·40	0·35	0·50	0·35	0·30	0·50	0·35	0·40	0·47	0·50	0·40	0·30	0·45	0·47
Sr ppm	HCl/HNO_3	10	10	20	12	20	20	25	5	15	10	15	20	15	18	10	25
†CO_2 %	See text	45·4	46·2	45·1	41·6	45·0	43·5	38·2	45·5	43·0	45·9	46·7	46·0	46·1	37·9	40·8	36·8
†Free C %	See text	0·03	0·1	0·2	0·3	0·3	0·2	0·7	0·2	0·3	N.D.	0·05	0·1	0·1	0·9	0·1	0·3
†P_2O_5 %	See text	0·001	0·012	0·052	0·028	0·026	0·022	0·063	0·034	0·304	0·011	0·008	0·009	0·010	0·036	0·014	0·096
Fe as metal %	See text	2·1	1·8	1·2	1·2	1·1	0·6	1·6	1·3	6·1	1·4	0·8	0·8	0·9	7·4	10·3	15·2

2. SHALES

Sample		42305	42306	42307	42308	42309	42310	42312	42313	42314	42316	42318	42326	42327	42330	42332	42333
Depth (m)		186·2	190·2	190·5	191·5	191·7	192·0	193·5	195·7	198·7	201·9	206·6	212·5	213·3	216·7	218·8	219·3
	Digestion																
Fe_2O_3 %	$HF/HClO_4$	2·0	3·0	1·9	2·0	2·1	1·7	1·7	1·7	1·6	1·6	1·3	3·6	2·6	1·9	1·7	1·1
MnO %	$HF/HClO_4$	0·03	0·03	0·10	0·17	0·14	0·14	0·08	0·15	0·23	0·14	0·05	0·27	0·25	0·01	0·03	0·08
MgO %	$HF/HClO_4$	2·32	3·15	3·48	4·64	3·48	5·10	2·98	4·97	5·80	3·48	2·82	8·32	6·80	2·82	3·32	3·81
CaO %	$HF/HClO_4$	2·24	0·13	3·22	3·65	3·20	5·04	1·80	4·26	5·44	4·62	1·96	3·56	5·56	0·64	1·68	2·50
Na_2O %	$HF/HClO_4$	0·07	0·07	0·07	0·08	0·08	0·08	0·08	0·06	0·06	0·07	0·08	0·06	0·07	0·08	0·09	0·20
K_2O %	HF/H_2SO_4	10·1	9·76	9·52	10·8	10·0	9·27	11·9	6·38	7·35	7·47	8·91	5·54	6·87	9·28	8·43	8·79
Cu ppm	$HF/HCl/HClO_4$	60	80	110	70	65	60	60	50	40	60	85	70	75	80	90	40
Pb ppm	$HF/HCl/HClO_4$	<10	40	25	25	30	30	20	20	10	15	20	20	25	20	20	15
Zn ppm	$HF/HCl/HClO_4$	160	300	180	160	180	175	180	150	185	145	205	40	165	170	225	20
Ni ppm	$HF/HCl/HClO_4$	150	165	165	150	150	135	180	135	90	135	105	120	120	180	180	30
V ppm	HCl/HNO_3	100	160	100	85	100	60	75	25	25	12	100	150	60	100	100	25
Ba %	HCl/HNO_3	0·05	0·05	0·12	0·10	0·05	0·05	0·02	0·07	0·10	0·07	0·05	0·20	0·05	0·05	0·05	0·02
Sr ppm	HCl/HNO_3	5	5	12	8	10	20	20	20	5	<5	10	12	10	20	5	8
CO_2 %	See text	2·2	0·3	2·6	5·5	3·7	6·9	2·8	5·6	6·6	7·3	2·8	4·1	7·1	0·8	1·7	3·2
Free C %	See text	2·1	2·5	1·7	1·8	1·9	1·6	2·6	2·1	1·4	1·7	2·7	4·6	2·9	2·6	2·3	2·3
P_2O_5 %	See text	0·082	0·064	0·082	0·146	0·092	0·089	0·051	0·083	0·074	0·119	0·080	0·148	0·090	0·050	0·075	0·078
Fe as metal %	See text	1·4	2·1	1·3	1·4	1·5	1·2	1·2	1·2	1·1	1·1	0·9	2·5	1·8	1·3	1·2	0·8

3. MISCELLANEOUS ROCK FROM THE DOLOMITE UNIT

		Impure Dolomites			Dolomitic Shale	*Siliceous* Contact Rock	Transition Zone Shales	
	Sample	42302	42303	42325	42317	42336	42335	42338
	Depth (m)	177·9	178·5	210·7	204·4	223·35	223·0	224·85
	Digestion							
Fe_2O_3 %	HF/HClO$_4$	2·3	2·6	1·9	1·7	9·6	4·7	6·7
MnO %	HF/HClO$_4$	0·34	0·35	0·62	0·21	0·06	0·04	0·03
MgO %	HF/HClO$_4$	20·9	16·4	12·8	5·47	1·49	4·30	4·31
CaO %	HF/HClO$_4$	16·2	15·8	15·8	7·6	2·10	0·86	0·90
Na_2O %	HF/HClO$_4$	0·02	0·03	0·04	0·07	0·01	0·08	0·24
K_2O %	HF/H_2SO_4	0·12	0·30	0·42	7·11	0·24	8·19	6·87
Cu ppm	}	20	20	20	85	20	60	85
Pb ppm	} HF/HCl/	25	20	15	10	20	20	25
Zn ppm	} HClO$_4$	45	55	20	165	25	110	330
Ni ppm	}	45	60	10	180	30	105	150
V ppm	}	25	25	12	75	125	125	175
Ba %	} HCl/HNO_3	0·20	0·15	0·33	0·13	0·02	0·05	0·02
Sr ppm	}	5	10	22	10	5	15	10
CO_2 %	}	19·0	25·4	28·0	11·1	2·8	1·0	0·8
Free C %	} See text	1·2	1·0	0·5	2·0	0·2	2·3	3·7
P_2O_5	}	0·021	0·050	0·022	0·059	0·003	0·068	0·076
Fe as metal		1·6	1·8	1·3	1·2	6·7	3·3	4·7

4. IRON FORMATION

		MAGNETITE—RICH PHASES								
	Sample	Transition Zone 42337	Transition Zone 42340B	42341D	42342	42343D	42345D	42347	42348D	42349D
	Depth (m)	223·4	225·2	225·7	225·8	226·3	226·8	227·3	228·3	228·9
	Digestion									
Fe_2O_3 %	HF/HClO$_4$	68·6	56·0	72·3	76·9	70·5	83·4	77·3	83·2	78·2
MnO %	HF/HClO$_4$	0·28	0·41	0·03	0·02	0·01	0·01	0·02	0·01	0·01
MgO %	HF/HClO$_4$	3·48	4·97	0·91	0·48	0·99	0·56	0·86	0·53	0·80
CaO %	HF/HClO$_4$	3·22	13·6	1·72	0·77	0·70	0·62	0·96	0·41	0·34
Na_2O %	HF/HClO$_4$	0·02	0·05	0·20	0·30	0·05	0·07	0·24	0·28	0·34
K_2O %	HF/H_2SO_4	0·60	0·60	0·34	0·32	0·27	0·25	0·23	0·25	0·24
Cu ppm	HF/HClO$_4$	25	20	10	10	20	10	5	5	5
Pb ppm	HCl/HNO_3	20	20	65	60	70	60	55	55	55
Zn ppm	HF/HClO$_4$	30	30	13	15	40	20	15	15	10
Ni ppm	HF/HClO$_4$	60	60	45	40	50	55	30	35	30
Ba ppm	HCl/HNO_3	500	1700	ND	175	ND	ND	150	125	ND
Sr ppm	HCl/HNO_3	20	10	10	ND	5	75	5	70	ND
CO_2		13·3	26·6	2·63	1·00	0·84	0·87	1·34	0·46	0·44
Free C %	}	0·8	0·2	0·05	0·03	0·04	0·04	0·06	0·02	0·07
P_2O_5	} See Text	0·059	0·068	0·043	0·040	0·043	0·056	0·027	0·075	0·047
Fe as metal	}	48·0	39·2	50·6	53·8	49·3	58·3	54·1	58·2	54·7

	SILICEOUS PHASES							Carbonate Riebeckite Phase	Composite Sample
Sample	42341L	42343L	42344	42345L	42346*	42348L	42349L	42350	42340X
Depth (m)	225·7	226·3	226·7	226·8	227·2	228·3	228·9	229·2	225·2–229·25
Fe_2O_3 %	9·8	2·7	2·9	6·0	22·3	8·3	8·8	13·7	32·3
MnO %	0·16	0·01	0·06	0·03	0·03	0·12	0·54	0·30	0·13
MgO %	4·06	0·06	2·24	1·57	3·98	2·40	3·05	3·16	2·57
CaO %	6·65	0·04	2·81	0·95	0·15	4·73	32·2	21·4	6·58
Na_2O %	0·17	$<$0·01	$<$0·01	0·01	0·01	0·51	0·67	2·36	0·13
K_2O %	0·22	0·06	0·05	0·25	0·20	0·04	0·24	0·12	0·24
Cu ppm	10	5	5	5	12	10	5	10	10
Pb ppm	20	$<$5	55	55	10	15	40	40	40
Zn ppm	10	10	10	13	30	10	10	10	20
Ni ppm	30	15	20	20	25	20	30	20	25
Ba ppm	100	100	200	250	ND	250	300	125	(100)
Sr ppm	20	ND	460	370	ND	30	75	50	20
CO_2	11·1	0·03	4·00	1·10	0·14	6·70	30·5	18·3	8·2
Free C %	0·06	0·04	0·03	0·04	0·02	0·12	0·06	0·07	0·03
P_2O_5	0·13	0·014	0·008	0·020	0·010	0·033	0·14	0·021	0·060
Fe as metal	6·9	1·9	2·0	4·2	15·6	5·8	6·2	9·6	22·6

ND = Not detected

* = Chert-minnesotaite rock

† = In this, and subsequent tables, analyses of CO_2, free C and P_2O_5 by Government Chemical Laboratories

The shales are unusual in their high potassium content. This potassium is not recognizable in thin section except by staining. (A yellow stain is given with sodium cobaltinitrite). The potassium content is comparable with that in shales reported from Minnesota (Weiss, 1954), Scotland (Bowie and others, 1966), Mount Isa (Croxford, 1964-5) and the Rhodesian Copperbelt (Darnley, 1959-60) but exceeds the world Clarke figure by a factor of 2 to 3 (see later discussion).

The non-carbonate carbon also exceeds that suggested by Pettijohn (1957, p. 344) for the average shale by a factor in excess of 3, though the value is much lower than that reported for other black shales e.g. 13.1 per cent in shales at Dry Gap, Georgia (Pettijohn, 1957, p. 362).

The shales contain variable amounts of carbonate. In many cases this is dolomite, but in some samples the carbonate is mainly calcite (e.g. 42306, 42310, 42316, 42332). In all cases magnesium is present in excess of that required for the carbonate mineral. This magnesium represents that present in the phyllosilicates illite and chlorite. Iron is probably present both in the phyllosilicates and in the opaques. Trace elements have higher values than the dolomites with the exception of manganese and barium. The values for Cu, Pb, Ni, V and Zn fall within the ranges suggested by Turekian and Wedepohl (1961), Hawkes and Webb (1962) and Krauskopf (1967). The phosphate is overall slightly higher in the shales than in the dolomites (see Fig. 49) but is not of major significance. Strontium values are very low.

The dolomites proper show relative uniformity over the extent of the core sampled (Fig. 48). There are no major trends apparent except at the bottom near the iron formation where there is an increase in iron, and some depletion of magnesium. An exception occurs at 209.6 m where the dolomite contains appreciable iron and a higher phosphate content. The increase in iron is matched by some depletion of magnesium.

The shales have a more variable composition though whether the differences in composition reflect genuine trends is not certain. A possible trend is that shown in Figure 48 for K_2O.

TRANSITION ZONE

A transition zone is considered to extend between the iron formation and the dolomite unit from 223.0 m to 225.2 m (approximately). This zone contains two bands with high magnetite content at 223.4 m (42337) and 225.2 m (42340B) but is characterized by the relative abundance of carbonate and the presence of high-potassium shales as in the dolomite unit. In the magnetite-rich bands the iron content, expressed as Fe_2O_3, reaches over 55 per cent but even in other layers, compared with the dolomite unit, the overall iron content is high with a minimum value (of Fe_2O_3) of about 5 per cent. Chert with minnesotaite, and ferrostilpnomelane also become evident (223.35 m and 224.85 m) respectively, indicating the close relationship of this phase with the underlying iron formation proper. Compared with the overlying rocks this zone is distinguished by the presence of calcite (and/or siderite) as well as dolomite in the carbonate-rich samples. Alkali metals and the trace elements determined fit well into the pattern of the shale or carbonate facies of the dolomite unit as appropriate, and the trace metal values of the two iron-rich bands are more similar to values in the overlying rocks than they are to the magnetite-rich bands in the iron formation proper.

IRON FORMATION

Examination of the analyses for the various bands of the iron formation reveals the massive inherent variability between adjacent mesobands. For this reason, and for other comparative purposes, a composite taken from the whole of the core from 225.2 m to the end of the core at 229.25 m is presented (42340X). This analysis (the average of duplicate samples) shows moderate to high Fe_2O_3, CaO and MgO values with appreciable carbon dioxide, and low overall concentrations of alkali metals. The trace element content, including the free carbon and the phosphate content, is also low.

The bulk chemistry scarcely reflects the composition of any single band. The magnetite-rich bands show high iron values, but differences in the nature of the associated minor minerals have caused moderate variations in calcium, magnesium and carbon dioxide values. Sodium and potassium are universally low, though there seems to be some tendency for Na_2O values to rise with depth (this is reflected not only in the magnetite-rich phases, but also in the silicate-rich phases). Of interest is the relatively high value of lead in the magnetite-rich phase. Presumably lead (and nickel) can be found in the magnetite. Both lead and nickel are present in lower concentrations in the siliceous phases and the copper and zinc values are very low indeed. Barium and strontium appear very variable and related neither to iron nor to carbonate minerals. The phosphate content of these magnetite-rich phases is quite low.

The composition of the siliceous phases is more variable than that of the magnetite phases, reflecting the changes in mineralogy. There is a variable iron content, mainly in minnesotaite and stilpnomelane, more rarely in magnetite (42346) or riebeckite. There is a very variable carbonate, calcium and magnesium content and both dolomite and calcite co-exist.

Barium is more abundant in this phase than in the magnetite phase, and so, overall, is strontium, though the amount of this element is very variable and it seems to behave independently of any particular mineral. Sodium varies from very low (?absent) to 2.36 per cent Na_2O in phases containing riebeckite.

Potassium values are quite low indicating that K-bearing phyllosilicates are absent. The presence of appreciable magnesium in the chert-minnesotaite phase (227.2 m, 42346) indicates that it might be appropriate to consider the minnesotaite as an iron-rich talc some distance from the end member.

DISCUSSION

IRON FORMATION

It is quite rare to get adequate samples of unmineralized iron formation from the Hamersley Range area which are fresh enough for an analytical evaluation. Such samples as have been analysed have been derived mainly from drill cores, and from the walls of steep-sided or overhanging gorges. Until recently the greater part of the economic interest in the area has lain with the Brockman Iron Formation which occurs stratigraphically above the Marra Mamba Iron Formation in the Hamersley Group of rocks. Between these two iron formations lie (oldest first) of the order of 300 m of varied dolomite (the Wittenoon Dolomite), iron formation and shale (the Mount Sylvia Formation) and further shale, dolomite and chert (the Mount McRae Formation). Within the Brockman Iron Formation the most studied portion has been the Dales Gorge Member. Analyses of the Brockman Iron Formation and the Boolgeeda Iron Formation (which occurs at the top of the Hamersley Group, 100 to 1 000 m above the Brockman Iron Formation) are presented in Trendall and Blockley (1970, p. 134). These authors also present the results of analysis (as composites) of selected mesoband types from the Dales Gorge Member.

The complete analysis 42340X, when compared with the Brockman and Boolgeeda Iron Formations, shows that the iron formation in the Millstream No. 9 drill core contains rather less iron than either of the other two formations. It is also richer in carbon dioxide (i.e. in carbonate content) than most of the samples analysed and reported in Trendall and Blockley (1970, p. 134, 5), though the wide fluctuation of carbon dioxide reported for the various samples may mean that all these iron formations have very variable compositions. The calcium content of 42340X (6.6 per cent CaO) exceeds the published calcium values of the other iron formations by a factor of 2 to 3. Magnesium figures are similar for all analyses. Sodium and potassium values given by Trendall and Blockley for the Dales Gorge Member of the Brockman Iron Formation are essentially similar to the present analysis, but the Joffre Member of the Brockman

Iron Formation, and the Boolgeeda Iron Formation are richer in potassium than either the Dales Gorge Member, or the present iron formation analysis. Trendall and Blockley postulate (1970, p. 138) that the higher potassium values of the Joffre Member and the Boolgeeda Iron Formation may be caused by the presence of sericitic phyllosilicates in these rocks. In the light of the mineralogy of the shales of the dolomite unit it appears possible that their higher K_2O values may be represented by fine-grained feldspar.

The phosphorus content of this iron formation is lower than that of the Dales Gorge Member and the Boolgeeda Iron Formation. Iron ore from the Marra Mamba Iron Formation is known to be lower in P_2O_5 than that from the Brockman Iron Formation (Mining Magazine, Aug. 1974, p. 87); it appears that this is a fundamental property of the Marra Mamba Iron Formation, and may assist in the stratigraphic siting of the iron formation investigated here.

Trendall and Blockley did not publish any analyses of magnetite-rich bands though they have given various complete and partial analyses (1970, p. 139 ff) of various individual mesoband types. Their analyses are a mixture of composites of mesoband types and individual mesobands, which collectively can be grouped into composites. Their analyses contrast with the analyses presented here which are all from single mesobands within the core. There are widely differing proportions of carbon dioxide, and its related cations, but comparable analyses can be found in the Brockman Iron Formation.

Trendall and Blockley present no trace element determinations.

The iron formation composite is compared with published analyses of other magnetite-rich iron formations in Tables 20 (major elements) and 21 (trace elements). This core of iron formation contains less iron than most other iron formations and more calcium. It contains slightly more carbon dioxide than most of the other iron formations (the Temiscamie Iron Formation being a notable exception). The iron contents are only slightly lower than values reported for the Biwabik Iron Formation and the Pongola beds. By contrast, as noted during the comparison with other West Australian iron formations, the calcium values are appreciably higher, by factors varying between 1.5 and 3. The number of analyses is limited and the inferences drawn are therefore somewhat tentative, but it does appear that this iron formation is unique in its calcium content (in magnetite facies rocks). Values of other major elements are comparable with those of other deposits. Some analysts do not report values for Na_2O and K_2O; whether these oxides were not determined or not detected is not always clear. The phosphorus value is slightly lower than most of the other analyses.

Very few trace element values appear in the literature and Table 21 shows those which have been found. However, even these determinations are scarcely comparable since most of them have been derived from rocks which contain either dominant, or, at least, appreciable hematite. The nickel and barium values of the examined iron formation are comparable with the other published figures, however copper, zinc and strontium are possibly low. No firm conclusions can be inferred from this comparison.

The origins of iron formation are discussed by Trendall and Blockley (1970, chapter 9) and no evidence is revealed by the present chemical study to disprove their general hypotheses.

THE TRANSITION ZONE

Transition zones from iron formation to adjoining rocks are not well recorded in the literature, possibly because the main interest has lain in the potentialities of the iron formations for the location of iron ore bodies and possibly because near-surface weathering and alteration has masked many of the effects.

It is clear, however, that in this drill core there is an approximate 2.2 m band of overlap between the iron formation below and the dolomite unit above.

The iron content remains high but the dominantly siliceous phase of the iron formation is replaced by carbonate (with minor shale). Apart from their iron values, the retention of a little free silica (e.g. at 223.35 m 42336) and the presence of calcite with dolomite, the remainder of the lithology is like that of the overlying dolomite unit. However, the last traces of the iron formation may be weakly represented by sample 42323 at 209.6 m. This specimen contains much higher iron than the remaining samples from the dolomite suite.

THE DOLOMITE UNIT

The two major items of interest are the presence of high potassium in the shale layers and the high manganese in the dolomite proper.

Average shale contains 3 to 4 per cent K_20 (Krauskopf, 1967) but high potassium shales are not particularly rare. Examples of such shales are noted by Berg (1952) in Minnesota and Wisconsin; Bowie and others (1966), in Scotland; Croxford (1964-5), at Mount Isa; Darnley (1959-60), in Rhodesia; Granger and Raup (1964), in Arizona; Schmitt (1924) and Weiss (1954) in Minnesota; Shearer (1918), in Georgia; and Tester and Atwater (1934) in various places. Trendall and Blockley (1970, p. 148) record the presence of high potassium shales occurring in the Brockman Iron Formation but do not remark on the high values.

The above authors are divided about the origin of the potassium in these shales. Croxford (1964-65) reports the presence of volcanic shards in shales at Mount Isa, and a mineralogy for the rock of K-feldspar 70-80 per cent, ferroan dolomite 10 per cent, quartz 5 per cent, accessories 1-2 per cent. The K-feldspar has the composition $Or_{98.3}$ $Ab_{1.7}$ An_0 and is believed by Croxford to have once been a low-temperature orthoclase phase (?adularia), though it is largely microcline in its present state. Croxford considered that the potassium was derived from connate water and reacted with volcanic glass to form the orthoclase. He reports the highest values of all authors for K_2O in shales, 12.45 to 13.42 per cent in four samples.

Darnley (1959-60) showed that argillites of the Roan sediments of Rhodesia contained from about 6 per cent K_20 to over 11 per cent K_20. In some cases the potassium was present in biotite/sericite, in others in K-feldspar. He believed the origin of this potassium to be metasomatic.

The greater part of the remaining authors believe that K-feldspar has ultimately formed from clay minerals following collection of potassium from sea or interstitial water by the clays. A sequence of montmorillonite-illite (with chlorite)-K-feldspar is postulated. The mechanisms of K-fixation by montmorillonite in alkaline environments have been reasonably established (Reitemeier, 1951; Nanz, 1953; Grim and Johns, 1954, and Whitehouse and McCarter, 1958—reference cited by Bowie and others, 1966) and are believed to occur by diagenesis. In the process sodium is given up to surrounding waters/solutions. Berg (1952) and Gruner and Thiel (1937) directly, and Bowie and others (1966) indirectly, argue the additional step to K-feldspar without demonstrating the mechanism. The origin of the potassium remains a problem.

Conway (1943) believed that the rate of removal of potassium from the ocean reached a peak in or around the late Precambrian. Many of the potassic shales and rocks cited above are from this general period. Granger and Raup (1964) identify K-rich siltstones of the Dripping Springs Quartzite with 6 to 7 per cent low-sodium K-feldspar as Proterozoic. Berg's (1952) illustration is from the Upper Cambrian Franconia Formation. The Minnesota specimens (Weiss 1954; Schmitt, 1924) are Ordovician. The Scottish "fucoid" beds are Cambrian (Bowie and others, 1966). The Mount Isa rocks are Lower Proterozoic. The present sediments are Lower Proterozoic. There is thus some tenuous support for Conway, however, the origin of the potassium remains unclear.

Trendall and Blockley (1970, p. 112) illustrate in photomicrographs the presence of volcanic shards in the shales of the Dales Gorge Member of the Brockman Iron Formation. Petrological

(7)—46009

TABLE 19. SUMMARY VALUES FOR THE TWO MAIN PHASES IN THE DOLOMITE UNIT, AND FOR MAGNETITE-RICH MESOBANDS IN THE IRON FORMATION

	Dolomite (n = 14)		Shale (n = 17)		Magnetite-Rich Bands A(n = 7)		Magnetite-Rich Bands B(n = 9)	
	χ	σ	χ	σ	χ	σ	χ	σ
Fe_2O_3 %	2·89	2·95	2·13	0·90	77·40	4·90	74·04	8·50
MnO %	0·95	0·13	0·11	0·08	0·02	0·01	0·09	0·15
MgO %	19·06	1·81	4·21	1·59	0·73	0·21	1·51	1·59
CaO %	27·71	1·35	2·96	1·68	0·79	0·46	2·48	4·26
Na_2O %	0·04	0·02	0·08	0·03	0·21	0·11	0·17	0·12
K_2O %	0·50	0·24	8·74	1·64	0·27	0·04	0·34	0·15
Cu ppm	19	6	68	18	9	5	12	8
Pb ppm	22	6	21	8	60	5	51	18
Zn ppm	41	31	161	63	18	10	21	10
Ni ppm	40	30	135	39	41	9	45	12
V ppm	17	25	82	44	....	....	....	....
Ba ppm	3 980	710	680	430	64	81	294	551
Sr ppm	15	5	11	6	23	34	22	29
CO_2 %	44·01	2·89	3·78	2·33	1·08	0·75	5·28	8·98
Free C %	0·23	0·26	2·30	0·73	0·04	0·02	0·14	0·25
P_2O_5 %	0·04	0·08	0·09	0·03	0·05	0·01	0·05	0·01

χ = mean; σ = standard deviation;
n = number of samples

N.B. Samples from the transition zone 223·0 to 225·2 m have been excluded from the calculations because of their evidently changed nature, except that the two magnetite bands in the transition zone have been included in the calculation for the last two columns

TABLE 20. COMPARISON OF THE MAJOR ELEMENT CHEMISTRY OF THE IRON FORMATION WITH OTHER PUBLISHED VALUES (NON-AUSTRALIAN)

%	1	2	3	4	5	6	7	8	9	10	11
SiO_2		34·44	35·86	45·66	39·50	22·70	50·90	46·40	40·71	41·83	43·28
Al_2O_3		0·85	1·57	0·28	0·44	0·31	6·25	0·90	2·32	0·92	0·08
Fe_2O_3	32·3	30·54	38·56	19·16	29·21	22·07	20·00	18·70	21·04	33·21	36·14
FeO	*	22·06	20·26	21·28	18·51	23·20	14·40	19·71	20·10	14·66	16·54
MgO	2·57	2·30	1·74	2·73	2·00	3·88	2·00	2·98	3·15	1·96	1·33
CaO	6·58	1·72	0·51	1·04	2·71	4·49	0·85	1·60	2·63	1·90	0·62
Na_2O	0·13	0·0	}0·02 (Na₂O + K₂O)					0·04	1·05		0·13
K_2O	0·24	0·13						0·13	0·57		trace
H_2O^+		0·44	0·60	1·54			}1·30 (H_2O^+ + H_2O^-)	1·60	0·91		0·09
H_2O^-		0·17	0·06					0·32	0·07		
TiO_2		0·02	0·04		0·040	0·014	0·30	0·04	0·12	0·21	0·22
P_2O_5	0·060	0·07	0·14	0·085			0·05		0·25	0·072	0·14
MnO	0·13	0·21	0·16		0·12	1·06	1·85	0·63	0·29	0·07	0·04
CO_2	8·2	7·36	0·60	7·54	6·22	21·88	1·10	6·90	6·56	0·12	1·84 (L.O.I.)
C	0·03	0·04		0·12	0·017	0·016		0·17			
Fe (total)	22·6							28·36		34·59	38·15

* Iron expressed as Fe_2O_3; FeO not determined

L.O.I. indicates loss on ignition

Blank spaces indicate lack of (published) analyses

1. Iron formation. Composite 42340X, this study
2. Magnetite iron-formation. Ironwood iron-formation; quoted in James, 1966, p.w21
3. Magnetite-quartz rock. Sakasogan (Krivoi Rog) Series, Ukraine ; quoted in James, 1966, p.w. 21.
4. Magnetite chert. Biwabik Iron Formation, Mesabi, Minnesota; quoted in James, 1966, p.w21
5. & 6. Magnetite chert rock, Temiscamie Iron Formation, Quebec; quoted in James, 1966, p.w21
7. Magnetite-siderite slate. Pongola beds, Swaziland System, southeast Transvaal; quoted in James, 1966, p.w21
8. Weighted mean, Biwabik Iron-formation, Mesabi, Minnesota. Bayley and James, 1973, p.942
9. Kuruman Iron Formation, S. Africa.Average of nine analyses. Quoted in Beukes, 1973, p.989
10. Magnetite quartzite, Kursk Magnetic Anomaly, USSR. Plaksenko and others, 1973, p.92
11. Magnetite quartzite, Tarikhan deposit, Aldan Shield USSR. Vorona and others, 1973, p.246

TABLE 21. COMPARISON OF TRACE ELEMENT COMPOSITIONS OF THE IRON FORMATION WITH OTHER PUBLISHED TRACE ELEMENT DATA

	1	2	3	4	5
Cu ppm	10	34	22(6–50)	*(6–8)	30–50
Pb ppm	40				30–80
Zn ppm	20				40–60
Ni ppm	25	23	21(7–170)	*(10–20)	10–20
Ba ppm	100	53	179(34–1000)	27(10–46)	
Sr ppm	20	72			

1. Iron formation; present study. Composite 42340X
2. Magnetite quartzite, Kursk Magnetic Anomaly; Plaksenko and others, 1973. p.93
3. Itabirite (hematite-rich), Casa de Pedra deposit, Minas Gerais, Brazil; Dorr 1973, p.1012. Values given are means, figures in brackets the range. Eighty-nine samples were analysed
4. Dolomite Itabirite; Dorr, 1973, p.1012. Figures have same significance as item 3. Six samples analysed. * Mean values not given
5. Iron Formation (Hematite, magnetite, martite) Bel Park Dala, Kazakhstan; Alexandrov, 1973, p.1050. Spectrographic analyses—ranges only

examination of the present suite of samples has revealed no traces of shards, however, the possibility of a volcanic source cannot be ruled out. The shales are relatively rich in carbon (or hydrocarbons) and some features in the adjoining dolomites suggest the presence of fossil material. It is possible that the shale bands represent "sudden death" sedimentation with volcanic activity not only contributing debris but also killing the then living organisms. The junctions of shale with dolomite are commonly sharp, if somewhat undulatory, and the shales vary from very thin (1-5 mm) to thin (1-2 cm), indicating the abrupt changes which took place in what must have been a relatively short period of time. It is possible that carbonate sedimentation took place at a uniform rate. The sudden bursts of clastic material represented by the shales may have produced local, more rapid deposition. The carbonate content of the shales may therefore reflect carbonate precipitation at a standard rate, overprinted (or diluted) by the clastic components. The low sodium content precludes against the feldspar being normal igneous feldspar. The identification of adularia (by X-ray diffraction) in the present investigation and the absence of visible detrital K-feldspar suggest that at least the greater part of the K-feldspar in these shales is of authigenic origin with a volcanic (tuffaceous) component and, possibly, a sea water component.

Turning to the dolomitic rock proper, the main points of interest are the consistent overall composition and the presence of high manganese values throughout the entire length of the column analysed. The high magnesium content renders the dolomite in this area unsuitable as a metallurgical flux.

The high manganese content is of greater interest, for the levels are high enough for the rock to have potential as a source of manganese ores. The lateral equivalent of the Wittenoom Dolomite in the Oakover River Basin is the Carawine Dolomite, which is known to be appreciably manganiferous (de la Hunty 1963, 1965; Campana and others, 1972), and acts as host ("enclosing rock", Campana and others' terminology) for manganese mineralization—Woodie Woodie, Ripon Hills. The origins of this mineralization are not absolutely clear, though, ultimately, the manganese is believed to have been derived from the Carawine Dolomite (de la Hunty, 1963; A. Hickman, pers. comm.). Rocks of comparable age and lithology in the Kuruman District of South Africa are also manganiferous and are the hosts of manganese mineralization (Frankel, 1958). In the dolomite unit the manganese is evidently an inherent feature of the rock as its close relationship with calcium and magnesium must mean that the manganese is a component of the carbonate. It was therefore present at or before the crystallization of the dolomite. A comparable situation, with comparable manganese values, occurs in the "deep Bangombé" borehole in the manganiferous deposit of Moanda, Gabon (Weber, 1973).

It was stated earlier that certain relict features in the dolomite and in the transition zone are reminiscent of fossil material. Trendall and Blockley (1970, p. 85) note that algal structures have been recognized in the Carawine Dolomite at Woodie Woodie. If the features in the rocks of the Millstream core are demonstrated to be of organic origin, they will be among the few known fossils of this age from the Hamersley area.

A major problem is that the greater part of the minerals have been transformed by diagenesis, and very little non-recrystallized material has been recognized. Evidence of recrystallization and diagenesis is found in the rhombic growth of dolomite (and siderite), the presence of abundant stylolites at certain intervals, the presence of authigenic feldspars, the random growth of riebeckite and the late development of pyrite. Other features include the infilling of apparent compaction cracks, the growth of carbonate grains across, and including, trains of opaque grains and late stage veining by dolomite and, rarely, quartz. Not all these features were noted in any one specimen but there is no reason to exclude any part of the sequence from the recrystallization process.

Original features of the rock are believed to include primary disposition of opaques, particularly the carbonaceous opaques, and the intraformational breccias which, though not sampled, are present near the top of the column.

There is no evidence from this core to show whether the rock before recrystallization was dolomitic or not. The presence of calcite within the shales suggests that calcite might have been the primary carbonate, though the reverse has been postulated by Trendall and Blockley for the Brockman Iron Formation. These authors (1970, p. 129) consider that calcite which is associated with some of the shales is secondary.

Chemical conditions, since diagenesis at least, have been reducing as is shown by the retention of the organic carbon, and by the presence of pyrite and magnetite. The presence of intraformational breccias, of varying thicknesses of shale, and of possible organic, ?planktonic and algal remains, suggests a shallow water environment of deposition possibly with subsidence occurring at a rate corresponding with the rate of deposition. The lack of large clastic grains indicates generally quiet conditions with a general absence of detritus.

CONCLUSIONS

This study has consisted of an investigation of the transition from an iron formation unit to an overlying dolomite unit of the Wittenoom Dolomite.

The main features shown by the study are:

(i) The tremendous variability of composition of the various mesobands of the iron formation.

(ii) The close similarity of composition of the iron formation to other magnetite-rich, Precambrian banded iron formations throughout the world. The main differences lie not in the mineralogy, but in the proportion of iron, which at 22.6 per cent Fe is lower and in the proportion of calcium (6.6 per cent CaO) which is higher than in most other iron formations.

(iii) The presence of a distinct transition zone between the iron formation and the dolomite unit has been recognized. This zone, which is approximately 2.2 m thick, has, for the most part, the dolomite unit facies of dolomite with shales, but additionally contains two magnetite-rich bands and rare chert with minnesotaite. This zone is richer in iron and is also probably richer in calcium than the overlying part of the Wittenoom Dolomite.

(iv) The lower part of the dolomite unit consists of rather featureless dolomite punctuated by thin (2 mm-2 cm) bands of shale. The dolomite is dark in colour and contains visible oily hydrocarbons at 179.5 m. Contacts between shale and dolomite are normally abrupt though much of the dolomite has shaly partings.

(v) The dolomite of the dolomite unit approximates to the theoretical composition for the mineral dolomite with some substitution of manganese for magnesium. The manganese content is high compared with normal dolomite (averaging 0.95 per cent MnO) but is similar to that in dolomites of similar age in the Oakover River area, W.A., in Gabon and in South Africa.

(vi) The shales in the dolomite unit are abnormally high in potassium which is present as adularia, a low-sodium, K-feldspar. This feldspar is believed to have developed authigenically from illite. The origin of the potassium is unknown, but a tuffaceous source is suspected.

(vii) The conditions of formation of the various rocks/phases are uncertain because of extensive diagenesis and recrystallization. However it appears likely that all phases, except the shales, were once chemical precipitates. Shallow water sedimentation is suggested and the reducing conditions may have developed concurrently with diagenesis. The shales are considered to be transformed products of vulcanism (volcanic ash) possibly with other clastic components.

ACKNOWLEDGEMENTS

The help and advice of members of the Government Chemical Laboratories, in particular Messrs D. Burns, M. Costello (chemical analysis) and R. Clarke and L. Bastian (X-ray diffraction) is gratefully acknowledged.

REFERENCES

Alexandrov, E. A., 1973, The Precambrian iron formations of the Soviet Union: Econ. Geol. v. 68, no. 7, p. 1035-62.

Bayley, R. W., and James, H. L., 1973, Precambrian iron formations of the United States: Econ. Geol. v. 68, no. 7, p. 934-959.

Berg, R. R., 1952, Feldspathised sandstone: Jour. Sed. Petrol. v. 22, p. 221-223.

Beukes, N. J., 1973, Precambrian iron formations of Southern Africa: Econ. Geol. v. 68, no. 7, p. 960-1004.

Bowie, S. H. N., Dawson, J., Gallagher, M. J., and Ostle, D., 1966, Potassium-rich shales in the Cambrian of northwest Scotland: Inst. Mining and Metall., Lond., Trans., v. 75, Bull. 714, p. 125-145.

Campana, B., Cocquio, S., and Jaques, J.-M., 1972, Les gîtes de ferro-manganèse des Ripon Hills (Est Pilbara, Australia Occidentale): Bull. Ver. Schwerz. Petrol.-Geol. u.-lng v. 39, no. 95, p. 42-63.

Conway, E. J., 1943, The chemical evolution of the ocean: Royal Irish Acad. Proc. v. 48B, no. 9, p. 161.

Croxford, N. J. W., 1964-5, Origin and significance of volcanic potash-rich rocks from Mt. Isa: Inst. Mining and Metall., Lond., Trans., v. 74, p. 33-43.

Darnley, A. G., 1959-60, Petrology of some Rhodesian Copperbelt orebodies and associated rocks: Inst. Mining and Metall., Lond., Trans., v. 69, p. 137-73. Discussion p. 371-398, 540-569, 699-719.

Davy, R., 1975, A geochemical investigation of part of the Millstream no. 9 diamond drill core; methods and results: West. Australia Geol. Survey Geochemical Rept. no. 1 (unpublished).

Deer, W. A., Howie, R. A., and Zussman, J., 1962, Rock-forming minerals: New York, Wiley, (5 vol.).

de la Hunty, L. E., 1963, The geology of the manganese deposits of Western Australia: West. Australia Geol. Survey Bull. 116, 122 p.

——— 1965, Investigation of manganese deposits in the Mt. Sydney-Woodie Woodie area, Pilbara Goldfield: West. Australia Geol. Survey Ann. Rept. 1964, p. 45-49.

Dorr, J. Van-n., II, 1973, Iron formation in South America: Econ. Geol. v. 68, no. 7, p. 1005-1022.

Frankel, J. J., 1958, Manganese ores from the Kuruman district, Cape Province, South Africa: Econ. Geol. v. 53, no. 5, p. 577-597.

Gruner, J. W., and Thiel, G. A., 1937, The occurrence of fine-grained authigenic feldspar in shales and silts: Am. Mineralogist v. 22, p. 842-6.

Granger, H. C., and Raup, R. B., 1964, Stratigraphy of the Dripping Spring Quartzite, southeastern Arizona: U.S. Geol. Survey Bull. 1168.

Grim, R. E., and Johns, W. D., 1954, Clay mineral investigation of sediments in the northern Gulf of Mexico: National Academy Sci., Washington, D.C., National Research Council pub. 327, p. 81-103.

Hawkes, H. E., and Webb, J. S., 1962, Geochemistry in mineral exploration: New York, Harper and Row, 416 p.

James, H. L., 1966, Geochemistry of the iron-rich sedimentary rocks: *in* Fleischer, M., (Ed.) "Data of Geochemistry", 6th edn., U.S. Geol. Survey. Prof. Paper 440-W.

Krauskopf, K. B., 1967, Introduction to Geochemistry: New York, McGraw-Hill, 721 p.

Kriewaldt, M. J. B., and Ryan, G. R., 1967, Pyramid, W.A.: West. Australia Geol. Survey 1 : 250 000 Geol. Series Explan. Notes.

MacLeod, W. N., 1966, The geology and iron deposits of the Hamersley Range area, Western Australia: West. Australia Geol. Survey Bull. 117.

Nanz, R. H. (Jr.)., 1953, Chemical composition of Precambrian slates, with notes on the geochemical evolution of lutites: Jour. Geol. v. 61, p. 51-64.

Pettijohn, F. J., 1957, Sedimentary rocks: New York, Harper and Row, 718 p.

Plaksenko, N. A., Koval, I. K., and Shchogolev, I. N., 1973, Precambrian ferruginous-siliceous formations associated with the Kursk Magnetic Anomaly: *in* Genesis of Precambrian iron and manganese deposits, Unesco, Proc. Kiev Symp. 1970, p. 89-103.

Reitemeier, R. F., 1951, The chemistry of soil potassium: *in* Advances in Agronomy, New York, Academic Press, v. 3, p. 113-164.

Schmitt, H. A., 1924, Possible potash production from Minnesota shale: Econ. Geol. v. 19, p. 72-83.

Shearer, H. K., 1918, The slate deposits of Georgia: Georgia Geol. Survey Bull. no. 34.

Tester, A. C., and Atwater, G. I., 1934, The occurrence of authigenic feldspars in sediments: Jour. Sed. Petrol. v. 4, p. 23-31.

Trendall, A. F., and Blockley, J. G., 1970, The iron formations of the Precambrian Hamersley Group, Western Australia: West. Australia Geol. Survey Bull. 119.

Turekian, K. K., and Wedepohl, K. H., 1961, Distribution of the elements in some major units of the earth's crust: Geol. Soc. America Bull. v. 72, p. 175-192.

Vorona, I. D., Kravchenko, V. M., Pervago, V. A., and Frumkin, I. M., 1973, Precambrian ferruginous formations of the Aldan shield: *in* Genesis of Precambrian iron and manganese deposits, Unesco, Proc. Kiev Symp. 1970, p. 243-247.

Weber, F., 1973, Genesis and supergene evolution of the Precambrian sedimentary manganese deposits at Moanda (Gabon): *in* Genesis of Precambrian iron and manganese deposits, Unesco, Proc. Kiev Symp., 1970, p. 307-322.

Weiss, M. P., 1954, Feldspathised shale from Minnesota: Jour. Sed. Petrol. v. 24, p. 270-274.

Whitehouse, U. G., and McCarter, R. S., Diagenetic modification of clay mineral types in artificial sea water: National Academy Sci., Washington, D.C., National Research Council pub. 566, p. 81-119.

THE NULLAGINE METEORITE

by J. D. Lewis

ABSTRACT

A small meteorite recovered in 1973 near the township of Nullagine (21° 52′ S, 120° 07′ E), Western Australia, weighed 102 g and is an almost complete stone. The Nullagine meteorite is a moderately metamorphosed bronzite chondrite and contains rare chromite chondrules. The meteorite contains approximately 11 per cent iron and 8 per cent sulphides. Neumann bands are prominent in the iron and some of the sulphide has been remobilized by shock veins.

INTRODUCTION

During the regional mapping of the Nullagine Sheet in 1973 by the Geological Survey of W.A., a small stony meteorite was recovered by Mr. R. Thom. It was found 5 km north of Nullagine township, by the side of the Great Northern Highway, (approx: 21° 52′ S, 120° 07′ E), in the Pilbara district of N.W. Western Australia. A brief search of the area did not reveal further finds or evidence of an impact crater in the surrounding surface rubble of weathered Archean sediments.

The meteorite has been designated the Nullagine meteorite after the township near which it was found. The name has been approved by West Australian Meteorite Committee.

GENERAL DESCRIPTION AND MORPHOLOGY

The meteorite, as collected, weighed 102.25 g and apart from a chip on one corner is a complete stone (Fig. 50A and B). The stone is irregular in shape with maximum dimensions of about 5 x 4 x 3 cms and a "kite" shaped cross section. A very thin (ca. 0.1 mm) matt brown oxidised fusion crust covers the whole meteorite except for the small broken section which reveals an oxidised chondritic core. Depressions on two of the larger faces probably represent the original shape of the stone rather than regmaglypts. No features due to orientation in flight can be seen.

STRUCTURE AND PETROGRAPHY

On a cut surface the chondritic nature of the meteorite is obscured by a general oxidation which extends uniformly throughout the mass. Metal and sulphide particles are visible however, and a thin section reveals that oxidation has not extended beyond formation of a thin film of hydrated iron oxides on the original minerals.

Modal analysis of a polished mount of the Nullagine meteorite gave the following analysis:

Mineral	*Per cent*
Silicates	77.6
Kamacite	11.1
Troilite	6.0
Taenite	2.2
Chromite	1.1
"Iron oxides"	2.0

The silicate phase is predominantly chondritic with probably only 10 per cent as interstitial olivine and pyroxene grains. The opaque minerals form a large part of the interchondrule material but troilite is also found marginally in many chondrules and a few chondrules consists predominantly of chromite. "Iron oxides" noted in the modal analysis are the weathered products of the kamacite and troilite; their probable composition is goethite. They could probably be distributed proportionately to determine the original metal and sulphide content of the unweathered meteorite.

Chondrules

A wide variety of chondrules is present (Fig. 50E), ranging in size from about 0.2 mm to 2 mm in diameter. The chondrules are commonly spherical or ovoid but some are polygonal and perhaps one third of the chondrules are broken.

Fine-grained excentroradial orthopyroxene chondrules are the most prominent type and include the largest and the smallest chondrules. These chondrules are typically spherical and the degree of crystallization varies from devitrified glass through feathery fans of orthopyroxene to stout radiating prisms of orthopyroxene. Variations include chondrules which crystalized about a small central euhedral pyroxene crystal and a few containing small acicular orthopyroxene crystals arranged to form a "spherulite".

Porphyritic chondrules, containing euhedral to subhedral olivine and orthopyroxene in a devitrified groundmass, are the commonest type. Individual olivine crystals vary from about 0.01 mm to 1 mm long. Most porphyritic chondrules contain only olivine crystals and the proportion of olivine varies from chondrules of packed anhedral olivine grains with minimal interstitial material to those in which the olivines are euhedral and the devitrified groundmass contains abundant needles of orthopyroxene.

Few porphyritic chondrules contain only orthopyroxene but there are a number in which orthopyroxene predominates, either as euhedral prisms 0.2-0.5 mm long or as more acicular prisms up to 1 mm long (Fig. 50D).

A distinctive type of porphyritic chondrule are those which contain a high proportion of interstitial devitrified glass. In these chondrules olivine may form small outline skeletal crystals only, or skeletal additions to earlier formed euhedral olivines, while orthopyroxene forms randomly orientated, small, ghost crystals. Occasionally small skeletal olivines have nucleated on the surface of the chondrules and the crystallites are directed inwards (Fig. 50D). The textures shown by these chondrules are probably quench textures but with cooling taking place more rapidly than for the barred chondrules.

Barred chondrules are not uncommon in the Nullagine meteorite but the most distinctive form (Fig. 50E), consisting of a small number of broad parallel olivine bars in optical continuity with a granular olivine rim, is the least common. In the example illustrated the interstitial material consists of fine grained acicular needles of orthopyroxene. More commonly the barred olivine chrondrules are polygonal and consist of one or more sets of narrow olivine plates, with up to 30 plates per set and no rim (Fig. 50C). Despite the apparent regularity of the arrangement of the sets of olivine plates, Dodd and Calef (1971) have shown that the olivines are probably randomly orientated rather than twinned.

Barred chondrules of orthopyroxene are also found although some are probably fortuitous sections through coarsely crystaline excentroradial chondrules. Olivine bars can also be seen traversing some orthopyroxene rich chondrules and in a few there appear to be alternate bars of olivine and orthopyroxene, sometimes on such a fine scale that the chondrule appears to be an excentroradial chondrule of olivine.

As an intermediate type between the barred and porphyritic chondrules many chondrules contain individual, large porphyritic olivines which have grown from a skeletal barred crystal and now enclose small blebs and trains of devitrified glass.

Chromite rich chondrules will be described later but mention must be made of a few small chondrules which contain diopside. The two such chondrules observed are small, about 0.2 mm across, polygonal and contain a few acicular diopside crystals in a devitrified glassy matrix. Diopside is also plentiful however as an exsolution product of orthopyroxene where it occurs most commonly as marginal lamellae parallel to the 100 polysynthetic twinning. Less well defined lamellae and zones of diopside are also present internally in some of the larger orthopyroxene crystals. Exsolution blebs of diopside are common in the fine-grained excentroradial chondrules.

The orthopyroxene of the Nullagine meteorite is commonly homogeneous and has straight extinction but a few crystals show well defined polysynthetic twinning and a small extinction angle, indicating inversion from clino-bronzite (Binns 1970). Frequently the homogenization is incomplete and the crystal has the appearance of a strained orthopyroxene.

Small low relief and low birefringance patches within the groundmass of some chondrules are probably plagioclase but nowhere have they developed into well shaped crystals.

Opaque Minerals.

Kamacite and troilite are the principal opaque minerals of the Nullagine meteorite and together they constitute more than half of the interchondrule mesostasis. Both form large cuspate grains up to 1 mm across, and are moulded onto the chondrules and interstitial silicates.

Throughout most of the meteorite the individual grains of kamacite and troilite are single crystals but within a few millimetres of the fusion crust the grains have been partly or completely recrystallized to an aggregate of small equiaxed crystals usually less than 0.1 mm across. Troilite has always been more completely recrystallized than adjacent kamacite grains. Except near the fusion crust kamacite shows well developed Neumann bands (Fig. 51E) and some of the troilite shows a strained extinction.

Kamacite is almost entirely moulded onto the chrondules but troilite also occurs as small spherical droplets in the marginal parts of chondrules and occasionally as small droplets within chondrules.

Kamacite and troilite are never intergrown in the Nullagine meteorite but occasionally a large subhedral crystal of troilite is enclosed by kamacite. Taenite is only present to the extent of 2 per cent and forms small irregular grains often intergrown with troilite (Fig. 51C). More rarely taenite is found in association with kamacite. Etch patterns indicate a high nickel content for the taenite. Some taenite crystals have a spongy internal structure (Fig. 51D) which appears to be a myrmekitic style intergrowth between high and low nickel taenite.

According to Ramdohr (1973) chromite is the most variable mineral in stoney meteorites. This is true of the Nullagine meteorite where chromite can be found as individual large subhedral crystals, up to 0.1 mm across, as anhedral interstitial crystals, as irregular aggregates and as a major or minor component of chondrules. Two generations of chromite are probably present. Early formed chromite is found as small euhedral crystals in chondrules and possibly in the irregular aggregates.

A later chromite phase is moulded on the silicates of the interstitial material but is euhedral towards kamacite and troilite. This later phase is the commonest and appears to be preferentially associated with troilite and taenite (Fig. 51C). Being a brittle mineral chromite is easily fractured and several crystals now consist of aggregates of shard-like fragments.

Chromite aggregates range up to about 0.2 mm across, are irregularly shaped and appear to consist of a number of small octahedra welded together. Centrally the chromite has often aggregated to a degree that excludes silicates but marginally small laths of silicate minerals form a considerable proportion of the aggregate.

In chondrules chromite varies from a few small euhedral grains in a normal chondrule, to chondrules which consist principally of chromite. Scattered chromite grains in chondrules are fairly common, making up 20 per cent in one example. Chromite rich chondrules, however, are small, usually about 0.2 mm across, and contain about 60-70 per cent chromite. In the few samples located in the Nullagine meteorite the chromite forms predominantly as octahedra which appear to have matted together, but occasionally the crystals are prismatic (Fig. 51A). The silicate material in such chondrules is, according to Ramdohr (1967), mainly plagioclase but in the Nullagine meteorite it has not been identified. One chromite chondrule contains many small blebs of troilite (Fig. 51B).

Metamorphism.

Both thermal and shock metamorphic effects are visible in the meteorite. Thermal metamorphism is evidenced by the turbidity of former glassy portions of the meteorite, the almost complete elimination of low-Ca clinopyroxene and the presence of a little interstitial plagioclase. The chondrules, however, are strongly delineated which suggests that the temperature of metamorphism did not reach extreme values (van Schmuss and Wood 1967).

Low grade shock metamorphism is shown by the presence of strained extinction and, more rarely, twinning in the troilite and Neumann bands in the kamacite (Fig. 51E). Strain in the troilite is not common but Neumann bands are almost universal in the iron phase except near the fusion crust; their presence indicates that the meteorite was subjected to high energy shock after it had cooled down (Uhlig 1955). A few shock veins are also present and these usually contain a dark glass, crystal fragments and sometimes anastomosing veins of secondary troilite (Fig. 51E). Iron is only rarely found in these shock veins but adjacent to the vein it is sometimes recrystallized to a very fine-grained polycrystalline aggregate which truncates the Neumann bands in the main mass.

The history of the Nullagine meteorite, as revealed by its metamorphism, indicates that the original mass was first metamorphosed at temperatures above 550° C (van Schmuss and Wood 1967) and probably near 900° C (Binns 1967). At a temperature probably below 300° C (Uhlig 1955) the mass exploded, causing the shock metamorphism and the angular shape of the present specimen. Passage through the atmosphere then gave rise to the fusion crust and marginal recrystallization of the metal and sulphide fractions.

CLASSIFICATION

Olivine from the Nullagine meteorite, determined by the Weissenberg X-ray method of Pryce (1970), has the following cell dimensions: $a = 4.767 \pm 0.002$ Å, $b = 10.249 \pm 0.003$ Å, $c = 6.001 \pm 0.0025$ Å which correspond to a composition of Fa 19 ± 1. The meteorite is therefore an H group or olivine bronzite chrondrite according to the data of van Schmuss and Wood (1967, p. 750, table 1). Petrographically the Nullagine meteorite falls in either type 4 or 5 of the above author's classification. The presence of turbid glass in some chondrules and the well defined outlines of the chondrules suggest type 4, whereas the structural state of the low-Ca pyroxene and the recrystallized nature of the matrix suggest type 5.

Using the classification of Binns (1967) the presence of diopside in association with the orthopyroxene indicates an olivine bronzite chondrite of the transitional group.

The Nullagine meteorite is, then, an H5 or transitional group olivine-bronzite chondrite.

ACKNOWLEDGEMENTS

The author would like to thank Dr. R. A. Binns of the University of Western Australia for helpful discussion and M. Pryce of the Government Chemical Laboratories for determination of the olivine.

Figure 50. (opposite)
A and B. Two views of the Nullagine meteorite.
C. Small barred olivine chondrule.
D. Porphyritic chondrule containing only orthopyroxene (upper), and spherical, glassy chondrule with small skeletal olivines nucleated on the surface of the chondrule (lower).
E. Photomicrograph showing the variety of chondrules present in the Nullagine meteorite.

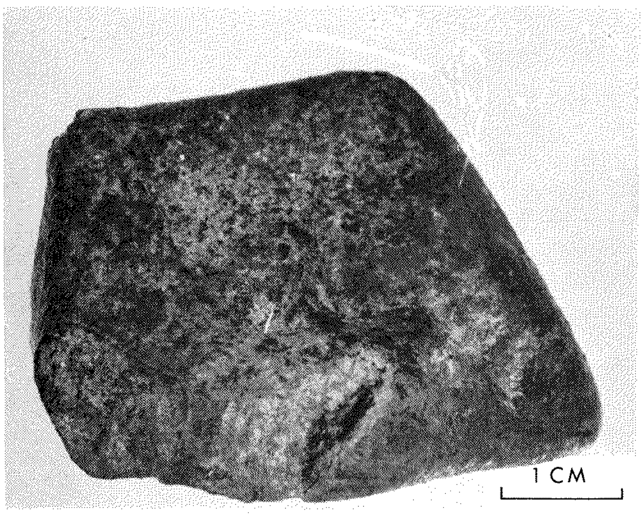

A

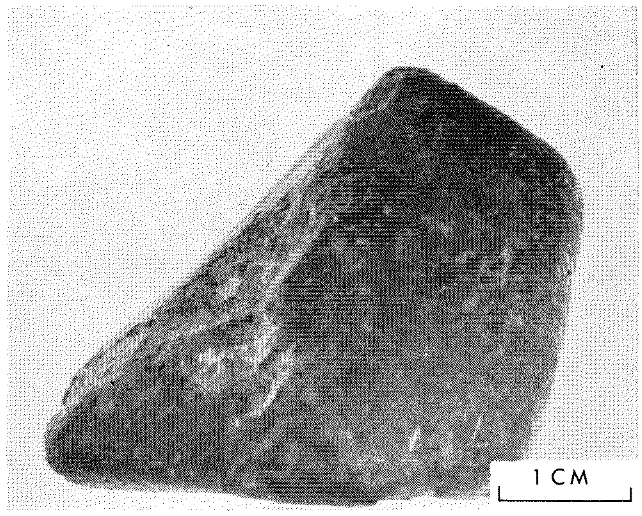

B

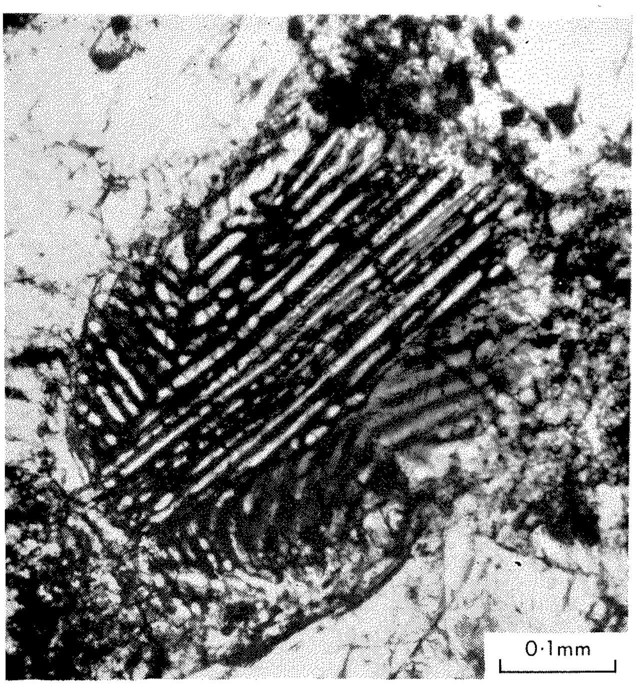

C

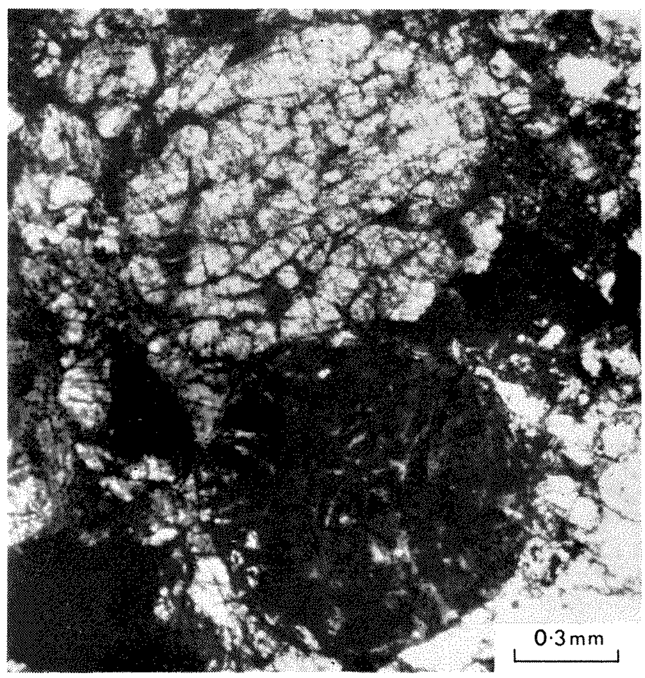

D

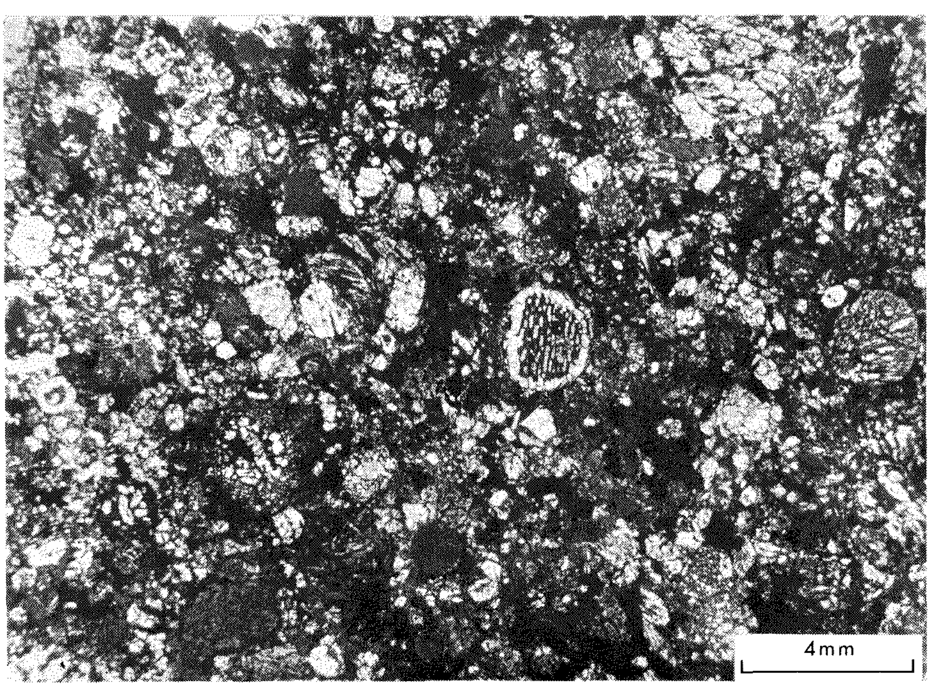

E

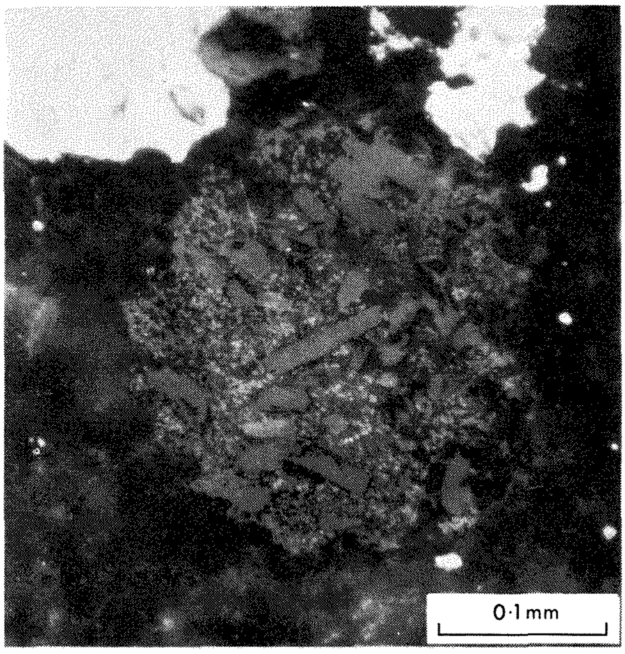

A

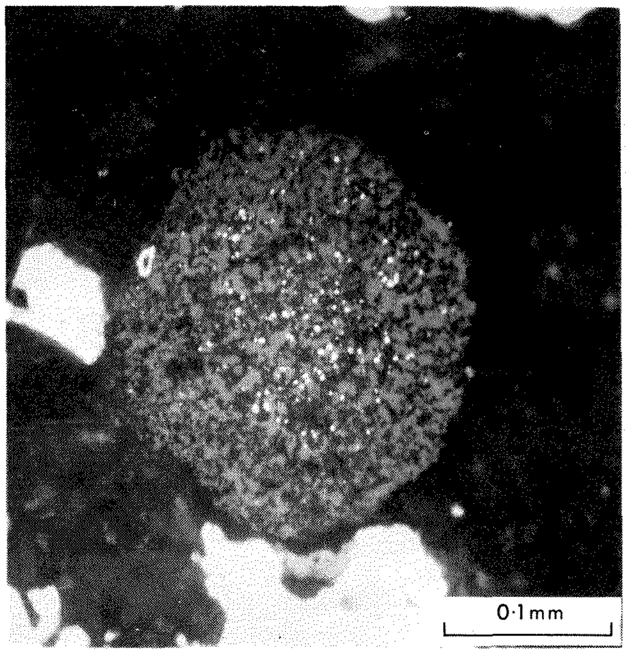

B

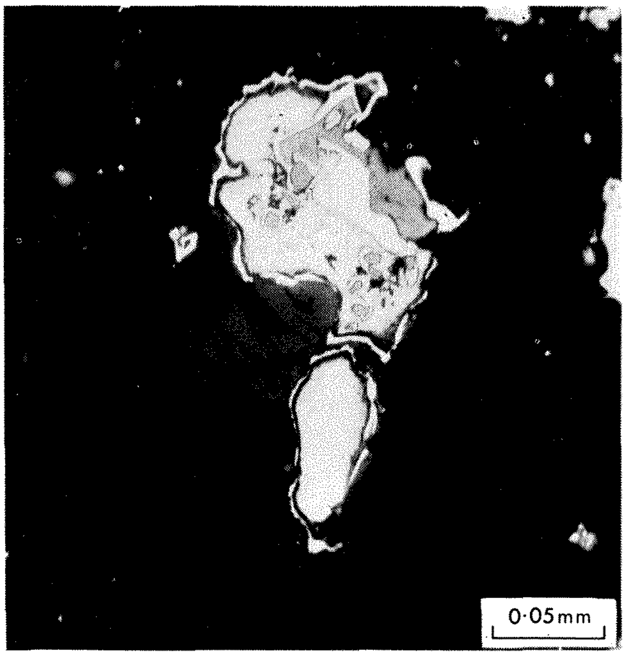

C

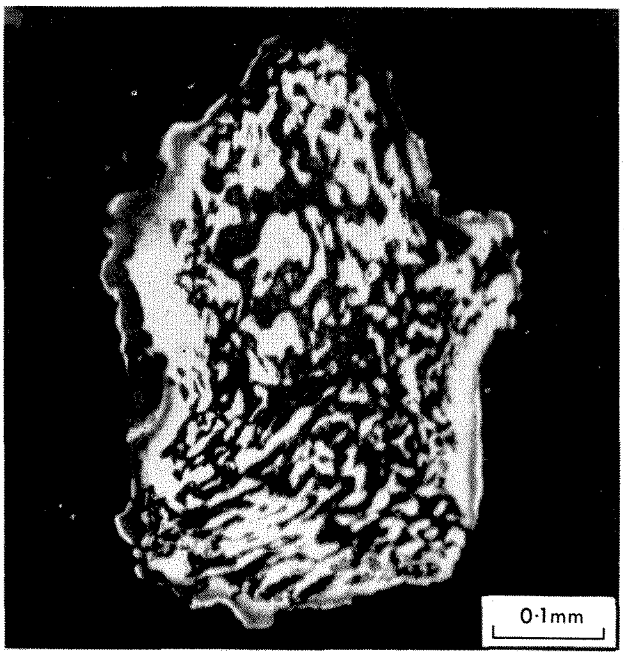

D

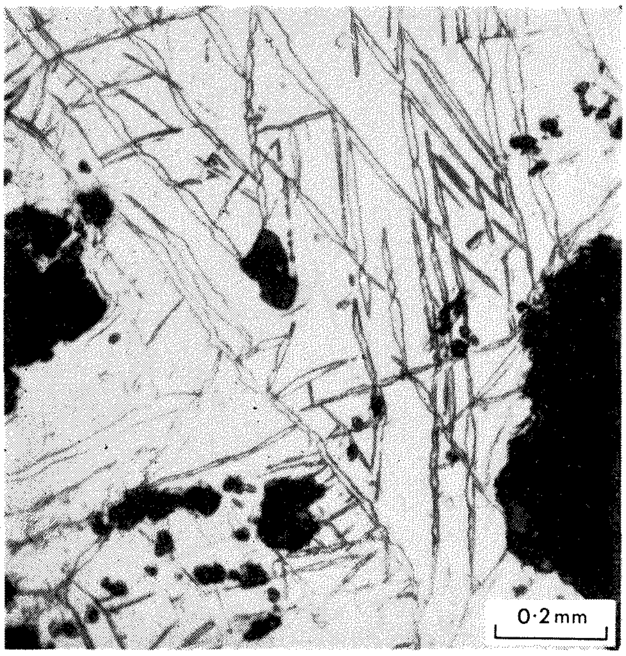

E

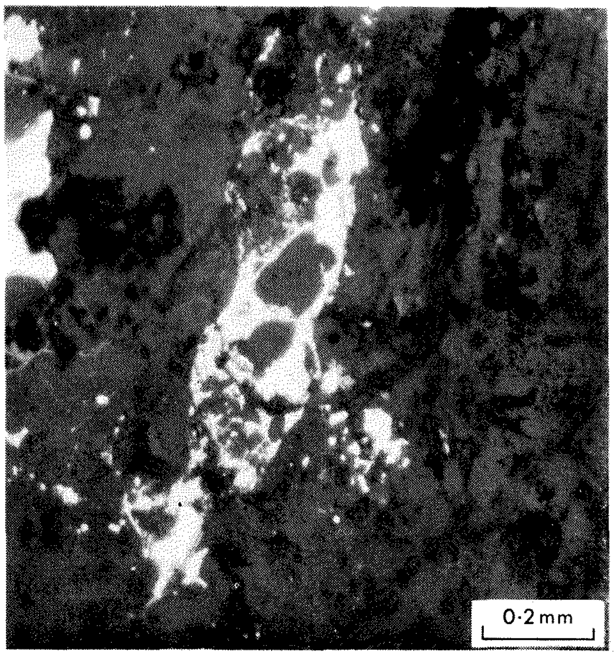

F

Figure 51. (opposite).
A. Chromite rich chrondrule with prismatic chromite.
B. Chromite rich chondrule containing small blebs of troilite. In this example the original chromite euhedra have been partly fused together.
C. Taenite (nital etched) intergrown with troilite and moulded onto a large chromite grain.
D. Taenite (nital etched) showing myrmekitic style intergrowth of high and low Ni varieties.
E. Neumann bands in kamacite (nital etched).
F. Remobilization of troilite along a shock vein. Small angular fragments of silicate minerals set in a network of troilite.

REFERENCES

Binns, R. A., 1967, Structure and evolution of non-carbonaceous chondritic mateorites: Earth and Planetary Sci. Letters v. 2, p. 23-28.

——— 1970, Pyroxenes from non-carbonaceous chondritic meteorites: Mineralog. Mag. v. 37, p. 649-669.

Dodd, T. R., and Calef, C., 1971, Twinning and intergrowth of olivine crystals in chondritic meteorites: Mineralog. Mag. v. 38, p. 324-327.

Pryce, W. M., 1970, A Weissenberg goniometer for Straumanis position films with 8 : 1 ratio: Jour. Physics E.: Sci. Instr. v. 3, p. 1026.

Ramdohr, P., 1967, Chromite and chromite chondrules in meteorites—I: Geochim. et Cosmochim. Acta v. 31, p. 1961-1967.

——— 1973, The Opaque Minerals in Stony Meteorites: Elsevier, Amsterdam, 245 p.

Uhlig, H.H., 1955, Contribution of Metallurgy to the origin of meteorites, Pt. II—The significance of Neumann bands in meteorites: Geochim. et Cosmochim. Acta v. 7, p. 34-42.

Van Schmuss, W. R., and Wood, J. A., 1967, A chemical—petrologic classification for the chondritic meteorites: Geochim. et Cosmochim. Acta v. 31, p. 747-765.

PRELIMINARY GEOCHRONOLOGICAL RESULTS FROM TWO PILBARA PORPHYRY BODIES

by A. F. Trendall

ABSTRACT

The Bamboo Creek Porphyry and the Spinaway Porphyry are two stratiform bodies of porphyry within the Hardey Sandstone (Fortescue Group) in two separate parts of its outcrop in the eastern Pilbara area of Western Australia. Similarity of petrography and intrusion shape, as well as stratigraphic equivalence, suggest correlation of the two porphyry bodies. However, Rb/Sr isotopic analyses of nine samples of Spinaway Porphyry, and of ten samples of Bamboo Creek Porphyry, give computed isochrons of 2 124 ± 195 m.y. and 2 820 ± 516 m.y. respectively. A large age difference cannot be satisfactorily reconciled with the geological evidence. On the other hand, if the two porphyries are accepted from geological evidence as closely coeval, and the age of both, on regional grounds, is accepted to be close to that of the Spinaway Porphyry isochron, the isotopic analyses of the Bamboo Creek Porphyry samples are not easily reconciled with their petrography and chemistry. Nevertheless, this second course appears to be the most reasonable one, pending further evidence.

INTRODUCTION

The purposes of this paper are to report and discuss the results of Rb/Sr isotopic analyses of 19 whole-rock samples from two stratiform bodies of felsic porphyry near the base of the Fortescue Group in the eastern Pilbara area of Western Australia; specifically, these results are relevant to the geological history of an area roughly enclosed between latitudes 21° and 22° S and longitudes 119° 30′ and 120° 30′ E, representing the eastern and western parts respectively of the Marble Bar and Nullagine 1:250 000 Sheet areas.

Although the data reported are consistent with more than one hypothesis concerning the age and emplacement of the porphyry, they are nevertheless significant, and as there is no immediate prospect of further work a published record is desirable.

GEOLOGICAL SETTING AND NOMENCLATURE

The broad regional tectonic and geochronological significance of both the porphyry bodies, under the single name Bamboo Creek Porphyry, were discussed by de Laeter and Trendall (1971); the following brief outline supplies only enough background to allow this paper to be read and understood in isolation.

During the early Proterozoic, steady sinking of a land surface eroded across Archaean rocks led to the development of an ovoid depositional basin—the Hamersley Basin—over an area of some 150 000 km² of what is now the northwestern part of Western Australia. The material which accumulated within it was at first volcanic and volcanoclastic, then largely chemically precipitated, and finally clastic, and this sequence broadly corresponds with the three divisions—Fortescue Group, Hamersley Group, and Wyloo Group—into which the remaining part of its contents are now stratigraphically subdivided. Later uplift led to the removal of much of this material, and the present northern edge of the basin is marked by a regional unconformity in which the negligibly disturbed Fortescue Group dips very gently southwards off the Archaean rocks of the Pilbara Block.

This great unconformity runs sinuously but consistently east-southeastwards from the coast for some 400 km before its course becomes more irregular, swinging northwards and back towards the west. As a result, in the area under immediate attention, two lobes of the unconformity, one from the northeast and the other from the south, are opposed across a gap about 20 km wide in which the Archaean floor of the basin is re-exposed. Within a clastic unit clearly identifiable as equivalent in the lower part of the Fortescue Group of both lobes there is present also in each lobe a stratiform body of similar porphyry.

Noldart and Wyatt (1962) mapped and described the southern and northern outcrops of porphyry as part of a single, presumably originally continuous, body called the Bamboo Creek Porphyry. They noted earlier divergence of opinion as to whether it was intrusive or extrusive, and also described some new evidence for both types of origin.

Hickman (in prep.), as a result of recent re-mapping of the Nullagine 1 : 250 000 Sheet area by himself and Mr. R. Thom, proposes to retain the name Bamboo Creek Porphyry for the porphyry north of the exposure gap, and to apply the name Spinaway Porphyry (Lipple, 1975) to that south of it. Both form stratiform bodies within the Hardey Sandstone of the Fortescue Group, probably up to about 100 m thick. Hickman (in prep.) records local evidence that the Bamboo Creek Porphyry is at least in part extrusive, and that the Spinaway Porphyry is intrusive. He nevertheless appreciates that the evident similarity in lithology and intrusion shape, as well as the stratigraphic continuity of the host sandstone, make a supposition of original direct continuity attractive.

MATERIAL USED

The samples analysed were collected by Dr. A. H. Hickman. Nine were taken from the Spinaway Porphyry and ten from the Bamboo Creek Porphyry.

Samples 32559 A-I (9), from the Spinaway Porphyry were collected at lat.21° 46′ S, long.120° 05′ E, 15 km north of Nullagine from cliffs 100 m west of Great Northern Highway.

The individual samples, each weighing about 2 kg, were collected from the central part of the sheet over an exposure area of about 0.5 ha to give a variable sample separation of about 5 to 25 m.

These nine samples are not distinguishable from one another in macroscopic appearance, and consist of massive, fresh, homogeneous, felsic porphyry. Abundant greyish yellow-green (5 GY 7/2) plagioclase phenocrysts mostly between 2 and 10 mm in longest diameter, less abundant and slightly smaller rounded phenocrysts of pink (5 RP 8/2) potassium feldspar, and corroded phenocrysts of quartz about the same size as the plagioclase phenocrysts, are set in a bluish-grey (5 B/6/1) aphanitic matrix. Darker and more coarsely granular patches in this matrix may represent digested xenoliths.

Thin section examination shows clearly that the shapes of all three phenocryst types are those characteristic of late modification, including resorption. The quartzes are well rounded and in places deeply embayed, the plagioclase (albite) has slightly rounded and corroded subhedral outlines, while the potassic feldspar is deeply embayed and irregular. Lamellar twinning and glomerocryst structure is typical of the albite phenocrysts, whose green colour is due to abundant inclusions of fibrous pumpellyite and chlorite; epidote, fluorite and carbonate are less abundant. The potassic feldspar is untwinned, with highly irregular patchy extinction, and is charged with exsolved hematite dust.

The matrix consists of a random mesh of slender "laths", about 0.5 mm long, which consist of quartz which is optically continuous in a pattern independent of the lath forms. The laths are assumed to be quartz paramorphs after tridymite. The interstitial areas contain either finely fibrous brownish-green chlorite or a fine (0.02-0.05 mm) mosaic of potassic feldspar, or a mixture of both. There are wide variations in textural detail in the matrix, which has a locally variable minor content of opaque mineral, carbonate, sphene and epidote. Larger concentrations of chlorite may be pseudomorphous after pyroxene.

Samples 32995 A-J (10), from the Bamboo Creek Porphyry were collected at Bamboo Creek (120° 13′ 30″ E; 20° 55′ 30″ S). They were collected over an area of about 0.25 ha within 30 m of the lower contact of the porphyry; approximate sample separation was 5 to 10 m.

Like the porphyry material from the Spinaway Porphyry, each sample weighed about 2 kg; the ten samples are not distinguishable from each other in macroscopic appearance and consist of massive, fresh, homogeneous, felsic porphyry. While these rocks are closely similar to those from the Spinaway Porphyry in that they contain both green and pink feldspar phenocrysts as well as quartz in a fine-grained grey matrix, there are macroscopic differences in colour and relative abundance of these constituents which are related to significant differences apparent in thin section.

The matrix is a darker bluish-grey (5 B 4/1) than in the Spinaway Porphyry samples, as also are the dusky yellow-green (5 GY 5/2) plagioclase phenocrysts; the phenocrysts of potassic feldspar are of the same pink (5 RP 8/2) colour. All three phenocryst types are of roughly equal size (2-10 mm), and also of approximately equal abundance.

In thin section the plagioclase phenocrysts of these rocks are so abundantly sericitized that their composition cannot be accurately determined; in addition they appear more corroded than those in the Spinaway Porphyry. The potassic feldspar phenocrysts show the same patchy extinction and irregular forms as their possible southern counterparts, but differ in having abundant carbonate alteration.

The matrix of these rocks from the Bamboo Creek Porphyry shows no sign of the lath-like quartz texture, but is a very fine-grained aggregate of quartz, feldspar and sericite. Chlorite and opaque minerals are also present in irregular scattered aggregates in the matrix.

In summary, while the analysed samples from the Spinaway Porphyry and Bamboo Creek Porphyry are distinctively different in both macroscopic and thin section appearance, the differences would be accepted by most petrographers as those to be expected within a single igneous rock body.

ANALYTICAL PROCEDURES

With one exception, all instruments and methods used were the same as those described by de Laeter and others (1974). The exception is that the Sr^{87}/Sr^{86} values of Table 22 were normalized to a Sr^{88}/Sr^{86} value of 8.365 to give a mean value of 0.710 3 for replicate analyses of NBS 987 standard. The resultant age difference of about 0.13 per cent is not large enough to affect comparison with other ages reported from the Western Australian Institute of Technology Laboratory, where the more usual 8.375 2 normalizing value has now been adopted.

RESULTS

The measured Rb/Sr (XRFS) and Sr^{87}/Sr^{86} ratios are shown in Table 22 together with the calculated Rb^{87}/Sr^{86} values. All errors are at the 95 per cent confidence level. The data also appear in Figure 52 together with two isochrons computed from them by the programme of McIntyre and others (1966). The 2 124 ± 195 m.y. age derived from the nine analyses of samples 32559 A-I, from the southern area, is a Model 4 age; the age of 2 820 ± 516 m.y. computed from the ten results of sample 32995 A-J, from the north, is a Model 3 age. The mean squares of weighted deviates (MSWD) for Model 1 ages of these two groups were 13.2 and 16.1 respectively, indicating that the scatter of points is well beyond experimental error, and is due to some "geological effect".

TABLE 22. ANALYTICAL DATA FOR NINE WHOLE-ROCK SAMPLES FROM THE SPINAWAY PORPHYRY (32559) AND TEN WHOLE-ROCK SAMPLES FROM THE BAMBOO CREEK PORPHYRY (32995)

Sample No.	Rb (ppm)	Sr (ppm)	Rb/Sr	Rb^{87}/Sr^{86}	Sr^{87}/Sr^{86}
32559 A	167	92	1·68 ± 0·02	4·93 ± 0·05	0·863 9 ± 0·001 0
32559 B	170	72	2·24 ± 0·02	6·60 ± 0·07	0·913 0 ± 0·004 0
32559 C	156	94	1·62 ± 0·02	4·74 ± 0·05	0·854 5 ± 0·005 0
32559 D	159	116	1·31 ± 0·01	3·80 ± 0·04	0·829 6 ± 0·001 9
32559 E	164	77	2·09 ± 0·02	6·14 ± 0·06	0·894 2 ± 0·001 5
32559 F	167	110	1·45 ± 0·01	4·24 ± 0·04	0·836 5 ± 0·002 0
32559 G	156	101	1·50 ± 0·02	4·39 ± 0·04	0·842 2 ± 0·002 6
32559 H	178	94	1·81 ± 0·02	5·31 ± 0·05	0·873 6 ± 0·010 0
32559 I	170	87	1·93 ± 0·02	5·67 ± 0·06	0·879 3 ± 0·006 3
32995 A	198	185	1·06 ± 0·01	3·10 ± 0·03	0·826 6 ± 0·001 5
32995 B	166	159	1·04 ± 0·01	3·04 ± 0·03	0·819 7 ± 0·001 3
32995 C	158	157	0·95 ± 0·01	2·77 ± 0·03	0·816 4 ± 0·002 1
32995 D	156	202	0·77 ± 0·01	2·24 ± 0·02	0·792 8 ± 0·001 0
32995 E	156	152	1·05 ± 0·01	3·06 ± 0·03	0·823 8 ± 0·001 3
32995 F	174	185	0·94 ± 0·01	2·68 ± 0·03	0·806 6 ± 0·002 8
32995 G	161	176	0·91 ± 0·01	2·64 ± 0·03	0·804 8 ± 0·003 4
32995 H	187	183	1·02 ± 0·01	3·01 ± 0·03	0·822 4 ± 0·001 4
32995 I	174	204	0·85 ± 0·01	2·79 ± 0·03	0·811 8 ± 0·000 4
32995 J	156	176	0·89 ± 0·01	2·54 ± 0·03	0·799 8 ± 0·000 7

Note: The Rb and Sr concentrations are preliminary results from loose powder samples, and have an accuracy of about ±5 per cent. The Rb/Sr ratios are from accurate measurements of these ratios on compressed pellets; they do not correspond exactly with the ratios that would be derived from the separate Rb and Sr values shown.

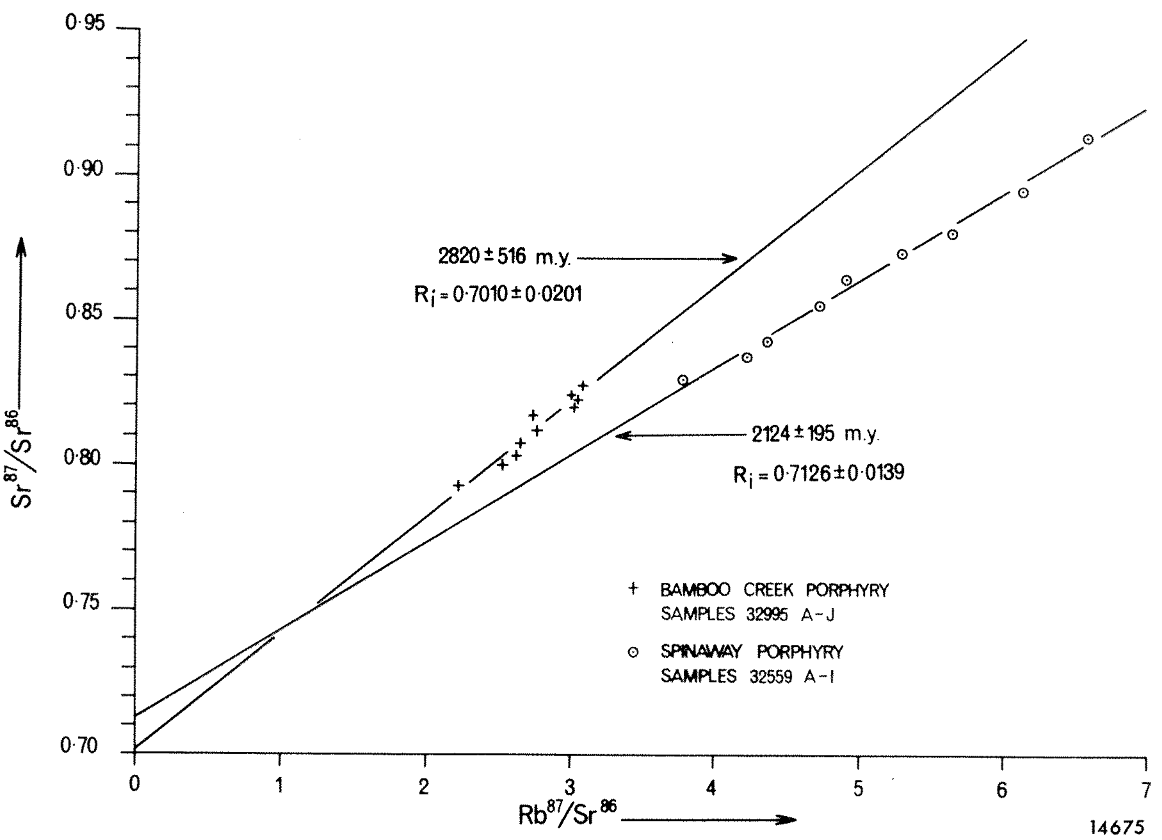

Figure 52. Isochron diagram for data of Table 22.

DISCUSSION

From Table 22 it is clear that, in respect to Rb and Sr chemistry, both porphyry bodies, as samples, have a comparable Rb content, but a Sr content differing by a factor of about 2. The means for samples 32559 and 32995 are, for Rb, 165 and 199 respectively, with an overlap in range of values, and for Sr, 94 and 178, with a gap of 36 ppm between the highest value (D) for 32559 and the lowest (E) for 32995. It is noteworthy that the samples with more abundant potassic feldspar phenocrysts (32995) unexpectedly have higher Sr values. The range of values for both Rb and Sr for both sets of samples is small. These features result in the lack of overlap between their Rb^{87}/Sr^{86} values, evident in Figure 52, and the comparatively narrow range in this ratio for each set.

It was evident from visual assessment of Figure 52 that the analyses of the two sets of samples did not define a single isochron, and separate isochrons for the two sets were therefore computed. The computed age for the Spinaway Porphyry, 2 124 ± 195 m.y., is consistent with its supposed intrusive relationship into the Hardey Sandstone, the best available younger and older limits on the age of which are 2 200 m.y. (de Laeter and others, 1974) and either 2 606 ± 128 m.y. or 2 329 ± 89 m.y. according to preferences in regional interpretation (Lewis and others, 1975). It is also consistent with its broad correlation with a number of other stratiform felsic bodies within the Fortescue Group and overlying Hamersley and Wyloo Groups (Fig. 53), as representatives of a regional igneous event at about 2 200 to 2 000 m.y.

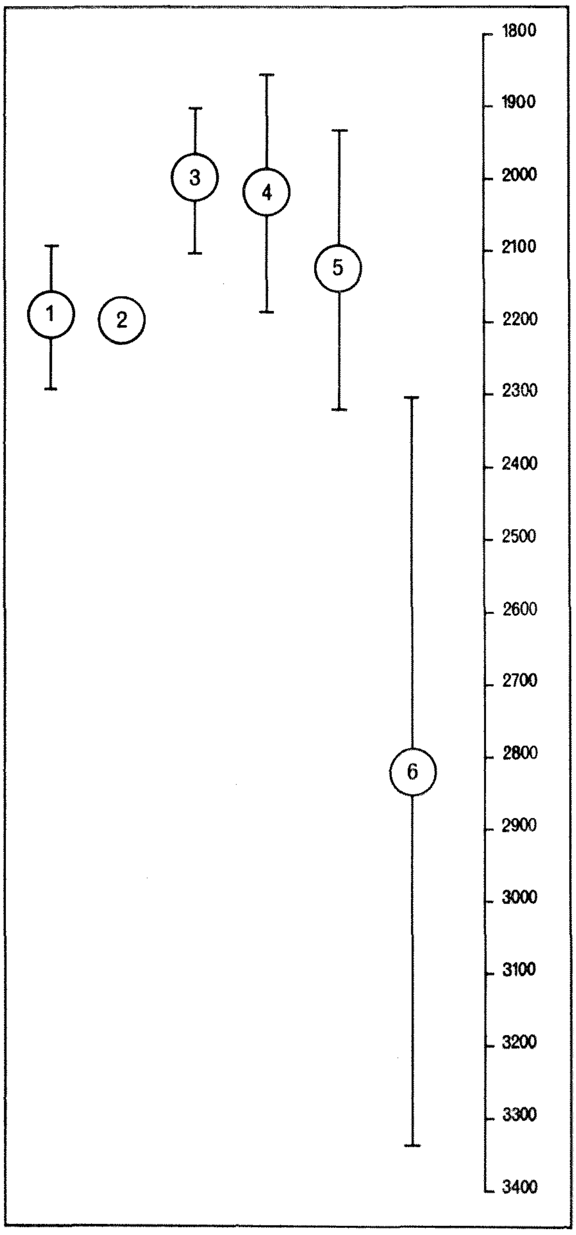

14676

Figure 53. Graphic comparison of age determinations from six stratiform bodies of felsic rock in the Pilbara and Hamersley Range areas:

1. 2 190 ± 100 m.y.; interbedded layers of acid igneous rocks in Fortescue Group (Compston and Arriens, 1968).
2. 2 196 ± 26 m.y.; granophyre intruded along basal unconformity of Fortescue Group (de Laeter and Trendall, 1971).
3. 2 000 ± 100 m.y.; Woongarra Volcanics (Compston and Arriens, 1968).
4. 2 020 ± 165 m.y.; layered acid igneous rocks interbedded in the Wyloo Group (Compston and Arriens, 1968).
5. 2 124 ± 195 m.y.; Spinaway Porphyry (this paper).
6. 2 820 ± 516 m.y.; Bamboo Creek Porphyry (this paper).

Further discussion of the regional relationship of determinations 1–4 above are given by de Laeter, Peers and Trendall (1974), in whose Figure 58 they are numbered 5, 6, 9 and 12 respectively.

The computed age for the Bamboo Creek Porphyry, of 2 820 ± 516 m.y., also represented in Figure 53, raises problems not presently capable of solution. If this order of age difference between the two porphyry bodies is real then it is remarkable, but not impossible, that two stratiform bodies of such similar rock were emplaced at the same stratigraphic level at times several hundreds of millions of years apart. The possible extrusive origin of the Bamboo Creek Porphyry, contrasted with the intrusion of the Spinaway Porphyry, is not a satisfying explanation of the age difference, since it would do little to reduce the coincidence involved, it would push the age of the initiation of the Hamersley Basin beyond the oldest limit of present credibility, and it would require a highly variable time-depression relationship for the basin. If, on the other hand, the older age of the Bamboo Creek Porphyry is dismissed as meaningless, it would be necessary to suppose that the analyses of Figure 52 fall, in fact, on a cluster of younger isochrons, parallel to each other and to that of the Spinaway Porphyry, or perhaps to an isochron of about 2 300 m.y. representing the overlap of error limits for both sets. In this case it would be necessary to explain why different subsets of closely spaced samples of Bamboo Creek Porphyry should have acquired different initial Sr^{87}/Sr^{86} ratios at the time of emplacement. Different proportions of ingested older potassic material would be the conventional explanation, but neither the very small spread in Rb/Sr ratios, nor the indistinguishable petrographies of the different samples, make this attractive.

Until more data are available the provisional acceptance of the Spinaway Porphyry age, and the rejection of that for the Bamboo Creek Porphyry, on grounds which cannot be convincingly argued, seems to involve least mental stress, but does not provide a satisfying reconciliation of the data presented.

ACKNOWLEDGEMENTS

The results reported here were obtained during the tenure of an Honorary Visiting Fellowship in the Physics Department, Western Australian Institute of Technology. I wish to thank Dr. J. R. de Laeter, former Head of that Department and now Dean of Applied Science, for his patient instruction in the instrumental techniques employed, and also to the following members of the Department for additional guidance and advice whenever it was needed; Mr. I. D. Abercrombie, Mr. M. T. McCulloch and Dr. K. J. R. Rosman in mass spectrometry, and Mr. W. W. Thomas in XRFS procedures.

REFERENCES

Compston, W., and Arriens, P. A., 1968, The Precambrian geochronology of Australia: Canadian Jour. of Earth Sciences, v. 5, p. 561-583.

de Laeter, J. R., and Trendall, A. F., 1971, The age of the Gidley Granophyre: West. Australia Geol. Survey Ann. Rept. 1970, p. 62-67.

de Laeter, J. R., Peers, R., and Trendall, A. F., 1974, Petrography, chemical composition, and geochronology of two dolerite sills from the Precambrian Weeli Wolli Formation, Hamersley Group: West. Australia Geol. Survey Ann. Rept. 1973, p. 82-91.

Hickman, A. H., in prep., Explanatory notes on the Nullagine 1 : 250 000 Geological Sheet, W.A.: West Australia Geol. Survey Rec. 1975/5 (unpublished).

Lewis, J. D., Rosman, K. J. R., and de Laeter, J. R., 1975, The age and metamorphic effects of the Black Range dolerite dyke: West. Australia Geol. Survey Ann. Rept. 1974, p. 80-88.

Lipple, S. L., 1975, Definitions of new and revised stratigraphic units of the Eastern Pilbara Region: West. Australia Geol. Survey Ann. Rept. 1974, p. 58-63.

McIntyre, G. A., Brooks, C., Compston, W., and Turek, A., 1966, The statistical assessment of Rb-Sr isochrons: Jour. Geophys. Research v. 71, p. 5459-5468.

Noldart, A. J., and Wyatt, J. D., 1962, The geology of portion of the Pilbara Goldfield: West Australia Geol. Survey Bull. 115, 199 p.

PALYNOLOGY OF THE YARRAGADEE FORMATION IN THE ENEABBA LINE BOREHOLES

by J. Backhouse

ABSTRACT

The Late Jurassic and Early Cretaceous *Dampieri, Baculatisporites* and *Cicatricosisporites* Zones recognized in the Watheroo Line boreholes are present in the Eneabba Line boreholes, but the highest zone (*Concavus* Zone) is absent. In addition, a distinctive microflora with contemporaneous microplankton and diverse remainé forms is recorded from the Otorowiri Siltstone Member in five boreholes. This unit occurs at the base of the *Cicatricosisporites* Zone. The overall composition of the palynogolical assemblages in each zone does not differ significantly from the Watheroo Line.

INTRODUCTION

The Eneabba Line boreholes (referred to as E.L. in this report) are located just north of latitude 30° S and extend from south of Carnamah to the coast north of Snag Island (Fig. 54). Drilling commenced in 1972 and was completed towards the end of 1974.

The Late Jurassic and Early Cretaceous Yarragadee Formation was intersected in boreholes E.L. 1 to 7 and also in Dathagnoorarra No. 1 borehole. Side-wall cores were obtained from all boreholes except Dathagnoorarra No. 1 from which ditch cutting samples were processed. A few conventional cores were cut in shallow subsidiary boreholes on the same sites as the main boreholes.

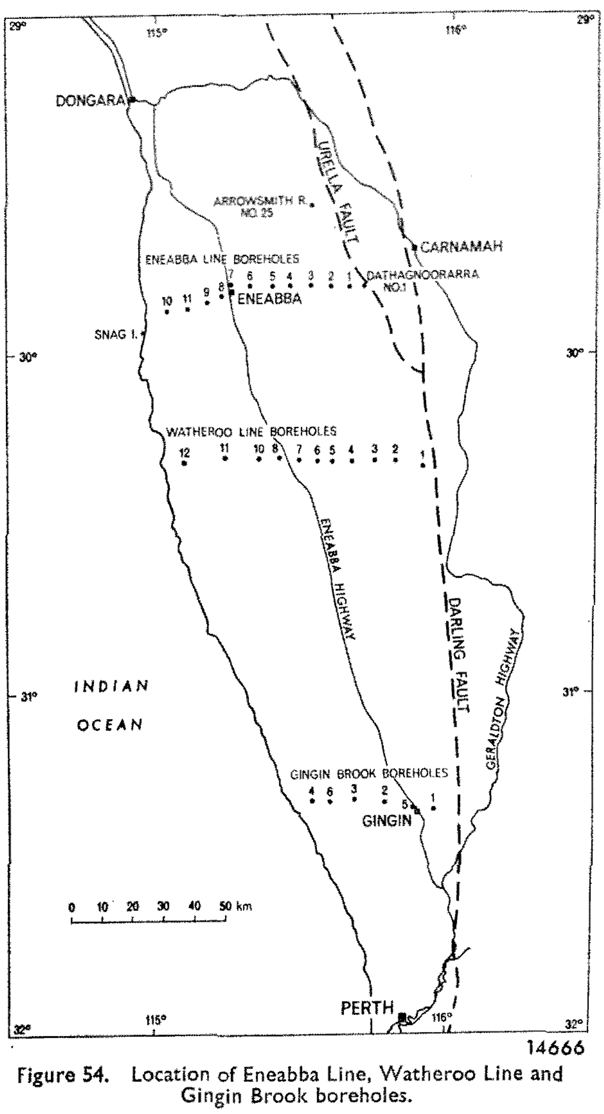

Figure 54. Location of Eneabba Line, Watheroo Line and Gingin Brook boreholes.

The position of the samples is shown in Figure 54, and the distribution of palynomorphs from the samples is set out in Table 23.

The microflora of the Yarragadee Formation in the Eneabba Line boreholes is comparable with the previously described microfloras from the same formation in the Gingin Brook and Watheroo Line boreholes (Ingram 1967a, Backhouse 1974). A major difference is the occurrence in the Eneabba Line of the characteristic microflora associated with the Otorowiri Siltstone Member in the Arrowsmith River boreholes (Ingram. 1967b). This microflora forms a prominent marker zone in the five eastern boreholes.

ZONATION

Three of the zones described in the Watheroo Line, the Late Jurassic *Dampieri* and *Baculatisporites* Zones and the Early Cretaceous *Cicatricosisporites* Zone can be recognised in the Eneabba Line. The uppermost zone, the *Concavus Zone,* is not represented in any sample so far examined. Spores and pollen grains, characteristic of these zones, are illustrated in Backhouse (1974).

DAMPIERI ZONE

Palynomorph assemblages from E.L. 6 and E.L. 7 belong to the *Dampieri* Zone. As in the Watheroo Line, samples from this zone are dominated by *Araucariacites australis* Cookson, *Zonalapollenites* spp. and bisaccate pollen grains, and *Cyathidites* spp. are common.

However, unlike the samples from the Watheroo Line, *Klukisporites* spp. are sometimes very common and *Classopollis* type pollen is rare. The following forms occur which were not recorded from the *Dampieri* Zone in the Watheroo Line:

Concavisporites jurienensis Balme
Contignisporites cooksonii (Balme)
C. multimuratus Dettmann
Coronatispora telata (Balme)
Dictyophyllidites sp.
Ischyosporites crateris Balme
Inaperturopollenites turbatus Balme

BACULATISPORITES ZONE

This assemblage zone occurs above the *Dampieri* Zone and below the first appearance of *Cicatricosisporites australiensis* (Cookson) which marks the *Cicatricosisporites* Zone. In the Eneabba Line many samples from this zone are barren or yielded only sparse assemblages. As in the Watheroo Line *Baculatisporites comaumensis* (Cookson) and *Osmundacidites wellmanii* Couper are more abundant in this zone and *Microcachryidites antarcticus* Cookson occurs for the first time. Other forms to occur for the first time are:

Aequitriradites acusus (Balme)
A. hispidus Dettmann and Playford
Cyathidites concavus Balme
Lycopodiumsporites facetus Dettmann
L. nodosus Dettmann
Trilobosporites sp.

CICATRICOSISPORITES ZONE

The *Cicatricosisporites* Zone starts with the first occurrence of *C. australiensis* which in the Eneabba Line first appears in the Otorowiri Siltstone Member and then is recorded sporadically throughout this zone. One species, *Pilosisporites notensis* Cookson and Dettmann, which first occurs in this zone in the Watheroo Line also first occurs in this zone in the Eneabba Line. However, *C. concavus,* which first occurs in this zone in the Watheroo Line, is known from the *Baculatisporites* Zone in the Eneabba Line. *M. antarcticus* is noticeably more common in this zone in the Eneabba Line.

TABLE 23. PALYNOMORPHS FROM THE ENEABBA LINE BOREHOLES

PALYNOMORPHS	E.L.7						E.L.6				E.L.5					E.L.4							E.L.3					E.L.2								E.L.1					
	645	589.5	446	315	247	120	393.5	380.5	264	154	688	631.5	556.5	421.5	375	643	404	296	282	267	238	156.5	490.8	490	450	323	151	598	515	479	433	384	366	277	206	694	684	345	294	278	197
Aequitriradites spp.															X				X		X		X	X	X		X	X	X	X	X	X	X	X			X	X	X	X	X
Araucariacites australis	X	X	X	X	X	X	X	X	X	X				X	X			X	X	X	X		X	X	X	X		X		X	X	X	X	X	X	X	X	X	X	X	X
Baculatisporites comaumensis			X												X		X	X		X	X	X	X	X	X	X	X			X	X	X	X	X	X		X	X	X	X	X
Ceratosporites equalis															X			X						X	X		X	X					X	X	X			X	X		X
Cicatricosisporites australiensis																							X	X			X			X	X	X			X				X		X
Classopollis spp.	X	X	X	X			X							X					X	X	X		X	X	X	X	X	X		X	X	X	X				X	X		X	X
Concavisporites jurienensis	X				X				X	X					X					X		X	X	X		X	X					X			X						
Contignisporites cooksonii	X	X	X			X		X	X	X				X	X				X	X	X		X	X	X	X	X	X	X	X	X	X	X					X	X	X	X
C. multimuratus					X			X	X	X					X			X	X	X	X	X	X	X	X	X	X	X		X	X		X	X	X		X	X		X	X
Coronatispora perforata																								X	X		X				X			X					X	X	
C. telata			X												X					X		X						X	X	X	X	X	X		X	X	X	X	X	X	X
Cyathidites australis	X							X							X		X	X	X	X			X	X	X	X	X	X	X	X	X	X	X	X	X		X	X	X	X	X
C. concavus																												X	X		X		X					X			X
C. minor	X	X		X	X	X	X		X	X			X				X	X		X	X	X	X	X	X	X	X	X	X		X	X	X	X	X		X	X	X	X	X
Densoisporites velatus																			X	X				X	X	X	X					X							X	X	
Dictyophyllidites sp.	X	X	X	X	X		X		X	X							X			X	X				X		X	X				X							X	X	X
Dictyotosporites complex																									X	X	X				X		X	X	X						
Foraminisporis dailyi																											X	X													
Foveosporites canalis									X											X		X	X		X		X	X	X	X			X		X		X			X	X
Foveotriletes parviretus																										X	X	X	X		X	X	X	X	X	X				X	X
Ginkgocycadophytus nitidus																		X		X	X				X		X				X	X	X				X	X		X	
Gleicheniidites senonicus	X	X		X	X		X		X								X	X		X	X	X		X		X		X	X	X	X	X	X		X		X	X	X	X	
Inaperturopollenites turbatus	X	X		X						X													X	X																	
Ischyosporites crateris		X						X	X	X		X					X				X	X	X	X	X	X	X	X	X	X	X	X	X	X				X	X	X	X
Januasporites spinulosus																																X							X		
Klukisporites scaberis	X	X	X	X			X	X		X			X		X					X	X	X		X	X	X	X	X	X	X	X		X	X	X	X		X	X	X	X
K. sp.		X		X	X	X			X	X									X																						X
Laevigatosporites spp.					X																							X	X						X						X
Leptolepidites major		X													X							X			X	X					X		X		X		X			X	
L. verrucatus			X								X				X				X	X	X	X			X		X	X		X		X	X	X	X		X	X	X	X	X
Lycopodiacidites asperatus	X	X		X	X			X	X	X										X	X	X	X			X	X	X	X	X			X		X	X	X				X
Lycopodiumsporites austroclavatidites	X	X	X				X				X	X	X	X	X				X	X		X	X	X	X	X	X	X	X	X	X				X	X	X	X	X	X	X
L. circolumenus												X		X	X				X	X		X		X	X	X	X			X		X	X	X	X	X	X			X	X
L. eminulus																		X			X			X	X	X	X		X	X		X	X			X	X	X		X	X
L. facetus																X									X			X					X		X		X			X	
L. nodosus														X			X									X										X		X			
Matonisporites crassiangulatus									X																X	X		X				X	X		X					X	X
M. sp.							X		X																																
Microcachryidites antarcticus															X		X	X	X	X	X		X	X	X	X	X	X		X	X	X	X	X	X	X	X	X	X	X	X
Murospora florida	X							X		X	X			X	X		X		X			X		X	X	X	X	X	X	X	X	X	X	X				X	X	X	X
Neoraistrickia truncata		X	X					X					X	X	X			X	X	X	X	X	X	X	X	X	X	X			X	X	X		X			X	X	X	
Nevesisporites vallatus																									X	X					X		X					X		X	X
N. sp.																					X				X	X	X				X	X	X					X	X	X	X
Obtusisporites sp.	X	X						X	X	X							X								X	X	X	X	X				X								
Osmundacidites wellmanii						X	X	X			X	X	X		X	X	X	X	X	X	X	X	X	X	X		X	X	X		X		X	X	X	X	X	X	X	X	X
Pilosisporites notensis																										X															X
Polypodiidites sp.																							X	X	X	X		X		X	X	X	X						X		X
Staplinisporites caminus					X		X	X	X	X			X							X		X															X				X
Stereisporites antiquasporites																								X	X																
Trilobosporites sp.									X									X					X	X	X	X	X	X			X	X	X	X	X		X	X	X	X	X
Zonalapollenites dampieri	X	X	X	X	X	X	X		X	X				X	X		X	X	X	X	X		X	X	X	X	X	X	X	X	X	X	X	X	X	X	X	X	X	X	X
Z. segmentatus			X	X			X		X												X		X		X	X	X	X		X		X							X		
Z. trilobatus	X	X		X			X		X	X									X					X	X		X			X	X	X						X	X	X	
bisaccate pollen	X	X	X	X	X	X	X	X	X	X	X	X	X	X	X	X	X	X	X	X	X	X	X	X	X	X	X	X	X	X	X	X	X	X	X	X	X	X	X	X	X
remanié forms				X						X				X					X	X	X	X	X	X	X					X								X			
microplankton																																									
Chytroeisphaeridia sp.																			X	X			X															X			
Komewuia sp.																			X	X			X	X																	
Meiourogonyaulax sp.																			X				X		X													X			
Micrhystridium spp.																					X									X										X	
Veryhachium spp.																		X	X	X			X	X	X			X		X						X		X	X		

X = present   Depths in metres

14668

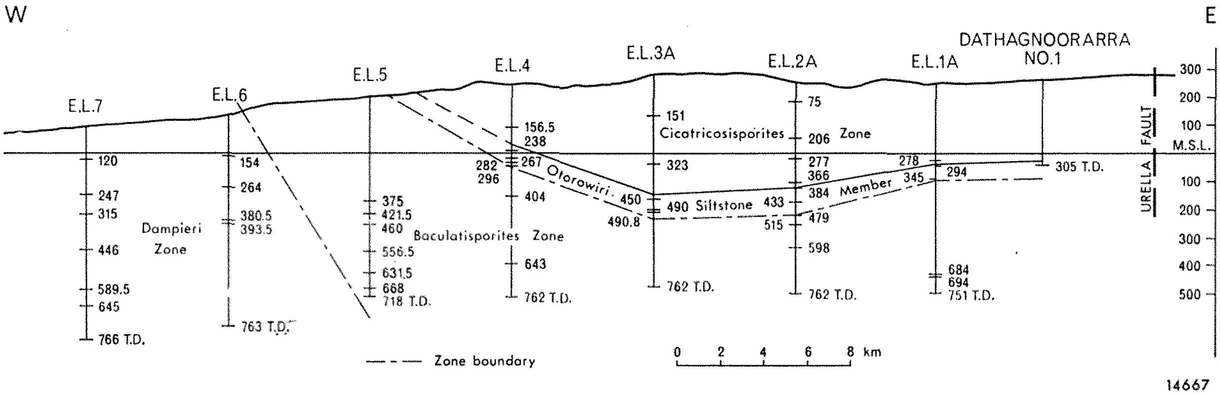

Figure 55. Palynological correlation of Eneabba Line boreholes.

OTOROWIRI SILTSTONE MEMBER

The type section of the Otorowiri Siltstone Member was defined by Ingram (1967b) in Arrowsmith River No. 25 borehole, approximately 27 km north of E.L. 3. During the Eneabba Line drilling the member was encountered in Dathagnoorarra No. 1 and E.L. 1-4 boreholes, and it crops out between E.L. 4 and E.L. 5 (D.P. Commander pers. comm.). It occurs in a syncline, becoming thicker in the centre and reaching a maximum intersected thickness of 99 m in E.L. 2 (Fig. 55).

In the Arrowsmith River area the Otorowiri Siltstone Member is characterized by a rich and diverse association of remanié palynomorphs. Spores and pollen of Devonian, Early and Late Permian, Early Triassic and Middle to Late Triassic age, and dinoflagellates of Late Jurassic age were identified by Ingram (1967b). In the Eneabba Line boreholes spores and pollen of Early Triassic and Permian age are common but there is only one definite occurrence of a remanié Devonian spore—a single specimen of *Hymenozonotriletes lepidophytus* Kedo from E.L. 2A at 479 m. This is of particular interest as this species has a very restricted age range of late Famennian to early Tournaisian. Several samples contain remanié Late Jurassic microplankton including *Adnatosphaeridium aemulum* (Deflandre), *Gonyaulacysta perforans* (Cookson and Eisenack), *Leiofusa jurassica* Cookson and Eisenack and *Wanaea clathrata* Cookson and Eisenack.

Thin walled dinoflagellates and a few acritarchs are present in small numbers in some samples. The dinoflagellates are tentatively referred to the genera *Meiourogonyaulax, Komewuia* and *Chytroeisphaeridia*. These are not considered to be remanié forms.

Komewuia sp. and other microplankton have been recorded from the Quinns Shale Member of the Yarragadee Formation in offshore wells drilled by West. Australian Petroleum Pty. Ltd. (Williams in Moyes, 1971), and *C. australiensis* seems to first appear at about the same stratigraphic level. There is also a similarity between gamma-ray logs of the Otorowiri Siltstone Member in the Eneabba Line boreholes and the Quinns Shale Member in offshore wells. It seems likely that both the Otorowiri Siltstone Member and the Quinns Shale Member occur at the base of the *Cicatricosisporites* Zone and are of the same age. This is contrary to the opinion of Cockbain and Playford (1973), who suggested that the Quinns Shale Member was slightly older than the Otorowiri Siltstone Member.

CONCLUSIONS

The biostratigraphy of the Yarragadee Formation in the Eneabba Line boreholes differs significantly from that in the Watheroo Line in two ways:

(1) The Otorowiri Siltstone Member microflora is present in the Eneabba Line at the base of the *Cicatricosisporites* Zone. The Eneabba Line is closer to the Arrowsmith River area, where the Otorowiri Siltstone Member microflora was first recognized, and the member appears to lens out between the Eneabba and Watheroo Lines of boreholes.

(2) The *Concavus* Zone of the Watheroo Line zonation was not encountered in any borehole on the Eneabba Line. This is probably because sediments from a higher stratigraphic level were sampled in the Watheroo Line.

REFERENCES

Backhouse, J., 1974, Stratigraphic palynology of the Watheroo Line boreholes, Perth Basin: West. Australia Geol. Survey Ann. Rept. 1973, p. 99-103.

Cockbain, A. E., and Playford, P. E., 1973, Stratigraphic nomenclature of Cretaceous rocks in the Perth Basin: West. Australia Geol. Survey Ann. Rept. 1972, p. 26-31.

Ingram, B. S., 1967a, A preliminary palynological zonation of the Yarragadee Formation in the Gingin Brook bores: West. Australia Geol. Survey Ann. Rept. 1966, p. 77-79.

——— 1967b, Palynology of the Otorowiri Siltstone Member, Yarragadee Formation: West. Australia Geol. Survey Ann. Rept. 1966, p. 79-83.

Moyes, C. P., 1971, Gage Roads No. 2 well completion report: West. Australia Petroleum Pty. Ltd., Petroleum Search Subsidy Report. (unpublished).

MACROFOSSILS FROM THE CRETACEOUS OF THE PERTH BASIN

by K. Grey and A. E. Cockbain

ABSTRACT.

The bivalve *Maccoyella* Etheridge 1892 is recorded for the first time from the Early Cretaceous Leederville Formation. A probable trigoniid bivalve, tentatively identified as *Pterotrigonia* van Hoepen 1929, and the desmoceratid ammonite *Puzosia* Bayle 1878 are illustrated from the mid-Cretaceous Osborne Formation. The discovery of these specimens extends their known geographical occurrence to the Perth Basin, and confirms the ages assigned to these formations on palynological evidence.

INTRODUCTION

Cretaceous sediments in the Perth Basin have only sparse outcrops and are known mainly from borehole sampling. Macrofossils are rarely encountered in such material, and even fragmentary and poorly preserved specimens assume substantial significance in any consideration of the faunal elements of the associated sediments.

Two boreholes and a shallow quarry in the Perth Basin (Fig. 56) have recently yielded fragments of macrofossils. These discoveries extend the known geographical occurrence of these fossils, and provide further evidence for the Cretaceous age assigned to the sediments on the basis of spore and microplankton dating.

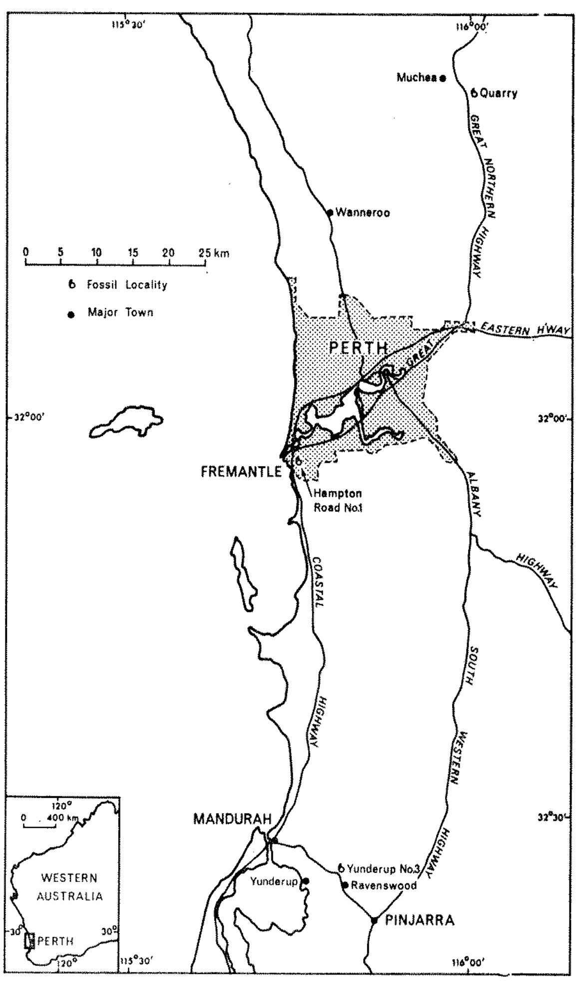

Figure 56. Perth Basin - localities of macrofossils from the Cretaceous.

STRATIGRAPHY

Cockbain and Playford (1973) revised the nomenclature of the Cretaceous rocks of the Perth Basin. The succession is summarized in Figure 57. The bivalve *Maccoyella* Etheridge 1892 is recorded from the Leederville Formation, a unit of the Warnbro Group, and the probable trigoniid bivalve ?*Pterotrigonia* van Hoepen 1929 and the desmoceratid ammonite *Puzosia* Bayle 1878 are recorded from the Osborne Formation, a unit of the Coolyena Group. Detailed descriptions of these formations are given by Cockbain and Playford (1973). Details of the localities and lithologies of each of the specimens are given with the specimen descriptions.

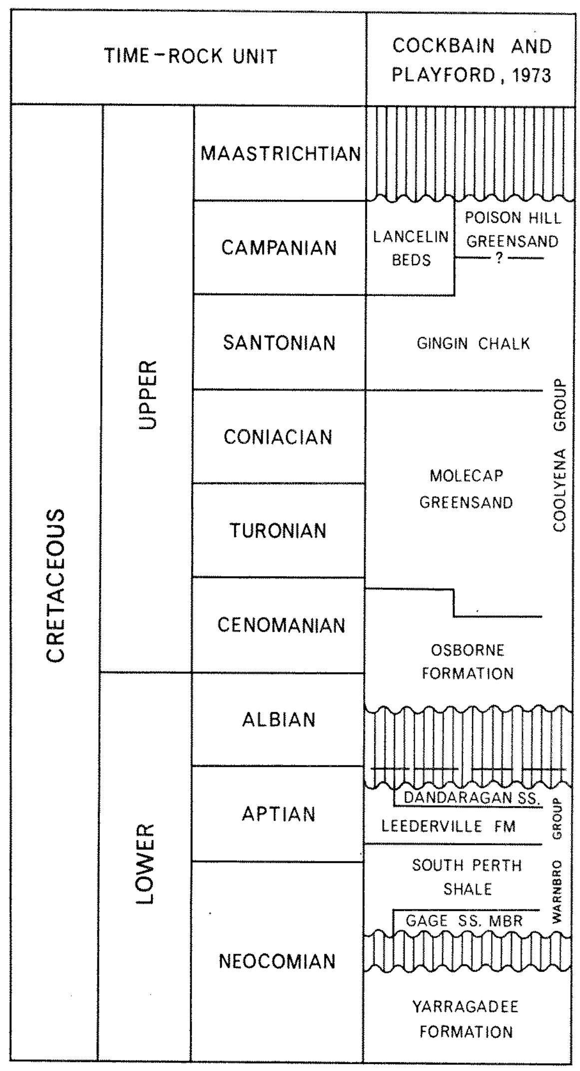

Figure 57. Cretaceous stratigraphic nomenclature, Perth Basin.

THE BIVALVE *MACCOYELLA* FROM THE LEEDERVILLE FORMATION

Yunderup No. 3 borehole is situated north of the Mandurah to Pinjarra road, near Ravenswood, lat. 32° 35′ S, long. 115° 50′ E. The borehole was drilled to a total depth of 115 m and passed through a sequence of sands and clays which are considered to be part of the Leederville Formation (D. P. Commander, pers. comm. 1973). A cuttings sample from a depth of 46 m consists of coarse sand with shale and fragments of the bivalve *Maccoyella* (G.S.W.A. registered No. F8470).

SYSTEMATIC PALAEONTOLOGY

Phylum MOLLUSCA
Class BIVALVIA
Subclass PTERIOMORPHIA
Order PTERIOIDA
Suborder PTERIINA
Superfamily PECTINACEA
Family OXYTOMIDAE
Genus MACCOYELLA Etheridge 1892

Maccoyella sp. cf. *M. barklyi* (Moore)
Figure 58A-D

cf. 1870 *Avicular barklyi* Moore; p. 245, pl. 11, fig. 1, 2.

cf. 1902 *Maccoyella barklyi* (Moore); Etheridge Jr.: p. 17, pl. 2, figs. 3-5, pl. 3, figs. 4-5, pl. 4, figs. 3-4.

1961 *Maccoyella* aff. *barklyi* (Moore); Cox: p. 16, pl. 1, fig. 14.

cf. 1966 *Maccoyella barklyi* (Moore); Ludbrook: p. 150, pl. 5, figs. 1-7.

Description: The material consists of about 30 shell fragments of the umbonal region. The largest fragment is 8.5 mm in length and 6.5 mm in height; most fragments are of left valves, a few are right valves.

The left valve is inflated with a slightly overhanging umbo. There are about 14 primary ribs which are fairly widely spaced and are crossed by prominent growth lines; where ribs and growth lines intersect a weak spine may be developed. Secondary ribs are inserted between the primaries. The right valve is somewhat flatter, with a posterior ear and a prominent anterior byssal notch. Most right valves are either smooth or weakly ribbed.

Remarks: On the basis of the degree of inflation and the rib count, the Yunderup specimens are compared with *M. barklyi,* which however is a much larger form.

Age: The sample is dated as Early Cretaceous on the basis of palynomorphs. The sample contains the microplankton: *Dingodinium cerviculum, Wetzeliella* sp., *Ascodinium* sp.; the spores *Gleicheniidites* sp. and *Contignisporites cooksonii;* the foraminifer *Marginulina;* plant fragments and fish teeth. Stratigraphically the sample comes from the Leederville Formation. Although fragmentary bivalve remains have long been known from the Leederville Formation and South Perth Shale, this is the first record of *Maccoyella* from these beds.

Distribution: This is the first record of *Maccoyella* from the Perth Basin, although the genus is widely known from Australia and has been recorded from the following places in Western Australia:

Carnarvon Basin: Cox (1961) records *M.* sp. aff. *M. barklyi, M.* sp. aff. *M. corbiensis, M.* sp. aff. *M. moorei* and *M.* sp. from the Nanutarra Formation.

Canning Basin: No undoubted record of *Maccoyella* has been found from the Canning Basin. Brunnschweiler (1954) records *Maccoyella* 'almost indistinguishable from *Maccoyella corbiensis*' from the Alexander Formation which is now believed to be Oxfordian in age. Cox (1961) identifies specimens from the Alexander Formation as 'indistinguishable from *M. barklyi*'. However, Brunnschweiler (1960) describes *Meleagrinella maccoyelloides* from the same formation, and Dickins (in Veevers and Wells, 1961, Appendix 4) refers to '*Meleagrinella maccoyelloides* Brunnschweiler, 1960 (previously referred to as Maccoyella sp.)'. It is probable that the Alexander Formation *Maccoyella* in fact is a species of *Meleagrinella.*

Officer Basin: The following species are recorded by Skwarko (1967) from the Samuel Formation and the Bejah Claystone: *M.* sp. cf. *M. barklyi, M.* sp. aff. *M. corbiensis, M.* sp, cf. *M. reflecta* and *M.* sp.

Eucla Basin: In a review of earlier work, Lowry (1970) notes the presence of *M. corbiensis* in the Madura Formation.

Maccoyella is essentially an Early Cretaceous genus. As shown above, the Late Jurassic record from the Alexander Formation is probably due to misidentification. Ludbrook (1966) gives the stratigraphic range of *M. barklyi, M. corbiensis, M. reflecta* and *M. umbonalis* as Aptian, and the range of *M. rockwoodensis* as Albian. The presence of *M.* sp. cf. *M. barklyi* in the Leederville Formation of Yunderup No. 3 borehole would suggest that the unit is of Aptian age. This is in agreement with the Neocomian-Aptian age for the unit established on palynological grounds.

A PROBABLE TRIGONIID FROM THE OSBORNE FORMATION

The specimen (Western Australian Museum Registered No. 74.528) was supplied by Mr. G. W. Kendrick of the Western Australian Museum. The sample is a dark grey siltstone from a shallow quarry at the east side of the road, 4.5 km southeast of Muchea, lat. 31° 35′ S, long. 116° 01′ E. The material was collected from strata that were formerly mapped as the Bullsbrook Beds but are now considered to belong to the Osborne Formation.

SYSTEMATIC PALAEONTOLOGY

Phylum MOLLUSCA
Class BIVALVIA
Subclass PALAEOHETERODONTA
Order TRIGONIOIDA
Superfamily TRIGONIACEA
Family TRIGONIIDAE
Subfamily PTEROTRIGONIINAE
Genus PTEROTRIGONIA van Hoepen 1929

?Pterotrigonia sp. indet.

Fig. 58E

Description: The specimen is a poorly preserved external mould of the right valve of a bivalve mollusc. The impression was illuminated so as to bring it into positive relief on the accompanying photograph; hence the impression appears to be a left valve.

The specimen is almost certainly a trigoniid and probably belongs to the genus *Pterotrigonia.* However, the preservation is such that the identification is tentative.

Age: Microplankton and foraminifers have been recovered from the same formation in nearby drillholes and indicate an Albian to Cenomanian age.

Distribution: Trigoniids are quite common in Lower Cretaceous rocks in Australia (and indeed in other circum-Indian Ocean countries). The only other Cretaceous record from the Perth Basin is of *Pterotrigonia* from the Maxicar Beds (Cockbain and Playford 1973, p. 29).

A DESMOCERATID AMMONITE FROM THE OSBORNE FORMATION

An ammonite fragment (G.S.W.A. registered No. F8651) was recovered from a core sample of the Hampton Road No. 2 borehole during palynological sampling. The borehole is sited near the junction of Hampton Road and Knutsford Street, Fremantle, lat. 32° 03′ S, long. 115° 46′ E. Details of the borehole are on file at the Geological Survey of Western Australia.

The core sample, taken between a depth of 121 and 131 m, consists of a dark grey siltstone with grains of glauconite and is from the Osborne Formation. The specimen was identified as an indeterminate species of *Puzosia* by Dr. M. K. Howarth of the British Museum (Natural History).

SYSTEMATIC PALAEONTOLOGY

Phylum MOLLUSCA
Class CEPHALOPODA
Order AMMONOIDEA
Family DESMOCERATIDAE
Genus PUZOSIA Bayle 1878

Puzosia sp. indet.

Fig. 58 F, G.

Description: The fossil is a poorly preserved fragment of the last whorl with the aperture missing. The specimen has a rounded whorl with flattened sides; weak ribs are present but are distinct only on the outer part; sinuous constrictions are present and are separated by approximately four ribs.

Remarks: The extremely poor preservation of the specimen precludes identification at species level.

Age: The genus *Puzosia* ranges from the Early Albian to Late Turonian and therefore confirms a mid-Cretaceous age for the Osborne Formation. Few macrofossils have been recorded from this formation, but an Albian to Cenomanian age is indicated by microplankton.

Distribution: This is the first record of *Puzosia* from the Perth Basin. Cretaceous ammonites have previously been described from Western Australia by Etheridge (1913), Spath (1926, 1940) and Brunnschweiler (1959, 1966). Etheridge described specimens from the Gingin Chalk and these were later reassessed by Spath (1926), who noted a resemblance of some of the specimens to *Parapuzosia.* Spath (1940) described ammonites from the Maastrichtian of the Carnarvon Basin including the puzosiid *Kitchinites.*

CONCLUSIONS.

The discovery of the macrofossils described above has increased our knowledge of the faunas of the Perth Basin. *Maccoyella* is indicative of paralic sediments and shallow marine basins (Skwarko 1967), a conclusion also indicated by the sporadic occurrence of microplankton in onshore sections of the Leederville Formation. The Osborne Formation contains abundant microplankton and the marine nature of these sediments is further emphasized by the presence of *Puzosia* and *?Pterotrigonia.* Skwarko (1963, p. 9) regards the presence of various trigoniids in Western Australia as indicative of "widespread though marginal marine incursions of the Australian continent".

Figure 58. (opposite).

A, B, C, D, *Maccoyella* sp. cf. *M. barklyi.* — all x 6.
A. Exterior, left valve.
B. Interior, left valve.
C. Exterior, right valve.
D. Interior, right valve
E. ?*Pterotrigonia* sp. indet., external mould of right valve x 4.
F, G. *Puzosia* sp. indet. F. lateral view, G. ventral view x 2.

REFERENCES

Brunnschweiler, R. O., 1954, Mesozoic stratigraphy and history of the Canning Desert and Fitzroy valley, Western Australia: Geol. Soc. Australia Jour., v. 1, p. 35-54.

——— 1960, Marine fossils from the Upper Jurassic and the Lower Cretaceous of Dampier Peninsula, Western Australia: Australia Bur. Mineral Resources Bull. 59.

——— 1959, New Aconeceratinae (Ammonoidea) from the Albian and Aptian of Australia: Australia Bur. Mineral Resources Bull. 54, p. 1-20.

——— 1966, Upper Cretaceous Ammonites from the Carnarvon Basin of Western Australia. I—The heteromorph *Lytoceratina:* Australia Bur. Mineral Resources Bull. 60.

Cockbain, A. E., and Playford, P. E., 1973, Stratigraphic nomenclature of Cretaceous rocks in the Perth Basin: West. Australia Geol. Survey Ann. Rept. 1972, p. 26-31.

Cox, L. R., 1961, The molluscan fauna and probable Lower Cretaceous age of the Nanutarra Formation of Western Australia: Australia Bur. Mineral Resources Bull. 61.

Etheridge, R., Jr., 1902, A monograph of the Cretaceous invertebrate fauna of New South Wales: New South Wales Geol. Survey Palaeontology Mem. 11.

——— 1913, The Cretaceous Fossils of the Gingin "Chalk": West. Australia Geol. Survey Bull. 55, p. 9-25.

Lowry, D. C., 1970, Geology of the Western Australian part of the Eucla Basin: West. Australia Geol. Survey Bull. 122.

Ludbrook, N. H., 1966, Cretaceous biostratigraphy of the Great Artesian Basin in South Australia: South Australia Geol. Survey Bull. 40.

Moore, C., 1870, Australian Mesozoic geology and palaeontology: Geol. Soc. London Quart. Jour., v. 26, p. 226-261.

Skwarko, S. K., 1963, Australian Mesozoic Trigoniids: Australia Bur. Mineral Resources Bull. 67.

——— 1967, Lower Cretaceous Mollusca of the Great Artesian Basin type in the Gibson Desert, central Western Australia: Australia Bur. Mineral Resources Bull. 75.

Spath, L. F., 1926, Note on two ammonites from the Gingin Chalk: Royal Soc. West. Australia Jour. v. 12, p. 53-55.

——— 1940, On Upper Cretaceous (Maestrichtian) ammonoidea from Western Australia: Royal Soc. West. Australia Jour. v. 26, p. 41-57.

Veevers, J. J., and Wells, A. T., 1961, The geology of the Canning Basin, Western Australia: Australia Bur. Mineral Resources Bull. 60.

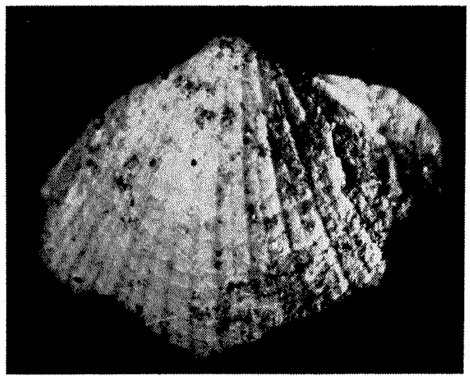
A

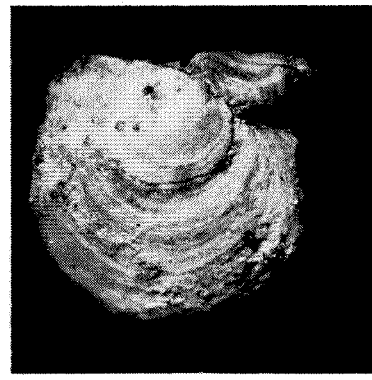
C

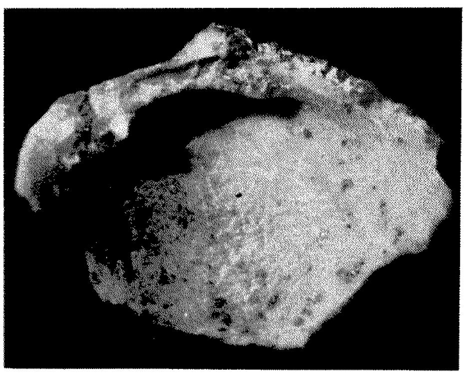
B


D


E


F


G

INDEX

46009/8/75

By Authority: WILLIAM C. BROWN, Government Printer